SISSA
Scuola
Internazionale
Superiore di
Studi Avanzati

Physics Area - PhD course in
Statistical Physics

Topologically Frustrated Quantum Spin Chains

Candidate:
Vanja Marić

Advisor:
Fabio Franchini

Academic Year 2020-21

Acknowledgements

First and foremost, I would like to thank my advisor Fabio Franchini, for introducing me to the world of research, for his constant guidance and various discussions. There wouldn't be anything in this thesis without him.

I gratefully acknowledge Salvatore Marco Giampaolo, for constant collaboration on the research presented in the thesis, various suggestions and discussions. His contribution is crucial and invaluable.

Many thanks to Gianpaolo Torre and Domagoj Kuić for the collaboration on topics related to the thesis.

My PhD was spent at two different institutions, SISSA in Trieste and Ruđer Bošković Institute in Zagreb. I would like to thank the Statistical Physics group at SISSA for a very stimulating environment and the transferred knowledge. The first year of my PhD, spent in Trieste, was a very enriching scientific and human experience. A special role here was played by the colleagues from the same year: Eduardo, Gennaro, Gianluca, Giuseppe, Xhek and my wonderful officemate Riccarda. The majority of the rest of my PhD was spent at Ruđer Bošković Institute in Zagreb. I would like to express my gratitude to the Division of Theoretical Physics at Ruđer for a pleasant and productive working environment. For this being a nice period special thanks go to the PhD students: Domagoj, Georgios, Irena, Jahmall, Mihovil and other with whom I had the privilege to interact.

Finally, I thank my parents, Vesna and Predrag, for their unwavering support.

Abstract

Frustration in many-body spin systems is a situation where the spins cannot orient themselves to fully minimize the interactions with their neighbors. It is caused, in general, by competing interactions or by the lattice structure, as in the antiferromagnets on non-bipartite lattices. Over the years frustrated systems have been studied substantially, since frustration can destabilize the antiferromagnetic order, lead to different phases of matter and induce various exotic properties.

Frustration can be caused also by a choice of boundary conditions, i.e. the lattice topology. For instance, a ring with an odd number of sites is non-bipartite, which makes antiferromagnets in this setting frustrated. The subject of this thesis are zero-temperature one-dimensional quantum systems exactly in this setting.

The major content is discussing how such a simple setting can influence the antiferromagnetic order, by studying spin-1/2 chains with discrete symmetries, whose breaking is related to the onset of the order. After reviewing the known results on topological frustration, dealing with non-thermodynamic quantities, we develop an approach for studying symmetry breaking, that is both suitable for exact analytical computations and meaningful for discussing the order also in a finite system. It consists of the realization that many spin-1/2 chains without external magnetic fields, such as the quantum XY chain, possess anticommuting global symmetries when the number of lattice sites is an odd number, implying the ground-state degeneracy already in a finite system.

In this framework, we discover that topological frustration, despite being induced only by the choice of boundary conditions and even/odd system size choice, can affect the magnetization in the thermodynamic limit and system's quantum phase transitions. We find that topological frustration can destroy local order, create a site-dependent magnetization that varies in space with an incommensurate pattern, induce a first-order quantum phase transition that is not present without frustration and modify the nature of a second-order transition, by destroying local order at both sides of the transition and preserving only non-local string order parameters. All these results indicate the incompleteness of the approach to quantum many-body systems, based on the Ginzburg-Landau theory, that tries to capture the properties of the system by taking the system size to infinity before computing the observables and neglects the influence of the chain length as a relevant scale.

We find that topological frustration can affect also non-equilibrium properties, by considering a local quantum quench setup. Namely, we study the Loschmidt echo and find it displays qualitatively and quantitatively different behavior for antiferromagnetic rings with an even and odd number of sites. Most of all, the differences become clearer for large system sizes, thus allowing to distinguish in a simple out-of-equilibrium experiment a system made by a certain, large, number of spins from the one with a single additional spin.

The thesis also contains a mathematical part. In studying order parameters of models mappable to free fermions, Toeplitz determinants with symbols that possess a part proportional to the delta function arise. We derive asymptotic formulas for this type of determinants.

List of Publications

Publications related to this thesis:

[1] **V. Marić**, S. M. Giampaolo, D. Kuić and F. Franchini,
The Frustration of being Odd: How Boundary Conditions can destroy Local Order,
New J. Phys. **22**, 083024 (2020).

[2] **V. Marić**, S. M. Giampaolo and F. Franchini,
Quantum Phase Transition induced by Topological Frustration,
Commun. Phys. **3**, 220 (2020).

[3] **V. Marić** and F. Franchini,
Asymptotic behavior of Toeplitz determinants with a delta function singularity,
J. Phys. A: Math. Theor. **54**, 025201 (2020).

[4] G. Torre, **V. Marić**, F. Franchini and S. M. Giampaolo,
Effects of defects in the XY chain with frustrated boundary conditions,
Phys. Rev. B **103**, 014429 (2021).

[5] **V. Marić**, F. Franchini, D. Kuić and S. M. Giampaolo,
Resilience of the topological phases to frustration,
Sci. Rep. **11**, 6508 (2021).

Preprints related to this thesis:

[6] **V. Marić**, S. M. Giampaolo and F. Franchini,
The fate of local order in topologically frustrated spin chains,
arXiv:2101.07276.

[7] **V. Marić**, G. Torre, F. Franchini and S. M. Giampaolo,
Topological Frustration can modify the nature of a Quantum Phase Transition,
arXiv:2101.08807. Submitted to SciPost Physics.

[8] G. Torre, **V. Marić**, D. Kuić, F. Franchini and S. M. Giampaolo,
An odd thermodynamic limit for the Loschmidt echo,
arXiv:2105.06483. Submitted to SciPost Physics.

Contents

Chapter 1

Introduction

1.1 Frustration in Spin Systems

In classical magnetic systems the spins orient themselves to satisfy the interactions with the other spins. At zero temperature, in ferromagnets the spins are aligned as their nearest neighbors, while in antiferromagnets the Néel order, with neighboring spins pointing in the opposite directions, is realized. Introducing sufficiently strong thermal or quantum fluctuations, by increasing the temperature or changing a Hamiltonian parameter, this magnetic order gets destroyed and the system exhibits a thermal or a quantum phase transition [9–11]. This simple picture can account for the behavior of a vast number of spin-systems. Yet, the set of possible behaviors of spin-systems is much more rich, one of the most important phenomena that enables it being *frustration*.

Frustration is a term that describes the situation where spins in a system cannot find an orientation to fully satisfy the interactions with their nearest neighbors [12]. In general, frustration is caused either by competing interactions or by the lattice structure, or a combination of both. Over the years frustrated systems have been a subject of a lot of research. On one side, because many real magnetic systems are frustrated, and on the other, because frustrated magnetism presents an excellent ground to discover new states of matter and to test and improve theories [12, 13]. Let us review some of the effects of frustration, first focusing on classical, and then on quantum systems.

In classical systems with competing interactions some of the most spectacular effects due to frustration are high ground-state degeneracy, existence of several phases in the ground-state phase diagram, multiple phase transitions with increasing temperature, reentrant phase with no long-range order below an ordered phase on a temperature scale, disorder lines and partial disorder at equilibrium [12]. They can be found already among the exactly solvable Ising models with nearest and next-to-nearest neighbor interactions, the most famous, containing many of these phenomena, being the $J_1 - J_2$ model on the square lattice [12]. A central property of these and of general frustrated systems is high ground state degeneracy. The parts of the phase diagrams of the models with competing interactions where alternative ground states are close to degeneracy are likely, in general, to have the highest effects of frustration. Consequently, these parts are of primary theoretical interest. Note, however, that it might be difficult to realize experimentally such a setting, with precise relation between different interaction strengths. The other kind of frustration, that arises only because of the lattice structure, avoids this problem[13].

Frustration that is caused by the lattice structure is termed *geometrical* frustration [13]. It arises, most notably, in antiferromagnetic systems on non-bipartite lattices. The standard example for introducing the concept is the antiferromagnetic Ising triangle, a building unit of the Ising antiferromagnet on a triangular lattice. Aligning

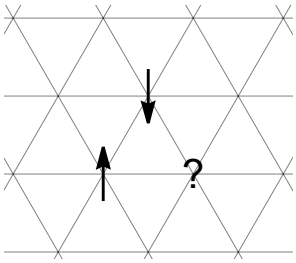

FIGURE 1.1: Geometrical frustration in the Ising antiferromagnet on the triangular lattice. Fixing two nearest neighbor spins to point in the opposite directions, it is impossible for their common neighbor to point oppositely from both.

two nearest neighbor spins on the triangle to point in the opposite directions, it is impossible for their common neighbor to point oppositely from both, as presented in Figure 1.1. In fact, the Ising antiferromagnet on a triangular lattice provided the first results on geometrical frustration [14, 15], where it was noticed that the model has different properties from ferromagnets or bipartite antiferromagnets. In geometrically frustrated systems lattice itself may destabilize Néel order and create high ground state degeneracy. For instance, the aforementioned Ising antiferromagnet on a triangular lattice [16] and the classical Heisenberg antiferromagnet on the pyrochlore lattice [17, 18], of corner sharing tetrahedra, do not posses long range order at any finite temperature.

Geometrical frustration induces also other exotic phenomena. The high ground state degeneracy of geometrically frustrated systems is related to the non-zero residual entropy, found already in the Ising antiferromagnet on the triangular lattice [14], and the spin ice phenomenon [19]. The dependence of the magnetic susceptibility on the temperature in geometrically frustrated systems is peculiar and is, in fact, an important revealing property of geometrical frustration [13]. Algebraic decay of correlations without criticality can arise in the presence of geometrical frustration [20, 21]. Furthermore, geometrical frustration can be a platform to realize emergent properties, such as artificial light [20, 21] and magnetic monopoles [22, 23].

Another interesting effect of geometrical frustration is order by disorder [24]. Since the high ground state degeneracy in geometrically frustrated antiferromagnets is not a consequence of a symmetry, but a rather accidental, the spectrum of thermal fluctuations around different ground states may be different. Thus at small finite temperature some ground states may have greater contribution to the free energy than the other and, moreover, it may happen that those states have some degree of long-range order. In this way fluctuations can enhance the order that is not present at zero temperature, rather than destroying it. Hence "order by disorder" [13, 25]. Notably, through this mechanism a coplanar order in the Heisenberg model on the Kagome lattice of corner sharing triangles is established [26]. In quantum systems, to which we now turn, a similar order by disorder phenomenon is possible, with the quantum fluctuations playing the role of thermal fluctuations in classical systems [13, 25].

In quantum systems the definition of frustration as a competition between terms in the Hamiltonian promoting different types of arrangement could be applied as well. In this sense, frustration could be of a purely quantum origin, because of the non-commutativity of different local terms in the Hamiltonian and the entaglement in the ground state [27, 28]. Some measures have also been introduced to distinguish this purely quantum contribution to frustration [29, 30]. However, to avoid calling

a large number of quantum phases frustrated, the term frustration in quantum systems is usually reserved for its classical origin, whether it comes from competing interactions or the lattice structure. Note that the notion of unfrustrated systems, in this sense, is different from the notion of frustration-free Hamiltonians [31], whose ground state minimizes all local terms.

Of quantum systems those with $SU(2)$-symmetric interactions typically receive the most of the attention. In such systems a notable quantum phase that can arise as a simple way to overcome frustration is the valence bond crystal phase, where the neighboring spins are paired into rotationally invariant singlets or "valence bonds". The system exhibts long-range order in these building blocks and no long-range order in spin-spin correlation functions [32, 33]. An example is the spin-1/2 Heisenberg model on the checkerboard lattice [34, 35]. An alternative phase that can arise in the presence of frustration is the resonating valence bond spin liquid phase, with different long distance properties and different magnetic excitations [32, 33]. In the spin-1/2 Heisenberg model on kagome and pyrochlore lattices, that have received a lot of theoretical attention, it is, for instance, still not completely clear which of the two phases is realized [32, 33]. Another model that has received a considerable attention, although the nature of its phase in the frustrated regime is not completely clarified yet, is the $J_1 - J_2$ Heisenberg model on the square lattice [33], where frustration is caused by competing nearest neighbor and next-to-nearest neighbor interactions. In this model several phenomena that are relevant for a wider class of two-dimensional frustrated quantum magnets have been discovered: classical degeneracy, destruction of long-range order by quantum fluctuations, break down of the spin-wave expansion, opening of a spin gap, order by disorder and possibly spontaneous translational symmetry breaking [33].

In one dimension, it is known that, even without frustration, quantum fluctuations can suppress magnetism and give rise to a variety of zero-temperature spin-liquid phases [36, 37], as in the exactly solvable antiferromagnetic Heisenberg chain [36–42]. Adding frustration, through competing nearest neighbor and next-to-nearest neighbor interactions, on top of it, can induce additional types of spin liquid phases with exotic properties [36]. For instance, the $J_1 - J_2$ Heisenberg chain exhibits a valence bond crystal phase, with incommensurate correlations and breaking of the lattice translation symmetry, through a spontaneous dimerization [33, 43–46]. The dimerization can be understood simply by considering the exactly solvable Majumdar-Ghosh point [47].

Frustration induces thus many exotic properties, both in classical and quantum systems. We have mentioned only the theoretical results, but there is many experimental results, motivating and confirming the theory [48–52]. For the end, let us mention the geometrical frustration in the context of the Ginzburg-Landau theory, a unifying theory of continuous phase transitions [53, 54]. The latter, justified by a microscopic averaging through a coarse-graining procedure [53], leads to the concept of universality [9, 53, 55]: Different physical systems exhibit the same critical behavior, irrespectively of the microscopic details, provided they have the same spatial dimension and order parameter symmetry. Geometrical frustration throws, in a sense, the antiferromagnets outside the range of validity of the theory, since it makes their properties strongly dependent on the lattice structure and, therefore, non-universal.

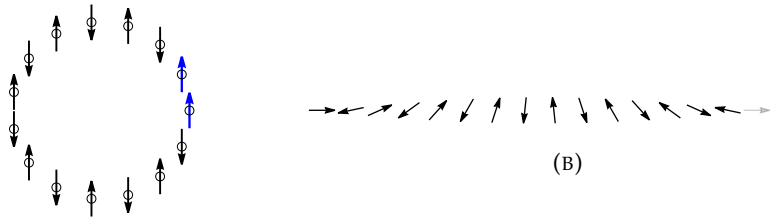

(A) (B)

FIGURE 1.2: Geometrical frustration arises if antiferromagnetically interacting spins are set on a ring with an odd number of sites. For classical Ising spins (a) the ground state configurations contain a ferromagnetic bond, while for classical Heisenberg spins (b) it is energetically more favorable to realize long-wavelength spin waves. We call the periodic boundary conditions with an odd number of sites *frustrated boundary conditions*, and the frustration arising from it in antiferromagnets *topological frustration*.

1.2 Topological Frustration

Geometrical frustration can be caused also simply by a choice of boundary conditions, i.e. by the lattice topology, in which case we term it *topological* frustration. For instance, a ring with an odd number of lattice sites is non-bipartite, which makes one-dimensional antiferromagnets in this setting frustrated. In this setting the spins cannot be aligned so that they all point oppositely from their nearest neighbors. This brings us to the topic of this thesis, one-dimensional quantum systems exactly in this setting, i.e. periodic boundary conditions with an odd number of lattice sites, that we term shortly *frustrated boundary conditions* (FBC). FBC are not the only setting inducing topological frustration in one dimension. For instance, antiperiodic, i.e. twisted, boundary conditions frustrate the ferromagnets, which can be often related to the setting that we study.

It is instructive to see how topological frustration arises in one-dimensional classical systems. For antiferromagnetic classical Ising spins-1/2 with FBC, described by the Hamitonian $H = \sum_{j=1}^{N} \sigma_j \sigma_{j+1}$, where the possible values are $\sigma_j = \pm 1$ and N is odd, the energy minimizing configuration has necessarily a ferromagnetic bond (see Figure 1.2) and the ground energy is $-N+2$. On the other hand, for classical Heisenberg or O(2) interactions, described by $H = \sum_{j=1}^{N} \mathbf{s}_j \cdot \mathbf{s}_{j+1}$ where $\mathbf{s}_j$ are unit vectors with three or two components respectively, it becomes energetically more favorable to tilt the spins and to form spin waves in the presence of frustration. To demonstrate this, let us focus on two components only. Each spin $\mathbf{s}_j$ can then be described by the angle θ_j with the x-axis, and the interactions can be written as $\mathbf{s}_j \cdot \mathbf{s}_{j+1} = \cos(\theta_{j+1} - \theta_j)$. Studying the first derivatives of the Hamiltonian with respect to the angles θ_j, it is easy to see that configurations that extremize the energy are those with a constant angle difference $\theta_{j+1} - \theta_j = q$ for all j. In these configurations, in order to account for the periodicity of the chain, the quantity Nq has to be necessarily a multiple of 2π. For even N the energy is minimized simply by $q = \frac{2\pi}{N}\frac{N}{2} = \pi$, describing Néel order $\mathbf{s}_{j+1} = -\mathbf{s}_j$. For odd N, however, the value $q = \pi$, and accordingly perfect Néel order, is not possible. The energy is minimized instead by the closest possible values, $q = \frac{2\pi}{N}\frac{N\pm 1}{2} = \pi \pm \pi/N$. The energy of these configurations is $N \cos q = -N + \pi^2/2N + O(N^{-3})$. It is, in particular, lower than the energy of the configurations with a single ferromagnetic bond, equal to $-N+2$. Denoting the unit vectors along x and y-axis by $\mathbf{e}_1$, $\mathbf{e}_2$, the spins in these ground state

configurations form a long-wavelength spin-wave

$$\mathbf{s}_j = (-1)^j \left[\cos\left(\frac{\pi}{N} j \pm \theta_N\right) \mathbf{e}_1 \pm \sin\left(\frac{\pi}{N} j \pm \theta_N\right) \mathbf{e}_2 \right]. \tag{1.1}$$

This configuration is shown in Figure 1.2, where it is assumed that the chain propagates in the direction that lies in the plane spanned by $\mathbf{e}_1$ and $\mathbf{e}_2$.

These simple classical examples illustrate the concept of topological frustration and the way it arises in one dimension. Naturally, the real question is what happens when quantum or thermal fluctuations are introduced. This thesis deals with the former, in one dimension.

The interest in the topologically frustrated quantum spin chains is three-fold. The first is along the line of interests in frustrated systems in general. Topological frustration, as we will see, also provides a way for evading the standard antiferromagnetic order and leads to new phases of matter, which can lead further to insights about general theories. Here, the insight is about the influence of the boundary conditions and the even/odd system size choice, which trigger topological frustration, on antiferromagnetic phases of matter. It is an important result of its own that these choices can have any significant effects in large systems with only local interactions.

Second, studying topological frustration in quantum chains might provide some insight on geometrical frustration in quantum systems in general, which is a field of research where getting exact results can be very hard. Clearly, the advantage of topologically frustrated spin chains is all the machinery that exists to deal with one-dimensional quantum systems [31, 37, 56].

Third, topologically frustrated spin chains are interesting physical systems on their own. One-dimensional systems are not anymore only a theorist's toy. There are now many experimental realizations of one-dimensional systems [37] and with cold atoms, for instance, it is possible to tailor various interactions [57–61]. Thus, a theoretically discovered property might be considered for the realization in the real world.

1.2.1 Older Results on Topological Frustration

A particularly notable result on topological frustration is a discovery from 1980s that topological frustration can affect the energy gap above the ground state [62, 63]. Namely, ferromagnetic quantum Ising chain with adjustable boundary conditions has been studied and it has been shown, analytically, that, with periodic and free boundary conditions the gap closes exponentially with the system size N, while with antiperiodic boundary conditions the gap closes only algebraically, as $1/N^2$. It is algebraic, but not like at criticality, where it closes as $1/N$. Note that with an odd number of sites the Ising ferromagnet with antiperiodic boundary conditions is equivalent, through a direct unitary mapping, to the Ising antiferromagnet with periodic boundary conditions, i.e. FBC, a setting that is the focus of this thesis. The authors suggest that these puzzling discovered phenomena are associated with topological excitations. In the same papers, also other boundary conditions, parametrized by the interaction strength at a single bond in the system, have been addressed numerically and it has been found that antiperiodic boundary conditions are a transition point, between algebraic and exponential closing of the gap. Soon afterwards, these results have been recovered analytically using random walk and perturbation theoretic arguments [64]. Influenced by these works, it has also been discovered soon that the transfer matrix mass gap of the classical two-dimensional

Ising model on a square lattice also depending on the boundary conditions vanishes exponentially or algebraically [65].

Essentially the same problem of the energy gap in the Ising chain was revisited, in a different form, more recently [66]. In agreement with the previous works, it has been shown that the gap in the antiferromagnetic Ising chain with periodic boundary conditions closes exponentially or algebraically, depending on whether we follow even ($N = 2M$) or odd system sizes ($N = 2M + 1$), corresponding to FBC, respectively towards infinity ($M \to \infty$). This work was motivated by the quantum adiabatic algorithm, for which the implications of a possibility of only an algebraically small gap have been discussed.

A few years later, the problem of the dependence of the gap in the Ising chain with adjustable boundary conditions, i.e. a one bond defect, has been revisited in [67]. It has been discussed how a bond defect can drive a quantum phase transition from a magnet phase, in which the gap closes exponentially, to a kink phase, in which the gap instead closes algebraically. Furthermore, a universal scaling behavior has been discovered close to the transition point. Namely, the theory of a finite size scaling at first-order quantum phase transitions [68], that would here be driven by the external magnetic field in the direction of the order parameter spin operator, has been applied. The scaling functions for the low-level energy differences and the two-point correlation function have been computed, from which the universal behavior has been inferred. A similar phenomenology can also be induced by two local magnetic fields at the boundaries of an open chain, that are aligned with the order parameter spin operator and point in the opposite directions [69], therefore inducing frustration. Increasing the strength of the boundary fields the system goes from a magnetic phase, where the gap closes exponentially, to a kink phase, where the gap closes algebraically, and close to the transition the low energy properties show a universal scaling behavior. Let us note that the algebraic closing of the gap has also been discovered in the quantum XY chain in a transverse field with FBC [70].

It should be noticed that in all these examples the presence of frustration in the spin chain is accompanied by an algebraic gap above the ground state, while the absence of frustration comes with an exponentially small gap. In fact, in the case of the exponentially small gap, the system can be considered gapped, since above the two lowest energy states, which can be considered quasi-degenerate, there is a finite gap, that does not close in the thermodynamic limit. On the other hand, in the case of algebraic gap the two lowest energy states are a part of the band, with a macroscopic number of states, in which the energy gap between the states closes in the thermodynamic limit. In the presence of frustration, the system is therefore gapless. The frustration in these examples, thus, turns the behavior of the system from gapped to gapless. We note that gapless excitations in the presence of frustration are not relativistic and are, thus, different from criticality.

The two-point correlation functions of order parameter spin operators have been studied in more details in [71], in the context of the quantum Ising chain with FBC. Together with [67], the result establishes that correlations in the ground state acquire a peculiar correction, with respect to the unfrustrated case, at distances comparable to the system size N. For two spins separated by a large distance r, the correction is the factor $(1 - 2r/N)$, implying that the correlations of the most distant spins on the ring, separated by distance $r = (N - 1)/2$, for a unit cell of size unity, vanish as $1/N$. However, letting first the system size to infinity and then looking at correlations the effects of topological frustration in the spin-correlation functions are destroyed. As shown in [72], the same behavior of the spin-correlation functions is

also a property of the whole lowest energy band of the model, with consequences to the low-temperature behavior. Note that, although the final result of [71, 72] is correct, there are some issues with the analytical content of the asymptotic analysis, as we comment in Chapter 9.

The entanglement entropy in the ground state of the same model, with generalizations to XYZ chain in a transverse field, is also found to differ from the unfrustrated model, when, in the bipartition of the system, the sizes of both subsystems are comparable to the system size [73]. The entanglement entropy violates the area law, while not diverging with the system size. Its behavior is well fitted by a universal law, derived from a conjectured single-particle picture.

The aforementioned results deal with systems out of criticality, but there are also some results for critical systems. Different proportionality constant with different boundary conditions has been discovered in the closing of the gap of the quantum Ising chain at a critical field [74]. In XXZ chain some finite-size effects related to FBC have been discovered [75]. Furthermore, it has been shown that in several critical spin chains a difference between even and odd antiferromagnetic rings arises in spin correlation functions at distances comparable to the system size [76]. Finally, let us mention that FBC have been recognized to be special in the antiferromagnetic Heisenberg chain, even before all these results [38].

Summarizing the older results discussed in this section, we conclude that topological frustration closes the gap above the ground state, by making it algebraic yet different from criticality, it suppresses the ground state spin-correlation functions at distances comparable to the system size and induces corrections to the entanglement entropy.

1.2.2 Non-Equilibrium Dynamics

Since the topological frustration closes the gap above the ground state, it is natural to expect its influence on the non-equilibrium dynamics of the system. For instance, as recognized in [67], the size dependence of the spectral gap determines the conditions for the nearly adiabatic quantum dynamics [77, 78] so topological frustration is relevant in this context. We are going to deal, in Chapter 2, with the consequences for the quantum quench protocol [78–81], perhaps the simplest and most widely studied way to bring the system out of equilibrium.

1.2.3 Spontaneous Symmetry Breaking

The primary goal of this thesis is to discuss whether and how topological frustration can affect the order parameter of antiferromagnetic phases, i.e. the (staggered) magnetization. In one dimension, the ground states of quantum systems with continuous symmetries are disordered, according to the quantum analog of the Mermin-Wagner theorem [11, 82–85]. Thus, we study how topological frustration affects the antiferromagnetic order in quantum spin chains with discrete symmetries, whose breaking is related to the onset of the order. In this section we cover different approaches for studying symmetry breaking in such systems, and compare the frustrated and unfrustrated case.

Ground State Degeneracy in the Thermodynamic Limit

The first symmetry breaking framework we cover is based on the realization that although the ground state might be single, and therefore respecting the symmetries

of the Hamiltonian, in the thermodynamic limit there might be the ground state degeneracy.

Let us focus on the quantum Ising chain [10, 86], the prototype model for quantum phase transitions, given by the Hamiltonian

$$H_0 = J \sum_{j=1}^{N} \sigma_j^x \sigma_{j+1}^x + h \sum_{j=1}^{N} \sigma_j^z. \tag{1.2}$$

Here σ_j^α, for $\alpha = x, y, z$, are Pauli matrices with support at site j, N is the system size and periodic boundary conditions $\sigma_{j+N}^\alpha = \sigma_j^\alpha$ are imposed. The spins interact ferromagnetically (antiferromagnetically) for $J = -1$ ($J = 1$) and are subject to a transverse field h. The Hamiltonian commutes with the parity operator $\Pi^z \equiv \bigotimes_{j=1}^{N} \sigma_j^z$, which constitutes the Z_2 symmetry of the model. The spontaneous breaking of this symmetry is associated to the existence of the non-vanishing order parameter, the longitudinal magnetization $\langle \sigma_j^x \rangle$ in the ground state. Note that when N is even the ferromagnet $J = -1$ and antiferromagnet $J = 1$ are related by a unitary transformation $\sigma_j^x \to (-1)^j \sigma_j^x$, that consist of rotating every other spin around the z-axis by an angle π, while for odd N there is no such unitary transformation.

Let us first examine the unfrustrated case, focusing on the antiferromagnet $J = 1$ and even N, while the ferromagnet has analogous phenomenology, of course. From the exact solution by mapping to free fermions [10, 56, 86], it is known that at $h = 1$ the model exhibits a quantum phase transition from the ordered magnetic phase at $h \in (0, 1)$, with non-zero value of the ground state magnetization, to the paramagnetic phase $h > 1$, with zero magnetization. In a finite system there is no symmetry breaking. The ground state is single, with a definite Π^z parity and, therefore, zero magnetization. However, in the magnetic phase, the first excited state, that carries opposite Π^z parity, is separated by an energy gap that is exponentially small in N. This quasi-degeneracy becomes exact in the thermodynamic limit, which makes it possible to form ground state superpositions, that break Π^z parity and have a non-zero magnetization. For $h \to 0$ these superpositions correspond to the states $|g_1\rangle \equiv |+-+-\ldots+-\rangle$ and $|g_2\rangle \equiv \Pi^z |g_1\rangle = |-+-+\ldots-+\rangle$, where by $|\pm\rangle$ we denote the eigenstate of σ^x with the eigenvalue ± 1. The same phenomenology arises in the antiferromagnet with free boundary conditions. This illustrates the symmetry breaking mechanism based on the ground state degeneracy in the thermodynamic limit.

The exact value of the magnetization is [56, 86]

$$\langle \sigma_j^x \rangle_{g_1} = (-1)^{j+1} (1 - h^2)^{1/8}. \tag{1.3}$$

Typically, this value is inferred from the spin-correlation functions $\langle \sigma_j^x \sigma_{j+r}^x \rangle$ at large distances r, using the cluster decomposition principle [11, 87, 88]

$$\lim_{r \to \infty} \left(\langle \sigma_j^x \sigma_{j+r}^x \rangle - \langle \sigma_j^x \rangle \langle \sigma_{j+r}^x \rangle \right) = 0, \tag{1.4}$$

but a direct computation has also been performed [89]. The phenomenology in the model with free boundary conditions is the same [86, 90].

Now let us examine the odd N case. From the works [62–64, 66, 67] mentioned in section 1.2.1 it is known that, while there are no effects of frustration in the paramagnetic phase, in the magnetic phase the energy gap above the ground state now closes algebraically as $1/N^2$, instead of exponentially as without frustration. Moreover, the

ground state is now a part of a band of states and the system is gapless. This can be understood simply from the lowest-order perturbation theory in h. Let us assume thus that $0 \ll h \ll 1$ and apply the perturbation theory.

At the classical point $h = 0$ the ground-state manifold is $2N$-fold degenerate, corresponding to N different positions where the ferromagnetic bond can be placed and two different orientations of the spins. The ground state energy is equal to $-N + 2$, because of the presence of a ferromagnetic bond. We call these ground states the kink states. Let us denote by $|j\rangle$, for $j = 1, 2, \ldots, N$, the kink state with the ferromagnetic bond $\sigma_j^x = \sigma_{j+1}^x = 1$ and the remaining bonds antiferromagnetic. The other kink states, with the ferromagnetic bond $\sigma_j^x = \sigma_{j+1}^x = -1$ and the remaining bonds antiferromagnetic, can then be written as $\Pi^z |j\rangle$.

Turning on a small positive magnetic field h, the translationally invariant Π^z-symmetric states split in energy. These are the states

$$|q, \pm\rangle = \frac{1 \pm \Pi^z}{\sqrt{2N}} \sum_{j=1}^{N} e^{iqj} |j\rangle , \tag{1.5}$$

where the momentum q can assume any value from the set $\{2\pi k/N : k = 0, 1, \ldots, N-1\}$, and their parity is $\Pi^z = \pm 1$. Their energies are obtained by diagonalizing the perturbation, as presented in Appendix A, and are given by

$$E_{q,\pm} = -(N-2) \pm 2h \cos q. \tag{1.6}$$

The ground state, in particular, is given by $|g\rangle \equiv |0, -\rangle$ and it is single. The energy gap above the ground state does not close exponentially with N, as without frustration, but only algebraically as $1/N^2$.

The ground state being single, there is no magnetization. From the perturbation theory, as presented in Appendix A, we obtain the spin correlation functions

$$\langle \sigma_j^x \sigma_{j+r}^x \rangle_g = (-1)^r \Big(1 - \frac{2r}{N}\Big). \tag{1.7}$$

For most distant spins on the ring, separated by $r = (N-1)/2$, we have $\langle \sigma_j^x \sigma_{j+r}^x \rangle \sim 1/N$ so the correlations vanish in the infinite system. Interestingly, this is in agreement with the value of the magnetization and the cluster decomposition principle. The exact results do not change this picture [71, 73].

However, there are important differences from the paramagnetic phase. Here, in the double scaling limit $1 \ll r \ll N$ the spin-correlations acquire the same, non-zero, value as without frustration. Furthermore, the system is gapless and, as discussed in the next section, by introducing symmetry breaking fields in the Hamiltonian it is possible to select the ordered ground states.

Symmetry Breaking Fields

Another way to study order parameters is to introduce symmetry breaking fields, aligned with the order parameter spin operator, and let them to zero after the thermodynamic limit [11]. Adding symmetry breaking fields to the Hamiltonian (1.2) we get the Hamiltonian

$$H = H_0 + \sum_{j=1}^{N} \lambda_j \sigma_j^x, \tag{1.8}$$

where λ_j specify the value of the field at different sites. The ground state $|g\rangle$ of H is now, in general, single and exhibits non-zero magnetization.

Let us focus first on the unfrustrated case, the antiferromagnet with N even, in particular. Although the model (1.8) is not anymore exactly solvable, it is easy to understand, using perturbation theory in λ, that taking the staggered field

$$\lambda_j = (-1)^{j+1}\lambda \tag{1.9}$$

results in the spontaneous magnetization

$$\lim_{\lambda\to 0^{\pm}} \lim_{N\to\infty} \langle \sigma_j^x \rangle = \pm(-1)^j (1-h^2)^{1/8}, \tag{1.10}$$

for $h \in (0,1)$. The staggered field, out of the two-fold degenerate ground state manifold in the thermodynamic limit, simply selects the state with the antiferromagnetic order that minimizes the energy. This is what constitutes the symmetry breaking framework based on symmetry breaking fields. Note also that the opposite sign of λ yields the magnetization of the opposite sign, so the line $h \in (0,1)$, $\lambda = 0$, represents the first-order quantum phase transition.

For odd N there is, actually, an ambiguity with the staggered field. As the magnetization in the classical ground states, the staggered field cannot be completely staggered, but one bond is necessarily singled out where two neighboring fields are equal. The notation (1.9), in particular, selects this to be the bond between the sites $j = 1$ and $j = N$, where $\lambda_1 = \lambda_N$. The staggered field thus breaks the translational invariance. In this case, due to the gapless nature of the frustrated system without symmetry breaking fields, the perturbation theory in λ is a complicated problem. Still, a simple perturbation theory in h can be performed, telling us that, for $0 \ll h \ll 1$, one of the two classical Néel states, $|-+-\ldots+-\rangle$ or $|+-+\ldots-+\rangle$, depending on the sign of λ, is the ground state $|g\rangle$. The magnetization is thus expected to be the same as in the unfrustrated case, except for a single ferromagnetic bond that breaks the translational invariance.

If we decide to break the translational invariance, we can also consider other symmetry breaking terms. We can even consider a local symmetry breaking field, present only at site $j = N$,

$$\lambda_j = \delta_{j,N}\lambda. \tag{1.11}$$

For even N, it's easy to understand using perturbation theory in λ, that even this local symmetry breaking term will select the same antiferromagnetic order as the global staggered field, described by (1.10).

For odd N, however, the situation is much more complicated. Again, we can resort to the perturbation theory in h. For $h = 0$ there are N ground states, which are the kink states that have $\sigma_N^x = -1$ for $\lambda > 0$ and $\sigma_N^x = 1$ for $\lambda < 0$. Turning on a small positive h the degeneracy is lifted. The new ground state is obtained by diagonalizing the perturbation in the subspace spanned by the aforementioned N kink states, as done in Appendix A. We find that the ground state is single and the system is gapless, with the energy gap above the ground state closing as $1/N^2$. The magnetization in the ground state is for $\lambda > 0$ given by

$$\langle \sigma_j^x \rangle_g = (-1)^{j+1} \left\{ 1 - \frac{2}{N+1}\left(j+\frac{1}{2}\right) + \frac{1}{(N+1)\sin\left(\frac{\pi}{N+1}\right)} \sin\left[\frac{2\pi}{N+1}\left(j+\frac{1}{2}\right)\right] \right\}, \tag{1.12}$$

while for $\lambda < 0$ the sign is opposite. It is presented in Figure 1.3. Note that the

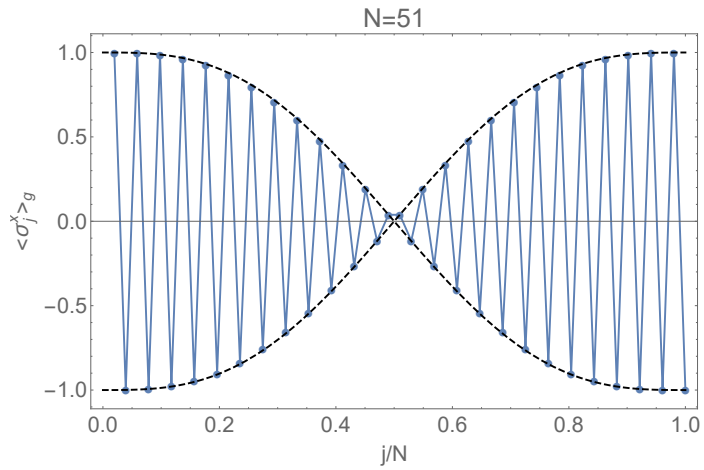

FIGURE 1.3: The ground state magnetization (1.12) at different sites of the lattice of $N = 51$ spins, for the quantum Ising chain with a local symmetry breaking field, obtained from a perturbative approach. The magnetization, represented by blue circles, joined to guide the eye, is staggered, but modulated over the ring. The modulation is in a large system described by the functions $\pm(1 - 2x + \sin(2\pi x)/\pi)$, for $x = j/N$, represented by the dashed lines.

magnetization respects the mirror symmetry around site N, where the local field is placed. The magnetization is staggered, but does not represent the standard simple antiferromagnetic order. For $N \gg 1$ we have

$$\langle \sigma_j^x \rangle_g = (-1)^{j+1} \left[1 - \frac{2j}{N} + \frac{1}{\pi} \sin\left(\frac{2\pi j}{N} \right) \right] + O(N^{-1}), \tag{1.13}$$

where we can see that the magnetization is modulated over the ring, by functions $\pm(1 - 2x + \sin(2\pi x)/\pi)$, for $x = j/N$. The modulation is such that the maximal absolute value of the magnetization is at the site $j = N$, where the field is placed, while the minimal value, of order $1/N$, is at the diametrically opposed bond on the ring, reflecting the mirror symmetry of the Hamiltonian around the site where the symmetry breaking field is localized. Note that the modulated antiferromagnetic order discovered here is similar to the one that we have discovered in the exactly solvable quantum XY chain with FBC [2], that will be the subject of Chapter 4.

The point of the presented perturbative calculation is to notice how in the presence of topological frustration the notion of taking the thermodynamic limit and afterwards computing the quantities of interest might be ambiguous. With a local symmetry breaking field the ground state magnetization with FBC is site-dependent, and, although locally antiferromagnetic, it takes different values at different parts of the ring. Focusing on different parts of the ring and letting the system size to infinity would yield different information about the system. The presented system has to be considered as a whole.

We have considered a global staggered symmetry breaking field and a local one, present at a single site. With FBC they yield different behavior of the magnetization, and taking other configurations of symmetry breaking fields could yield results different from both. Due to large classical ground state degeneracy different perturbations to the classical Hamiltonian select different states with different properties. The sensitivity to perturbations due to large ground state degeneracy, discovered here, is, in fact, a common property in frustrated magnetism [25].

Ground State Degeneracy due to Anticommuting Symmetries

There is also another approach to symmetry breaking, that we have discovered in [1] in the context of the XYZ chain. It does not work for the the discussed quantum Ising chain, but works for a large class of spin chains in the absence of external magnetic fields.

Let us consider the Hamiltonian

$$H = \sum_{(j,l)} (J^x_{j,l}\sigma^x_j\sigma^x_l + J^y_{j,l}\sigma^y_j\sigma^y_l + J^z_{j,l}\sigma^z_j\sigma^z_l), \tag{1.14}$$

where the couplings $J^\alpha_{j,l}$, for $\alpha = x, y, z$, describe the interactions of spin components α between the sites j and l, and the sum is over all distinct pairs of j and l. For instance, in one-dimension the XYZ chain [56] is the special case $J^\alpha_{j,l} = J^\alpha \delta_{|j-l|,1}$, and the XY chain [56, 91] has further $J^z = 0$.

We recognize that Hamiltonian (1.14) commutes with each of the parity operators $\Pi^\alpha = \bigotimes_{j=1}^N \sigma^\alpha_j$, for $\alpha = x, y, z$, where N is the system size ($[H, \Pi^\alpha] = 0$). This expresses the fact that the Hamiltonian is invariant under the transformation $\sigma^\alpha_j \to -\sigma^\alpha_j \ \forall j$, for each choice of α. Crucially, we also recognize that, irrespectively of the values of the couplings and the lattice geometry, we have the following property. While different parity operators commute when N is even ($\left[\Pi^\alpha, \Pi^\beta\right] = 0$ for $N = 2M$), when N is odd different parity operators anticommute ($\left\{\Pi^\alpha, \Pi^\beta\right\} = 2\delta_{\alpha,\beta}$ for $N = 2M + 1$).

These properties have an important consequence on the structure of the Hamiltonian eigenstates when N is odd. The consequence is that, in this case, every eigenstate is at least two-fold degenerate. Namely, suppose we diagonalize the Hamiltonian simultaneously with Π^z, and let $|\psi\rangle$ be the simultaneous eigenstate, with $\Pi^z = 1$ and some energy. Since different parity operators anticommute, the state $\Pi^x |\psi\rangle$ (or $\Pi^y |\psi\rangle$) is also an eigenstate of the Hamiltonian, with the same energy, but with $\Pi^z = -1$. The states $|\psi\rangle$ and $\Pi^x |\psi\rangle$ have, thus, the same energy but are orthogonal. The same conclusion holds also for more general Hamiltonians than the one in (1.14), when they possess the discussed symmetries.

The ground state manifold, in particular, is at least two-fold degenerate. Furthermore, for each ground state choice there is a parity symmetry that is broken and for each parity symmetry of the Hamiltonian there is a ground state that breaks it. Magnetization is, thus, in general, non-zero already in a finite system. For instance, an eigenstate of Π^x breaks the Π^z symmetry and can exhibit a non-zero expectation value of σ^x_j. Thus, as with the symmetry breaking fields, the magnetization can, in principle, be computed in a finite system and followed towards the thermodynamic limit ($N = 2M + 1, M \to \infty$). However, in this approach no other limits are required after the thermodynamic limit to discuss the order parameter and, as we will see, in some exactly solvable models this approach is also suitable for analytical computations. In this thesis we work within this symmetry breaking framework to discuss the influence of topological frustration on the order parameter. Since the frustration inducing setting on which we focus are periodic boundary conditions with an odd number of lattice sites, the requirement for odd N is satisfied automatically.

1.2.4 Boundary Conditions and Local Order

Since topological frustration is triggered by a choice of boundary conditions, which typically, quite in agreement with intuition, do not influence the bulk, macroscopic,

properties of the system, it is not obvious at all that topological frustration can have any such effects. We would like to comment here topological frustration in this context.

Let us first note that, although boundary conditions typically do not influence the bulk properties of the system, there are known exceptions. It has been discovered that the free energy (density) of the six-vertex model takes different values depending on whether periodic or domain-wall boundary conditions are imposed [92]. Furthermore, it is known that this difference is intimately related to the appearance of a macroscopic phase separation in real space when domain-wall boundary conditions are imposed. The latter allow only ordered configurations close to the boundaries and, due to strong correlations, induce ordered regions extending macroscopically from the boundaries, that are sharply separated by the so-called arctic curve from a central, also macroscopic, disordered region [93–98]. A similar phenomenon of a phase separation due to boundary conditions appears also in other tilling problems [99–104].

That being said, we recognize that tilling problems and fixed boundary conditions seem a rather special from the point of view of the influence of the boundaries. For systems with local interactions, such as Ising or Heisenberg, it can indeed be proven rigorously that boundary conditions, such as free or periodic, do not influence the free energy in the thermodynamic limit. Let us focus on a quantum system of N spins. If the system is described by the Hamiltonian H then the free energy is given by

$$f = -\frac{1}{N\beta}\mathrm{Tr}\left(e^{-\beta H}\right), \tag{1.15}$$

where β is the inverse temperature. A different Hamiltonian results, naturally, in a different value of the free energy. For two different Hamiltonians, H_1 and H_2, describing interactions in such a system, it can be shown [105, 106] that the corresponding free energies, denoted by f_1 and f_2, satisfy the bound

$$|f_1 - f_2| \leq \frac{1}{N}\left\|H_1 - H_2\right\|. \tag{1.16}$$

In fact, the relation holds for any Hermitian operators H_1 and H_2 acting on the same, finite-dimensional, vector space. Note that at zero temperature, i.e. $\beta = +\infty$, where the free energy is given simply by the ground state energy, the same bound holds, and is, in fact, more immediate. Now, if the two local Hamiltonians differ only by boundary conditions, such as free or periodic, then the norm of the difference, $\|H_1 - H_2\|$, is $O(1)$ as $N \to \infty$. It follows from (1.16) that the difference between the free energies vanishes in the thermodynamic limit $N \to \infty$. Boundary conditions thus do not influence the free energy. A similar argument can be used to show that even and odd system sizes cannot have a different thermodynamic limit for the free energy. Classical Hamiltonians can be dealt with using similar methods [105, 106]. We conclude that topological frustration cannot affect the free energy in the thermodynamic limit.

For this reason we might expect that topological frustration cannot affect the bulk, local, order. In the end, in Landau symmetry breaking theory [11, 54, 107, 108], or more generally the Ginzburg-Landau theory [53, 54], the free energy is the fundamental quantity. The value of the order parameter is the one that minimizes the free energy. And although the Landau theory was originally developed for classical systems and some quantum phases violate it, as the topological ones, the theory has still been widely successful in the quantum regime [109].

Leaving aside the question whether boundary conditions can influence the order in other classical models, let us claim that, at least in the quantum case, the free energy alone does not contain sufficient information to discuss order parameters. For instance, we have seen that a local symmetry breaking field, which does not contribute to the free energy in the thermodynamic limit, in the unfrustrated antiferromagnet introduces the energy splitting between two different antiferromagnetic states. The sign of such a field determines the sign of the staggered magnetization in the ground state. Moreover, we have seen that such a local field can result in a different kind of ground state order between the frustrated and unfrustrated case. Local contributions to the Hamiltonian are not negligible and their details can carry important information. Thus, the property that boundary conditions do not influence the free energy does not preclude their influence on the order in the ground state.

1.3 Organization of the Thesis and Main Results

This thesis presents the work the author of the thesis has done during his PhD with his collaborators from the Ruđer Bošković Institute in Zagreb. The thesis is based on the publications, and papers still under evaluation, related to this work. The contribution of the author in these works is the majority of the analytical computations and the participation in the writing, while the author acknowledges his collaborators for the majority of numerical work and the creation of the majority of figures. One chapter of the thesis is devoted to each paper. While this introductory chapter has presented a general motivation for studying topological frustration, we give separate introductions for different chapters, and in each chapter we make conclusions. We end the main part of the thesis by a general conclusion. After the conclusion there are different appendices, referenced in different chapters, that give the details of the calculations done in the thesis. The main results, chapter by chapter, are the following.

- In Chapter 2 we exploit the property that topological frustration closes the gap above the ground state to construct a quantum quench protocol in which the Loschmidt echo displays different features, qualitatively and quantitatively, for antiferromagnetic rings with even and odd number of sites. The emphasis is on the quantum Ising chain, but we argue that the phenomenology is general. This chapter is based on [8].

- In Chapter 3 we study the quantum XYZ chain with FBC, within the symmetry breaking framework based on anticommuting symmetries. The leading interaction in the model is set to be antiferromagnetic, and the other ones ferromagnetic. It is shown that topological frustration destroys local order. The emphasis is on the quantum XY chain, where we are able to compute all the quantities of interest analytically. This chapter is based on [1].

- In Chapter 4 we study the transition in the quantum XY chain when also the subdominant interaction becomes antiferromagnetic. It is thus discovered that topological frustration can induce a quantum phase transition. The incommensurate antiferromagnetic order, characterized by a site-dependent magnetization modulated over the ring, is discovered here. This chapter is based [2].

- In Chapter 5 we study the effects of defects, that break translational invariance, on the orders discovered in the quantum XY with FBC in the previous chapters. It is shown that, depending on the type of defects, the incommensurate antiferomagnetic order can survive their presence. This chapter is based on [4].

- In Chapter 6, using perturbative arguments, we study more general models within the symmetry framework based on anticommuting symmetries. It is shown that the vanishing of the local order and the appearance of the incommensurate antiferromagnetic order are phenomena that go beyond the specific models studied previously, and it is discussed how the momentum of the degenerate ground states determines which possibility occurs. This chapter is based on [6].

- In Chapter 7, by studying the exactly solvable 2-Cluster Ising model, we demonstrate that topological frustration can destroy local order at both sides of a quantum phase transition. The transition can then be characterized only by non-local quantities, so topological frustration has modified its nature. This chapter is based on [7].

- In Chapter 8, motivated by the discovered effects of topological frustration on magnetic phases, we examine several models exhibiting symmetry protected topological order. The results suggest that symmetry protected topological phases of one dimensional systems are not affected by topological frustration. This chapter is based on [5].

- The Chapter 9 is a mathematical part of the thesis, where we derive the asymptotic formulas for determinants of large Toeplitz matrices whose symbols posses a part proportional to a delta function. This is the type of determinants that appears in studying the order parameters of topologically frustrated spin chains mappable to free fermions. This chapter is based on [3].

Chapter 2

An Odd Thermodynamic Limit for the Loschmidt Echo

It has been known [62–64, 66] that topologically frustrated spin chains are gapless (see also Chapter 1). In this chapter we exploit this property to construct a (local) quantum quench protocol in which the Loschmidt echo displays different features, qualitatively and quantitatively, for the antiferromagnetic rings with even and odd number of lattice sites. Consequently, measuring the Loschmidt echo in an experiment would enable distinguishing antiferromagnetic rings made of N and $N+1$ spins, for arbitrarily large N. We employ the prototypical quantum Ising chain to illustrate this phenomenology, and argue that it is general for antiferromagnetic spin rings. This chapter is based on [8].

2.1 Introduction

Quantum dynamics has been a very active field of research in the new century. A sufficiently weak system-environment coupling has been achieved with ultra-cold atoms on optical lattices [110–112], enabling us to perform reliable experiments on the unitary dynamics of closed quantum systems. Stimulated by the experimental progress, the theoretical questions about relaxation and the presence or absence of thermalization [81, 113–116] have been studied intensively. Perhaps the most widely studied, and the simplest, way of bringing a system out of equilibrium is the *quantum quench* protocol [78–81]. Here, the system is prepared in the ground state of an initial Hamiltonian and it is let suddenly to exhibit a unitary evolution governed by a different Hamiltonian, obtained, for example, by changing suddenly a Hamiltonian parameter, such as the magnetic field.

Developments in quantum dynamics have lead to conceptual advancements in the foundations of statistical mechanics [117–120] and, furthermore, older concepts, such as the quantum phase transition [10], have received their characterizations in terms of dynamic quantities. Quantum phase transitions are defined as points of the non-analyticity of the ground state energy, and are accompanied by the gapless energy spectrum and the change in the behavior of the order parameter [10]. In a dynamical setting, there is, for instance, evidence [121] that order parameters are best enhanced for quenches in the vicinity of quantum critical points. However, even a more basic quantity, the Loschmidt echo (LE) [122, 123] has been proposed to be used as a witness of quantum criticality [124].

The Loschmidt echo $\mathcal{L}(t)$ is defined as the squared absolute value of the overlap between the initial and the evolved state at time t. Namely, suppose that the system is prepared in the ground state $|g\rangle$ of the initial Hamiltonian H_0, and then, suddenly, at $t = 0$, it is left to evolve unitarily by Hamiltonian H_1. The LE can then be defined

as

$$\mathcal{L}(t) = \left| \langle g | \, e^{-\imath H_1 t} \, | g \rangle \right|^2 . \tag{2.1}$$

It is a quantity related also to the work probability distribution function [125, 126]. Following the initial work [124], a substantial evidence [127–135] has been collected that the LE of quenches to quantum criticality is characterized by an enhanced decay and periodic revivals, although there are known exceptions [136]. Importantly, LE can be experimentally measured by coupling the system of interest to an auxiliray two-level system, where the LE is the measure of the decoherence of the auxiliary system [122, 124, 129, 137].

Here we show that the Loschmidt echo can be used to distinguish an antiferromagnetic spin-1/2 ring consisting of N elements from the one consisting from a single additional element, i.e. of total $N+1$ elements, for arbitrarily large N. It is known that in such systems, depending on whether we follow the even or odd system sizes towards the thermodynamic limit, the energy spectrum is gapped or gapless respectively [62–64, 66] (see also Chapter 1), due to the presence of topological frustration for odd N. Thus, similarly as bringing the system to criticality, topological frustration closes its spectral gap, although the gapless excitations in frustrated chains are not relativistic. We exploit the spectral differences for even and odd N to construct a (local) quantum quench protocol in which the LE displays different features, qualitatively and quantitatively, for the two cases. Consequently, measuring the LE in an experiment would enable distinguishing systems made of N and $N+1$ spins, for arbitrarily large N.

2.2 Results

2.2.1 General argument

A deeper insight in the time behavior of the LE can be obtained by expanding the initial state in terms of the eigenstates $|n\rangle$ of the perturbed Hamiltonian H_1:

$$\mathcal{L}(t) = \left| \sum_n e^{-\imath E_n t} |c_n|^2 \right|^2 , \qquad c_n = \langle n | g \rangle \, . \tag{2.2}$$

In the general (nontrivial) case, the state $|g\rangle$ is not an eigenstate of the Hamiltonian H_1 and thus several coefficients c_n assume a non-vanishing value and the time evolution of the LE depends on their relative weights. Roughly speaking, we can arrange the possible behaviors into two large families. The first is made of the cases in which one of the coefficients is much greater, in absolute value, than the sum of all the others. As a consequence, denoting by $|0\rangle$ the eigenstate of H_1 for which c_n reaches the maximum, from eq. (2.2) we recover that the LE will be characterized by oscillations with an average value close to the identity and oscillation amplitudes bounded from above by $(1 - |c_0|^2)|c_0|^2$. On the other hand, if none of the c_n dominates over the others, we can obtain an evolution characterized by a more complex pattern with larger oscillation amplitudes.

These two prototypical behaviors for the LE are generally associated with different properties of the physical systems [138, 139]. For example, the first trend type characterizes systems in which H_0 shows an energy gap that separates the ground state from the set of the excited states [128, 129]. Let us consider a quench with $H_1 = H_0 + \lambda H_p$, where λ is the parameter whose non-zero value brings the system

out of equilibrium and the eigenvalues of H_p are of the order of unity [123, 140]. In this case, assuming that λ is much smaller than the energy gap, the coefficient $\langle g_1|g\rangle$, where $|g_1\rangle$ is the ground state of H_1, is expected to be much larger than all the others. Consequently, LE is expected to display the dynamics of the first kind. On the other side, for systems in which the ground state of H_0 is a part of a narrow band that, in the thermodynamic limit, tends to a continuous spectrum, as at quantum criticality, the perturbation λH_p may induce a non-negligible population in several low-energy excited states [141], resulting in the time evolution of the second kind.

Typically, these different spectrum properties do not turn into one another by changing the number of elements that make up the system. Indeed, the presence or the absence of the gap in the energy spectrum is related to the different symmetries of the Hamiltonian, which are, usually, size-independent. Hence, keeping all other parameters fixed and increasing the number of elements, we expect the same kind of time-evolution, with finite-size effects that reduce with the system size up to some point at which the dependence of the LE on the number of constituents is almost undetectable. To have a LE evolution that changes as the number of elements turns from even to odd and vice-versa, we need a system in which also the shape of the energy spectrum is strongly dependent on it.

However, as we have seen in Chapter 1, while the antiferromagnetic rings with an even number of lattice sites ($N = 2M$, $M \to \infty$) are gapped, those with an odd number of lattice sites ($N = 2M + 1$, $M \to \infty$) are, due to topological frustration, gapless [62–64, 66], with the ground state being a part of a narrow band of states. Hence the properties of the spectral gap depend dramatically on whether the size of the system is an even or odd number.

However, this property alone is not sufficient to ensure a dependence of the dynamics of the LE on the size of the system like the one we are looking for. The perturbation that acts on the initial Hamiltonian must also be chosen carefully. On the one hand, as the states in the lowest energy band of the frustrated system are identified by different quantum numbers (namely, their momenta), the perturbation should break the symmetry these numbers reflect, to ensure that the eigenstates of the perturbed Hamiltonian can have a finite overlap in the whole band (otherwise, we expect that the initial state would overlap only with states carrying the same quantum number). On the other hand, in the unfrustrated system we want that the ground state of the unperturbed Hamitonian has a significant overlap only with one of the eigenstates of the perturbed Hamiltonian, to have a simple evolution of the first kind. The unfrustrated system in a symmetry broken phase has an (asymptotically) degenerate ground state manifold. We want the perturbation to preserve the symmetry of the Hamiltonian not to mix different ground states.

2.2.2 Quantum Ising chain

To clarify these arguments and to provide a specific example, let us discuss a paradigmatic model, i.e. the antiferromagnetic Ising chain in a transverse magnetic field with periodic boundary conditions [10, 56, 86]. This well-known model is described by the Hamiltonian

$$H_0 = \sum_{j=1}^{N} \left(\sigma_j^x \sigma_{j+1}^x + h\sigma_j^z \right). \tag{2.3}$$

Here σ_j^α with $\alpha = x, y, z$ stands for the Pauli operators defined on the j-th lattice site, h is the relative weight of the local transverse field, N is the length of the ring and periodic boundary conditions imply that $\sigma_{N+j}^\alpha = \sigma_j^\alpha$. As we can see from eq. (2.3), the

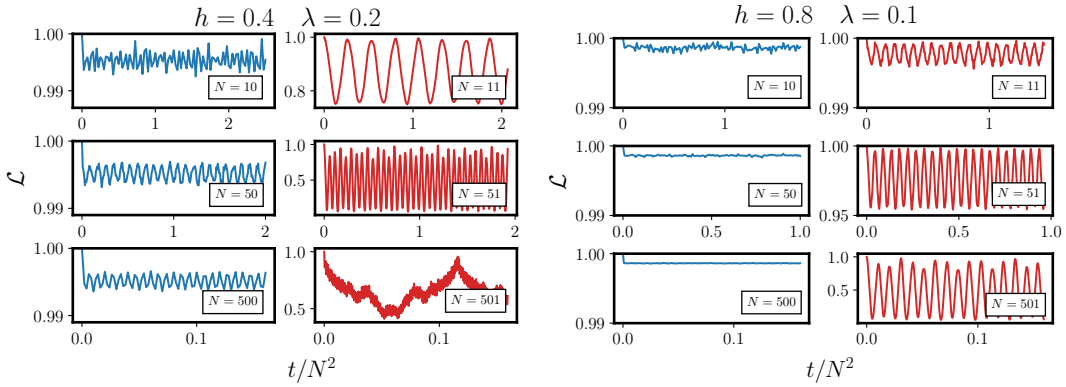

FIGURE 2.1: Loschmidt echo comparison between frustrated and unfrustrated chains of similar length N, fixing the magnetic field and the perturbation parameter respectively to $h = 0.4$, $\lambda = 0.2$ (left plot) and $h = 0.8$, $\lambda = 0.1$ (right plot). The time is rescaled for a better comparison. For even N (unfrustrated systems), due to the negligible hybridization with the first excited states, the LE presents small oscillations around a value near one (left columns). For odd N instead the higher number of hybridized states results in a strong sensitivity of the LE oscillations to the system parameters.

system has the parity symmetry with respect to the z-spin direction, i.e. $[H_0, \Pi^z] = 0$, where $\Pi^z = \bigotimes_{i=1}^{N} \sigma_i^z$. This means that the eigenstates of H_0 can be arranged in two sectors, corresponding to two different eigenvalues of Π^z. Moreover, the model in eq. (2.3) is also invariant under spatial translation which implies that there exists a complete set of eigenstates of H_0 made of states with definite lattice momentum [2].

In the range $0 < h < 1$, for $N = 2M$ the system shows two nearly degenerate lowest energy states with opposite parity and an energy difference closing exponentially with the system size [56, 142] while all the other states remain separated by a finite energy gap. When $N = 2M + 1$, topological frustration sets in and the unique ground state becomes part of a band in which states of different parities alternate. In this case the gaps between the lowest energy states close algebraically as $1/N^2$ [62–64, 67, 70, 71, 73].

A simple perturbation that satisfies the criteria we discussed above is $H_p = \sigma_N^z$, breaking the translational invariance which classifies the eigenstates of H_0, while preserving the parity symmetry. Thus, we have

$$H_1 = H_0 + \lambda\, \sigma_N^z, \tag{2.4}$$

and we assume that $\lambda \ll 1$, i.e. we assume that λ is much smaller than the energy gap above the two quasi-degenerate ground states in the unfrustrated case. Here λ is assumed to be small, but independent of N. A global quench where H_1 preserves the parity and breaks the translational invariance, for example through a modulated or a random transverse field, could also be considered. However, it is important that the perturbation is not large enough to complicate the evolution of the LE in the unfrustrated case, which we want to be of the first kind. Furthermore, we are looking for a simple, unambiguous, system-size independent protocol, for which the local quench is suitable.

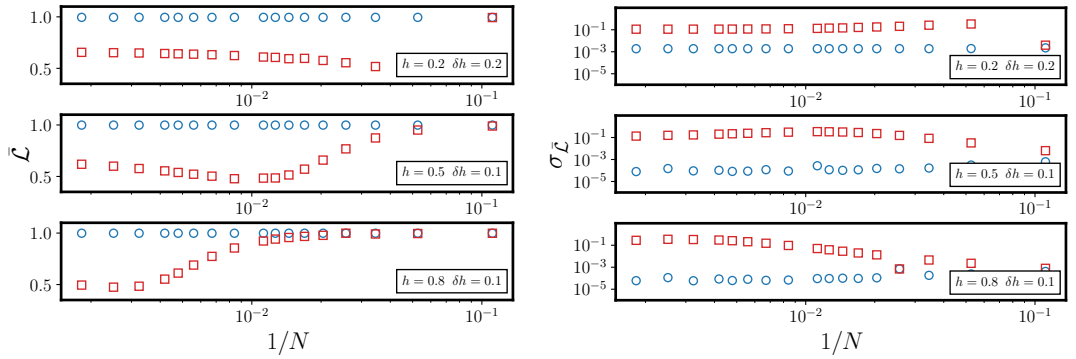

FIGURE 2.2: Comparison between the result for frustrated (red squares) and unfrustrated (blue circles) chains of the time-average (left panel) and of the standard deviations (right panel) of the LE for several sets of parameters as a function of the inverse system length. Differently from the frustrated case, the unfrustrated time average is mostly size independent. The standard deviation for the frustrated case is always larger, even a few orders of magnitude, than the one of the unfrustrated case.

Since H_1 is not invariant under spatial translations, we cannot diagonalize it analytically as is possible for H_0, by exploiting the usual approach based on the Jordan-Wigner transformation followed by a Bogoliubov rotation [56]. Nevertheless, we can resort to the diagonalization procedure reported in [91], which allows us to diagonalize numerically the Hamiltonians (2.3) and (2.4) in an efficient way [4], and thus to calculate the LE (see the Methods section for the details). The results obtained are summarized in Fig. 2.1, where several behaviors of the LE for even N and odd $N+1$ sizes are compared.

The results fit well in the qualitative picture we have discussed in the first part. When N is even and hence the system is not frustrated the LE presents small noisy oscillations around a value close to unity, see Fig. 2.1. The average value is almost independent from the parameters, while oscillations reduce as the system size increases. This behavior reflects the fact that, λ being small, the initial state shares a significant overlap only with one of the lowest eigenstates of H_1 and the contributions from all other states above the gap produce fast oscillations that average out in the long time limit.

For the frustrated case $N = 2M + 1$ instead, the picture is completely different. The LE exhibits decays and periodic revivals, similarly to its behavior in quenches to critical points [124, 127–135]. Here, because of the closing of the gap, the same perturbation hybridizes several states, which thus contribute to the evolution of the LE. Finite-size effects become important, since by increasing the chain length the density of states changes and thus also the number of states which get hybridized. These considerations imply a strong sensibility of the LE oscillation frequency and amplitude to all the parameters in the setting.

The results presented in Fig. 2.1 make it clear that the behaviors of the LE for even and odd N are completely different. To go beyond this qualitative assessment, we can make a quantitative comparison of the difference between these two behaviors, by considering the time averaged value of the LE $\bar{\mathcal{L}}$ over a long period of time, ideally infinite. This analysis, whose results can be found in the left panel of Fig. 2.2, clearly shows that for the unfrustrated case (blue circles) the time average is almost

independent from the size of the ring, while for the frustrated one (red squares) there is a significant dependence on the ring size, with an asymptotic value in the thermodynamic limit which differs from the even chain length case. The similarity between the frustrated and unfrustrated values for small systems can be easily understood by taking into account that in the frustrated model, for small N, the gap between the ground state and the other states in the lowest energy band can be bigger than the perturbation amplitude, hence giving life to an unfrustrated-like behavior for the LE.

As we wrote above, since H_p breaks the spatial invariance, it is impossible to obtain an exact expression for the LE. For the unfrustrated case, it is possible to develop a cumulant expansion [125] which provides the correct evolution of the LE, but its reliability hinges on a clear separation of scales between the strength of the perturbation and the energy gap. When N is odd, the gap closes and for sufficiently large system size this approach fails. Nonetheless, to gain some insight into the LE when the system is frustrated, we can resort to a perturbation theory around the classical point $(h = 0)$ and derive an analytic expression which can be compared to our numerical results. Within this approach, we first compute the initial (ground) state of H_1 considering, in the beginning, $\lambda\sigma_N^z$ as the perturbation to the Hamiltonian at the classical point $(h = 0)$, and then bringing back the term $h\sum_j \sigma_j^z$ as a second-order perturbation term. By construction, this approach is justified for $0 < h \ll \lambda \ll 1$. The effect of the local term $\lambda\sigma_N^z$ is to split the initial $2N$ degenerate states into three groups. In particular, the ground space becomes two-fold degenerate, separated by an energy gap of order λ from $2N-4$ degenerate states, on top of which, separated by a gap of the same value, there are two other degenerate states. The second perturbation term $h\sum_j \sigma_j^z$ does not act significantly on the two two-dimensional manifolds but removes the macroscopic degeneracy, creating an intermediate band of $2N-4$ states.

Exploiting this perturbative analysis (see the Methods section for details), we obtain for the LE

$$\mathcal{L}(t) = \left| \frac{2}{N(N-1)} \sum_{k=1}^{(N-1)/2} \tan^2\left[\frac{(2k-1)\pi}{2(N-1)}\right] \exp\left\{ -\imath 2ht \cos\left[\frac{(2k-1)\pi}{N-1}\right]\right\} + \frac{2}{N}\exp\left[\imath t(\lambda+h)\right]\right|^2 . \tag{2.5}$$

In Fig. 2.3 we compare the analytical results in eq. (2.5) with the numerical data and we find a substantial agreement between the two in the region $h \ll \lambda$ (see the upper panel). It is also worth noting that the two methods give similar results even when h and λ are comparable (middle panel of Fig. 2.3). The main difference between the two behaviors is, apparently, only a rescaling of the oscillation frequency that seems to be underestimated in the perturbative approach.

In the thermodynamic limit the term proportional to $2/N$ in eq. (2.5) can be neglected and the expression of the LE can be approximated as: $\mathcal{L}(t) \simeq \mathcal{F}\left(\frac{2ht}{N^2}\right)$ where the function $\mathcal{F}(x)$ is given by

$$\mathcal{F}(x) = \lim_{M\to\infty} \left| \frac{1}{2M^2} \sum_{k=1}^{M} \tan^2\left[\frac{(2k-1)\pi}{4M}\right] \exp\left\{ -\imath x(2M+1)^2 \cos\left[\frac{(2k-1)\pi}{2M}\right]\right\}\right|^2 \tag{2.6}$$

The function in eq. (2.6) is somewhat reminiscent of the Weierstrass function [143] and indeed it displays a continuous, but nowhere differentiable behavior. While

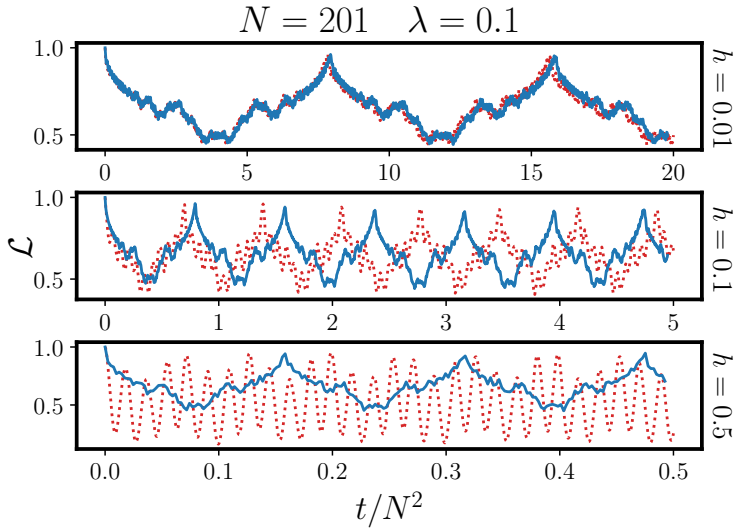

FIGURE 2.3: Loschmidt echo's comparison between the numerics (dotted red line) and the analytic expression eq. (2.5) (blue line) for a spin chain of length $N = 201$ and for $\lambda = 0.1$. The time is rescaled for a better comparison. The results are in agreement for $h = 0.01$, that corresponds to the limit $0 < h \ll \lambda \ll 1$ (upper panel, the curves are mostly superimposed). We also find similar results when h and λ are comparable, as shown in the middle panel for the case $\lambda = h = 0.1$. Finally, in the lower panel the failure of the approximation for $h = 0.5$ is shown, where the value of the magnetic field is beyond the assumed range of validity.

its emergence in such a simple context is remarkable, we remark that such fractal curves [144, 145] were already observed in LE evolution [146]. Furthermore, similar curves were also observed in quenches to multicritical points [131, 135], where as in our case the LE displays the period of revivals proportional to N^2. Presumably, an important reason behind this similarity is that both at the studied multicritical points and in the studied topologically frustrated spin chain the spectral gap closes quadratically with the system size.

2.3 Conclusions

We have analyzed the behavior of the LE in short-range antiferromagnetic one-dimensional spin systems with periodic boundary conditions in the presence of a perturbation that violates translational invariance, but leaves unaffected the parity, namely a local magnetic field. Under these conditions, the LE shows an anomalous dependence on the number of elements in the system. When this number is even, LE shows small random oscillations around a value very close to unity that is almost independent from the system size, and the amplitude of these oscillations tend to decrease with the size increasing until it disappears in the thermodynamic limit. On the contrary, in the presence of a ring made out of an odd number of sites, the oscillations are large and do not disappear in the thermodynamic limit while the average value is strongly dependent on the system size. The presence of two different behaviors can be traced back to the difference in the energy spectrum for even and odd N, that arises from the presence of topological frustration in the latter case. These general results have been tested in a paradigmatic model, the Ising model

in the transverse field, using both exact diagonalization methods and perturbation theory.

The LE can thus be used to distinguish the spin chains with N and $N+1$ sites, for arbitrarily large N. This result is especially relevant taking into account that LE is an experimentally accessible quantity, by looking at the decoherence of a two-level system interacting with the spin system [122, 124, 129, 137]. Our result is also interesting if we take into account that LE plays a fundamental role in several problems of current interest in quantum thermodynamics such as quantum work statistics [125, 126] and information scrambling [126, 147].

2.4 Methods

2.4.1 Exact results by mapping to free fermions

Let us provide a detailed description of the method exploited to obtain the data on the Ising model. Our starting point is to observe that, for spin systems that can be mapped to free-fermionic models, eq. (2.1) can be rewritten in the following form [128, 129]:

$$\mathcal{L}(t) = |\det(1 - \mathbf{r} + \mathbf{r}e^{-\imath \mathbf{C} t})|. \tag{2.7}$$

Here

$$\mathbf{\Delta}^\dagger = (c_1^\dagger, \ldots, c_N^\dagger, c_1, \ldots, c_N), \tag{2.8}$$

describes the fermionic operators, $\mathbf{C}$ is the matrix coefficient of the Hamiltonian H_1 in the fermionic language, i.e.

$$H_1 = \frac{1}{2}\mathbf{\Delta}^\dagger \mathbf{C} \mathbf{\Delta}, \tag{2.9}$$

and $\mathbf{r} = \langle g| \Delta_i^\dagger \Delta_j |g\rangle$ is the two-point fermionic correlation matrix in the initial state. The hermiticity requirement for the Hamiltonian fixes the matrix $\mathbf{C}$ to be of the block-form

$$\mathbf{C} = \begin{pmatrix} \mathbf{S} & \mathbf{T} \\ -\mathbf{T} & -\mathbf{S} \end{pmatrix}, \tag{2.10}$$

where $\mathbf{S}$ is a symmetric and $\mathbf{T}$ an antisymmetric matrix.

It is useful to rewrite the $\mathbf{r}$ matrix in terms of the correlation functions of the Majorana operators. Following [91] we define

$$A_i = c_i^\dagger + c_i, \quad B_i = \imath(c_i^\dagger - c_i). \tag{2.11}$$

Exploiting eq. (2.11) and the fact that, since $|g\rangle$ is the ground state of H_0, $\langle g| A_i A_j |g\rangle = \langle g| B_i B_j |g\rangle = \delta_{ij}$ it is straightforward to obtain:

$$\mathbf{r} = \frac{1}{4}\begin{pmatrix} 2\mathbf{I} + \mathbf{G} + \mathbf{G}^\intercal & \mathbf{G} - \mathbf{G}^\intercal \\ -\mathbf{G} + \mathbf{G}^\intercal & 2\mathbf{I} - \mathbf{G} - \mathbf{G}^\intercal \end{pmatrix}, \tag{2.12}$$

with $G_{ij} = -\langle g| B_i A_j |g\rangle$.

Therefore, to calculate the LE it remains to evaluate the correlation matrix G on the ground state of the unperturbed Hamiltonian H_0 and the matrix C linked to H_1. Both can be determined following the same approach. Exploiting the Jordan-Wigner transformation

$$c_j = \left(\bigotimes_{l=1}^{j-1} \sigma_l^z\right)\frac{\sigma_j^x + \imath\sigma_j^y}{2}, \quad c_j^\dagger = \left(\bigotimes_{l=1}^{j-1} \sigma_l^z\right)\frac{\sigma_j^x - \imath\sigma_j^y}{2}, \tag{2.13}$$

we map the spin system to a quadratic fermionic one. In fact, due to non-locality of the Jordan-Wigner transformation the Hamiltonians in eq. (2.3) and eq. (2.4) cannot be written as a quadratic form (2.9). However, they commute with the parity operator $\Pi^z = \bigotimes_{i=1}^{N} \sigma_k^z$ and it is possible to separate them into two parity sectors, corresponding to the eigenvalues $\Pi^z = \pm 1$, so that in each sector they are a quadratic fermionic form. In the following, we can restrict ourselves to the Hamiltonians H_0 and H_1 only in the odd sector ($\Pi^z = -1$) since the ground state of the quantum Ising model (2.3) with frustrated boundary conditions and $h > 0$ belongs to it [70, 73]. There, they can be written in the form of eq. (2.9), up to an additive constant. In particular, the matrix $\mathbf{C}$ for H_1 in the odd sector, present in eq. (2.7), can be obtained easily by inspection.

The matrix $\mathbf{G}$ can be found easily from the exact solution of the quantum Ising chain with frustrated boundary conditions [70, 73]. However, for a more efficient numerical implementation we follow the approach from ref. [91, 129], where we write H_0 in the odd sector in the form of eq. (2.9) and where

$$G_{ij} = -\left(\mathbf{\Psi}^{\mathsf{T}}\mathbf{\Phi}\right)_{ij}, \tag{2.14}$$

with the matrices $\mathbf{\Phi}$ and $\mathbf{\Psi}$ being formed by the vectors given by the solution of:

$$\Phi_k(\mathbf{S}-\mathbf{T})(\mathbf{S}+\mathbf{T}) = \Lambda_k^2\Phi_k, \tag{2.15}$$
$$\Phi_k(\mathbf{S}-\mathbf{T}) = \Lambda_k\Psi_k. \tag{2.16}$$

Here Λ_k are the free-fermionic energies. Their sign is a matter of choice. Transforming Λ_k to $-\Lambda_k$ corresponds simply to switching the creation and the annihilation operator, and to transforming Φ_k (Ψ_k) into $-\Phi_k$ ($-\Psi_k$). It is important to note that the parity requirements do not allow for the ground state of H_0 to be the vacuum state for free fermions with positive energy [70, 73]. Thus, assuming the eigenvalues Λ_k^2 in eq. (2.15) are labeled in ascending order, the ground state corresponds to the vacuum state of fermions with $\Lambda_1 < 0$ and the remaining energies Λ_k positive.

2.4.2 Perturbation theory near the classical point

Let us now turn to provide some more details on the perturbative approach to the LE near the classical point in the presence of topological frustration. The first step consists of finding the ground state of the Hamiltonian H_0 in eq. (2.3), treating the term $h\sum_j \sigma_j^z$ as a perturbation. It is known that, at the classical point, in the presence of an odd number of spins the interplay between periodic boundary conditions and antiferromagnetic interactions gives rise to a $2N$-fold degenerate ground state manifold. Such a space is spanned by the kink states $|j\rangle$ and $\Pi^z|j\rangle$, $j = 1, 2, \ldots N$ with energy $-(N-2)$, that have one ferromagnetic bond $\sigma_j^x = \sigma_{j+1}^x = \pm 1$ respectively, the others being antiferromagnetic ($\sigma_k^x = -\sigma_{k+1}^x$ for $k \neq j$). The excited states outside this manifold are separated from the ground space by an energy gap of order unity so that we can neglect them in a perturbative approach. By considering the magnetic field the $2N$-fold degeneracy is removed and a narrow-band of states is created, with a gap that separates the ground state from the other elements of the band closing as $1/N^2$ (see Appendix A.1 for more details). To the lowest order in perturbation theory in h we found for the initial state appearing in eq. (2.1), that is

for the ground state of the unperturbed system, the expression:

$$|g\rangle = \frac{1}{\sqrt{N}} \sum_{j=1}^{N} \frac{1-\Pi^z}{\sqrt{2}} |j\rangle \,. \tag{2.17}$$

The next step is to find the lowest energy states of the Hamiltonian H_1 in eq. (2.4) through a perturbation theory both for $h > 0$ and $\lambda > 0$, and of the basis of this to compute the Loschmidt echo. The details of this calculation are given in Appendix B, while its main points are given in the following. Since we first apply the perturbation theory in λ while we consider h as a second-order perturbation, we are assuming that $h \ll \lambda \ll 1$. Also in this case we start from the $2N$ degenerate ground space formed by the kink states and we treat the term $\lambda\sigma_N^z$ as a perturbation. Again we find that the degeneracy is removed and, at this point, the system shows two-fold degenerate ground states:

$$|\psi_\pm\rangle = \frac{1 \pm \Pi^z}{2}(|N-1\rangle \mp |N\rangle), \tag{2.18}$$

separated by an energy gap equal to λ from $2N-4$ degenerate kink states. Above this macroscopically degenerate manifold, separated by a gap λ there are other two states:

$$|\phi_\pm\rangle = \frac{1 \pm \Pi^z}{2}(|N-1\rangle \pm |N\rangle) \tag{2.19}$$

We now consider the second-order perturbation $h\sum_j \sigma_j^z$. Its effect on the $|\psi_\pm\rangle$ and $|\phi_\pm\rangle$ states is only a shift in the energy respectively of $\mp h$. Furthermore, it creates a band of states from the kink ones given by:

$$|\xi_\pm, m\rangle = \frac{1 \pm \Pi^z}{\sqrt{N-1}} \sum_{j=1}^{N-2} (-1)^j \sin\left(\frac{m\pi}{N-1} j\right) |j\rangle \,, \tag{2.20}$$

with $m = 1, 2, \ldots, N-2$. The energies of the discussed eigenstates are given by

$$E(\psi_\pm) = -(N-2) - (\lambda + h), \tag{2.21}$$

$$E(\phi_\pm) = -(N-2) + \lambda + h, \tag{2.22}$$

$$E(\xi_\pm, m) = -(N-2) \mp 2h \cos\left(\frac{m\pi}{N-1}\right). \tag{2.23}$$

The calculation of the Loschmidt echo is now straightforward. From the definition eq. (2.1), expressing the initial state eq. (2.17) in terms of the eigenstates of the perturbed model eq.s (2.18), (2.19), and (2.20) and applying the evolution operator $e^{-\imath H_1 t}$ we finally obtain the expression in eq. (2.5).

Chapter 3

Topological Frustration can destroy Local Order

In this chapter, which is based on [1], we show that topological frustration can destroy the order parameter of the system. We study the quantum XYZ chain without external fields and with both antiferromagnetic and ferromagnetic interactions, set on the ring with an odd number of sites (frustrated boundary conditions). In this setting we are able to apply the approach to symmetry breaking based on the exact ground state degeneracy due to anticommuting symmetries, discussed in section 1.2.3, in which we can, already in a finite system, compute the magnetizations that are traditionally used as order parameters to characterize system's phases. When ferromagnetic interactions dominate, we recover magnetizations that in the thermodynamic limit lose any knowledge about the boundary conditions and are in complete agreement with standard expectations. On the contrary, when the system is governed by antiferromagnetic interactions, due to topological frustration the magnetizations decay algebraically to zero with the system size and are not staggered, despite the AFM coupling. We term this behavior *mesoscopic ferromagnetic magnetization*. Hence, in the antiferromagnetic regime, our results show an unexpected dependence of spin expectation values on the choice of boundary conditions.

3.1 Introduction

In section 1.2.4 we have discussed the boundary conditions in the context of the possibility to influence local order. Let us just note here that the older results on topological frustration, discussed in section 1.2.1, also bring some evidence pointing towards it, through a single, symmetric, ground state above which the energy gap closes only algebraically [62–64, 66, 67], i.e. not exponentially, and through the two–point function [67, 71, 73], which vanishes for the most distant spins in the ring, as discussed also in section 1.2.3. Crucially, here we consider the magnetization directly within a symmetry breaking framework.

After introducing the system under consideration, we will recap the two complementary approaches to extract the order parameter in the absence of frustration and then apply the same techniques to the case with frustration. Doing so, first we show that our technique yields the expected results in the former case, and then we apply it to the frustrated case.

3.2 The spin chains and their properties

We consider an anisotropic spin–$\frac{1}{2}$ chain with Hamiltonian

$$H = \sum_{j=1}^{N} \cos\delta \left(\cos\phi\, \sigma_j^x \sigma_{j+1}^x + \sin\phi\, \sigma_j^y \sigma_{j+1}^y \right) - \sin\delta \sigma_j^z \sigma_{j+1}^z , \tag{3.1}$$

where σ_j^α, with $\alpha = x, y, z$, are Pauli operators and N is the number of lattice sites, which we henceforth set to be odd $N = 2M+1$. Crucially, we apply periodic boundary conditions $\sigma_{j+N}^\alpha = \sigma_j^\alpha$.

The model is expected to exhibit a quantum phase transition every time two of the couplings are, in magnitude, equal and greater than the third [148] (in that case, the model becomes equivalent to a critical XXZ chain [56]). Dualities are connecting different rearrangements of the couplings along the x, y, and z directions [148]. Moreover, to avoid additional effects (and degeneracies) that will be the subject of subsequent chapters, we will allow only one antiferromagnetic (AFM) coupling (namely, along the x direction), letting the other two to favor a ferromagnetic alignment. We thus limit the range of the anisotropy parameters such that $\phi \in [-\pi/2, 0]$ and $\delta \in [0, \pi/2]$, so that the phase transition is at $\phi = -\pi/4$ (for $\tan\delta < 1/\sqrt{2}$) and separates two phases characterized by a two–fold degenerate ground state. In particular, for $\phi \in [-\pi/2, -\pi/4)$ the phase favors a ferromagnetic alignment along the y direction (yFM), while for $\phi \in (-\pi/4, 0]$ the dominant interaction is AFM along the x direction (xAFM) and thus *topologically frustrated*.

With no external field, we can adopt the approach to symmetry breaking based on anticommuting symmetries for odd N, discussed in section 1.2.3. All three parity operators along the three axes $\Pi^\alpha = \bigotimes_{j=1}^{N} \sigma_j^\alpha$ commute with the XYZ Hamiltonian in eq. (3.1) ($[H, \Pi^\alpha] = 0$). Since we are considering systems made by an odd number of sites $N = 2M+1$, the Π^α do not commute with one another, but rather anti-commute ($\{\Pi^\alpha, \Pi^\beta\} = 2\delta_{\alpha,\beta}$), and actually fulfill a a non-commuting algebra $\left[\Pi^\alpha, \Pi^\beta\right] = \imath\, \varepsilon^{\alpha,\beta,\gamma} 2(-1)^{\frac{N-1}{2}} \Pi^\gamma$, which is essentially SU(2). This structure implies that every state is exactly degenerate an even number of times, also on a finite chain. If $|\Psi\rangle$ is an eigenstate, say, of Π^z, then $\Pi^x |\Psi\rangle$, that differs from $\Pi^y |\Psi\rangle$ by a global phase factor, is also an eigenstate of the Hamiltonian with opposite z–parity but with the same energy.

Applying an external magnetic field h along, say, the z–direction leaves only Π^z to commute with the Hamiltonian, thus restoring the original $\mathbb{Z}_2$ symmetry the model is known for and breaking the exact finite-size degeneracy between the states [10, 56]. Nonetheless, up to a critical value of h, it is known that the induced energy split is exponentially small in the system size [142] and thus that the degeneracy is restored in the thermodynamic limit, representing one of the simplest, and most cited, examples of spontaneous symmetry breaking (SSB) [10]. To simplify things, let us set $\delta = 0$, so that eq. (3.1) describes an anisotropic XY chain [56, 91]. For $|h| < 1$ we are in the SSB phase. This means that, although a ground state with definite z–parity necessarily has zero expectation value concerning σ_j^x and σ_j^y, in the thermodynamic limit the degeneracy allows to select a ground state which is a superposition of different z–parities, which can thus display a spontaneous magnetization in the x or y direction. In the yFM phase we expect the order parameter $m_y \equiv \langle \sigma_j^y \rangle$ to be finite, while in the xAFM the non–vanishing order parameter should be the staggered magnetization $m_x \equiv (-1)^j \langle \sigma_j^x \rangle$.

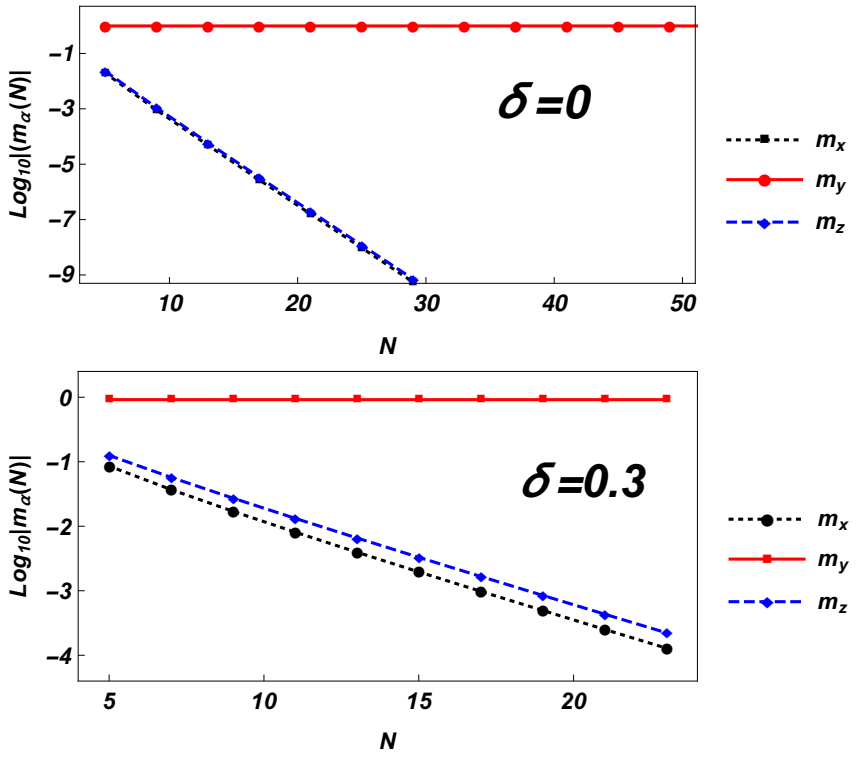

FIGURE 3.1: Magnetizations along the three axes (in absolute value) as a function of the chain length for the yFM phase at $\phi = -1.32$. The upper panel dots represent the data obtained by setting $\delta = 0$ and using the "trick" discussed in the text to evaluate the magnetizations as determinants of $\frac{N-1}{2} \times \frac{N-1}{2}$ matrices, while the dots in the lower one are obtained taking $\delta = 0.3$ and using exact numerical diagonalization. Regardless of the value of δ, m_y quickly saturates to its asymptotic finite value, while m_x and m_z decay to zero exponentially fast, as shown by the best fit lines (plots presented in logarithmic scale).

3.3 The ferromagnetic case

Let us now turn back to the system in eq. (3.1) and focus on the ferromagnetic region $\phi \in [-\pi/2, -\pi/4)$. The (quasi–)long–range order represented by the order parameter can be extracted in two ways: from the two–point function or by selecting a suitable superposition of states at finite sizes and then following their magnetization toward the thermodynamic limit. The former takes advantage of the cluster decomposition property [11, 87, 88]

$$\lim_{r\to\infty} \langle \sigma_j^\alpha \sigma_{j+r}^\alpha \rangle - \langle \sigma_j^\alpha \rangle \langle \sigma_{j+r}^\alpha \rangle = 0, \tag{3.2}$$

to extract the order parameter from the large distance behavior of the system's two–point correlators.

Exploiting the Jordan-Wigner Transformation [56, 91, 149], which maps the spin degrees of freedom into spin-less fermions:

$$c_j = \left(\bigotimes_{l=1}^{j-1} \sigma_l^z\right) \frac{\sigma_j^x + \imath\sigma_j^y}{2}, \quad c_j^\dagger = \left(\bigotimes_{l=1}^{j-1} \sigma_l^z\right) \frac{\sigma_j^x - \imath\sigma_j^y}{2}, \tag{3.3}$$

the XY model can be brought into a free fermionic form. Before doing so, however, states must be separated according to their parity Π^z, since negative (positive) parity corresponds to (anti-)periodic boundary conditions applied to the fermions. Thus, the XY chain Hamiltonian can be written as

$$H = \frac{1+\Pi^z}{2} H^+ \frac{1+\Pi^z}{2} + \frac{1-\Pi^z}{2} H^- \frac{1-\Pi^z}{2} \,, \tag{3.4}$$

where the exact expressions of H^+ and H^- can be found in Appendix C.2. From these Hamiltonians it is possible to determine, following the method described in details in Appendix C.2, the fundamental two–point correlation functions. These correlations are expressed as the determinant of a Toeplitz matrix, whose asymptotic behavior can be evaluated analytically [150]:

$$\langle \sigma_j^x \sigma_{j+r}^x \rangle \overset{r\to\infty}{\simeq} \frac{2}{\pi\sqrt{1-\cot^2\phi}} \frac{\cot^r\phi}{r} \tag{3.5}$$

$$\langle \sigma_j^y \sigma_{j+r}^y \rangle \overset{r\to\infty}{\simeq} \begin{cases} \sqrt{1-\cot^2\phi}\left[1+\frac{4}{\pi}\left(\frac{\cot\phi}{1-\cot^2\phi}\right)^2 \frac{\cot^r\phi}{r^2}\right] & r=2m \\ \sqrt{1-\cot^2\phi}\left[1+\frac{2}{\pi}\left(\frac{\cot\phi}{1-\cot^2\phi}\right)^2 \frac{1+\cot^2\phi}{\cot\phi}\frac{\cot^r\phi}{r^2}\right] & r=2m+1 \end{cases} \tag{3.6}$$

$$\langle \sigma_j^z \sigma_{j+r}^z \rangle \overset{r\to\infty}{\simeq} \begin{cases} 0 & r=2m \\ -\frac{2}{\pi}\frac{\cot^r\phi}{r^2} & r=2m+1 \end{cases} \tag{3.7}$$

From these large r behavior, taking into account the cluster decomposition hypothesis, we can extract the different magnetizations $m_\alpha \equiv \langle \sigma_j^\alpha \rangle$, obtaining

$$m_x = m_z = 0, \qquad m_y = \left(1-\cot^2\phi\right)^{1/4} \,. \tag{3.8}$$

However, on an odd–length chain at $h = 0$, exploiting the symmetries that we have already illustrated, we can provide a direct way to evaluate the different magnetizations even in finite systems. In fact, if $|g_z\rangle$ is one of the degenerate ground states with definite z–parity which can be constructed in terms of the Bogoliuobov fermions [56], we can generate a ground state with definite x–parity (y–parity) as $|g_x\rangle \equiv \frac{1}{\sqrt{2}}(1+\Pi^x)|g_z\rangle$, ($|g_y\rangle \equiv \frac{1}{\sqrt{2}}(1+\Pi^y)|g_z\rangle$). All these states have a vanishing magnetization in the orthogonal directions while along their own axes we have

$$\begin{aligned} \langle g_x|\,\sigma_j^x\,|g_x\rangle &= \langle g_z|\,\sigma_j^x\Pi^x\,|g_z\rangle = \langle g_z|\,\tilde{\Pi}_j^x\,|g_z\rangle \,, \\ \langle g_y|\,\sigma_j^y\,|g_y\rangle &= \langle g_z|\,\sigma_j^y\Pi^y\,|g_z\rangle = \langle g_z|\,\tilde{\Pi}_j^y\,|g_z\rangle \,, \end{aligned} \tag{3.9}$$

where $\tilde{\Pi}_j^\alpha \equiv \bigotimes_{l\neq j}\sigma_l^\alpha$ for $\alpha = x, y$. These states are the analytical continuation at $h = 0$ of the zero–temperature "thermal" ground state that spontaneously breaks the $\mathbb{Z}_2$ symmetry.

Note that in this way, we turn the calculation of the expectation value of an operator defined on a single–spin with respect to a ground state with a mixed z–parity into that of a string made by an even number of spin operators on a definite z–parity state, which is a standard problem. Thus the RHS of eq. (3.9) can be written again as the determinant of a Toeplitz matrix, whose asymptotic behavior can be studied analytically, similarly to what has been done in [90]. This "trick" can be understood as originating from the fact that, at zero external fields, the chain in eq. (3.1) has a

particle/hole duality and that, on a chain with an odd number of sites, the symmetry relates states with different parities. The result of such analysis reproduces eq. (3.8), proving the consistency of the two methods of evaluation for the order parameters. More details on this direct approach in Appendix C.5.

While for $\delta = 0$ we can evaluate the magnetizations using the analytical "trick", for $\delta \neq 0$ we have to resort to numerical solutions. In Fig. 3.1 we present some typical results for the finite size magnetizations for the XY and XYZ chain, showing a quick exponential decay in N of m_x and m_z to zero and a fast saturation of m_y (note that each plotted magnetization m_α is calculated with respect to the corresponding ground state $|g_\alpha\rangle$).

3.4 The frustrated case

We now turn to the case with $\phi \in (-\pi/4, 0]$, where the boundary conditions induce topological frustration. For $\delta = 0$, the model can be solved through the same steps used in the traditional cases and exactly mapped into a system of free fermions. In the ferromagnetic phase, the degeneracy between the different parity states is due to the presence of a single negative energy mode (only in one of the parity sectors), whose occupation lowers the energy of those states. With frustration, the negative energy mode moves into the other parity sector and, because of the parity selection rules in (3.4), it cannot be excited alone. Therefore, the effect of frustration is that the lowest energy states in each parity sector in (3.4) are not admissible.

The two degenerate ground states thus carry the signature of a single delocalized excitation and lie at the bottom of a band of states in which this excitation moves with different momenta (with an approximate Galilean dispersion relation). Hence, another effect of topological frustration is to close the gap that would otherwise exist, as in the older results on topological frustration, discussed in section 1.2.1.

Let us then repeat the extraction of the order parameters in the xAFM phase, following the same procedure we followed for yFM. However, in the present case, the analytical computation of the spin correlations along the x and y directions requires the knowledge of the asymptotic behavior of a new type determinants, whose symbol contains a delta function with a peak at the momentum of the excitation. We have studied such determinants in [3], that is the subject of Chapter 9, where we also present the details of the analytical computation of the results presented here. The computation of the correlations along z do not require these techniques and it is given in Appendix C.5. The results are

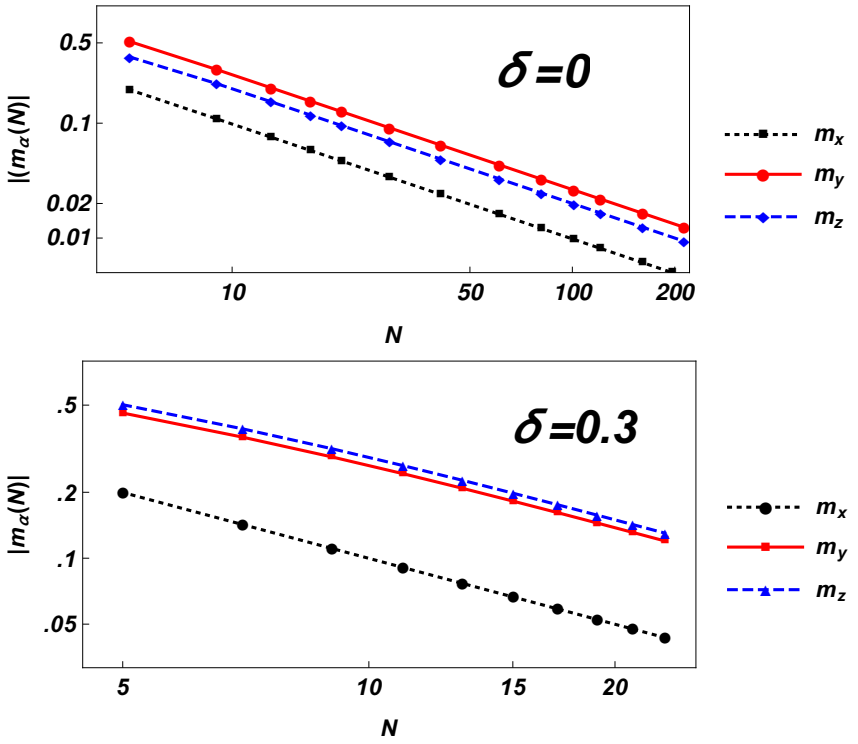

FIGURE 3.2: Magnetizations along the three axes (in absolute value) as a function of the chain length for the xAFM/MFM phase at $\phi = -0.25$. The upper panel dots represent the data obtained by setting $\delta = 0$ and using the "trick" discussed in the text to evaluate the magnetizations as determinants of $\frac{N-1}{2} \times \frac{N-1}{2}$ matrices, while the dots in the lower one are obtained taking $\delta = 0.3$ and using exact numerical diagonalization. Regardless of the value of δ, we see how all magnetizations decay algebraically to zero, as shown by the best fit lines (plots presented in log–log–scale).

$$\langle \sigma^x_j \sigma^x_{j+r} \rangle \overset{r\to\infty}{\simeq} \begin{cases} \sqrt{1-\tan^2\phi}\left(1-\frac{2r}{N}\right)\left[1+\frac{4}{\pi}\left(\frac{\tan\phi}{1-\tan^2\phi}\right)^2\frac{\tan^r\phi}{r^2}\right] & r=2m \\ -\sqrt{1-\tan^2\phi}\left(1-\frac{2r}{N}\right)\left[1+\frac{2}{\pi}\left(\frac{\tan\phi}{1-\tan^2\phi}\right)^2\frac{1+\tan^2\phi}{\tan\phi}\frac{\tan^r\phi}{r^2}\right] & r=2m+1 \end{cases} \tag{3.10}$$

$$\langle \sigma^y_j \sigma^y_{j+r} \rangle \overset{r\to\infty}{\simeq} \begin{cases} \frac{2}{\pi\sqrt{1-\tan^2\phi}}\frac{(-\tan\phi)^r}{r}+2^{\frac{5}{2}}\frac{1}{1+\tan\phi}\frac{(-\tan\phi)^{\frac{r}{2}}}{N\sqrt{\pi r}} & r=2m \\ \frac{2}{\pi\sqrt{1-\tan^2\phi}}\frac{(-\tan\phi)^r}{r}+2^{\frac{3}{2}}\frac{(-\tan\phi)^{\frac{1}{2}}+(-\tan\phi)^{-\frac{1}{2}}}{1+\tan\phi}\frac{(-\tan\phi)^{\frac{r}{2}}}{N\sqrt{\pi r}} & r=2m+1 \end{cases} \tag{3.11}$$

$$\langle \sigma^z_j \sigma^z_{j+r} \rangle \overset{r\to\infty}{\simeq} \begin{cases} 0 & r=2m \\ -\frac{2}{\pi}\frac{\tan^r\phi}{r^2}+2^{\frac{3}{2}}\sqrt{1-\tan^2\phi}\frac{(-\tan\phi)^{\frac{r-1}{2}}}{N\sqrt{\pi r}} & r=2m+1 \end{cases} \tag{3.12}$$

While they imply quite clearly that $m_y = m_z = 0$ (in accordance with expectations), the extraction of m_x is more subtle: using the standard prescription of taking $N \to \infty$ first, one would get $m_x = \left(1-\tan^2\phi\right)^{1/4}$. However, one could argue [73]

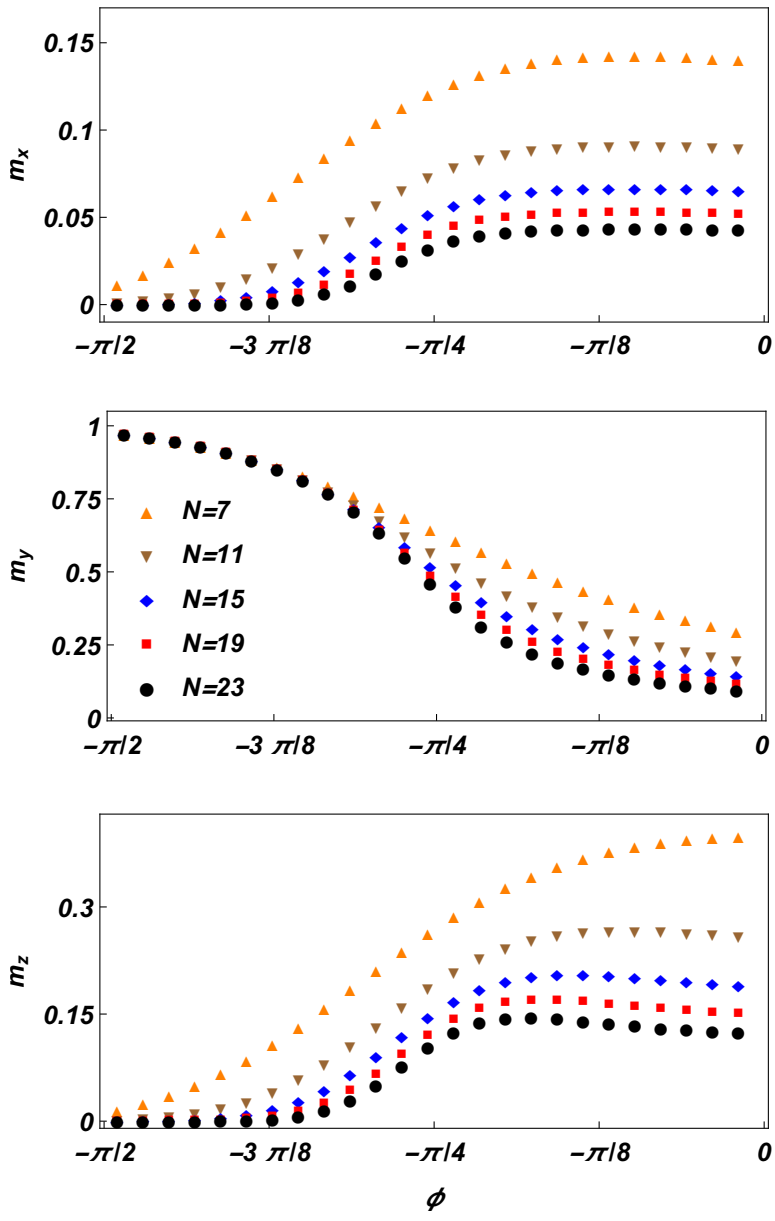

FIGURE 3.3: Plot of the magnetizations as a function of ϕ for $\delta = 0.3$ and several system sizes. The yFM phase ($\phi < -\pi/4$) shows a fast approach to saturation, while for the frustrated case the decay toward zero is algebraically slow.

that a better procedure would be to evaluate eq. (3.10) at antipodal points $r \sim N/2$ to minimize the correlations and then take the thermodynamic limit. In this way, one would get $m_x = \frac{1}{N}\left(1-\tan^2\phi\right)^{1/4} \overset{N\to\infty}{\to} 0$. Note also that there are systems where the violation of the cluster decomposition principle has been discovered [151].

It is thus important that we can directly access the single spin magnetization using eq. (3.9). Once more, for the XY chain the expectation values can be cast as determinants of Toeplitz matrices, whose behaviors are depicted in the upper panel of Fig. 3.2: all magnetizations are characterized by an algebraic decay to zero with the system size. The analytical results for are given in Appendix C.5, and demonstrate clearly this property.

Several elements are surprising in these results. The most evident one is that FBC kills the magnetization in the x–direction, that on an open or even-length chain would be finite. Note that a finite magnetization can be measured in any finite system, although it decreases algebraically with the system size, a phenomenon we term "*mesoscopic magnetization*". Quite surprisingly, however, this finite–size magnetization is *not staggered*, but rather ferromagnetic–looking (thus, we will call the AFM phase with FBC, a *mesoscopic ferromagnetic* phase, MFM). In hindsight, we could have expected this, since a staggered magnetization would have not been compatible with PBC with an odd number of sites (note that this problem does not arise for the 2-point function).

These analytical outcomes are corroborated by exact numerical diagonalization results, which allow us to extended our analysis to the XYZ ($\delta \neq 0$) ring, (see the lower panel of Fig. 3.2). In Fig. 3.3 we plot the behavior of the magnetizations as a function of ϕ for $\delta = 0.3$ for several chain lengths N: while in the yFM phase there is little dependence on N, as the saturation values are reached quickly, in the MFM phase we observe the slow, algebraic decay toward zero of the order parameters.

It is rather surprising that a finite chain, unable to sustain AFM order, would nonetheless generate a ferromagnetic spontaneous magnetization and that in any finite system, a phase with a dominant interaction along the x direction would show the weakest spontaneous magnetization in that direction, with m_y being the strongest one (once more, these magnetizations refer to different states $|g_\alpha\rangle$). Finally, we remark that FBC also seem to somewhat spoil the cluster decomposition, since the non–staggered mesoscopic magnetization we find is not compatible with (3.10), although both of them vanish in the thermodynamic limit.

3.5 Conclusions

We have presented a comparative study of the ferromagnetic and AFM frustrated case for the XYZ chain, showing that, contrary to expectations, the boundary conditions are able to destroy local order. We have done so, by realizing that, with no external field, we can exploit the anticommuting parity symmetries to construct an exact ground state at finite sizes that breaks the $\mathbb{Z}_2$ symmetry. For the XY chain, we can express the one-point function as a determinant of a Toeplitz matrix and evaluate it analytically, while for the interacting cases we can numerically diagonalize the model and calculate the expectation values. We benchmarked these procedures on a ferromagnetic phase with FBC to show that they reproduce the expected results eq. (3.8), while in an AFM phase the magnetizations, while finite in a finite chain, decay toward zero algebraically in the thermodynamic limit. Furthermore, despite a dominant AFM interaction, no magnetization shows a staggered behavior: we thus term this phase generated by FBC a mesoscopic ferromagnetic phase (MFM).

Nonetheless, we should remark that our results are fully consistent with a straightforward perturbative calculation starting from the classical frustrated Ising chain, similar to the one in [67, 69], as we show in Appendix C.7. Our important contribution is that we have found an exact way to approach the thermodynamic limit and to calculate the order parameter.

Our results are surprising because they show that, within the symmetry breaking framework that we have adopted, the boundary conditions can influence the bulk behavior of a system, by destroying local order. Let us end with a couple of observations about this strange phenomenology. The first is that FBC provide a non–local contribution to the system since frustration arises from an incompatibility between local and global order. Thus, it is possible that the discovered phenomenology has some topological origins. Another, somewhat more technical angle, is that in our class of models, the single spin magnetization is dual to a non–local correlator (see eq. (3.9)). From this point of view, it is not surprising that a non–local function is sensitive to the boundary conditions. Nonetheless, we have to admit that it seems to us a rather strange to consider single–site magnetizations as non–local quantities.

Chapter 4

Topological Frustration can induce a Quantum Phase Transition

In the previous chapter, we have already proved that when only one antiferromagnetic interaction dominates over ferromagnetic ones, topological frustration destroys local order (expressed by the spontaneous magnetization) in the thermodynamic limit, and replaces it with mesocopic ferromagnetic order. Here we focus on the transition that occurs when also the second interaction in the quantum XY chain becomes AFM. This transition is characterized, even at finite size, by a level crossing associated with a discontinuity in the first derivative of the free energy at zero temperature (i.e., the ground state energy). In the new phase, the ground state becomes four-fold degenerate and this increased degeneracy allows for the existence of a different magnetic order. The order is characterized by a staggered magnetization as in the standard AFM case, but with a modulation that makes its amplitude slowly varying in space. The results are surprising not only because we find a different kind of order, but also because the quantum phase transition, signaled by the discontinuity, does not exist with other boundary conditions (BC), such as open (OBC) or periodic (PBC) boundary conditions with an even number of sites N. This chapter is based on [2].

4.1 Results

4.1.1 Level crossing

Continuing the analysis of the previous chapter, we focus on the quantum XY chain [91] at zero field with FBC. Even if the discovered phenomenology is not limited to this model, it is useful to focus on it, because exploiting the well–known Jordan–Wigner transformation [91, 149] we can evaluate all the quantities that we need with an almost completely analytical approach. The Hamiltonian describing this system reads

$$H = \sum_{j=1}^{N} \cos\phi\ \sigma_j^x \sigma_{j+1}^x + \sin\phi\ \sigma_j^y \sigma_{j+1}^y\ , \tag{4.1}$$

where σ_j^α, with $\alpha = x, y, z$, are Pauli matrices and N is the number of spins in the lattice. Having assumed frustrated boundary conditions, we have that $N = 2M + 1$ is odd and $\sigma_j^\alpha \equiv \sigma_{j+N}^\alpha$. The angle $\phi \in (-\frac{\pi}{4}, \frac{\pi}{4})$ tunes the relative weight of the two interactions, as well as the sign of the smaller one. Hence, while the role of the dominant term is always played by the AFM interaction along the x-direction, we have that the second Ising–like interaction switches from FM to AFM at $\phi = 0$.

As discussed in the previous chapter, the symmetries of Hamiltonian 4.1 imply an exact ground-state degeneracy even in finite chains and thus the possibility to

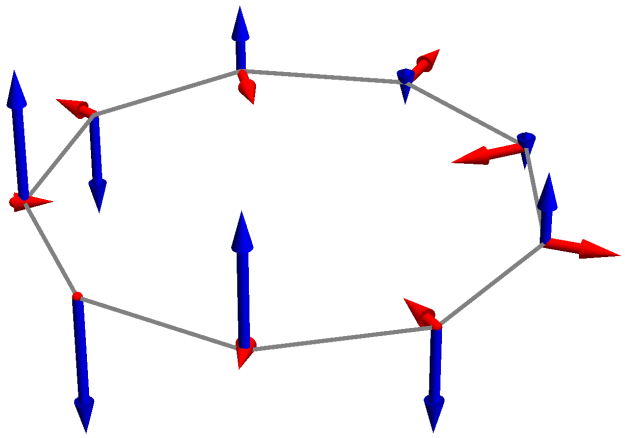

FIGURE 4.1: Site dependent magnetizations along x (Blue darker arrows) and y (Red lighter arrows) for each spin of a lattice with $N = 9$ sites. The magnetizations are obtained setting $\phi = \frac{\pi}{8}$ and recovering the maximum amplitudes $f_x \simeq 0.613$ and $f_y \simeq 0.329$, see discussion around eq. (4.7).

select states with a definite magnetization within the ground state manifold. Furthermore, it is possible to directly evaluate the magnetization of these states: having it as a function of the number of sites of the chain, we can take the thermodynamic limit and thus recover directly its macroscopic value, without resorting to the usual approach making use of the cluster decomposition. Let us repeat the reasoning. Regardless of the value of ϕ, the Hamiltonian in eq. (4.1) commutes with the parity operators ($\Pi^\alpha \equiv \otimes_{i=1}^N \sigma_i^\alpha$), i.e. $[H, \Pi^\alpha] = 0$, $\forall \alpha$. At the same time, since we are considering odd N, different parity operators satisfy $\{\Pi^\alpha, \Pi^\beta\} = 2\delta_{\alpha,\beta}$, hence implying that each eigenstate is at least two-fold degenerate: if $|\psi\rangle$ is an eigenstate of both H and Π^z, then $\Pi^x |\psi\rangle$, that differs from $\Pi^y |\psi\rangle$ by a global phase factor, is also an eigenstate of H with the same energy but opposite z–parity.

Using the standard techniques [56], that consist of the Jordan-Wigner transformation and a Fourier transform followed by a Bogoliubov rotation (more details in Appendix C.2), the Hamiltonian can be reduced to

$$\begin{aligned} H &= \frac{1+\Pi^z}{2} H^+ \frac{1+\Pi^z}{2} + \frac{1-\Pi^z}{2} H^- \frac{1-\Pi^z}{2} , \\ H^\pm &= \sum_{q \in \Gamma^\pm} \varepsilon(q) \left(a_q^\dagger a_q - \frac{1}{2} \right) . \end{aligned} \tag{4.2}$$

Here a_q ($a_q^\dagger$) is the annihilation (creation) fermionic operator with momentum q. The Hilbert space has been divided into the two sectors of different z-parity Π^z. Accordingly, the momenta run over two disjoint sets, corresponding to two sectors: $\Gamma^- = \{2\pi k/N\}$ and $\Gamma^+ = \{2\pi(k+\frac{1}{2})/N\}$ with k ranging over all integers from 0 to $N-1$. The dispersion relation reads

$$\begin{aligned} \epsilon(q) &= 2\left|\cos\phi\, e^{i2q} + \sin\phi\right| , \; q \neq 0, \pi , \\ \epsilon(0) &= -\epsilon(\pi) = 2\left(\cos\phi + \sin\phi\right) , \end{aligned} \tag{4.3}$$

where we note that only $\epsilon(0), \epsilon(\pi)$ can become negative.

The eigenstates of H are constructed by populating the vacuum states $|0^\pm\rangle$ in the two sectors and by taking care of the parity constraints. The effect of frustration is

that the lowest energy states are not admissible due to the parity requirement. For instance, from eq. (4.3) we see that, assuming $\phi \in (-\frac{\pi}{4}, \frac{\pi}{4})$, the single negative energy mode is $\epsilon(\pi)$, which lives in the even sector ($\pi \in \Gamma^+$). Therefore the lowest energy states are, respectively, $|0^-\rangle$ in the odd sector and $a_\pi^\dagger |0^+\rangle$ in the even one. But, since both of them violate the parity constraint of the relative sector, they cannot represent physical states. Hence, the physical ground states must be recovered from $|0^-\rangle$ and $a_\pi^\dagger |0^+\rangle$ considering the minimal excitation coherent with the parity constraint.

While for $\phi < 0$ there is a unique state in each parity sector that minimizes the energy while respecting the parity constraint (and these states both have zero momentum), for $\phi > 0$ the dispersion relation in eq. (4.3) becomes a double well and thus develops two minima: $\pm p \in \Gamma^-$ and $\pm p' \in \Gamma^+$, approximately at $\pi/2$ (for their precise values and more details, see Methods 4.3.1). Thus, for $\phi > 0$ the ground state manifold becomes 4-fold degenerate, with states of opposite parity and momenta. This degeneracy has a solid geometrical origin, which goes beyond the exact solution to which the XY is amenable, and has to do with the fact that, with FBC, the lattice translation operator does not commute with the mirror (or chiral) symmetry, except than for states with 0 or π momentum (see Appendix C.4). Thus, every other state must come in degenerate doublets of opposite momentum/chirality. In accordance to this picture, a generic element in the four-dimensional ground state subspace can be written as

$$|g\rangle = u_1 |p\rangle + u_2 |-p\rangle + u_3 |p'\rangle + u_4 |-p'\rangle \ , \tag{4.4}$$

where the superposition parameters satisfy the normalization constraint $\sum_i |u_i|^2 = 1$, $|\pm p\rangle = a_{\pm p}^\dagger |0^-\rangle$ are states in the odd z-parity sector and $|\pm p'\rangle = \Pi^x |\mp p\rangle = a_{\pm p'}^\dagger a_\pi^\dagger |0^+\rangle$ are the states in the even sector (for the second equality, that holds up to a phase factor, see Methods 4.3.2).

Hence, independently from N, once FBC are imposed, the system presents a level crossing at the point $\phi = 0$, where the Hamiltonian reduces to the classical AFM Ising. The presence of the level crossing is reflected on the behavior of the ground state energy E_g, whose first derivative exhibits a discontinuity

$$\left.\frac{dE_g}{d\phi}\right|_{\phi\to 0^-} - \left.\frac{dE_g}{d\phi}\right|_{\phi\to 0^+} = 2\Big(1 + \cos\frac{\pi}{N}\Big), \tag{4.5}$$

which goes to a nonzero finite value in the thermodynamic limit. The presence of both a discontinuity in the first derivative of the ground state energy, and a different degree of degeneracy even at finite sizes, is coherent with a first-order quantum phase transition [10].

However, such a transition is present only when FBC are considered. Indeed, without frustration, hence considering either OPC or PBC conditions in a system with even N, the two regions $\phi \in (-\frac{\pi}{4}, 0)$ and $\phi \in (0, \frac{\pi}{4})$ belong to the same AFM phase, have the same degree of ground-state degeneracy, and exhibit the same physical properties [90, 91]. Hence it is the introduction of the FBC that induces the presence of a quantum phase transition at $\phi = 0$.

4.1.2 The magnetization

Having detected a novel phase transition, we need to identify the two phases separated by it. In Chapter 3 we have proved that the two-fold degenerate ground

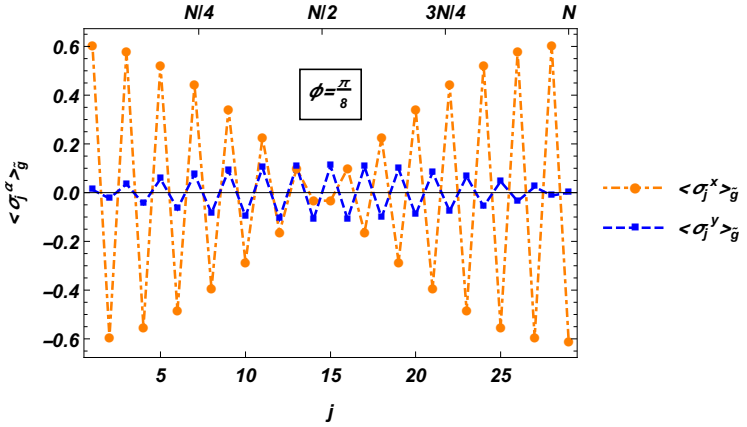

FIGURE 4.2: Plot of the site dependent magnetizations along x (orange points) and y (blue ones) for each spin of a lattice with $N = 29$ sites. The magnetizations are obtained setting $\phi = \frac{\pi}{8}$. The dashed lines are a guide to the eye to show the almost staggered order, while the modulation in space is given by eq. 4.7.

state for $\phi < 0$ is characterized by a ferromagnetic mesoscopic order: for any finite odd N, the chain exhibits non-vanishing, site-independent, ferromagnetic magnetizations along any spin directions. These magnetizations scale proportionally to the inverse of the system size and, consequently, vanish in the thermodynamic limit. For suitable choices of the ground state, this mesoscopic magnetic order is present also for $\phi > 0$ but, taking into account that now the ground state degeneracy is doubled, the new phase can also show a different magnetic order, that is forbidden for $\phi < 0$. However, from all the possible orders that can be realized we can, for sure, discard the standard staggerization that characterizes the AFM order in the absence of FBC. In fact, for odd N, it is not possible to align the spins perfectly antiferromagnetically, while still satisfying PBC. In a classical system, the chain develops a ferromagnetic defect (a domain wall) at some point, but quantum-mechanically this defect gets delocalized and its effect is not negligible in the thermodynamic limit as one would naively think.

To study the magnetization let us consider a ground state vector that is not an eigenstate of the translation operator:

$$|\tilde{g}\rangle = \frac{1}{\sqrt{2}}\left(|p\rangle + e^{\imath\theta} |p'\rangle \right) , \tag{4.6}$$

where θ is a free phase. We compute the expectation value of spin operators on this state. Having broken translational invariance, we can expect the magnetization to develop a site dependence, which can be found by exploiting the translation and the mirror symmetry (see Methods 4.3.2), giving

$$\langle \sigma_j^\alpha \rangle_{\tilde{g}} \;=\; (-1)^j \cos\left[\pi \frac{j}{N} + \lambda(\alpha, \theta, N) \right] f_\alpha \, , \tag{4.7}$$

where $f_\alpha \equiv |\langle p| \sigma_N^\alpha |p'\rangle|$. The two phase factors, whose explicit dependence on the arbitrary phase θ is given in Appendix C.6.1, are related as $\lambda(y, \theta, N) - \lambda(x, \theta, N) = \pi/2$, which corresponds to a shift by half of the whole ring between the x and y magnetization profiles. The obtained spatial dependence, depicted in Figure 4.1 and 4.2, thus breaks lattice translational symmetry, not to a reduced symmetry as in the

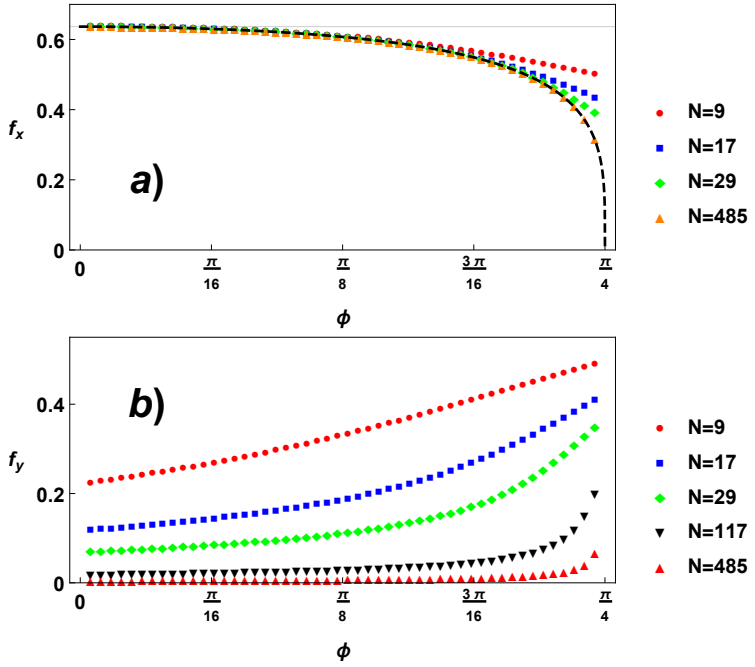

FIGURE 4.3: Behavior of matrix elements f_x (upper panel) and f_y (lower panel) as function of the Hamiltonian parameter ϕ for different sizes of the the system N.

case of the staggerization that characterizes the standard AFM order, but completely, since we have an incommensurate modulation that depends on the system size overimposed to the staggerization.

While the simple argument just presented explains how and why the magnetizations along x and y acquire a nontrivial spatial dependence, we still have to determine how their magnitudes scale with N. The magnitudes depend on the spin operator matrix elements $\langle p|\, \sigma_N^\alpha \,|p'\rangle$ and their evaluation is explained in Methods 4.3.3.

As we can see from Figure 4.3, we have two different behaviors for the magnetizations along x and y. While for the former we can see that it admits a finite non zero limit, which is a function of the parameter $\phi > 0$, the latter, for large enough systems, is proportional to $1/N$ (see also Figure 4.4) and vanishes in the thermodynamic limit. Hence, differently from the one along the y spin direction, the *"incommensurate antiferromagnetic order"* along x survives also in the thermodynamic limit. By exploiting perturbative analysis around the classical point $\phi = 0$ it is possible to show that, for $\phi \to 0^+$ and diverging N, f_x goes to $2/\pi$ (see Appendix C.7 for details). Moreover, numerical analysis has also shown that in the whole region $\phi \in (0, \pi/4)$ we have

$$\lim_{N\to\infty} |\, \langle p|\, \sigma_N^x \,|p'\rangle \,| = \frac{2}{\pi}(1 - \tan^2\phi)^{\frac{1}{4}} \,. \tag{4.8}$$

4.2 Conclusions

Summarizing, we have proved how, in the presence of FBC, the Hamiltonian in eq. (4.1) shows a quantum phase transition for $\phi = 0$. Such transition is absent both for OBC and for systems with PBC made of an even number of spins. This quantum phase transition separates two different gapless, non-relativistic phases that, even at a finite size, are characterized by different values of ground-states degeneracy: one

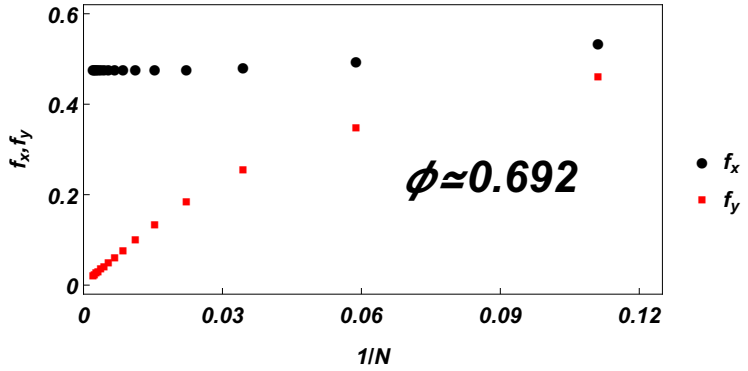

FIGURE 4.4: Dependence of the two $f_\alpha = |\langle p|\, \sigma_N^\alpha\, |p'\rangle|$ on the inverse of the size of the system $1/N$ for $\phi \simeq 0.692$. The black points represent the values obtained for f_x while the red squares stand for f_y

shows a two-fold degenerate ground-state, while in the second we have a four-fold degenerate one. This difference, together with the fact that the first derivative of the ground-state energy shows a discontinuity in correspondence with the change of degeneracy, supports the idea that there is a first-order transition.

The two phases display the two ways in which the system can adjust to the conflict between the local AFM interaction and the global FBC: either by displaying a mesoscopic ferromagnetism, whose magnitude decays to zero with the system size [1], as discussed in Chapter 3, or through an approximate staggerization, so that the phase difference between neighboring spins is $\pi\left(1 \pm \frac{1}{N}\right)$. For large systems, these $1/N$ corrections induced by frustration are indeed negligible at short distances. However, they become relevant when fractions of the whole chain are considered. Crucially, the latter order spontaneously breaks translational invariance and remains finite in the thermodynamic limit. Let us remark once more that, with different boundary conditions, all these effects are not present.

The results presented in this work are much more than an extension of those in Chapter 3, where we have already proved that FBC can affect local order. While there AFM was destroyed by FBC and replaced with a mesoscopic ferromagnetic order, here we encounter a different type of AFM order, which spontaneously breaks translational invariance, is modulated in an incommensurate way, and does not vanish in the thermodynamic limit. Most of all, the transition between these two orders is signaled by a discontinuity in the derivative of the free energy, indicating a first-order quantum phase transition.

The phase transition we have found resembles several well-known phenomena of quantum complex systems, without being completely included in any of them. A finite difference of the values of the free energy derivative at two sides of the transition characterizes also first-order wetting transitions [152–154], that are associated to the existence of a border. On the other hand, in our system, we cannot individuate any border, since the chain under analysis is perfectly invariant under spatial translations. Delocalized boundary transitions have already been reported and are called "interfacial wetting", but they differ from the phenomenology we discussed here, as they refer to multi-kink states connecting two different orders (prescribed at the boundary) separated by a third intermediate state [155].

The transition we have found, and the incommensurate order, might also be explored experimentally. To observe them, one could, for example, measure the magnetization at different positions in the ring. In the phase exhibiting incommensurate

AFM order, the measurements will yield different values at different positions, while in the other phase, exhibiting mesoscopic ferromagnetic order the values are going to be the same. One could also examine the maximum value of the magnetization over the ring. In the incommensurate AFM phase this value is finite, while in the other it goes to zero in the thermodynamic limit. The maximum of the magnetization over the ring thus exhibits a jump at the transition point.

The strong dependence of the macroscopic behavior on boundary conditions that we have found seemingly contradicts the Landau theory, that implicitly assumes microscopic changes, such as the boundary conditions, are negligible in the thermodynamic limit. Indeed, FBC are special, as the kind of spin chains we consider are the building blocks of every frustrated system [28–30, 156–158] , which are known to present peculiar properties. We can also speculate that FBC induce a topological effect that puts the system outside the range of validity of the standard theory. In fact, while in the ferromagnetic phases of the model the ground state degeneracy in the thermodynamic limit is independent of boundary conditions, in the parameter region exhibiting incommensurate AFM order the degeneracy is doubled with FBC, thus clearly depending on the (real space) topology of the system. But, there is a second more subtle connection. Indeed, while magnetic phases show symmetry-breaking order parameters, topological phases are characterized by the expectation value of a non-local string operator that does not violate the bulk symmetry of the system. In our system, as we have shown before, the value of the local magnetization is associated with the expectation value of the operator $\sigma_N^x \Pi^x = \bigotimes_{j=1}^{N-1} \sigma_j^x$, which is a string operator that does not break the parity symmetries of the model. However, while geometrical frustration induces some topological effects in the XY chain, interestingly, we have found evidence that suggests that topological phases are resilient to topological frustration [5], as we discuss in Chapter 8.

A natural question that emerges is how robust is the observed phenomenology to defects, that destroy the translational symmetry of the model. In fact, a common expectation is that such defect would pin the domain wall and restore the unfrustrated physics in the bulk. In Chapter 5 we address this question and show that a complex picture emerges depending on the nature of the defects, but that ultimately the incommensurate AFM order can survive under general conditions. Thus, the physics we have discussed here goes beyond fine-tuned properties, to a physically measurable phenomenon.

4.3 Methods

4.3.1 Ground state degeneracy

We have two different pictures depending on the sign of ϕ. For $\phi < 0$ the excitation energy, given by eq. (4.3), admits two equivalent local minima, one for each parity, i.e. $q = 0 \in \Gamma^-$ and $q = \pi \in \Gamma^+$. Consequently, the ground state is two-fold degenerate, and the two ground states that are also eigenstates of Π^z are $|g_0^-\rangle = a_0^\dagger |0^-\rangle$ and $|g_0^+\rangle = \Pi^x |g_0^-\rangle = |0^+\rangle$, where the last equality holds up to a phase factor. On the contrary, when ϕ becomes positive, the energy in eq. (4.3) admits, for each z-parity sector, two local minima at opposite momenta, $\pm p \in \Gamma^-$ and $\pm p' \in \Gamma^+$, where $p = \frac{\pi}{2}\left(1 - \frac{1}{N}\right)$ for a system size N satisfying $N \bmod 4 = 1$, $p = \frac{\pi}{2}\left(1 + \frac{1}{N}\right)$ for $N \bmod 4 = 3$ and $p' = \pi - p$.

4.3.2 Spatial dependence of the magnetization

To study the spatial dependence of the magnetization it is useful to introduce the unitary lattice translation operator T, whose action shifts all the spins by one position in the lattice as

$$T^\dagger \sigma_j^\alpha T = \sigma_{j+1}^\alpha, \quad \alpha = x, y, z \tag{4.9}$$

and which commutes with the system's Hamiltonian in eq. (4.1), i.e. $[H, T] = 0$. The operator T admits, as a generator, the momentum operator P, i.e. $T = e^{\imath P}$. Among the eigenstates of P, we have the ground state vectors $|\pm p\rangle$ and $|\pm p'\rangle$ with relative eigenvalues equal to $\pm p$ and $\pi \pm p' = \mp p$. A detailed definition of the operator and a proof of these properties is given in Appendix C.3. The latter equality allows to identify the ground states $a^\dagger_{\pm p'} a^\dagger_\pi |0^+\rangle$ with the states $\Pi^x |\mp p\rangle$.

We can exploit the properties of the operator T to determine, for each odd N, the spatial dependence of the magnetizations along x and y in the ground state $|\tilde{g}\rangle$ ($\langle \sigma_j^\alpha \rangle_{\tilde{g}}$ with $\alpha = x, y$), defined in eq. (4.6). In fact, taking into account that $|p\rangle$ and $|p'\rangle$ live in two different z-parity sectors, we have that the magnetization along a direction orthogonal to z on the state $|\tilde{g}\rangle$ is given by

$$\langle \sigma_j^\alpha \rangle_{\tilde{g}} = \langle \tilde{g} | \sigma_j^\alpha | \tilde{g} \rangle = \frac{1}{2} \left(e^{\imath\theta} \langle p | \sigma_j^\alpha | p' \rangle + e^{-\imath\theta} \langle p' | \sigma_j^\alpha | p \rangle \right). \tag{4.10}$$

The magnetization is determined by the spin operator matrix elements $\langle p | \sigma_j^\alpha | p' \rangle$, that can all be related to the ones at the site $j = N$. In fact, considering eq. (4.9) we obtain

$$\langle p | \sigma_j^\alpha | p' \rangle = e^{-\imath 2pj} \langle p | \sigma_N^\alpha | p' \rangle \ . \tag{4.11}$$

The advantage of this representation is that the matrix element $\langle p | \sigma_N^\alpha | p' \rangle$ is a real number for $\alpha = x$, and a purely imaginary one for $\alpha = y$, making it simple to express the magnetization. Let us illustrate the computation of the x magnetization, while the details for the y magnetization can be found in Appendix C.6.1. The special role of the site N is singled out by the choice made in the construction of the states through the Jordan-Wigner transformation. To prove that the matrix element is real it is useful to introduce the, unitary and hermitian, mirror operator with respect to site N, denoted as M_N, that makes the mirroring

$$M_N \sigma_j^\alpha M_N = \sigma_{-j}^\alpha, \quad \alpha = x, y, z, \tag{4.12}$$

and, in particular, leaves the N-th site unchanged. The operator satisfies $M_N |\pm p\rangle = |\mp p\rangle$, while the reflections with respect to other sites would introduce additional phase factors. A detailed definition of the mirror operators and discussion of their properties is given in C.4. Exploiting the properties of M_N we have then

$$\langle p | \sigma_N^x \Pi^x | -p \rangle = \langle -p | \sigma_N^x \Pi^x | p \rangle = (\langle p | \sigma_N^x \Pi^x | -p \rangle)^*, \tag{4.13}$$

so $\langle p | \sigma_N^x | p' \rangle$ is real. Evaluating $\langle p | \sigma_N^x | p' \rangle$ using the methods of the next section we can see that the quantity is actually positive, and therefore equal to its magnitude f_x. Then from eq. (4.10) and (4.11) we get the spatial dependence of the magnetization

$$\langle \sigma_j^x \rangle_{\tilde{g}} = \cos(2pj - \theta) \langle p | \sigma_N^x | p' \rangle . \tag{4.14}$$

Inserting the exact value of the momentum we get eq. (4.7) for $\alpha = x$, where the exact value of $\lambda(x, \theta, N)$ is given in Appendix C.6.1.

4.3.3 Scaling of the magnetization with N

The magnetization is determined by the matrix elements $f_\alpha = |\langle p|\, \sigma_N^\alpha\, |p'\rangle|$. To evaluate them we exploit a trick similar to the one used to compute the magnetization in Chapter 3.

Within the ground state manifold, we define the vectors

$$|g_\pm\rangle \equiv \frac{1}{\sqrt{2}}(|p\rangle \pm |-p\rangle), \tag{4.15}$$

and, further using the, already introduced, properties of the mirror operator M_N (see Appendix C.6.2 for details), we get

$$\langle p|\, \sigma_N^\alpha\, |p'\rangle \;=\; \frac{1}{2}\Big(\langle g_+|\, \sigma_N^\alpha \Pi^x\, |g_+\rangle - \langle g_-|\, \sigma_N^\alpha \Pi^x\, |g_-\rangle\Big)\,. \tag{4.16}$$

In this way, we represent a notoriously hard one point function in terms of standard expectation values of products of an even number of spin operators $\sigma_N^\alpha \Pi^x$, which can be expressed as a product of an even number (parity preserving) of fermionic operators. Using Wick's theorem, the expectation values can then be expressed as determinants and evaluated numerically efficiently (see Appendix C.6.2).

Moreover, in the limit $\phi \to 0^+$ the matrix elements can also be evaluated analytically using a perturbative approach (see Appendix C.7).

Chapter 5

XY Chain with Bond Defects

In the previous chapters we have shown that frustrated boundary conditions, that is, periodic boundary conditions with an odd number of lattice sites, can affect the bulk, local, order in antiferromagnetic systems. For the quantum XY chain in zero external fields, the usual antiferromagnetic order has been found to be replaced either by mesoscopic ferromagnetic order or by incommensurate AFM order. In this chapter we examine the resilience of these types of orders against a defect that breaks the translational symmetry of the model. We find that, while a ferromagnetic defect restores the traditional, staggered order, an AFM one stabilizes the incommensurate order. The robustness of the frustrated order to certain kinds of defects paves the way for its experimental observability. This chapter is based on [4].

5.1 Introduction

In general, it is known that the presence of defects in a spin chain can induce a very rich phenomenology [159] and can influence the system geometry [160]. The concept of topological frustration, in particular, is related to defects, as it is present depending on the nature of the interaction at a single bond in the system. In this line of research, it is known from the results by Campostrini *et al.* [67] that a one-bond defect drives a quantum phase transition in the quantum Ising antiferromagnet, between a *magnetic phase* when the defect favors a ferromagnetic order on a bond, and a *kink phase* with an AFM defect. The two phases are characterized by a different scaling of the energy gap above the ground state. The magnetic phase is gapped, with an exponential closing of the gap between the two quasi-degenerate ground states, while the kink phase is gapless, with the ground state being part of an energy band and an algebraic closing of the gap. The frustrated boundary conditions (FBC) represent exactly the transition point, with a universal scaling behavior of low energy properties close to it.

In this chapter we extend the analysis of chapters 3 and 4, by investigating how are the local orders in the quantum XY chain with frustrated boundary conditions, discovered there, affected by the presence of a localized defect. Under usual conditions, one does not expect that such defect can affect the system beyond some finite distance around it. Even more, since the ground state with FBC is interpreted as a single excitation state, the effect of a defect could be to localize this excitation, thus restoring the traditional order, except for an exponentially limited area whose relevance, in the thermodynamic limit, becomes negligible. These considerations are probably one of the reasons for which the aforementioned orders emerging with FBC have been overlooked for too long: they have been expected to be too weak against a defect and thus impossible to be detected experimentally. We will show that this picture is correct only when a ferromagnetic type defect (FTD), i.e. a defect

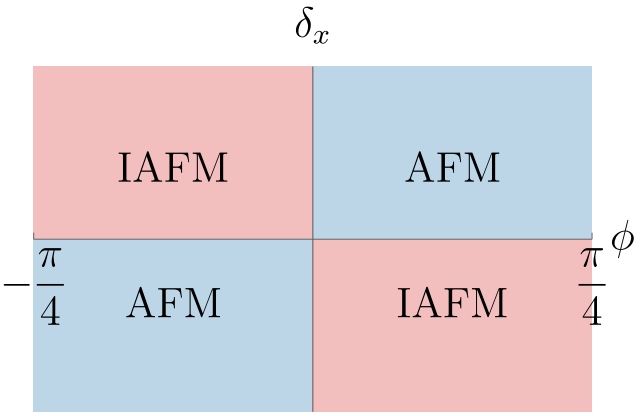

FIGURE 5.1: Schematic representation of different phases as a function of the system parameters. The interval $\phi \in (-\pi/4, \pi/4)$ corresponds to a dominating antiferromagnetic interaction along the x axis. When the defect of the form $(\delta_x \neq 0, \delta_y = 0)$ favours a ferromagnetic alignment (FTD), the effect of the defect is localized in a small region and outside it the standard AFM order is restored. On the other hand, when the defects tends to strengthen the antiferromagnetic interaction (AFTD) the incommensurate AFM order (IAFM) is realized.

that reduces the relative weight of the dominant AFM term, is considered. On the contrary, when we take into account an antiferromagnetic type defect (AFTD), i.e. a defect that locally increases the dominant AFM term, an incommensurate AFM order is induced in the system. This incommensurate AFM order holds a magnetic pattern very close to the one in Chapter 4, but is, differently from it, associated to a two-fold degenerate ground-state and not to a four-fold one. Furthermore, while the mesoscopic ferromagnetic order described in Chapter 3 does not seem to survive the presence of a defect, the incommensurate AFM order is found to be resilient also to the presence of a second defect, indicating that it can be observed under relatively general conditions with FBC. The emergence of two different orders (i.e. the standard AFM and the incommensurate staggered one) signals the existence of a quantum critical point (QPT) separating them. The QPT we observe with the defect is thus a similar phenomenology as the one observed in [67] for the quantum Ising chain, but due to the symmetries of our model, we are able to apply the approach to symmetry breaking based on anticommuting symmetries, discussed in section 1.2.3, and discuss local order.

This chapter is organized as follows. In Section 5.2 we introduce the model under study and briefly review its properties in the absence of defects. In Section 5.3 we describe the analytical and numerical techniques we use to analyze the effects of adding the defect, which requires particular care due to the gapless nature of the system without defects. In Section 5.4 we show and discuss the results for various types of perturbations. Conclusions and outlook are collected in Section 5.5.

5.2 The Model

We focus on the XY chain at zero fields with FBC and a local defect that, without the loss of generality, we set between the first and the last spin of the chain. Such a

system is described by the Hamiltonian

$$H = \sum_{j=1}^{N-1} \cos\phi\ \sigma_j^x \sigma_{j+1}^x + \sum_{j=1}^{N-1} \sin\phi\ \sigma_j^y \sigma_{j+1}^y + \\ + \cos(\phi+\delta_x)\ \sigma_N^x \sigma_1^x + \sin(\phi+\delta_y)\ \sigma_N^y \sigma_1^y, \tag{5.1}$$

where σ_j^α, for $\alpha = x, y, z$, are Pauli operators defined on the j-th spin and the FBC are achieved by imposing periodic boundary conditions $\sigma_{N+j}^\alpha \equiv \sigma_j^\alpha$ and an odd number N of lattice sites. The parameter ϕ tunes the relative strength between the interactions along the x and y directions, while δ_x and δ_y govern the strength of the defect along the x and y axis respectively. The presence of the defect in the interaction pattern destroys the translational invariance of the model and all its mirror symmetries, except the one with respect to the $(N+1)/2$-th spin.

This is, clearly, not the most general defect that we can consider. The reason behind our choice is that the Hamiltonian in eq. (5.1) still preserves the parity symmetries, $[H, \Pi^\alpha] = 0$ with $\Pi^\alpha = \bigotimes_{j=1}^N \sigma_j^\alpha$, with respect to all the three spin directions, $\alpha = x, y, z$, as the unperturbed model. This property is of particular relevance in our analysis, because, as in chapters 3 and 4, it implies an exact degeneracy for the ground state already in a finite system when N is odd. Again, since N is odd, parity operators anti-commute ($\{\Pi^\alpha, \Pi^\beta\} = 2\delta_{\alpha\beta}$). Hence, if the state $|\varphi\rangle$ is an eigenstate of both the Hamiltonian and one of the parity operators, say Π^z, the state $\Pi^x |\varphi\rangle$ is still an eigenstate of both H and Π^z but has the opposite Π^z eigenvalue. Hence, each eigenstate of the Hamiltonian is (at least) two-fold degenerate even at finite size. This degeneracy enables us to study the magnetization directly, even in a finite system, exploiting the trick introduced in chapters 3 and 4.

Before starting our analysis, let us briefly review here the main findings of chapters 3 and 4, that deal with the model obtained by setting $\delta_x = \delta_y = 0$ in eq. (5.1). For ϕ in the region $(-3\pi/4, -\pi/4)$ the dominant term is the ferromagnetic interaction along the y direction (yFM phase). In the thermodynamic limit, the two-fold degenerate ground state manifold is separated from the rest of the spectrum by a finite energy gap and admits a ferromagnetic magnetization along y-axis, $m_y = \langle \sigma_j^y \rangle$. This phenomenology is the same to the one that can be found taking into account open boundary conditions or an even number of spins [90, 91, 150]. On the contrary, due to topological frustration, a different type of order is found in the region $\phi \in (-\pi/4, \pi/4)$, where the antiferromagnetic interactions dominate. Without frustration, this region would be simply a x-AFM phase characterized by a staggered magnetization. Instead, assuming FBC, it is separated into two gapless regions (the energy gap closing as $1/N^2$), $\phi \in (-\pi/4, 0)$ and $\phi \in (0, \pi/4)$, characterized by different ground state degeneracies and different magnetization patterns. Moreover, the transition is accompanied by a finite discontinuity in the first derivative of the ground state energy at $\phi = 0$.

For $\phi \in (-\pi/4, 0)$, where the dominant antiferromagnetic interaction in the x direction competes with the ferromagnetic one in the y direction, the ground state manifold is two-fold degenerate. Although the dominant interaction along x is antiferromagnetic, the magnetization $m_x(j) = \langle \sigma_j^x \rangle$ (as well as $m_y(j), m_z(j)$) is found to be uniform, ferromagnetic, and decays algebraically with the system size to zero, as $1/N$, resulting in the zero value of the magnetization in the thermodynamic limit. Qualitatively, this behavior stems from the fact that with an odd number of sites with periodic boundary conditions, a staggered order cannot be sustained, and thus the delocalized kink contribution eventually destroys the AFM order. Because of these

properties, this order is termed *Mesoscopic Ferromagnetic Order* [1] (see Chapter 3).

For $\phi \in (0, \pi/4)$, where both interactions are antiferromagnetic, a more rich behavior is found. The ground state manifold is four-fold degenerate and it is possible to select ground states with different properties. While there are states that also exhibit mesoscopic ferromagnetic order, it is also possible to select states with a magnetization profile that varies in space with an incommensurate pattern and survives in the thermodynamic limit. Qualitatively, in this case, the system accommodates the frustration with a small shift in the staggered order, so that the magnetization varies as $\sin\left[\pi\left(1-\frac{1}{N}\right)j+\alpha\right]$: neighboring sites are almost perfectly staggered, but along the chain, the amplitude varies and at its minimum one finds a ferromagnetic bond. This new type of order has been termed *Incommensurate Antiferromagnetic Order* [2] (see Chapter 4).

5.3 Methods

The model in eq. (5.1) can be analyzed by mapping spins into spinless non-interacting fermions through the Jordan-Wigner transformations [91, 149]. Usually, in systems that can be solved exploiting the Jordan-Wigner transformation, followed by a Bogoliubov rotation in Fourier space, all the physical quantities can be obtained in terms of two-body correlation functions of Majorana operators that are determined analytically [90, 91, 161–163]. However, in the present case, the local perturbation explicitly breaks the invariance under spatial translation and, therefore, prevents the possibility to obtain analytical expressions for the Majorana correlation functions. Nevertheless, since the Hamiltonian in eq. (5.1), is quadratic in the spinless fermion operators, we construct an efficient algorithm, based on the work of Lieb *et al.* [91], to obtain a numerical evaluation of the whole set of Majorana correlation functions that allows to obtain all the analyzed quantities following the standard approach (see Appendix D.1 for details).

Usually, a finite longitudinal field is required to have a finite magnetization in the x-direction. The persistence of a finite value even after the removal of the field, after taking the thermodynamic limit, is the signature of a spontaneous symmetry breaking. However, in our case, we are working at zero fields to have an exact degeneracy between states with different parities, so that the system can exhibit a finite magnetization, even at a finite size, without the need to apply a symmetry-breaking field. Since the different parity operators do not commute with each other, any ground state vector necessarily breaks at least one of those symmetries. Once the magnetizations are obtained for a chosen N, we follow this value toward the thermodynamic limit to determine which order survives for large systems. Taking inspiration from the result obtained in the absence of defects [1, 2] (see chapters 3 and 4), we focus mainly on the study of the pattern of the magnetization in the x direction $m_x(j) = \langle \sigma_j^x \rangle$, which is maximized by taking into account the states with definite Π^x parity. The state with $\Pi^x = \pm 1$ reads

$$|g\rangle = \frac{1}{\sqrt{2}}(\mathbb{1} \pm \Pi^x)\,|g^-\rangle \ . \tag{5.2}$$

Here $|g^-\rangle$ is the ground state of the Hamiltonian in eq. (5.1) that falls in the odd sector of Π^z. Exploiting the trick introduced in Chapter 3, we can express the expectation value of σ_j^x on $|g\rangle$ with $\Pi^x = 1$ in terms of the expectation value of the

operator $\sigma_j^x \Pi^x$ on $|g^-\rangle$, i.e.

$$m_x(j) \equiv \langle g| \sigma_j^x |g\rangle = \langle g^-| \sigma_j^x \Pi^x |g^-\rangle , \tag{5.3}$$

which can be computed using the fermionic representation of the model, as discussed in Appendix D.1. The state with $\Pi^x = -1$ would just exhibit the magnetization $\langle \sigma_j^x \rangle$ of the opposite sign.

To further corroborate these results, we also employ an analytical perturbation theory, in two different ways. Treating either ϕ or δ_x in eq. (5.1) as a small parameter, we diagonalize the perturbation either in the kink state basis or just in the four-dimensional ground state manifold on the unperturbed model. Details are given in Appendix D.2. The first approach is more insightful and successful in describing the numerical results, while the second gives a more quantitative agreement for the incommensurate AFM order, although the truncation of the basis to just four states is only empirically justified.

While for defect strengths $\delta_{x,y}$ that go to zero sufficiently fast with the system size ($\delta_{x,y} \to 0$ as $N \to \infty$) the orders found with FBC should be preserved, we are interested in determining the resilience of these orders to the presence of a finite, fixed, defect, in the thermodynamic limit. To do so, we fix the strength (in absolute value) of the defect to be comparable with the energy width of the (unperturbed) lowest energy band, namely $|\delta_{x,y}| = |\phi|/10$. In this way, the defect always hybridizes several states of band.

In our analysis, we will have to face several different magnetization patterns and, hence, we have to find a way to discriminate among them. Even if, sometimes, it would be enough to look at a direct plot of the magnetizations to guess what kind of pattern is realized in the system, it is better to have a more quantitative way to discriminate between them. For this reason we decide to focus on the analysis of the Discrete Fourier Transform (DFT) of the magnetization:

$$\tilde{m}_x(k) \equiv \frac{1}{N} \sum_{j=1}^{N} m_x(j) e^{\frac{2\pi i}{N} kj}, \quad k = 1, \dots, N. \tag{5.4}$$

Hence, to determine the asymptotic behavior of the magnetization pattern in the thermodynamic limit, we will perform a finite size scaling analysis of the DFT, and compare the obtained result with some reference patterns.

For instance, the incommensurate AFM order has $\tilde{m}_x(k) \propto \delta_{k,\frac{N\pm1}{2}}$, while the mesoscopic ferromagnetic order would have $\tilde{m}_x(k) \propto \delta_{k,N}$, but with an amplitude decaying algebraically to zero as $N \to \infty$. Finally, a perfectly staggered order would have π-momentum, which is, however, not allowed by the quantization rules with FBC. The staggered order $m_x(j) = (-1)^j$, that has $m_x(N) = m_x(1)$ and the remaining bonds antiferromagnetic, would, on the other hand, be resolved over the allowed momenta as

$$\tilde{m}_x(k) \propto \frac{1}{1 + e^{-\frac{2\pi i}{N} k}} . \tag{5.5}$$

5.4 Results

In our analysis we study the behavior of the magnetization $m_x(j)$ in the presence of a defect for finite chains and then extrapolate the behavior in the thermodynamic limit. First we focus on the case where the defect affects only one spin direction, and then we switch to the case where the defect acts on both.

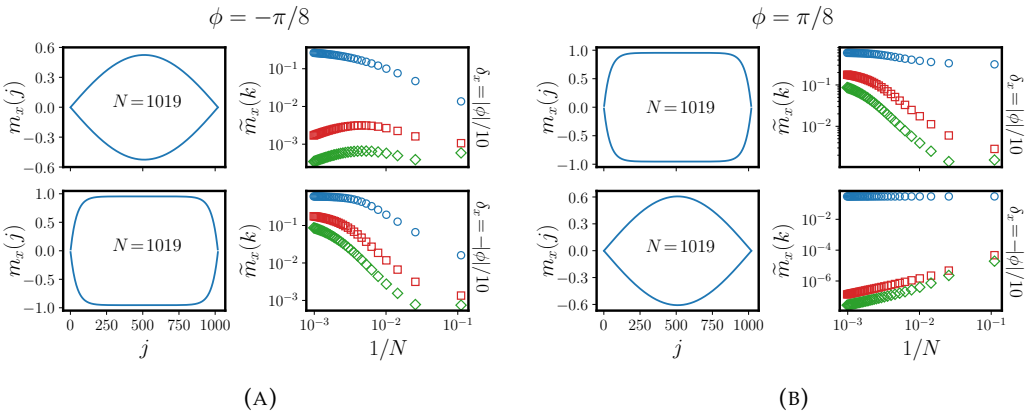

FIGURE 5.2: Magnetization $m_x(j) = \langle \sigma_j^x \rangle$ as a function of the site j for a chain made of $N = 1019$ spins (left), and the absolute value of its Discrete Fourier transform (DFT) (5.4) as a function of the inverse chain length, for chain lengths up to $N = 2001$ (right) and for different momenta: green diamonds $|\tilde{m}_x(\frac{N\pm5}{2})|$, red squares $|\tilde{m}_x(\frac{N\pm3}{2})|$, and blue circles $|\tilde{m}_x(\frac{N\pm1}{2})|$. The results are obtained considering the defect only along the x direction ($\delta_y = 0$). An antiferromagnetic defect yields an incommensurate AFM order, while a ferromagnetic one gives standard AFM order in the bulk (see text for discussion).

Before starting a detailed discussion, in Fig. 5.1 we depict a schematic phase diagram of the system in the presence of a defect with $(\delta_x \neq 0, \delta_y = 0)$, where we can see that the system shows two clearly different behaviors. As we can see from Fig. 5.2, when the defect tends to strengthen the AFM interactions, i.e. when an AFTD defect is considered, the max of the DFT $\tilde{m}_x(k)$, that is obtained for $k = \frac{N\pm1}{2}$, goes to a non-zero value as the system size diverges, while $\tilde{m}_x(k)$ vanishes for all other momenta. This picture is coherent with an incommensurate AFM order in which the site-dependent magnetization is proportional to $\sin\left[\pi(1-\frac{1}{N})j\right]$ as can also be seen from the plots of the envelopes obtained for $N = 1019$ spins. It is worth noting that the incommensurate AFM order is found both for $\phi \in (0, \pi/4)$ and for $\phi \in (-\pi/4, 0)$, although in the latter region, without perturbation, a mesoscopic ferromagnetic order was present. Thus an AFTD stabilizes the incommensurate AFM order, regardless of the order that characterizes the unperturbed underlying model.

A peculiar feature needs commenting: although one could naively expect that a stronger AFM bond would concentrate around the defect the largest magnetization amplitude, this is not the case and one observes the magnetization minimum at the defect. We do not have a proper qualitative explanation for this behavior, although the perturbative calculations below provide some technical justifications. It seems that the system prefers to have the most constant magnetization profile far away from the defect, so that at the center of the chain the order is hardly distinguishable from the unfrustrated one. Although the effect of FBC is to excite a single quasi-particle over the vacuum, we cannot characterize the observed position of the magnetization minimum as anything else but a many-body effect.

As we mentioned above, a single bond defect breaks all the mirror symmetries of the chain, except the one crossing the site $\frac{N+1}{2}$. Accordingly, the magnetization pattern with an AFTD satisfies this mirror symmetry with respect to this site and one can wonder how much this fact constraints its regular structure. Hence, a question that arises naturally is if the incommensurate AFM pattern survives even when the second localized defect is added to the Hamiltonian in eq. (5.1), to break also the

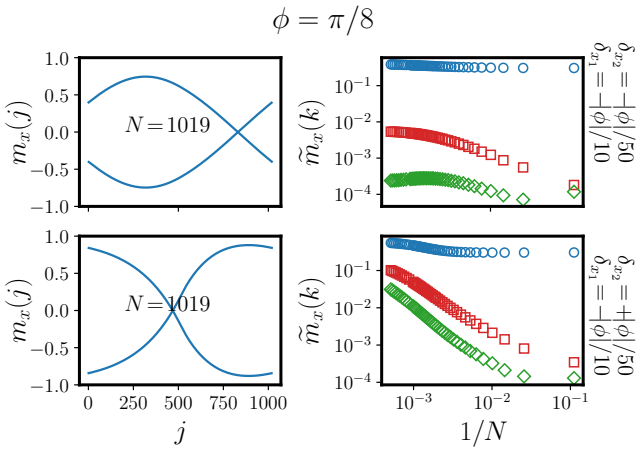

FIGURE 5.3: Magnetization with two bond defects, one between the first and the last spin of the chain (δ_{x_1}), and the second between the $\frac{N-1}{2}$-th and the $\frac{N+1}{2}$-th spin (δ_{x_2}). On the left, the magnetization $m_x(j) = \langle \sigma_j^x \rangle$ as a function of the site j for $N = 1019$ and on the right the absolute value of its Discrete Fourier transform (DFT) (5.4) as a function of the inverse chain length, up to $N = 2001$, for different momenta: green diamonds $|\widetilde{m}_x(\frac{N\pm5}{2})|$, red squares $|\widetilde{m}_x(\frac{N\pm3}{2})|$, and blue circles $|\widetilde{m}_x(\frac{N\pm1}{2})|$. The results are obtained considering the defects only along the x direction ($\delta_{y_1} = \delta_{y_2} = 0$). While in the case when both defects are AFTD (upper row) the DFT clearly signals the rising of a macroscopic incommensurate staggerization in which the magnetization on the j-th spin is proportional to $\sin\left[\pi(1-\frac{1}{N})j\right]$, when the smaller defect is FTD the system sizes considered are not sufficient to clearly characterize the emerging order.

remaining mirror symmetry. Thus, we introduce a smaller bond defect between the $\frac{N-1}{2}$-th and the $\frac{N+1}{2}$-th spins. The results for this case are presented in Fig. 5.3. Due to the second defect, the convergence of the DFT is quite slow and chains longer than $N = 2001$ would be required to clearly reach the asymptotic behavior, especially when the weaker defect is FTD. Nonetheless, when both defects are AFTD, it seems that once more an incommensurate AFM order is established, proving that its existence is not dependent on the presence of a mirror symmetry which needs to be respected. All these results indicate that, even under realistic experimental situations (i.e. without perfect translational invariance), the incommensurate AFM can exist and be observed. As a side note, while the defects are placed on the same bonds in both cases, with two AFTDs, the minimum of the magnetization is located at an intermediate point between them, while the FTD fixes it very close to itself, but not on it, probably because of a finite correlation length.

Turning back to the case of a single defect, the picture changes abruptly when the defect turns to be an FTD, i.e. when it starts to suppress the dominant antiferromagnetic interaction on one bond. Not only the maximum, but all $\widetilde{m}_x(k)$ go towards finite values, satisfying precise ratio rules, such as $\frac{\widetilde{m}_x(\frac{N\pm3}{2})}{\widetilde{m}_x(\frac{N\pm1}{2})} = \frac{1}{3}, \frac{\widetilde{m}_x(\frac{N\pm5}{2})}{\widetilde{m}_x(\frac{N\pm1}{2})} = \frac{1}{5}$ etc. This behavior is compatible with a perfectly staggered AFM order in the bulk, with deviations localized around the defect. As mentioned above, such bulk behavior would be characterized by a sharp peak at π, corresponding to a wavenumber $N/2$, which, being N odd, is not allowed. The aforementioned ratios can be easily obtained by taking the $N \to \infty$ limit of eq. (5.5) and reflect the expansion of a perfect AFM order

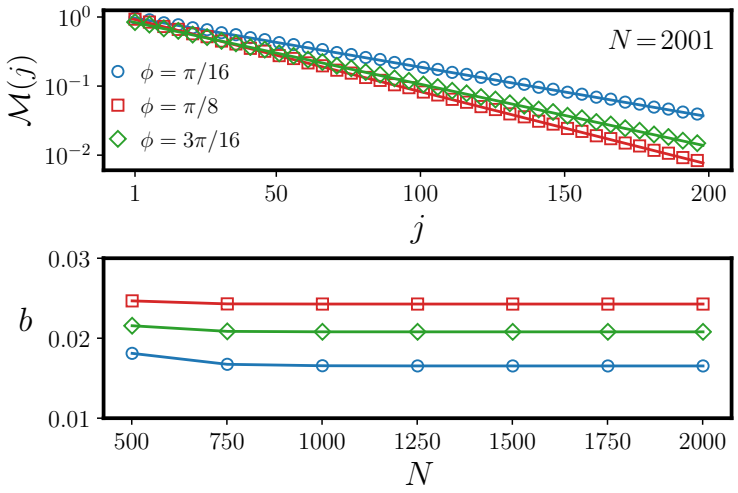

FIGURE 5.4: Upper panel: Behavior of $\mathcal{M}(j)$ as a function of j for a system made of 2001 spins, for different values of ϕ. Bottom panel: Size dependent numerical estimation of the exponential ratio b for different values of ϕ.

over the available wavenumbers, which are symmetrically distributed around $N/2$. As we can see also from the envelopes, the region affected by the presence of the defect is small because its effect decays exponentially. This fact can be better appreciated by looking at Fig. 5.4 where we have depicted the behavior of the function

$$\mathcal{M}(j) = \max_l |m_x(l)| - |m_x(j)|, \tag{5.6}$$

where $\max_j |m_x(j)|$ represents the value of the magnetizations in the bulk and the analysis of $\mathcal{M}(j)$ helps to understand the dimension outside which the effect of the defect is suppressed. As we can see from the figure, the effect decays exponentially $\mathcal{M}(j, \phi) \propto e^{-bj}$ with an exponential ratio b, that for large N becomes size independent. Hence, in the thermodynamic limit the magnetic pattern is similar to the one of a kink state.

However, Fig. 5.2 shows also another important result. By fixing the value of $\phi \in (-\frac{\pi}{4}, \frac{\pi}{4})$ and changing the defect from AFM to ferromagnetic (or vice-versa), we have an abrupt change of the magnetization pattern. At one side we have the standard AFM order with a localized defect and on the other an incommensurate staggerization. The existence of two different orders is compatible with the results by Campostrini *et al.* [67], mentioned before, although they did not consider the behavior of the local order: changing the defect from AFM to ferro (and viceversa) in a chain with FBC indeed drives the system across a QPT.

Finally, we note that different natures of the two magnetic orders are also visible in the spatial dependence of the spin correlation functions. Indeed, in Fig. 5.5 we show the spin correlation functions $\langle \sigma_1^x \sigma_j^x \rangle$ as a function of j, and we can see the following. For FTD the exponential decay $|\langle \sigma_1^x \sigma_j^x \rangle| = a + be^{-cj}$ is present, indicating the localization of the effect of the defect. On the other hand, with AFTD we have the linear behavior $|\langle \sigma_1^x \sigma_j^x \rangle| = a - b(j-1)$, that is a typical signature of the frustrated phase [1, 67, 70, 73].

We can get more insight and reach the same conclusions, about the different

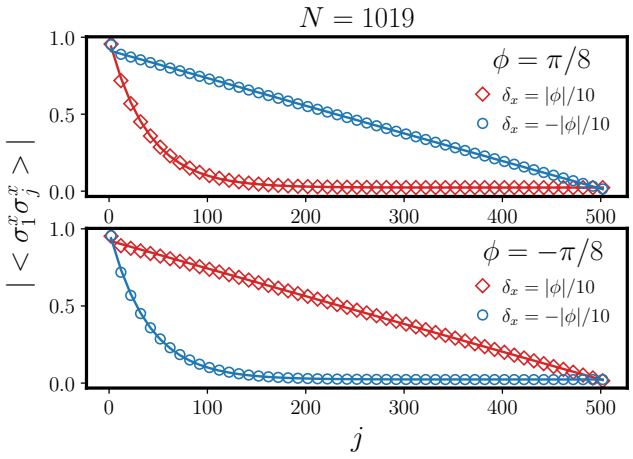

FIGURE 5.5: Spin correlation $|< \sigma_1^x \sigma_j^x >|$ as a function of the site j, for a chain made of $N = 1019$ spins. The defect is along the x direction. The exponential decay found for a FTD defect indicates the standard AFM order. On the other hand, the linear decay in the AFTD case is a typical signature of frustration.

magnetic order, through a perturbative analysis. We have done two different perturbation theories, which are presented in Appendix D.2. In both approaches, we are going to ignore every state separated by a finite energy gap from the ground states. However, the ground states are a part of a band of $2N$ states for which, in the thermodynamic limit, the gap vanishes, complicating any perturbative calculation. Thus, in our first approach, we worked around the point $\phi = 0$, and in this way, we provide a good picture explaining our numerical results. At $\phi = 0$ the ground state manifold is $2N$-fold degenerate, spanned by the "kink" states which have a ferromagnetic bond $\sigma_j^x = \sigma_{j+1}^x = \pm 1$ and an AFM bond between all other sites, for $j = 1, 2, \ldots N$. Adding the small interaction in the y direction, proportional to $\sum_j \sigma_j^y \sigma_{j+1}^y$, the kink states split in energy. By developing a method introduced in [69], we are then able to diagonalize the band of kink states under this term and do not need to deal with the complications emerging from a perturbative series with closing energy gaps. In the case of FTD, the ground states are, to the lowest order in the perturbation theory, simply the kink states with the ferromagnetic bond between the first and the last site ($\sigma_1^x = \sigma_N^x = \pm 1$), and the other states are separated by a finite energy gap, determined by δ_x. In the case of AFTD, the ground states are superpositions of kink states that have $\sigma_1^x = -\sigma_N^x$ and they belong to a band of states, in which the energy gap between the states closes as $1/N^2$, as in frustrated models without the defect [1, 2, 66, 71, 73]. Both of these cases are characterized by a two-fold degenerate ground-state manifold, as expected.

Having the ground states, to the lowest order in perturbation theory, the magnetization can be computed. In the case of an FTD, we find that for both signs of ϕ the magnetization is given by

$$m_x(j) = (-1)^j, \tag{5.7}$$

which represents the standard AFM staggerization, apart from the ferromagnetic bond placed where the defect is. The numerical results of Fig. 5.2 show indeed the standard staggered magnetization far from the defect, but zero value where the defect is placed. Thus the perturbation theory explains well the bulk behavior of the system, far from the defect. Close to $\phi = 0$ the correlation length is small and the

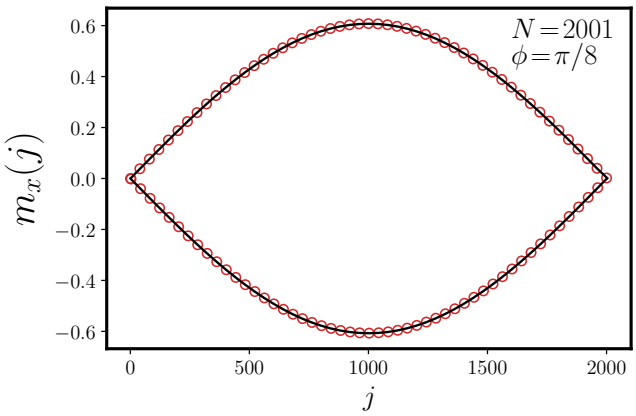

FIGURE 5.6: Comparison of the eq. (5.10) for the magnetization (solid black line), obtained using a perturbative approach, with the exact results (red dots), for a system made by $N = 2001$ spins and $\phi = \frac{\pi}{8}, \delta_x = -\frac{\pi}{80}$.

kinks are extremely well localized, while the numerics refers to a choice of a finite correlation length that provides a length scale over which the presence of the defect is felt before the bulk order ensues (see Fig. 5.4).

In the case of an AFTD, the perturbation theory predicts, for both signs of ϕ, the magnetization

$$m_x(j) = \frac{(-1)^j \sin\left[\frac{\pi}{N}\left(j-\frac{1}{2}\right)\right]}{N \sin\left(\frac{\pi}{2N}\right)} + \frac{1}{N}, \tag{5.8}$$

which is for large N well approximated by

$$m_x(j) = (-1)^j \frac{2}{\pi} \sin\left(\frac{\pi}{N} j\right). \tag{5.9}$$

This order is the incommensurate AFM order of Chapter 4, with a locally staggered magnetization, but modulated in magnitude over the length of the chain. Against naive expectations, but in agreement with the numerics, the modulation is such to have an exactly vanishing magnetization at the sites connected by the defect. This perturbative calculation validates well our numerical results of Fig. 5.2, both close and far from the defect.

The incommensurate AFM order is found whenever the defect is AFM, even though, without the defect, it is present only for $\phi \in (0, \pi/4)$ (see Chapter 4). Without the defect, this region possesses a four-fold degenerate ground-state manifold out of which it is possible to select the ground states exhibiting incommensurate AFM order. It is thus of interest to find which of these ground states are selected through a small antiferromagnetic defect. We answer this question in Appendix D.2.2, by doing a (degenerate) perturbation theory for small δ_x. In this case, we ignore the band above the ground states and consider the effect of the defect only on the GS manifold. Of course, the resulting lowest energy state is odd under the mirror symmetry passing across the site $\frac{N+1}{2}$. Combining the obtained ground state with the techniques developed in Chapter 4, for the magnetization in the thermodynamic limit we find,

$$m_x(j) = (-1)^j \frac{2}{\pi} (1 - \tan^2\phi)^{1/4} \sin\left(\frac{\pi}{N} j\right), \tag{5.10}$$

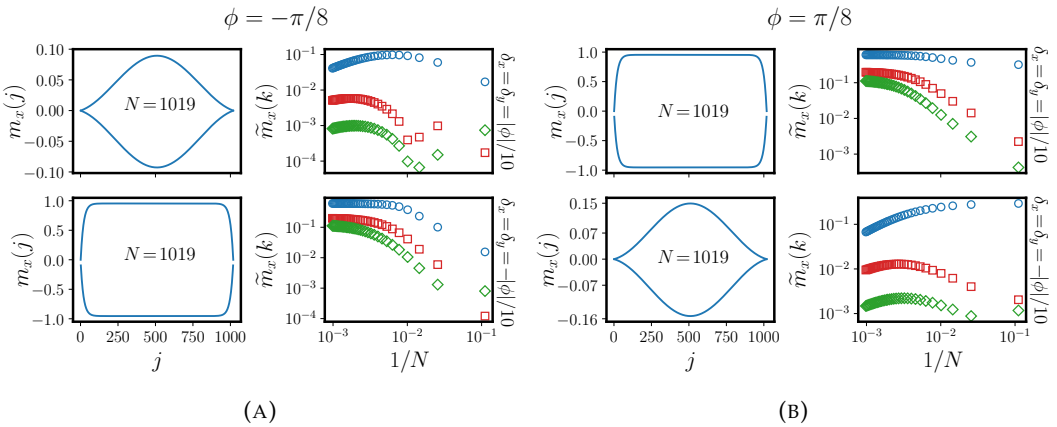

FIGURE 5.7: Magnetization $m_x(j) = \langle \sigma_j^x \rangle$ as a function of the site j for a chain made of $N = 1019$ spins (left), and the absolute value of its Discrete Fourier transform (DFT) (5.4) as a function of the inverse chain length (right), for different momenta: green diamonds $|\widetilde{m}_x(\frac{N-3}{2})|$, red squares $|\widetilde{m}_x(\frac{N-1}{2})|$, and blue circles $|\widetilde{m}_x(\frac{N+1}{2})|$. The defect is along both the x and y directions. An antiferromagnetic one yields mesoscopic magnetization that varies in space, while a ferromagnetic defect yields the standard AFM order in the bulk (see text for discussion).

which generalizes eq. (5.9) to the whole region $\phi \in (0, \pi/4)$ and is in good agreement with our numerical results, as presented in Fig. 5.6. Note that in the perturbation theory in δ_x we have neglected all excited states of the unperturbed model, including those belonging to the lowest energy band. While in the case of interest the procedure yields a result in agreement with numerics, this approach is not justified in general, because of the gapless nature of the unperturbed system. While the quantitative agreement of this approach with the numerics is quite surprising, it provides a geometrical explanation of the observed qualitative behavior. In fact, since the defect preserves the mirror symmetry across the site $\frac{N+1}{2}$, states (which always come in degenerate duplets or quadruplets) are hybridized to select the combination in each multiplet with definite mirror symmetry (with the odd one having lower energy): by explicit construction we observe that both states even or odd under mirror symmetry have vanishing magnetization at the defect, in the thermodynamic limit. At finite size, the former have a small ferromagnetic bond at the defect, while the latter exhibit exactly zero value of the magnetization at the defect.

While we did not find qualitative differences between a defect in the x and in the y direction, the same cannot be said when both are finite. We are now in presence of two defects which can agree or disagree in favoring a ferromagnetic or an antiferromagnetic alignment. A typical example of our numerical results for these cases is given in Fig. 5.7. In the case when both defects suppress the dominant antiferromagnetic interaction, we can see a picture completely analogous to the one with a single, FTD, defect. The behavior of the DFT is compatible with the Fourier transform of a single kink state and the real space magnetization envelope shows an exponential decay of the effect of the defect as we move away from it, to reach a regular AFM pattern in the bulk. Hence, in the thermodynamic limit the magnetic pattern represents, except in the vicinity of the defect, the standard AFM staggerization.

On the contrary, when both defects are AFTD, the DFT goes very slowly to zero in the thermodynamic limit, for all momenta, thus signaling that the magnetization

is mesoscopic and vanishes in the thermodynamic limit. As in the case $\delta_y = 0$, also in this case we can see that by fixing ϕ and turning the defect from AFM to ferro (or viceversa), we have that the magnetization pattern changes abruptly from the standard AFM one to the one with an incommensurate mesoscopic staggerization, signaling the QPT.

5.5 Conclusions

We have analyzed what happens to the properties of the model studied in chapters 3 and 4, i.e. the XY chain at zero fields with FBC, when a localized defect is added to the Hamiltonian. The resulting system has been characterized through the behavior, both at finite-sizes and in the thermodynamic limit, of the magnetization $m_x(j) = \langle \sigma_j^x \rangle$. Our motivation has been to challenge the naive expectation that a defect would immediately spoil the features discovered in chapters 3 and 4, since the effect of FBC is a single excitation in the system.

We have found that depending on the kind of defects we add, the system responds by selecting different types of orders. According to expectations, a defect in the Hamiltonian that reduces the relative weight of the dominant antiferromagnetic interaction restores the standard AFM order, except for a small region around the defect. On the contrary, if the bond defect favors an AFM alignment, we find an incommensurate AFM order: locally, two neighboring spins are anti-aligned, but along the chain the amplitude of the magnetization varies in space and vanishes at the defect. For a defect aligned along either the x or the y axis, this order is the same as the one in Chapter 4 and survives the thermodynamic limit. On the other hand, when the defect in both directions is considered, the amplitude of the, also site-dependent, magnetization vanishes as $N \to \infty$.

While the resurgence of the traditional AFM order is in line with the traditional expectation that FBC can be accounted for by single particle physics, the other orders challenge this point of view and promote a more many-body interpretation, as signaled by the fact that the largest amplitude of the magnetization is not placed at the AFM defect.

Let us note that the dependence of the order in our system on the details of the defects is in line with a general property of frustrated systems: the sensitivity to perturbations due to large classical degeneracy [25]. Here, the ground state degeneracy at the classical point $\phi = 0$ is extensive with N. Due to large degeneracy different perturbations can lift the degeneracy in a variety of different ways. It's important, in particular, that not all the defects select the standard AFM order.

Furthermore, these results corroborate the analysis in [67], indicating that translationally invariant systems with FBC lie at the transition between a magnetic phase, for a ferromagnetic defect that restores the unfrustrated order, and a kink phase, when the defect is AFM, and that the local order remains sensitive to subdominant contributions. Although the discovered transition is different from the one that is the subject of Chapter 4, it also indicates that topological frustration can be responsible for the existence of a quantum phase transition between different kinds of local order.

To conclude, in agreement with the results that FBC are the threshold for a QPT, we have shown that there is a sudden change in the local order driven by the defect. In this way, we have shown that translational invariance is not a necessary condition for the appearance of frustrated phases, paving the way to their experimental

observability and demonstrating that, close to FBC, the standard AFM order is not generically stable.

Chapter 6

General Systems

In chapters 3 and 4 we have shown that applying periodic boundary conditions with an odd number of sites (Frustrated Boundary Conditions, FBC) can destroy or modify local order in the antiferromagnetic XY chain, and a perfectly staggered order cannot be established there. Here, using perturbative arguments, we discuss the effects of FBC on a wide class of spin-1/2 chains (integrable or non-integrable) without external magnetic fields. Namely, we study spin chains whose Hamiltonians commute with the parity operators in all three spin directions, so that we can work within the symmetry breaking framework based on anticommuting parity symmetries, discussed in section 1.2.3. We establish that either a) local order decays to zero, algebraically (or faster) in the chain length, or b) there is a degeneracy which allows for a ground state choice that admits a finite magnetic order, which breaks translational symmetry. Which of the two possibilities is realized can also change if the thermodynamic limit is reached through a different choice of the sequence of chain lengths. The results are illustrated through examples. This Chapter is based on [6].

6.1 Introduction

In Chapter 3 we have shown that topological frustration can destroy the order parameter. The traditional order is staggered and quantum interactions resolve the conflict between it and the FBC with an interference pattern that effectively cancels the magnetization, leaving only a mesoscopic ferromagnetic order at finite sizes, that vanishes algebraically with the chain length. This phenomenology has later been enriched in Chapter 4, where we have found that the incommensurate antiferromagnetic order, characterized by a magnetization profile that varies in space with an incommensurate pattern, can arise. This type of order has been shown in Chapter 5 to be stable against antiferromagnetic (AFM) defects [4]. Furthermore, the boundary between the mesoscopic ferromagnetic order and the incommensurate AFM one is the first-order quantum phase transition, which exists only with FBC. All these results have established that, contrary to standard expectations, the boundary conditions can indeed affect the local, bulk behavior of a system, or, at least, that this is the case in presence of frustration.

It should, however, be remarked that the results discussed above have been found in specific (integrable) models and one should wonder about their general relevance. In this chapter, we address this issue and address the question of whether topological frustration generically destroys local order or creates a modulated AFM order with a site-dependent magnetization. As it is well known, local order parameters are central elements in Ginzburg-Landau theory. They are expectation values of local operators, with support over a finite range of lattice sites, which, given the symmetries of the system, should be zeroed and which, when they assume a value

other than zero, signal the spontaneous breaking of the symmetry and the establishment of a macroscopic order. We consider general spin-1/2 Hamiltonians with a dominant antiferromagnetic interaction, subject only to the symmetry constraint that they commute with the parity operators in all three spin directions, which describes a wide class of systems without external fields. In fact, this constraint is respected quite generally when the lattice has an odd number of sites. It allows us to work in the symmetry breaking framework based on anticommuting parity symmetries, discussed in section 1.2.3. Namely, it ensures an exact degeneracy in the ground state manifold (at least two-fold) and allows for the direct evaluation, even in a finite-size system, of the expectation values for all local operators, i.e. operators with support over a finite range of lattice sites. One can then follow the behavior of these observables toward the thermodynamic limit.

In this way, we show that three possibilities arise:

- if the system only admits ground states with zero momentum, the only possible order is not staggered (ferromagnetic) and is decaying algebraically (or faster) to zero with the system size, as in Chapter 3;
- if the model has an at least four degenerate ground state manifold with two GS momenta differing by π in the thermodynamic limit an incommensurate AFM order like that found in Chapter 4 can emerge. In this way the system indeed preserves a semblance of the order it has under generic boundary conditions, but with a modulation over the whole chain, which spontaneously breaks translational symmetry;
- if the relative momentum between the degenerate ground states does not approach π, no finite order can survive for large chain lengths.

In particular, these results imply that, when the boundary conditions kill the order parameter connected to the dominant interaction (namely, the magnetization), these systems are unable to develop any other type of order with support over a finite range of lattice sites, regardless of the type and nature of the other interactions in the Hamiltonian.

To determine the ground state properties and analyze the local order in generic systems, we will take advantage of the Hilbert space structure at a classical point (with simple domain wall as lowest energy states) and use a highly degenerate perturbation theory. This will allow us to classify whether in a finite neighborhood of the classical point any order vanishes in the thermodynamic limit or if a finite incommensurate order can emerge. While the amplitude of any order generally depends on the microscopic details of the model, its finiteness is a property of the given phase and thus to establish its existence (or lack thereof) it is sufficient just to consider a small finite parameter region. We will also corroborate these findings through the exact numerical diagonalization of a few examples, as well as the analytical solution of a series of Cluster-Ising models that showcase various phenomenologies.

6.2 Systems under consideration

We consider translational invariant spin-1/2 Hamiltonians with a dominant antiferromagnetic Ising interaction in one direction, say x, to which we add arbitrary interactions,

$$H = \sum_{j=1}^{N} \sigma_j^x \sigma_{j+1}^x + \lambda \sum_{j=1}^{N} H_j \,. \tag{6.1}$$

Here σ_j^α, for $\alpha = x, y, z$, are Pauli spin operators, λ is the ratio between the two interactions and we impose FBC, i.e. periodic boundary conditions ($\sigma_j^\alpha = \sigma_{j+N}^\alpha$) and odd N. The only restriction we apply to H_j is that it should commute with all three parity operators $\Pi^\alpha \equiv \bigotimes_{j=1}^N \sigma_j^\alpha$ ($[H, \Pi^\alpha] = 0$ for $\alpha = x, y, z$), so that the whole Hamiltonian becomes invariant under transformations $\sigma_j^\alpha \to -\sigma_j^\alpha \ \forall j$. All in all, this class of Hamiltonians describes a wide range of systems without magnetic fields and defects. The terms H_j can include, for example, nearest neighbor interactions such as $\sigma_j^\alpha \sigma_{j+1}^\alpha$ in directions other than $\alpha = x$, next-to-nearest-neighbor interactions such as $\sigma_j^\alpha \sigma_{j+2}^\alpha$ and, more generally, interactions $\sigma_j^\alpha \sigma_{j+l}^\alpha$ of spins separated by l sites. It also extends to arbitrary products of the terms above, as in the case of the cluster interactions $\sigma_j^y (\sigma_{j+1}^z \sigma_{j+2}^z \dots \sigma_{j+n}^z) \sigma_{j+n+1}^y$ for even integers n, on which we will focus later. Note that H_j can be a sum of different interactions with different weights. The index j in H_j indicates a reference site for the interaction, which is shifted in eq. (6.1) to ensure translational invariance.

On a chain with an odd number of sites N, the three parity operators Π^α do not commute. Instead, they anticommute ($\{\Pi^\alpha, \Pi^\beta\} = 2\delta_{\alpha,\beta}$) and realize a non-local $SU(2)$ algebra ($[\Pi^\alpha, \Pi^\beta] = \imath \varepsilon_{\alpha,\beta,\gamma} 2(-1)^{\frac{N-1}{2}} \Pi^\gamma$). Since the Hamiltonian (6.1) commutes with all Π^α, its ground state manifold is at-least two-fold degenerate (see section 1.2.3), and any ground state breaks at least one of the parity symmetries. Thus, in such a setting, it is always possible to break one of the Hamiltonian symmetries already in a finite system and to follow the behavior of the order to $N \to \infty$. Moreover, the same structure also allows for the direct computation of matrix elements between states with different parities, whose calculation usually either requires extremely cumbersome expressions of limited practical use or is achieved indirectly from certain expectation values by invoking the cluster decomposition property.

In particular, let $|g\rangle$ be an eigenstate of H and, simultaneously, an eigenstate of Π^x with eigenvalue equal to one, i.e. $\Pi^x |g\rangle = |g\rangle$. Since the parity operators mutually anticommute ($\{\Pi^\alpha, \Pi^\beta\} = 2\delta_{\alpha,\beta}$), it follows that the state $\Pi^z |g\rangle$ has the same energy but opposite parity with respect to Π^x, i.e. $\Pi^x \Pi^z |g\rangle = -\Pi^z |g\rangle$. States with different parities can be constructed through superpositions of states above and thus it is possible to calculate the ground state expectation value of operators $\mathcal{O}$ breaking one symmetry of the Hamiltonian by choosing a suitable ground state. For instance, for an eigenstate $|g\rangle$ of Π^x, the magnetization in the x direction can be calculated as $\langle g| \sigma_j^x |g\rangle$. On the other hand, the magnetization in the z direction can be evaluated on the state $|\tilde{g}\rangle = \frac{1}{\sqrt{2}}(\mathbf{1} + \Pi^z) |g\rangle$ and is equal to $\langle \tilde{g}| \sigma_j^z |\tilde{g}\rangle = \langle g| \sigma_j^z \Pi^z |g\rangle$.

6.3 Translational invariance and the ground state structure

Let us examine the structure of the ground states of the studied systems on the basis of general arguments. At the classical point $\lambda = 0$ the topological frustration does not allow for every spin to point oppositely to its nearest neighbors. Instead, the ground space is $2N$-fold degenerate, spanned by the "kink states", which have a single ferromagnetic bond (two spins aligned in the same direction), i.e. the "kink", and $N-1$ antiferromagnetic bonds (spins aligned in opposite directions). We denote by $|j\rangle$ the kink state in which the ferromagnetic bond is between sites j and $j+1$, with $\langle j| \sigma_j^x |j\rangle = 1$, while the kink state that we obtain flipping all the spins, i.e. $\Pi^z |j\rangle$, has $\langle j| \Pi^z \sigma_j^x \Pi^z |j\rangle = -1$. Above the states with a single kink there is an energy gap of order unity separating them from the states with three kinks (due to odd N an

even number of kinks is not allowed). At higher energies, one finds bands with a progressively growing number of kinks separated by order of unity gaps.

By turning on a small coupling λ in eq. (6.1), the degenerate states typically split in energy. For small λ (much smaller than the gap between the two lowest energy bands), the ground state will be described accurately within the single kink subspace. Assuming, thus, $|\lambda| \ll 1$ and neglecting, for the moment, the states with more kinks, because of translational invariance we write the ground states as

$$|s_p\rangle \equiv \frac{1}{\sqrt{N}} \sum_{j=1}^{N} e^{\imath pj} |j\rangle , \quad \Pi^z |s_p\rangle = \frac{1}{\sqrt{N}} \sum_{j=1}^{N} e^{\imath pj} \Pi^z |j\rangle . \tag{6.2}$$

Here $p = 2\pi k/N$, with k running over integers from 0 to $N-1$, is the lattice momentum, whose quantization is a result of periodic boundary conditions.

For progressively larger λ, the ground state will acquire contributions from states with more kinks. Because of the translational invariance, the states can still be labeled by their momentum p. To describe their structure let us introduce the translation operator T [2], a unitary operator that shifts cyclically the spins by one lattice site, i.e. $T^\dagger \sigma_j^\alpha T = \sigma_{j+1}^\alpha$, for $\alpha = x, y, z$ (see also Appendix C.3). The eigenvalues $e^{\imath p}$ of the translation operator fall on the unit circle, where the angle p defines the momentum of the state. Now, for any eigenstate of the model with momentum p, ground state in particular, the contributions coming from the subspaces with different number of kinks can be separated. For any state $|\boldsymbol{\beta}\rangle \equiv |\beta_1, \beta_2, \ldots, \beta_N\rangle \equiv \bigotimes_{j=1}^N |\beta_j\rangle$, where $|\beta_j\rangle \in \{|+\rangle, |-\rangle\}$ are eigenstates of the Pauli operator σ^x, we can construct the translationally invariant state

$$|\boldsymbol{\beta}, p\rangle = \frac{1}{\sqrt{N}} \sum_{j=0}^{N-1} e^{-\imath pj} T^j |\boldsymbol{\beta}\rangle , \tag{6.3}$$

with momentum p. For instance, the states $|s_p\rangle$ in (6.2) are given by $|\boldsymbol{\beta}\rangle = |+-+-\ldots+-+\rangle = |N\rangle$ (we have $|j\rangle = (T^\dagger)^j |N\rangle$). We can write then any ground state $|g_p\rangle$ of H with momentum p as

$$|g_p\rangle = \sum_{\boldsymbol{\beta}} c_{\boldsymbol{\beta}} |\boldsymbol{\beta}, p\rangle , \tag{6.4}$$

where the sum is over all different, and not equivalent by translation, states $|\boldsymbol{\beta}\rangle$, and the normalization implies $\sum_{\boldsymbol{\beta}} |c_{\boldsymbol{\beta}}|^2 = 1$. Here we say that two states, $|\boldsymbol{\beta}_1\rangle$ and $|\boldsymbol{\beta}_2\rangle$, are not equivalent by translation if $|\boldsymbol{\beta}_1\rangle \neq T^k |\boldsymbol{\beta}_2\rangle$ for any integer k. For instance, the states $|s_p\rangle$ in (6.2) are given by $c_{\boldsymbol{\beta}} = 1$ for $|\boldsymbol{\beta}\rangle = |+-+-\ldots+-+\rangle = |N\rangle$ and $c_{\boldsymbol{\beta}} = 0$ for states $|\boldsymbol{\beta}\rangle$ with more than one kink. Finally, we note that because of the symmetries of the model, the states $|g_p\rangle$ and $\Pi^z |g_p\rangle$ are orthogonal, but have the same energy. Hence, the ground-state manifold of the Hamiltonian in eq. (6.1) will be spanned by a certain number of pairs $|g_p\rangle$ and $\Pi^z |g_p\rangle$.

For a small λ compared to the energy gap at the classical point, i.e. for $|\lambda| \ll 1$, in the ground state (6.4) the contribution of the states $|\boldsymbol{\beta}, p\rangle$, and therefore the overlap $c_{\boldsymbol{\beta}}$, is expected to decrease fast with the number of kinks in the state $|\boldsymbol{\beta}\rangle$.

6.4 Matrix elements of local operators

In order to discuss local order we study the possible values of matrix elements of

local operators between different contributions in the ground state decomposition (6.4). Let us first neglect the contributions from the states with more than one kink and focus on one-kink subspace only. Afterwards, we are going to generalize the result to an arbitrary finite number of kinks. At this point let us recall that by local operators we mean all operators having support over a finite range of lattice sites, not scaling with N. Due to translation invariance, without losing generality we can assume that the operator has support over the first L sites (for some fixed integer L). Moreover, taking into account that Pauli spin operators together with the unit operator provide a basis at a single site, we have that a local operator can always be written as a linear combination of a finite number of monomials in the Pauli operators $\sigma_1^{\alpha_1}\sigma_2^{\alpha_2}\dots\sigma_L^{\alpha_L}$, where $\alpha_1,\alpha_2,\dots,\alpha_L \in \{0,x,y,z\}$ and $\sigma_j^0 = 1$. Thus, we can focus only on monomials in Pauli operators. Furthermore, each single monomial either commutes or anticommutes with a given parity operator. We are interested only in monomials that anticommute with some of the parity operators, whose non-zero expectation value would signal a breaking of a Hamiltonian symmetry. All such monomials fall into one of the two categories, a) and b), in the following theorem, that we prove:

Theorem 1. *Let $A \equiv \sigma_1^{\alpha_1}\sigma_2^{\alpha_2}\dots\sigma_L^{\alpha_L}$ be a product of Pauli operators, for some integer L. Let us consider two states (not necessarily different) of the form as in eq. (6.2), $|s_{p_1}\rangle$ and $|s_{p_2}\rangle$, and let us consider arbitrary superpositions $|g_j\rangle = (u_j\mathbf{1} + v_j\Pi^z)\,|s_{p_j}\rangle$, for $j = 1,2$, where $|u_j|^2 + |v_j|^2 = 1$. We have:*

a) if A is such that $\alpha_j \in \{0,x\}$ for all sites $j \in \{1,2,\dots,L\}$, with $\alpha_j = x$ for an odd number of sites j, then

$$|\langle g_1|\, A\, |g_2\rangle| \leq \frac{C_1}{N|\cos\frac{p_1-p_2}{2}|}. \tag{6.5}$$

b) if in A there is at least one site $j \in \{1,2\dots,L\}$ for which $\alpha_j \in \{y,z\}$, then

$$|\langle g_1|\, A\, |g_2\rangle| \leq \frac{C_2}{N}. \tag{6.6}$$

Here C_1 and C_2 are positive constants independent of N.

Note that the first term in (6.5) is well defined, since, by the quantization of the momenta, with N being odd and finite, we cannot have $p_1 - p_2 = \pm\pi$. The proof of the theorem takes into account that in the kink states apart from the kink there is Néel order, while the contributions of the kinks can be bounded. A more formal proof is provided in Appendix E, but its basic argument is the following.

In case *a)*, the operator A commutes with Π^x and hence the evaluation of $\langle g_1|\, A\, |g_2\rangle$ reduces to the evaluation of $\langle s_{p_1}|\, A\, |s_{p_2}\rangle$. Moreover, in this case, the kink states are also eigenstates of A, thus only matrix elements between the same kink state are different from zero and we have

$$\langle s_{p_1}|\, A\, |s_{p_2}\rangle = \frac{1}{N}\sum_{j=1}^{N} e^{-\imath(p_1-p_2)j}\,\langle j|\, A\, |j\rangle\,. \tag{6.7}$$

For $j < L$, A acts on a Neel state and we have $\langle j| A |j\rangle = c(-1)^j$, for some constant $c \in \{-1, 1\}$. The first term in eq. (6.5) is the result of inserting the above expectation in eq. (6.7) for the whole sum, while the second term is a correction due to the first L elements in the sum differing from the rest.

In the case *b)* we have to consider two different situations. If the number of sites with $\alpha_j \in \{y, z\}$ is even, the operator A commutes with Π^x and thus the evaluation of $\langle g_1| A |g_2\rangle$ reduces to the evaluation of $\langle s_{p_1}| A |s_{p_2}\rangle$, but the kink states are no more eigenstates of A. On the contrary, since the operator A flips some spins, the matrix elements between the same kink state vanish. Moreover, if the kink is outside the support of A, the matrix elements $\langle j| A |l\rangle$ also vanish because of orthogonality. Thus, we have

$$\langle s_{p_1}| A |s_{p_2}\rangle \quad = \quad \frac{1}{N} \sum_{j,l=1}^{N} e^{-\imath(p_1 j - p_2 l)} \langle j| A |l\rangle \ , \tag{6.8}$$

where the terms with $L < j, l < N$ vanish and we are left with, at most, $(L+1)^2$ terms of order one, suppressed by the overall factor $1/N$.

On the other hand, if the number of sites with $\alpha_j \in \{y, z\}$ is odd, the operator A anticommutes with Π^x and hence the evaluation of $\langle g_1| A |g_2\rangle$ reduces to the evaluation of $\langle s_{p_1}| A\Pi^z |s_{p_2}\rangle$. Analogously to the previous case we recognize that in the sum

$$\langle s_{p_1}| A\Pi^z |s_{p_2}\rangle \quad = \quad \frac{1}{N} \sum_{j,l=1}^{N} e^{-\imath(p_1 j - p_2 l)} \langle j| A\Pi^z |l\rangle \, , \tag{6.9}$$

there is at most $(L+1)^2$ non-vanishing terms, which are of order one and are suppressed by an overall factor that scales with the length of the ring.

The theorem can be generalized straightforwardly to the states with more kinks as follows.

Theorem 2. *Let $A \equiv \sigma_1^{\alpha_1} \sigma_2^{\alpha_2} \dots \sigma_L^{\alpha_L}$ be a product of Pauli operators, for some integer L. Let us consider two states of the type as in eq. (6.3), $|\boldsymbol{\beta}_1, p_1\rangle$ and $|\boldsymbol{\beta}_2, p_2\rangle$, with momentum p_1 and p_2 respectively.*

a) Let A be such that $\alpha_j \in \{0, x\}$ for all sites $j \in \{1, 2, \dots, L\}$, with $\alpha_j = x$ for an odd number of sites j. If $|\boldsymbol{\beta}_1\rangle$ and $|\boldsymbol{\beta}_2\rangle$ are different, and not equivalent by translation, then

$$\langle \boldsymbol{\beta}_1, p_1| A |\boldsymbol{\beta}_2, p_2\rangle = 0. \tag{6.10}$$

If $|\boldsymbol{\beta}_1\rangle = |\boldsymbol{\beta}_2\rangle$ then

$$|\langle \boldsymbol{\beta}_1, p_1| A |\boldsymbol{\beta}_2, p_2\rangle| \leq \frac{C_1}{N|\cos\frac{p_1 - p_2}{2}|}. \tag{6.11}$$

b) Let A be such that there is at least one site $j \in \{1, 2 \dots, L\}$ for which $\alpha_j \in \{y, z\}$. Then

$$|\langle \boldsymbol{\beta}_1, p_1| A |\boldsymbol{\beta}_2, p_2\rangle| \leq \frac{C_2}{N}. \tag{6.12}$$

Here C_1 and C_2 are positive constants independent of N, that depend only on L and the number of ferromagnetic bonds in the states $|\boldsymbol{\beta}_1\rangle$ and $|\boldsymbol{\beta}_2\rangle$.

The proof of Theorem 2 is similar to the one of Theorem 1, but more involved. The details are also given in Appendix E.

6.5 Local order in the ground state

Based on the derived theorems here we discuss the local order in the ground state, depending on the ground state momenta. The various ground states, labeled by momentum and parity, can be followed from the classical point $\lambda = 0$ to a finite λ perturbatively, and represented in terms of states with a progressively growing number of domain wall states. With generic boundary conditions, at some critical point $\lambda_c \neq 0$ the system will undergo a quantum phase transition, characterized by a change in the ground state properties, as well as by the non-analytic behavior of the ground state energy (density) in the thermodynamic limit [10]. Since this quantity is not sensitive to the choice of boundary conditions or the odd number of lattice sites, the phase transition point cannot be moved by applying FBC. However, a system can also cross smaller, non-extensive, discontinuities (boundary phase transitions), such as the one discussed in [2], due to a GS level crossing, which also mark a change in the ground state order. In any case, the order, or lack thereof, being a characteristic property of a phase between critical points, it is sufficient to study it in a small finite interval of λ to determine the nature of a given phase.

We make a natural assumption that in the regime $|\lambda| \ll 1$ the behavior of the local order is captured within the subspace spanned by states with a finite, bounded, although arbitrary, number of kinks. We note, for example, that the properties of the magnetization in the exactly solvable quantum XY chain can be captured already within the one-kink subspace [1, 2] (see Appendix C.7). We discuss also the contribution of the states with more kinks, since some interactions can involve preferably such states, and show that they do not change the obtained picture about the relation between the ground state momenta and local order.

If the system's ground space is only two-fold degenerate, i.e. if there exist only a particular momentum $p(N)$ (allowing for system size dependence), with the associated ground states $|g_{p(N)}\rangle$ and $\Pi^z |g_{p(N)}\rangle$, the theorems imply that the expectation values of local operators that break a Hamiltonian symmetry are $O(N^{-1})$. In particular, they vanish in the thermodynamic limit.

There is a simple explanation for this result if we look at the expectation value of σ_j^x. The states $|g_{p(N)}\rangle$ and $\Pi^z |g_{p(N)}\rangle$ have the same eigenvalue of the translation operator T. If the ground space is only two-fold degenerate, the consequence is that the expectation value of $\sigma_j^x = (T^\dagger)^j \sigma_N^x T^j$ is independent of j in any ground state. The leading interaction in the model being antiferromagnetic, the ferromagnetic order should not survive in the thermodynamic limit, so it vanishes.

The situation becomes more complex if the system admits a larger ground state degeneracy. Let us say that the system has $2d$-fold degenerate ground space and denote the ground state momenta by $p_1(N), p_2(N), \dots p_d(N)$, whose quantized value depends on the system size, and by $p_1^*, p_2^*, \dots, p_d^*$ the values they tend to in the thermodynamic limit, respectively. Then, unless $p_n^* - p_m^* = \pi$ for some n and m, the theorems imply again that there is no local parameters. On the other hand, if it is the case that $p_n^* - p_m^* = \pi$ for some n and m, then we can construct a ground state such as

$$|g(N)\rangle = \frac{1}{\sqrt{2}}(|g_{p_n(N)}\rangle + e^{\imath\theta} |g_{p_m(N)}\rangle), \tag{6.13}$$

for some phase θ, which exhibits a non-zero order parameter. To explain this it is sufficient to focus on the one-kink subspace, where $|g_{p(N)}\rangle = |s_{p(N)}\rangle$. Applying the procedure as in the proof of the Theorem 1 we find the site-dependent magnetization

$$\langle g(N)|\sigma_j^x|g(N)\rangle = \frac{\cos[(p_m(N)-p_n(N))j+\theta']}{N|\cos\frac{p_n(N)-p_m(N)}{2}|} + O(N^{-1}) \tag{6.14}$$

where the phase θ' is related to θ, but its explicit expression is not needed. Since $p_n(N) - p_m(N) = \pi + O(N^{-1})$, in the denominator the correction compensates the factor N and produces a nonvanishing value of the magnetization in the thermodynamic limit. Moreover, in the numerator it forces a slowly varying magnetization profile. In fact, while for neighboring sites σ_j^x is almost perfectly staggered, over the whole chain the $1/N$ correction adds up so that the amplitude of the order parameter varies and even locally vanishes at some points. Thus, the one in eq. (6.14) is not a standard AFM order and the phase θ' (θ) selects a breaking of translational symmetry (due to a ground state choice that is not an eigenstate of the translation operator). A nice example of this phenomenology was discussed for the quantum XY chain with two AFM interactions in Chapter 4. There, the model exhibits a four-fold degenerate ground space, with $p_1(N) = -p_2(N) = \pi/2 + (-1)^{(N+1)/2}\pi/2N$ so from (6.14) we get approximately the magnetization $\langle g|\,\sigma_j^x\,|g\rangle = \frac{2}{\pi}(-1)^j \cos\left(\frac{\pi}{N}j + \theta''\right)$, which was termed *incommensurate antiferromagnetic order*.

Finally, we should also remark that it is possible for the ground state degeneracy to depend on the system size and that a finite order parameter can be reached only through a precise sequence of system sizes. This is a peculiar phenomenon in the topologically frustrated models that has no counterpart in the unfrustrated ones. We are going to provide an example for this phenomenology, given by the n-Cluster-Ising chains. Before that, we examine the models with only two-body interactions.

6.6 Example: Models with two-body interactions

Let us consider models with only two-body interactions, both nearest-neighbor and beyond. Such models can be specified by interactions

$$H_j = \mu_1^y \sigma_j^y \sigma_{j+1}^y + \mu_1^z \sigma_j^z \sigma_{j+1}^z + \sum_{l=2,3,\ldots} \sum_{\alpha=x,y,z} \mu_l^\alpha \sigma_j^\alpha \sigma_{j+l}^\alpha, \tag{6.15}$$

in (6.1), where μ_l^α are the coefficients that describe the relative strength within the subleading interactions. In a realistic Hamiltonian it is expected that the interactions decay with distance ($|\mu_l^\alpha| > |\mu_{l+1}^\alpha|$), and in order not to deal with long-range interacting systems, which are known to have a peculiar phenomenology [164–167], we assume there is some cut-off value of l. We show that as long as the model in (6.15) is a small perturbation of the quantum XY chain, defined by $|\mu_1^y| \neq 1$ and zero remaining couplings, it shows the same phenomenology. The properties of the topologically frustrated quantum XY chain [1, 2] are thus not fine-tuned.

For this task we assume $|\lambda| \ll 1$ and diagonalize the Hamiltonian within the one-kink subspace, i.e. we perform the lowest order-perturbation theory, and determine the ground state momentum. We also assume that the XY chain coupling is much stronger than the others, i.e. $|\mu_l^\alpha| \ll |\mu_1^y|$ for $l \neq 1$ or $\alpha \neq y$.

It's easy to see that in the one-kink subspace the nearest neighbor interactions act by translating the kink by two sites, i.e.

$$\sum_{j=1}^{N} \sigma_j^\alpha \sigma_{j+1}^\alpha = T^2 + (T^\dagger)^2, \quad \alpha = y, z. \tag{6.16}$$

The interactions of the x-components of spins for different l only shift the energy of the states with different number of kinks and we neglect them. Finally, the matrix elements of the interactions $\sum_{j=1}^{N} \sigma_j^\alpha \sigma_{j+l}^\alpha$ for $\alpha = y, z$ beyond the nearest neighbor vanish in the one-kink subspace. Because of the latter the result will also hold when the couplings μ_l^α for $\alpha = y, z$ and $l > 1$ are comparable to μ_1^y.

It follows then that the energy of the translationally invariant states $|s_p\rangle$, $\Pi^z |s_p\rangle$, is

$$E_p = -(N-2) + 2(\mu_1^y + \mu_1^z)\cos(2p). \tag{6.17}$$

If $\mu_1^y < 0$ the ground state manifold is two-fold degenerate (with the momentum $p = 0$) and there is no local order in the thermodynamic limit. On the other hand, for $\mu_1^y > 0$ the degeneracy is four-fold, with ground state momenta $p_1(N) = -p_2(N) = \pi/2 + (-1)^{(N+1)/2}\pi/2N$ and the system exhibits incommensurate AFM order, discussed before. It follows that perturbing the XY chain with additional two-body interactions does not change its properties.

6.7 Example: Cluster-Ising models

To provide a specific example of a system where the existence of local order depends on the particular sequence of (odd) system sizes followed towards the thermodynamic limit, we consider the exactly solvable one dimensional n-Cluster-Ising models, defined by the Hamiltonian

$$H = \sum_{j=1}^{N} \sigma_j^x \sigma_{j+1}^x + \lambda \sum_{j=1}^{N} \sigma_j^y (\sigma_{j+1}^z \sigma_{j+2}^z \ldots \sigma_{j+n}^z) \sigma_{j+n+1}^y, \tag{6.18}$$

with n an even number (in order to commute with all the parity operators). While the solution of such models, obtained using an exact mapping to free fermions, is known for a few years [161–163, 168–170], under FBC a few subtleties have to be taken into account and are presented in Appendix F.

With FBC, we find that the ground state degeneracy of the n-Cluster-Ising models depends on the greatest common divisor (gcd) between the system size N and the size $n+2$ of the cluster in the many-body interactions. In particular, denoting $g \equiv \gcd(N, n+2)$, for $\lambda \in (0, 1)$ there are $4g$ ground states, while for $\lambda \in (-1, 0)$ the degeneracy is halved (at $\lambda = 0$ there is a level crossing, analogous to the one in the XY chain [2]). The ground state degeneracy of the topologically frustrated n-Cluster-Ising models is thus another example [171–173] how the question of divisibility of numbers can appear in quantum mechanics.

The degeneracy can be understood on the basis of the symmetries of the model. The details are given in Appendix F, while the main points are the following. The Hamiltonian (6.18) can be written as a sum of g commuting distinct Hamiltonians. Namely,

$$H = H^{(1)} + H^{(2)} + \ldots + H^{(g)}, \tag{6.19}$$

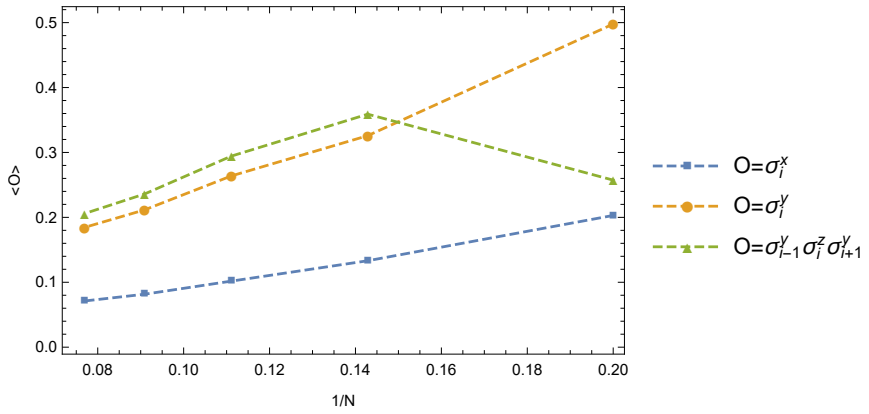

FIGURE 6.1: The parameters in Hamiltonian (6.22) are set to $\lambda_1 = -0.5$, $\lambda_2 = -0.25$ and the (odd) system sizes range from $N = 5$ to $N = 13$. The ground state manifold is found to be two fold degenerate. Accordingly, the ground state expectation values of different operators decay with N towards zero.

where $H^{(k)} = (T^\dagger)^k H^{(g)} T^k$ for $k = 1, 2, \ldots, g-1$, the different Hamiltonians $H^{(k)}$ mutually commute ($[H^{(k)}, H^{(l)}] = 0$) and they are invariant under translations by g lattice sites($[H^{(k)}, T^g] = 0$). Due to frustration, the ground state of H cannot minimize the energy of all $H^{(k)}$. On the other hand, it can be chosen as a ground state of $g-1$ Hamiltonians $H^{(k)}$ and the first excited state of the remaining one. Due to g possible choices of the excited one, the ground state degeneracy of H is at least g-fold. Since the Hamiltonians $H^{(k)}$ commute with T^g it can be shown that this degeneracy allows for the shift of the momentum by $2\pi/g$ in the ground space: If p is the ground state momentum, so is $p + 2\pi/g$. Going further, the mirror symmetry of H (the symmetry under the transformation $\sigma_j^\alpha \to \sigma_{-j}^\alpha$ for $\alpha = x, y, z$ and all j) implies that for each ground state with momentum p there is a ground state with momentum $-p$. Now, there are two-possible cases. The first one is that for any ground state momentum p the momentum $-p$ can be obtained by adding the certain number of increments $2\pi/g$ to p. The second case is that this is not possible. In the first case the mirror symmetry does not bring anything new so there are g distinct ground state momenta, while in the second there are $2g$ distinct ground state momenta. Taking into account also the parity symmetries, it follows that the ground state degeneracy is $2g$ in the first case, and $4g$ in the second. It requires the exact solution to see that the first case happens for $\lambda < 0$, and the second for $\lambda > 0$.

Thus, for $n = 0, 2$ there are 2 ground states for negative λ and 4 for positive one, for all odd N. The situation changes abruptly if we consider $n = 4$. Let us focus on $\lambda > 0$ and take into account separately two chain length sequences, $N = 12M + 1$ and $N = 12M + 3$ for integers M.

For $N = 12M + 1$ the ground space is 4-fold degenerate and the momenta are $p_1(N) = \frac{\pi}{6}\left(1 - \frac{1}{N}\right)$ and $p_2(N) = -p_1(N)$. Letting $M \to \infty$ we have $p_1^* - p_2^* = \frac{\pi}{3} \neq \pi$ and thus there is no finite local order parameters in the thermodynamic limit for these chain lengths. On the other hand, for $N = 12M + 3$ the ground space is 12-fold degenerate, with momenta $p_j(N) = (2j+1)\frac{\pi}{6} - (-1)^j \frac{\pi}{2N}$ for $j = 1, 2, \ldots, 6$. In this case we have, for instance, $p_4^* - p_1^* = \pi$ so the system can exhibit a non-zero magnetization. From (6.14) we find the magnetization $\langle \sigma_j^x \rangle = \frac{2}{\pi}(-1)^j \cos\left(\frac{\pi}{N} j + \theta\right)$, where the phase factor θ depends on the ground state choice.

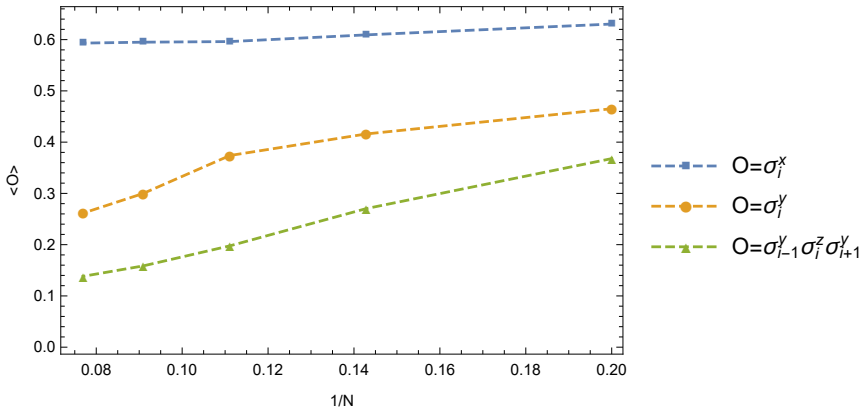

FIGURE 6.2: The parameters in Hamiltonian (6.22) are set to $\lambda_1 = 0.5$, $\lambda_2 = 0.25$ and the (odd) system sizes range from $N = 5$ to $N = 13$. The ground state manifold is found to be four fold degenerate, with the ground state momenta $p_1(N) = -p_2(N) = \pi/2 + (-1)^{(N+1)/2}\pi/2N$, as in the quantum XY chain with both interactions AFM [2]. The absolute value of the matrix elements $\langle p_1(N), \Pi^z = 1 | O | p_2(N), \Pi^z = -1 \rangle$ (the quantum numbers of the ground states are indicated) is shown, for different operators O. Since $p_1(N) - p_2(N) \overset{N\to\infty}{\to} \pi$ there is a ground state choice that exhibits the incommensurate AFM order, as the non-zero value for $O = \sigma_j^x$ in the plot illustrates.

6.8 Example: Exact numerical diagonalization of more complicated models

For the end, to corroborate our analytical results we are going to provide exact numerical results on more complicated models with FBC. Diagonalizing a model of interest simultaneously with one of the parity operators and the translation operator T it is possible to label the ground states by parity and momentum. It is not obvious how to construct T numerically. For this task we use a representation for T from [174], that reads

$$T = Q_{N,N-1} Q_{N-1,N-2} \dots Q_{3,2} Q_{2,1}, \tag{6.20}$$

where

$$Q_{j,l} \equiv \frac{1}{2}\left(1 + \sum_{\alpha=x,y,z} \sigma_j^\alpha \sigma_l^\alpha\right). \tag{6.21}$$

are the permutation operators between two sites. In this way the translation operator is expressed in terms of spin operators and can be implemented numerically.

We are going to examine two models. The first one is given by the Hamiltonian

$$H = \sum_{j=1}^{N} \sigma_j^x \sigma_{j+1}^x + \lambda_1 \sum_{j=1}^{N} \sigma_j^y \sigma_{j+1}^y + \lambda_2 \sum_{j=1}^{N} \sigma_j^y (\sigma_{j+1}^x \sigma_{j+2}^x) \sigma_{j+3}^y, \tag{6.22}$$

that includes the dominant Ising interaction in the x-direction, a subleading Ising interaction in the y direction and an additional four-body interaction. We have diagonalized the model for (odd) system sizes ranging from $N = 5$ to $N = 13$. Furthermore, we have focused on the expectation value of the spin operators σ_j^x, σ_j^y and of

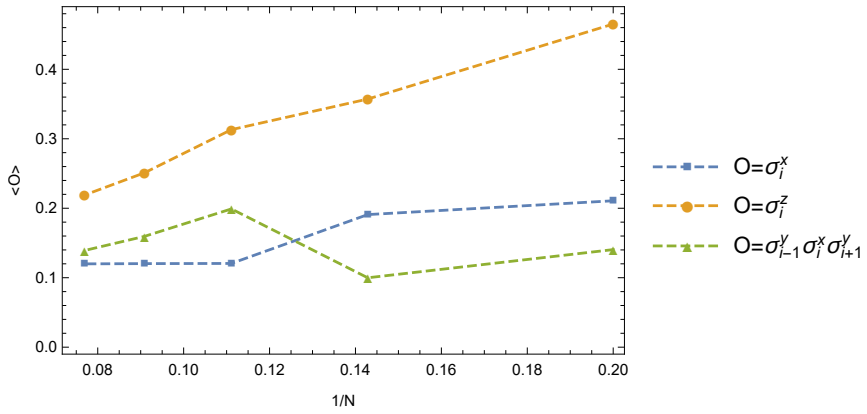

FIGURE 6.3: The parameters in (6.23) are set to $\lambda_1 = 0.5$, $\lambda_2 = 0.25$ and the (odd) system sizes range from $N = 5$ to $N = 13$. The ground state manifold is found to be four fold degenerate, with the ground state momenta $p_1(N), p_2(N)$ given in the text. The absolute value of the matrix elements $\langle p_1(N), \Pi^z = 1 | O | p_2(N), \Pi^z = -1 \rangle$ (the quantum numbers of the ground states are indicated) is shown, for different operators O. The difference $p_1(N) - p_2(N)$ does not go to π for $N \to \infty$, and accordingly local order decays to zero.

the operator $\sigma^y_{j-1}\sigma^z_j\sigma^y_{j+1}$, which are the order parameter operators associated to different interactions in (6.22). The results in Fig. 6.1 and 6.2 show, in accordance with our analytical results, that depending on the ground state momenta the local order goes to zero with N or there is a ground state choice with a finite (incommensurate AFM) order.

The second model we examine is obtained by adding an additional nearest neighbor interaction to the Cluster-Ising Hamiltonian in (6.18) for $n = 2$. It is given by the Hamiltonian

$$H = \sum_{j=1}^{N} \sigma^x_j \sigma^x_{j+1} + \lambda_1 \sum_{j=1}^{N} \sigma^y_j (\sigma^z_{j+1}\sigma^z_{j+2})\sigma^y_{j+3} + \lambda_2 \sum_{j=1}^{N} \sigma^z_j \sigma^z_{j+1}. \tag{6.23}$$

We have set the parameters to $\lambda_1 = 0.5$ and $\lambda_2 = 0.25$. Diagonalizing the model for (odd) system sizes ranging from $N = 5$ to $N = 13$ we find the same ground state momenta (and degeneracy) as in the model obtained by setting $\lambda_2 = 0$ and keeping the same λ_1, that we have solved analytically. The ground state momentum is given by

$$p_1(N) = \begin{cases} \frac{\pi}{4} - \frac{\pi}{4N}, & \text{N mod 8=1} \\ \frac{5\pi}{4} + \frac{\pi}{4N}, & \text{N mod 8=3} \\ \frac{5\pi}{4} - \frac{\pi}{4N}, & \text{N mod 8=5} \\ \frac{\pi}{4} + \frac{\pi}{4N}, & \text{N mod 8=7.} \end{cases} \tag{6.24}$$

and $p_2(N) = -p_1(N)$. The difference $p_1(N) - p_2(N)$ goes to $\pi/2$ for $N \to \infty$, which is different from π. Accordingly, the local order vanishes in the thermodynamic limit. The results in Fig. 6.3 illustrate this property.

6.9 Conclusions

We have studied generic Hamiltonians that commute with all three parity operators and examined the expectation values of local operators that break a Hamiltonian (parity) symmetry. With a dominant antiferromagnetic Ising interaction and in a setting that induces topological frustration we have shown that there are two possibilities: a) The expectation values of all such local operators decay algebraically, or faster, with the system size and vanish in the thermodynamic limit. b) There is a ground state choice that admits a finite magnetic order, but at the price of breaking the translational invariance. Which of the two possibilities is realized can also depend on the choice of the subsequence of (odd) chain lengths followed towards infinity, as the Cluster-Ising models demonstrate. We conclude that FBC are special for generic systems: since a perfect AFM order is not compatible with them, either the system disorders or spontaneously breaks translational symmetry. While these findings are probably not robust against a single ferromagnetic defect, we should stress once more that in Chapter 5 it was shown that the standard AFM order does not reappear in presence of at least one AFM defect, because, following also [67], FBC are at the verge of a phase transition and an AFM defect pushes the system into a phase that is either disordered or incommensurate. These results are intuitive from one side, but surprising from the point of view that the onset of local order is supposed to be independent from the applied boundary conditions and show once more that frustrated systems (even weakly frustrated ones) belong to a different class of systems altogether.

Chapter 7

Topological Frustration can modify a Quantum Phase Transition

Ginzburg-Landau theory [53, 54] of continuous phase transitions implicitly assumes that microscopic changes are negligible in determining the thermodynamic properties of the system. In this chapter we provide an example that clearly contrasts with this assumption. We show that topological frustration can destroy local order at both sides of a continuous quantum phase transition, by considering the 2-Cluster Ising chain with frustrated boundary conditions. While with other boundary conditions each of two phases is characterized by its own local order parameter, with frustration no local order can survive. We construct string order parameters to distinguish the two phases, but having proved that the transition cannot be characterized by local order parameters, topological frustration has modified its nature. This chapter is based on [7]

7.1 Introduction

In the previous chapters we have seen that topological frustration (TF) can destroy and modify local order. Here we point out the existence of an even more surprising effect associated with TF than in the previous chapters. Namely, we investigate the case in which the orders on both sides of a second order quantum phase transition (QPT) are "staggered" and thus both incompatible with the frustrated boundary conditions (FBC). We show that, in some cases, FBC generate TF that prevents the emergence of any local order, as quantified by observables spreading over a finite support and breaking a Hamiltonian symmetry and hence the system remains locally disordered across the QPT. Since the scaling dimensions of local observables close to the phase transition are usually one of the most important quantities to determine the universality class at criticality [175], we have that, without local order, the quantum phase transition changes its nature in presence of TF with respect to the other physical situations.

We discover this phenomenology by considering the 2-Cluster Ising chain, an exactly solvable model. Although frustration can prevent the establishment of any local order, we expect that the singularity at the QPT indeed signals a rearrangement of the system, although on lengths scaling like the total system size. Exploiting the analytical solvability of the model in the example we consider, we prove the existence and provide the explicit expressions for string order parameters that replace the local ones in distinguishing the two phases. In this way, we provide a path for an extension of the Ginzburg-Landau theory, in the sense that the transition indeed separates different types of global orders. Thus, with TF the transition becomes akin

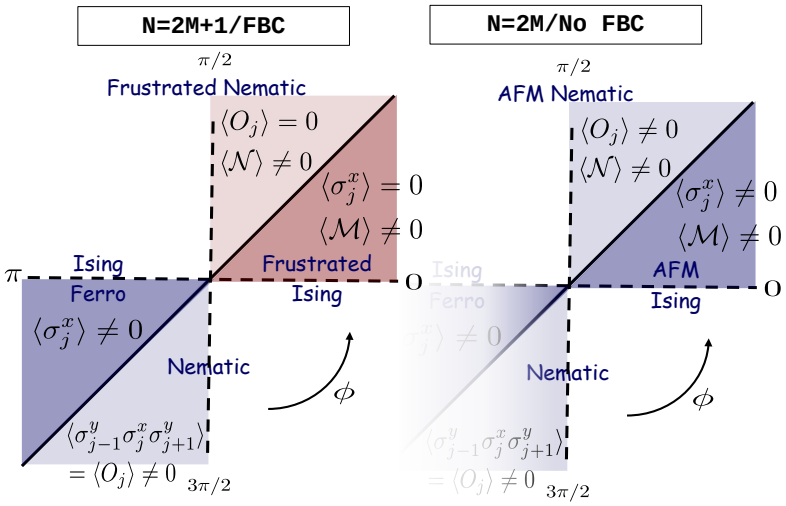

FIGURE 7.1: Relevant phase diagram of the 2-Cluster Ising model with Frustrated Boundary Conditions and its comparison with the established phase diagram with other BC.

to a topological one, although we are not able to provide a definite characterization in this respect.

7.2 The Model

We consider the so-called 2-Cluster Ising model, in which a short-range two-body Ising interaction competes with a cluster term acting simultaneously on four contiguous spins [170]:

$$H = \cos\phi \sum_{j=1}^{N} \sigma_j^x \sigma_{j+1}^x + \sin\phi \sum_{j=1}^{N} \sigma_{j-1}^y \sigma_j^z \sigma_{j+1}^z \sigma_{j+2}^y \tag{7.1}$$

$$= \cos\phi \sum_{j=1}^{N} \sigma_j^x \sigma_{j+1}^x + \sin\phi \sum_{j=1}^{N} O_j O_{j+1} \,. \tag{7.2}$$

Here and in the following σ_j^α ($\alpha = x, y, z$) stand for Pauli's operators on the j-th spin, $O_j = \sigma_{j-1}^y \sigma_j^x \sigma_{j+1}^y$ is the cluster operator [163] that allows to rewrite the cluster interaction term in a form resembling a two body one, ϕ is a parameter that allows to tune the relative weight between the two terms and the periodic boundary conditions imply that $\sigma_{j+N}^\alpha = \sigma_j^\alpha$, as well as $O_{j+N} = O_j$. Note that different cluster operators are mutually commuting ($[O_j, O_k] = 0$).

Usually, this model displays a second-order phase transition between two different ordered phases [170], depending on whether the Ising or the cluster terms dominate. However, by applying FBC (so setting N to be an odd number), when the interactions favor an antiferromagnetic alignment, TF sets in and the phase diagram modifies accordingly, as we will discuss and is previewed by the phase diagram in Fig. 7.1

In addition to the aforementioned quantum phase transition, this model possesses anticommuting parity symmetries, discussed in section 1.2.3, that are pivotal in our discussion of local order. Namely, the Hamiltonian in eq. (7.1) is invariant

under the transformation $\sigma_j^\alpha \leftrightarrow -\sigma_j^\alpha \ \forall \alpha$, which implies that, defining the parity operators as $\Pi^\alpha = \bigotimes_{l=1}^N \sigma_l^\alpha$, we have $\left[H, \Pi^\alpha\right] = 0 \ \forall \alpha$. Since we are considering the case of odd N, different parity operators anti-commute ($\left\{\Pi^\alpha, \Pi^\beta\right\} = 0$ for $\alpha \neq \beta$), implying that each eigenstate of the model is, at least, two-fold degenerate. Indeed, if $|\psi\rangle$ is an eigenstate of H with $\Pi^z = 1$, the state $\Pi^x |\psi\rangle$ has the same energy, but $\Pi^z = -1$. We stress that this symmetry is quite generic with FBC and is typically violated by the presence of external fields. Its importance is, as in the rest of the thesis, that it provides us a framework for symmetry breaking, bypassing the approach with the symmetry breaking fields, since the ground state degeneracy implies that any ground state vector breaks one of the invariances of the Hamiltonian and thus can display a finite magnetization in that direction. We will also use the fact that the mirror symmetry, which is the invariance under the transformation $\sigma_j^\alpha \leftrightarrow \sigma_{2k-j}^\alpha$, where k is the generic site of symmetry, implies that eigenstates either have 0 or π-momentum, or they appear as degenerate doublets [2] (see Appendix C.4).

The Hamiltonian in eq. (7.1) also enjoys other properties that are convenient for our analysis. Indeed, this model can be mapped exactly, although non-locally, to a free fermionic systems (see Appendix G) and exploiting this fact we can treat larger systems or even get exact analytical results. Moreover, a duality symmetry, consisting of the invariance of the Hamiltonian under the simultaneous exchange $\phi \leftrightarrow \frac{\pi}{2} - \phi$ and $\sigma_j^x \leftrightarrow O_j$, relates the Ising and the nematic phases.

When $\phi \in \left(\frac{3\pi}{4}, \frac{7\pi}{4}\right)$ the dominant interaction favors a ferromagnetic alignment and thus FBC do not induce any frustration, which sets in only in the remaining part of the phase diagram. Here, a double degenerate ground state (due to anticommuting parity symmetries) is separated by a finite energy gap from the other states and in the thermodynamic limit its behavior is indistinguishable from that with open boundary conditions studied in [170]. At $\phi = \frac{5\pi}{4}$ there is a quantum phase transition which separates two differently ordered phases. When the Ising interaction prevails over the cluster one, i.e. for $\phi \in \left(\frac{3\pi}{4}, \frac{5\pi}{4}\right)$, the system shows a ferromagnetic phase characterized by a non-zero value of the magnetization along x. On the other side of the critical point, when $\phi \in \left(\frac{5\pi}{4}, \frac{7\pi}{4}\right)$, we have that the system is in a nematic phase identified by the zeroing of the magnetizations in all directions and the simultaneous rise of a non-vanishing value for the expectation value of the nematic operator O_j.

On the contrary, when $\phi \in (0, \frac{\pi}{2})$, both the cluster and Ising interaction are "antiferromagnetic", and hence TF is induced in the system. Similarly to the phenomenology discussed in Chapter 4, the competition between two frustrated interactions increases the ground state degeneracy to four. Denoting by $|p\rangle$ a ground state vector in the odd sector of the z-parity with lattice momentum p, the GS manifold is spanned by four states, two in the odd sector $|\pm p\rangle$, and two in the even one $\Pi^x |\pm p\rangle$. The value of p depends on the value of N mod 8 and takes the value $p \simeq \frac{\pi}{4}$ or $p \simeq \frac{3\pi}{4}$. These states are surmounted by a band (of single particle) states, with the gap above the ground state closing as $1/N^2$ for large N.

7.3 Results

7.3.1 Local Order

As in the absence of TF, the ground-state energy displays a critical point when the relative weights of the two interactions coincide, see Fig. 7.2. On the contrary, several other physical aspects are completely spoiled. To highlight this fact, among all the

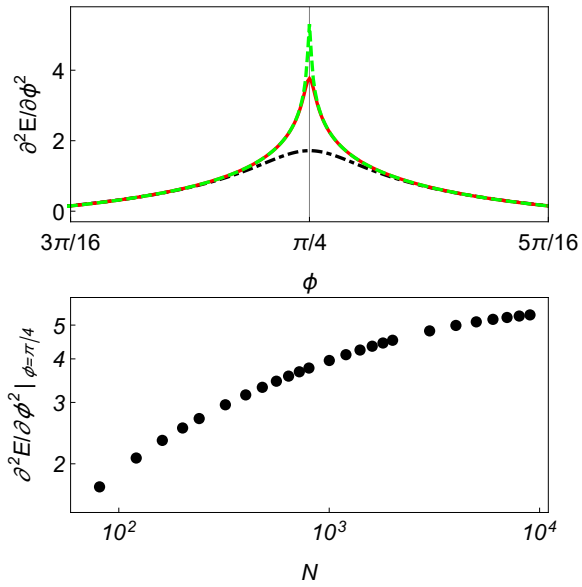

FIGURE 7.2: (Color online) - Upper Panel: second derivative of the ground-state energy density (i.e. the energy per site) as function of ϕ for different length of the system. $N = 81$ Black dot-dashed line, $N = 801$ Red solid line, $N = 8001$ Green Dashed line. Lower Panel: Dependence of the second derivative of the energy density evaluated for $\phi = \pi/4$ on the size of the system N.

elements in the manifold, we focus on two of them that capture two different spatial dependences of the order parameters,

$$\begin{aligned} |g_1\rangle &= \frac{1}{\sqrt{2}}\left(|p\rangle + \Pi^x |p\rangle \right), \\ |g_2\rangle &= \frac{1}{\sqrt{2}}\left(|p\rangle + \Pi^x |-p\rangle \right). \end{aligned} \tag{7.3}$$

As we wrote before, in the unfrustrated regimes the role of the order parameters is played by the expectation values of two operators, σ_j^x and O_j. They share the following properties: 1) they are defined on a finite subset of spins; 2) they commute with Π^x and anti-commute with Π^z. For an operator K_j, satisfying both 1) and 2), we have that its expectation value in the state $|g_1\rangle$ reduces to $\langle g_1| K_j |g_1\rangle = \langle p| \Pi^x K_j |p\rangle$ and, due to translational invariance we recover

$$\langle g_1| K_j |g_1\rangle = \langle p| \Pi^x K_N |p\rangle \qquad \forall j. \tag{7.4}$$

Hence, on $|g_1\rangle$ the order parameters assume the same value on each site of the system. On the contrary, $|g_2\rangle$ is not invariant under spatial translation, and we obtain

$$\langle g_2| K_j |g_2\rangle = \cos(2jp) \langle -p| \Pi^x K_N |p\rangle . \tag{7.5}$$

Therefore, on $|g_2\rangle$ the order parameters show an incommensurate periodic behavior.

Hence, to study the order parameters in the thermodynamic limit it is enough to analyze the dependence on N of $F_1(K_N) = \langle p| \Pi^x K_N |p\rangle$ and $F_2(K_N) = \langle -p| \Pi^x K_N |p\rangle$. This can be done borrowing the techniques developed in [1, 2] (chapters 3 and 4) and applied to this case in Appendix G. The general behavior for the magnetic ($K_N = \sigma_N^x$) and the nematic ($K_N = O_N = \sigma_{N-1}^y \sigma_N^x \sigma_1^y$) order parameter for $\phi \in (0, \frac{\pi}{4})$ is depicted

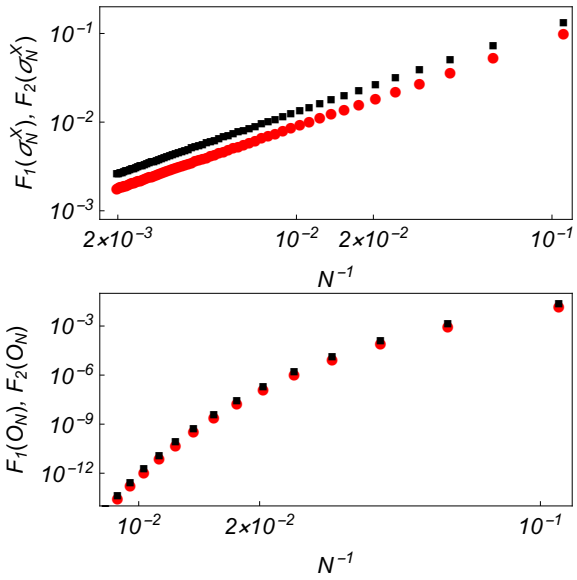

FIGURE 7.3: (Color online) - Dependence of $F_1(K_N) = \langle p|\,\Pi^x K_N\,|p\rangle$ (red dots) and $F_2(K_N) = \langle -p|\,\Pi^x K_N\,|p\rangle$ (black square) on the size of the system N at $\phi = \pi/8$ for different choices of K_N: upper panel $K_N = \sigma_N^x$, displaying a power law behavior; lower panel $K_N = O_N = \sigma_{N-1}^y \sigma_N^x \sigma_1^y$, showing an exponential decay. The data runs from $N = 9$ to $N = 505$.

in Fig. 7.3 as function of the (inverse) size of the system.

In accordance with the unfrustrated case, in the thermodynamic limit we would expect the system to be in a magnetic phase in which either $F_1(\sigma_N^x)$ or $F_2(\sigma_N^x)$ assumes a non-zero value, while both $F_1(O_N)$ and $F_2(O_N)$ vanish. However, while the exponential decay of the nematic order parameter is in agreement with this picture, Fig. 7.3 clearly shows that, in the thermodynamic limit, there is also no magnetic order since both $F_1(\sigma_N^x)$ and $F_2(\sigma_N^x)$ go to zero linearly with the inverse of the size of the system. Therefore, while in the non-frustrated models the system shows, in the region $\phi \in (0, \frac{\pi}{4})$, an antiferromagnetic order, the introduction of TF in the system induces a zeroing of the magnetic order parameter. In Appendix G we also show that this behavior survives the introduction of an AFM defect in the chain, proving, in accordance with Chapter 5, that the phenomenology we discuss is not restricted to purely translationally invariant systems. Moreover, recalling the duality symmetry held by the system, the behavior of the magnetic order parameter for $\phi \in (0, \frac{\pi}{4})$ is mirrored by the nematic order parameter for $\phi \in (\frac{\pi}{4}, \frac{\pi}{2})$. Hence, when FBC are imposed, the order parameters characterizing the two macroscopic phases of the unfrustrated models vanish at both sides of the critical point, making them unable to characterize the phase transition.

But we can go further. Indeed, we can prove that not only the magnetization and the nematic order parameter both vanish in both phases, but that this result extends to any possible local order parameter, i.e. to any expectation value of a local observable that anticommutes with at least one of the parity operators Π^α. In fact, in Chapter 6, we have shown that a wide class of topologically frustrated models, to which the 2-Cluster Ising also belongs, cannot exhibit a finite local order parameter in the vicinity of the classical antiferromagnetic point ($\phi = 0$) unless the difference between the momenta of two ground states tends to $\pm\pi$ in the thermodynamic limit. Since in our case we have that this difference tends to $\pi/2$, the expectation values of

all local observables that can play the role of the order parameter vanish in the thermodynamic limit close to the point $\phi = 0$ and, hence, we expect that they stay equal to zero until the quantum critical point at $\phi = \pi/4$ is reached. Moreover, applying the duality arguments, it follows that the expectation values of local observables must vanish also in the vicinity of the point $\phi = \pi/2$ and therefore also in the whole region $\phi = (\pi/4, \pi/2)$. As a consequence, since the expectation value of all such local observables vanishes at both sides of the critical point, there is no local order parameter that can characterize the quantum phase transition at either sides. To our knowledge, this is the first case in which topological frustration, and hence a change in the boundary conditions of a system, affects the thermodynamic phase of a spin system so deeply up to completely remove the presence of local order parameters.

7.3.2 String order

However, the result of Chapter 6 does not apply to operators whose support scales with the length of the chain and this fact discloses the possibility that the two macroscopic phases can be distinguished by string order parameters, whose presence is normally associated with some kind of phases with topological order [161, 163, 170, 176]. We have not been able to identify a strong geometric criterion to define the string order connected with TF, but, exploiting the microscopical structure of the model under consideration, we have indeed succeeded in constructing two string operators that suit our needs, namely:

$$\mathcal{M} = \prod_{k=1}^{I(N)} \left(\sigma^x_{4k-2}\sigma^x_{4k-1}\right); \quad \mathcal{N} = \prod_{k=1}^{I(N)} \left(O_{4k-2}O_{4k-1}\right), \tag{7.6}$$

where $I(N)$ depends on the length of the chain and it is equal to $\frac{N-1}{4}$ for $N \bmod 4 = 1$ and to $\frac{N+1}{4} - 1$ in case of $N \bmod 4 = 3$. Both operators commute with all the parity operators Π^α. It is easy to see that, defining $\mathcal{F}_{1,2}(\mathcal{K}) = \langle g_{1,2}|\mathcal{K}|g_{1,2}\rangle$ for a generic string operator $\mathcal{K}$ for which $[\mathcal{K}, \Pi^\alpha] = 0\ \forall \alpha$, we have $\mathcal{F}_1(\mathcal{K}) = \mathcal{F}_2(\mathcal{K})$.

These expectation values can be studied analytically using the asymptotic properties of determinants studied in [3] (see Appendix G), that are the subject of Chapter 9, and for $\mathcal{K} = \mathcal{M}, \mathcal{N}$ in the region $\phi \in (0, \pi/4)$ we obtain

$$\begin{aligned} \mathcal{F}_1(\mathcal{M}) &\overset{N\to\infty}{\simeq} (-1)^{I(N)}\frac{1}{2}(1-\tan^2\phi)^{\frac{1}{4}}, \\ \mathcal{F}_1(\mathcal{N}) &\overset{N\to\infty}{\simeq} 0\,. \end{aligned} \tag{7.7}$$

In the same region the finite-size results for $\mathcal{F}_1(\mathcal{M})$ and $\mathcal{F}_1(\mathcal{N})$ are depicted in Fig. 7.4, where it can be seen that the second goes to zero algebraically with the system size. In the thermodynamic limit the expectation value of the string operator goes continuously to zero at $\phi = \pi/4$, and can thus serve to characterize the quantum phase transition. This picture of the continuous quantum phase transition is coherent with the one inferred from the second derivative of the ground state energy. Of course, taking into account that $\mathcal{M}$ and $\mathcal{N}$ are one image of the other under the duality transformation, their behavior is mirrored in the region $\phi \in (\pi/4, \pi/2)$.

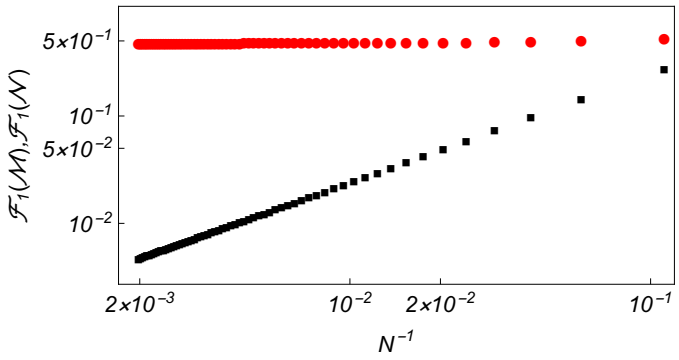

FIGURE 7.4: (Color online) - Dependence of $\mathcal{F}_1(\mathcal{M}) = \langle g_1| \mathcal{M} |g_1\rangle$ (Red dots) and $\mathcal{F}_1(\mathcal{N}) = \langle g_1| \mathcal{N} |g_1\rangle$ (Black squares) on the size of the system N at $\phi = \pi/8$. The data runs from $N = 9$ to $N = 505$ and shows the power law decay of one of the string order parameters, while the other remains finite in the thermodynamic limit.

7.4 Conclusions

We have shown how the presence of a TF, induced by the assumption of FBC in a system with antiferromagnetic interactions, can change the nature of the phase transition in a one-dimensional spin system. While in absence of such kind of frustration, the phases at different sides of the critical point admit two different (staggered) local order parameters, when TF comes into play such quantities vanish in the thermodynamic limit. And this fact is not limited to the expectation value of the operators associated to the order parameters without frustration, but extends to all the operators that can act as local order parameters.

These results lead to the rethinking within the standard approach to phase transitions. Indeed, usually, approaching a phase transition, only one length scale becomes important: that of the (dominant) correlation length (or the inverse mass gap). This is because the system size is already considered bigger than any other length scale and thus irrelevant. However, this is an idealization, since in practice it is much easier to reach a very large correlation length than to have a truly infinite system. Thus, approaching a critical point, it would be important to also consider scaling quantities that include the size of the system. While under all other boundary conditions this turns out not to be necessary, in presence of FBC this is not the case, as also already pointed out in Ref. [76], and the system size suppresses any local order. Nonetheless, the divergences of the correlation length that causes the discontinuity in the second derivative of the free energy can still be harvested to define an order (and disorder) parameter with different behaviors across the transition, but requires an observable spreading through the whole loop, that is, a string order. While we cannot guarantee that the string parameters that we defined in eq. (7.6) are the optimal ones to classify the phases, nor we can provide an interpretation for what they represent in this way, we have shown that the traditional elements of GLT mix differently in the presence of TF and provide a completely unexpected phenomenology.

From the results in Chapter 4, we can see that the quantum XY chain does not posses the phenomenology discovered here for the 2-Cluster Ising chain. In the quantum XY chain (4.1) at different sides of the QPT at $\phi = \pi/4$, on the other hand, there are ground states with different incommensurate AFM orders. From the results in Chapter 6 we can see that for n-Cluster Ising models for other (even) n it

can, in general, depend on the choice of the subsequence of (odd) system sizes followed towards infinity whether we will have the phenomenology as in the quantum XY chain or as in the 2-Cluster Ising model here. It would be interesting to explore further which systems posses the phenomenology discussed here and which don't.

Before concluding, we wish to underline that the results from this chapter are resilient to the presence of a localized AFM defect in the Hamiltonian, as we show in Appendix G, thus proving that the phenomenon we have discussed here cannot be considered simply as resulting from fine-tuning in the system parameters.

Chapter 8

Topological Frustration does not affect Topological Phases

In the previous chapters we have shown that one-dimensional antiferromagnetic spin models with frustrated boundary conditions, i.e. periodic boundary conditions with an odd number of elements, may show very peculiar behavior. Indeed, the presence of frustrated boundary conditions can affect local magnetic orders and system's quantum phase transitions. Motivated by these results, in this chapter we analyze the effects of the introduction of frustrated boundary conditions on several models supporting (symmetry protected) topological order, and compare our results with the ones obtained in other settings. We find that none of the analyzed topological order phases are altered by frustrated boundary conditions. This observation leads naturally to the conjecture that topological phases of one-dimensional systems are in general not affected by topological frustration. This chapter is based on [5].

8.1 Introduction

In the previous century various different classical phases of matter and continuous phase transitions were classified using the Landau symmetry breaking theory [107, 108]. When physicists begin to turn their attention to quantum phases, the Landau theory was successfully borrowed to describe also the quantum regime and it was believed that virtually all phases can be classified in this framework. However, in the late 1980s it became clear that there are quantum phases beyond the Landau paradigm and successively the concept of topological order was established [109]. Topological phases [109, 177–179] are quantum phases with different properties from any symmetry breaking states. They are characterized by the properties such as the topological ground state degeneracy, non-Abelian geometric phases and long-range entanglement. For instance, the topological ground state degeneracy depends on the system's topology and cannot be lifted by any local perturbations. In one dimension, only a weaker form of topological order can exist essentially, namely the Symmetry Protected Topological (SPT) order. [109, 179–183], where topological properties can occur only if symmetry requirements are imposed on the system and with the ground states exhibiting only short-range entanglement.

While in this thesis we have found many effects that topological frustration can have on antiferromagnetic phases of quantum spin chains, nothing has still been done for phases exhibiting (symmetry protected) topological orders, in which the system's topology indeed determines some system's properties. In the present chapter, our goal is to fill this gap. For this task we focus on several exactly solvable one-dimensional models known to exhibit the SPT order and analyze the effects of imposing frustrated boundary conditions on them.

At first, in Sec. 8.2, we study the so-called Cluster–Ising model [161, 162] that is a one–dimensional model, in which a three–body cluster interaction competes with an antiferromagnetic Ising one. Despite its apparent complexity, the model admits an analytical solution obtained by mapping the spin degrees of freedom into spinless fermions using the Jordan-Wigner transformation [91, 149]. Since there is an interplay between two different types of interactions, the model presents a transition between a phase dominated by the cluster interaction and one in which the leading term is the Ising one. While in the second region the system (usually) admits a magnetically ordered phase, when the cluster interactions dominate over the antiferromagnetic ones, the model is known to exhibit a symmetry protected topological order. We will show that, while the magnetic phase is deeply affected by the rising of topological frustration, the SPT ordered phase is insensitive to frustrated boundary conditions, a fact that we explain considering simple properties of the two and three body interactions. The fact that the sensitivity of the model to the change of boundary conditions is a function of the macroscopic phase and not only of the model considered, strongly suggests that such a property must extend to all other models that present SPT ordered phases.

To test such a suggestion we turn, in Sec. 8.3, to the AKLT chain [184, 185], which is a one-dimensional model, with a $SO(3)$ symmetric Hamiltonian, describing spin-1 degrees of freedom interacting antiferromagnetically. The model supports a unique ground state (up to boundary state degeneracies), separated from the rest of the eigenstates by a finite gap, and it exhibits exponentially decaying correlation functions. It is characterized by spins paired into valence-bonds and symmetry protected topological order [109, 182]. The model with periodic boundary conditions, including FBC, has been already studied in details [31, 185] so we simply summarize and discuss the results relevant for this work, showing that also in this model frustrated boundary conditions, which induce topological frustration, do not affect the model and its order.

Finally, in Sec. 8.4 we consider the last of the 1D topological models in our survey, namely the Kitaev chain [186]. With open boundary conditions, the Kitaev chain is known to be exactly mappable to the quantum XY chain in a transverse magnetic field [56, 90], but moving to periodic BC there are some subtleties, that play an important role when we wish to analyze the effect of frustration. In all cases, the Kitaev chain can be reduced to a free fermionic problem, and therefore diagonalized analytically [56, 91]. Exploiting this approach, we highlight that, regardless of the macroscopic phase, the Kitaev chain is completely unaltered by moving from an even to an odd number of sites (or viceversa).

Thus in all models analyzed we find that their symmetry protected topological orders are either resilient to the topological frustration imposed by frustrated boundary conditions, or that the system is such that frustrated boundary conditions do not introduce any incompatibility in the simultaneous minimization of the local and global structure of the Hamiltonian. These observations naturally drive us to conjecture that SPT ordered phases in one dimension are not affected by frustrated boundary conditions. This result could be, to some extent, counter intuitive. In fact, it shows that topological phases are not affected by the (real-space) topology of the system. Most of all, our conjecture places a further clear distinction between phases characterized by non-global order parameters, as the magnetic and the nematic ones, studied in previous chapters, and topologically ordered ones, at least in one dimension.

8.2 The Cluster-Ising model

8.2.1 The Model

Let us start by introducing the Cluster-Ising model. We consider a system made of spins-$\frac{1}{2}$, in which a two-body antiferromagnetic Ising pairing competes with a three-body cluster interaction. The Hamiltonian of such model reads

$$H = \cos\phi \sum_{j=1}^{N} \sigma_j^x \sigma_{j+1}^x + \sin\phi \sum_{j=1}^{N} \sigma_{j-1}^y \sigma_j^z \sigma_{j+1}^y, \tag{8.1}$$

where σ_j^α, for $\alpha = x, y, z$, are the Pauli operators on the j-th spin and the parameter ϕ allows to change the relative weight between the two terms. Since our goal is to study the effect of topological frustration, we assume periodic boundary conditions $\sigma_{j+N}^\alpha = \sigma_j^\alpha$ and that N is an odd number ($N = 2M+1$). Due to the existence of an analytical solution, the family of spin-1/2 cluster models was intensively studied in the past years [161–163, 168–170, 187]. For the Cluster–Ising model in eq. (8.1) it is well-known that for $\phi \in (-\pi/4, \pi/4)$ the model is in an antiferromagnetic Ising phase, for $\phi \in (3\pi/4, 5\pi/4)$ in a ferromagnetic phase, while for $\phi \in (\pi/4, 3\pi/4)$ and $\phi \in (-3\pi/4, -\pi/4)$, where the many-body interactions dominate over the Ising ones, the model exhibits a symmetry protected topological order. Such order can be characterized by a non-zero expectation value of the non-local string operator, defined as

$$O(r) = \sigma_1^y \sigma_2^x \Big(\bigotimes_{j=3}^{r} \sigma_j^z \Big) \sigma_{r+1}^x \sigma_{r+2}^y. \tag{8.2}$$

Before we start the detailed solution of the model based on the Jordan-Wigner transformation, let us make some general considerations. Both from the seminal Toulouse's works [156, 157] for classical models and from their generalization to the quantum regime [29, 30], we have that, to determine whether or not a model is geometrically or topologically frustrated, we need two elements. The first of these elements is a prototype model, i.e. a model in which frustration is absent. The second element is a set of local unitary operators, by which we try to reduce the model under analysis to the prototype one. If it is possible to find such a set of local unitary operations that map our Ising–like model into the prototype one, then the system is free from geometrical frustration. Otherwise, we have that the system is geometrically or topologically frustrated.

In the case of an antiferromagnetic Ising model the prototype model is the model in which each bond is turned into a ferromagnetic one. Let us now focus on the case of a one–dimensional lattice with periodic boundary conditions in which all bonds between neighboring spins are antiferromagnetic. Such model is exactly the Ising term of the Hamiltonian in eq. (8.1) and can be written as $\sum_{i=1}^{N} \sigma_i^x \sigma_{i+1}^x$. If N is even, the sign of all the terms $\sigma_j^x \sigma_{j+1}^x$ can be inverted simply by inverting every second spin, starting from $j = 1$, hence reducing it to a purely ferromagnetic Ising model and thus proving that the model is not frustrated. On the contrary, with odd N, the system is not bipartite and there is no such transformation, hence proving the presence of frustration.

Let us now consider the cluster term of the eq. (8.1), i.e. $\sum_j \sigma_{j-1}^y \sigma_j^z \sigma_{j+1}^y$. Differently from the Ising case, inverting every single spin of the lattice through a unitary operation generated by the spin operators σ_j^y it is always possible to change the global

sign of the model. As a consequence, the three-body cluster interaction is not expected to show any geometrical frustration. This should be contrasted to the case of the cluster interaction with an even number of sites, such as the 2-Cluster-Ising chain [163, 170], studied in chapters 6 and 7, which does not have topological order. According to the argument above, in these cases we expect for the frustration to be effective and indeed we have proven this to be the case in chapters 6 and 7.

When we have the simultaneous presence of both interactions, arguments like those just made become more complex. However, in the parameter region in which the Ising type interaction dominates over the cluster one, taking inspiration from arguments such as adiabatic deformation [188], we expect the system to present signatures of the presence of geometrical frustration. Viceversa, in the region dominated by cluster-type interaction, these signatures can be expected to be absent. Such region is expected to show a symmetry protected topological order [161], and therefore it is expected to be unaffected by the presence of frustration.

Let us now turn to the exact solution of the Cluster–Ising model in presence of frustrated boundary conditions. It is well known [161, 170] that it can be diagonalized exactly, using the Jordan–Wigner transformation

$$c_j = \left(\bigotimes_{l=1}^{j-1} \sigma_l^z\right) \frac{\sigma_j^x + \imath\sigma_j^y}{2}, \quad c_j^\dagger = \left(\bigotimes_{l=1}^{j-1} \sigma_l^z\right) \frac{\sigma_j^x - \imath\sigma_j^y}{2}, \tag{8.3}$$

that maps spins into spinless fermions. In the process of diagonalization, of which the details can be found in Appendix H.1, the Hamiltonian is divided in the two parity sectors of $\Pi^z = \bigotimes_{j=1}^N \sigma_j^z$,

$$H = \frac{1+\Pi^z}{2} H^+ \frac{1+\Pi^z}{2} + \frac{1-\Pi^z}{2} H^- \frac{1-\Pi^z}{2}\,, \tag{8.4}$$

and in each sector the Hamiltonian can be written in terms of free fermionic operators

$$H^\pm = \sum_{q\in\Gamma^\pm} \varepsilon_q \left(a_q^\dagger a_q - \frac{1}{2}\right), \tag{8.5}$$

where a_q are Bogoliubov fermions. The fermionic momenta q in eq. (8.5) belong to two different sets, respectively $q \in \Gamma^+ = \{\frac{2\pi}{N}(k+\frac{1}{2})\}$ for the even parity sector ($\Pi^z = 1$) and $q \in \Gamma^- = \{\frac{2\pi}{N}k\}$ for the odd one ($\Pi^z = -1$), where, in both cases, k runs over all integers between 0 and $N-1$.

To each fermionic momentum is associated an energy, given by

$$\begin{aligned} \varepsilon_q &= 2\sqrt{1+\sin 2\phi \cos 3q} && \forall\, q \neq 0, \pi, \\ \varepsilon_0 &= 2(\sin\phi + \cos\phi) && q = 0 \in \Gamma^-, \\ \varepsilon_\pi &= 2(\sin\phi - \cos\phi) && q = \pi \in \Gamma^+. \end{aligned} \tag{8.6}$$

It is worth noting that the momenta $0 \in \Gamma^-$ and $\pi \in \Gamma^+$ (since we study the case in which N is odd), are different from the others because: a) they do not have the corresponding opposite momentum; b) their energies can be negative.

From eqs. (8.6) it is easy to determine the ground states of the system starting from the vacuum of Bogoliubov fermions in the two sectors ($|0^\pm\rangle$), which, by construction, have positive parity $\Pi^z = 1$, and taking into account the modes with negative energy and the parity requirements. We are going to examine the antiferromagnetic phase and the cluster phase separately. To compute the ground state

expectation of observables it is going to be convenient to use the Majorana fermions, defined as

$$A_j = c_j^\dagger + c_j, \quad B_j = \imath(c_j^\dagger - c_j), \tag{8.7}$$

which are related to the spin operators as

$$A_j = \Big(\bigotimes_{l=1}^{j-1}\sigma_l^z\Big)\sigma_j^x\,, \quad B_j = \Big(\bigotimes_{l=1}^{j-1}\sigma_l^z\Big)\sigma_j^y. \tag{8.8}$$

On the basis of Wick theorem [189–192] the expectation values of observables are determined by the two-point correlators of Majorana fermions.

Antiferromagnetic phase

In studying the antiferromagnetic phase $\phi \in (-\pi/4, \pi/4)$ we focus on the parameter region $\phi \in (-\pi/4, 0)$ without loosing generality since to any ground state $|g(\phi)\rangle$ corresponds the ground state $|g(-\phi)\rangle = \Pi^x |g(\phi)\rangle$ In particular, the spin-correlations functions are the same in the two states, $\langle g(-\phi)|\, \sigma_1^x\sigma_{1+r}^x\, |g(-\phi)\rangle = \langle g(\phi)|\, \sigma_1^x\sigma_{1+r}^x\, |g(\phi)\rangle$, and, similarly, the magnetization $\langle g(\phi)|\, \sigma_j^x\, |g(\phi)\rangle = \langle g(-\phi)|\, \sigma_j^x\, |g(-\phi)\rangle$.

We find that the ground state degeneracy depends on whether (odd) N is divisible by 3. When N is not divisible by 3 the ground state is single, given by $|g\rangle = a_0^\dagger |0^-\rangle$, corresponding to the energy minimizing mode $q = 0$. When N is divisible by 3 there are three energy minimizing modes, given by $q = 0, 2\pi/3, -2\pi/3$. The ground state manifold is thus three-fold degenerate and a general ground state is a superposition

$$|g\rangle = (u_1 a_0^\dagger + u_2 a_{\frac{2\pi}{3}}^\dagger + u_3 a^\dagger_{-\frac{2\pi}{3}})\,|0^-\rangle\,, \tag{8.9}$$

where the normalization $\sum_{j=1}^3 |u_j|^2 = 1$ is assumed. However, regardless the dimension of the ground state manifold, it always falls into a single Π^z sector, with an energy gap above it that closes as $1/N^2$ for large (odd) N.

The Majorana correlators in the ground state (8.9) are found to be

$$\begin{aligned}\langle A_j A_l\rangle_g &= \delta_{jl} - \frac{2\imath}{N}(|u_2|^2 - |u_3|^2)\sin\Big[\frac{2\pi}{3}(j-l)\Big] \\ &\quad - \frac{2\imath}{N}\Big[(u_1^* u_2 - u_3^* u_1)e^{\imath\frac{\pi}{3}(j+l-1)} + \text{c.c.}\Big]\sin\Big[\frac{\pi}{3}(j-l)\Big],\end{aligned} \tag{8.10}$$

$$\begin{aligned}\langle B_j B_l\rangle_g &= \delta_{jl} - \frac{2\imath}{N}(|u_2|^2 - |u_3|^2)\sin\Big[\frac{2\pi}{3}(j-l)\Big] \\ &\quad - \frac{2\imath}{N}\Big[(u_1^* u_2 - u_3^* u_1)e^{\imath\frac{\pi}{3}(j+l+1)} + \text{c.c.}\Big]\sin\Big[\frac{\pi}{3}(j-l)\Big],\end{aligned} \tag{8.11}$$

$$\begin{aligned}-\imath\,\langle A_j B_l\rangle_g \overset{N\to\infty}{\simeq} &\int_0^{2\pi} \frac{\cos\phi + \sin\phi\, e^{-\imath 3q}}{|\cos\phi + \sin\phi\, e^{-\imath 3q}|} e^{-\imath q(j-l-1)}\frac{dq}{2\pi} \\ &- \frac{2}{N}\Big\{|u_1|^2 + (|u_2|^2 + |u_3|^2)\cos\Big[\frac{2\pi}{3}(j-l-1)\Big]\Big\} \\ &- \frac{2}{N}\Big[(u_1^* u_2 + u_3^* u_1)e^{\imath\frac{\pi}{3}(j+l)} + \text{c.c.}\Big]\cos\Big[\frac{\pi}{3}(j-l-1)\Big] \\ &- \frac{2}{N}\Big[u_2^* u_3\, e^{-\imath\frac{2\pi}{3}(j+l)} + \text{c.c.}\Big],\end{aligned} \tag{8.12}$$

while, for N not divisible by 3, the correlators can be reproduced from the previous expressions by taking formally $u_2 = u_3 = 0$. The exact finite-N result for the last

correlator can be found in Appendix H.1. In the correlators we can see corrections of order $1/N$, that would not be present in a model without topological frustration. Although they vanish in the thermodynamic limit, they cannot be neglected, as they can influence the spin-correlation functions at large distances, i.e. for a distance that scales with the dimension of the system. Indeed, as shown in Appendix H.1, we find the spin-correlation functions

$$\langle \sigma_1^x \sigma_{1+r}^x \rangle_g \overset{r\to\infty}{\simeq} (-1)^r (1-\tan^2\phi)^{3/4} \left(1 - \frac{2r}{N}\right). \tag{8.13}$$

The correlations at large distances r decay linearly and for the most distant spins on the ring, separated by $r \approx N/2$, they vanish in the thermodynamic limit. The magnetization order parameter also vanishes in the ground state, above which there is only an algebraically small gap, similarly to the quantum Ising chain with FBC [66, 67, 71, 73], discussed in Chapter 1. Thus, topological frustration affects the antiferromagnetic phase of the Cluster-Ising chain, closing the energy gap and destroying the magnetization and spin-correlations at large distances, which are the effects of topological frustration encountered throughout the whole thesis.

Cluster phase

We find that for $\phi \in (\pi/4, 3\pi/4)$ the ground state is $|g\rangle = |0^+\rangle$ and it is separated by a finite energy gap from the excited states above it. Similarly, for $\phi \in (-3\pi/4, \pi/4)$ the ground state is $|g\rangle = a_0^\dagger |0^-\rangle$, also with a finite energy gap above it. These two regions of the model's phase space are those known to display symmetry protected topological order [161, 170].

As shown in Appendix H.1, the correlators of Majorana fermions are $\langle A_j A_l \rangle_g = \langle B_j B_l \rangle_g = \delta_{jl}$ and

$$\langle A_j B_l \rangle_g \overset{N\to\infty}{\simeq} \imath \int_0^{2\pi} \frac{\sin\phi + \cos\phi\, e^{\imath 3q}}{|\sin\phi + \cos\phi\, e^{\imath 3q}|} e^{-\imath q(j-l+2)} \frac{dq}{2\pi}, \tag{8.14}$$

which is the same result as without frustration [161, 170], i.e. the same result would be obtained for even N. There is no corrections of order $1/N$ as in the antiferromagnetic phase.

The consequence of this result is that the expectation value of any bulk observable remains the same with frustrated boundary conditions, generic periodic BC or, arguably, open BC. Indeed, in the antiferromagnetic phase the effect of frustration arises as a correction to the Majorana correlation function. Since, any observable can be expressed in terms of Pauli spin-operators, while Pauli spin-operators can be expressed as a product of Majorana fermions, the expectation value of any observable can be expressed as an expectation of a product of Majorana fermions, which is by Wick theorem determined by two-point correlators of Majorana fermions. Therefore, since the two-point correlators of Majorana fermions are the same as without frustration for large N, and since the same applies for the Jordan-Wigner transformation (8.7), so is the expectation value of any bulk observable.

In particular, in Appendix H.1 we compute the expectation value of the string operator, obtaining

$$\langle O(r)\rangle_g \overset{r\to\infty}{\simeq} \begin{cases} (1-\cot^2\phi)^{\frac{3}{4}}, & \phi\in(\frac{\pi}{4},\frac{3\pi}{4}) \\ (-1)^r(1-\cot^2\phi)^{\frac{3}{4}}, & \phi\in(-\frac{3\pi}{4},-\frac{\pi}{4}) \end{cases} \tag{8.15}$$

as without frustration [170]. On the contrary, in the topologically ordered phases, the expectation values of the operators $\langle\sigma_j^\alpha\rangle$ for $\alpha = x,y,z$ are zero. Namely, since the ground state does not break the Π^z parity symmetry of the model we have immediately $\langle\sigma_j^x\rangle = 0$, $\langle\sigma_j^y\rangle = 0$, while the relation $\langle\sigma_j^z\rangle = 0$ follows from the equality $\sigma_j^z = -\imath A_j B_j$ and the property that the corresponding integral in (8.14) vanishes.

The non-zero expectation value of the non-local string operator, and zero expectation value of local observables, such as spin operators, characterizes the symmetry protected topological ordered phase in the Cluster-Ising model. It is, hence, proved that such a phase is not affected by FBC.

8.3 AKLT model

The AKLT model [184, 185] is a one dimensional model, describing spin-1 degrees of freedom interacting antiferromagnetically. It is defined by the $SO(3)$ symmetric Hamiltonian

$$H = \sum_{j=1}^{N}\left[\vec{S}_j\cdot\vec{S}_{j+1} + \frac{1}{3}(\vec{S}_j\cdot\vec{S}_{j+1})^2\right]. \tag{8.16}$$

The FBC are achieved by imposing an odd number of lattice sites $N = 2M+1$ and periodic BC $\vec{S}_{j+N} = \vec{S}_j$. Naively, we can expect that FBC induce frustration in the AKLT model, by considering its classical limit, namely the classical Heisenberg model, and thus neglecting the second term in eq. (8.16). As discussed in Chapter 1, with periodic boundary conditions and even N the energy is minimized by the perfectly staggered configuration $\vec{S}_j = -\vec{S}_{j+1}$. However, for odd N, corresponding to FBC, such a configuration is impossible because the lattice is not bipartite. Therefore, not all local terms in the Hamiltonian can be minimized simultaneously, and the Hamiltonian is frustrated.

Turning back to the quantum case, the AKLT Hamiltonian in eq. (8.16) acquires a (symmetry protected) topological order and it is thus an ideal candidate to test our conjecture that this property protects it from the effect of FBC. It is easy to check that eq. (8.16) can be written as a sum of projectors

$$H = 2\sum_{j=1}^{N}\left[P^{(2)}(\vec{S}_j,\vec{S}_{j+1}) - \frac{1}{3}\right], \tag{8.17}$$

where $P^{(2)}(\vec{S}_j,\vec{S}_l)$ projects the state of two spin-1 at sites j and l into their spin-2 representation.

The AKLT model with both open and periodic BC has been studied in detail in [185] (for a more pedagogical approach see the book [31]). It is known that the ground state is unique with PBC, and four-fold degenerate with open BC, with this degeneracy related to the existence of edge states and thus not influencing the expectation values of bulk observables, which are the same in the different ground states (similarly to what happens in the Cluster-Ising model and the Kitaev chain that we will analyze later). The AKLT ground state, with periodic boundary conditions, is

a valence-bond solid state. To show this, one represents each spin-1 degree of freedom through two spin-1/2 in their triplet representation. Then, these spin-1/2 on neighboring sites are paired as singlet to prevent the ferromagnetic alignment penalized by the Hamiltonian. Denoting by $|\alpha\rangle_j$, $|\beta\rangle_j$ the two spin-1/2 on the j-th site, the valence bond state is

$$|V\rangle_j \equiv \mathbf{V}^{\beta_j,\alpha_{j+1}}|\beta_j\rangle_j|\alpha_{j+1}\rangle_{j+1} = \frac{1}{\sqrt{2}}\Big(|\uparrow\rangle_j|\downarrow\rangle_{j+1} - |\downarrow\rangle_j|\uparrow\rangle_{j+1}\Big)\,, \tag{8.18}$$

where $\mathbf{V} \equiv \frac{1}{\sqrt{2}}\begin{pmatrix} 0 & 1 \\ -1 & 0 \end{pmatrix}$. We then construct the ground state of (8.16) as

$$|GS\rangle \equiv \prod_{l=1}^{N} \hat{P}_l^{(1)} \bigotimes_{j=1}^{N} |V\rangle_j\,, \tag{8.19}$$

where

$$\hat{P}_l^{(1)} \equiv \mathbf{P}^{\sigma}_{\alpha,\beta}|\sigma\rangle_j\langle\alpha|_j\langle\beta| = |+1\rangle_j\langle\uparrow\uparrow| + \frac{1}{\sqrt{2}}|0\rangle_j\Big(\langle\uparrow\downarrow| + \langle\downarrow\uparrow|\Big) + |-1\rangle_j\langle\downarrow\downarrow| \tag{8.20}$$

projects the two spin-1/2 into their spin-1 representation, with the Clebsch-Gordan coefficients $\mathbf{P}^{+1} \equiv \begin{pmatrix} 1 & 0 \\ 0 & 0 \end{pmatrix}$, $\mathbf{P}^{0} \equiv \frac{1}{\sqrt{2}}\begin{pmatrix} 0 & 1 \\ 1 & 0 \end{pmatrix}$, and $\mathbf{P}^{-1} \equiv \begin{pmatrix} 0 & 0 \\ 0 & 1 \end{pmatrix}$, and where the site $N+1$ is identified with the first, since periodic boundary conditions are assumed. As already discussed in [185], the only difference between having even or odd N is the need of a different index contraction in the spinorial representation of the valence bond state. However, the even-odd choice does not change the gapped nature of the system and the bulk behavior of the correlation functions [31, 185].

Moreover, the string order parameters that encode the topological order of the AKLT model

$$S_{j,l}^{(\alpha)} \equiv \langle GS|S_j^{\alpha} e^{\imath\pi\sum_{n=j+1}^{l-1} S_n^{\alpha}} S_l^{\alpha}|GS\rangle / \langle GS|GS\rangle\,, \tag{8.21}$$

$$S^{(\alpha)} \equiv \lim_{l-j\to\infty}\lim_{N\to\infty} S_{j,l}^{(\alpha)} = \frac{4}{9}\,, \tag{8.22}$$

for $\alpha = x, y, z$, remain non-zero and unchanged.

We thus conclude that the (symmetry protected) topological order of the AKLT model is not affected by frustrated boundary conditions.

8.4 Kitaev chain

The Kitaev chain [186] is a model of a spinless fermions topological superconductor, with the Hamiltonian

$$H = -\mu\sum_{j=1}^{N}\left(c_j^{\dagger}c_j - \frac{1}{2}\right) - \sum_{j=1}^{N}\Big[w\,(c_j^{\dagger}c_{j+1} + \text{h.c.}) - \Delta\,(c_j c_{j+1} + \text{h.c.})\Big]\,, \tag{8.23}$$

where μ is the chemical potential, w is the hopping amplitude and Δ is the superconducting gap. As we have done so far, also with the Kitaev model we will focus on the case of FBC, i.e. with periodic boundary conditions ($c_{j+N} = c_j$) and an odd number of lattice sites $N = 2M+1$. However, before we start the analysis of the case with

periodic boundary conditions, let us summarize the main results that were obtained for the open ones.

It is well-known that the Kitaev chain with open boundary conditions, that can be obtained from eq. (8.23) restricting the range of the second sum up to $j = N - 1$, can be mapped, inverting the Jordan-Wigner transformation in eq. (8.3), to the quantum XY chain in transverse field [56, 90, 91, 150]

$$H = -\sum_{j=1}^{N-1} \left[\frac{w+\Delta}{2} \sigma_j^x \sigma_{j+1}^x + \frac{w-\Delta}{2} \sigma_j^y \sigma_{j+1}^y \right] + \frac{\mu}{2} \sum_{j=1}^{N} \sigma_j^z. \tag{8.24}$$

Hence, exactly as the correspondent spin model, in the thermodynamic limit, it shows a phase transitions at $\mu = \pm 2w$. This quantum phase transition separates a topologically trivial phase for $|\mu| > 2|w|$ without edge modes in the open chain, from a topologically ordered phase $|\mu| < 2|w|$ characterized by the presence of Majorana edge modes. The latter, for the spin chain, was shown to be affected by FBC when the Ising term promotes an AFM order [1, 2, 73], with a phenomenology similar to that of the Cluster-Ising chain we discussed in Sec. 8.2.1. Due to the relation between the XY and the Kitaev chain, it is natural to wonder if the latter can also be affected by FBC, although we cannot compare the spinless model to a related classical one which is affected by frustration.

Moving from open to periodic boundary conditions, the exact equivalence between the fermionic and the spin model ceases to exist. The reason for such quite surprising result is connected to the fact that the Jordan-Wigner transformations breaks the invariance under spatial translation, by selecting a reference site. This implies that the interactions terms between the first and the last spin of the chain are no more mapped in a standard two–body fermionic term, but in a string term that makes it impossible to map a short-range fermionic model into a short range spin model. To provide an example, we have that the term $\sigma_N^x \sigma_1^x$ is mapped into the string operator $-\Pi^z (c_N^\dagger - c_N)(c_1^\dagger + c_1)$ where Π^z is the parity operator along the z axis that has support on the whole lattice. A similar result stands also for $\sigma_N^y \sigma_1^y$. When either $w \pm \Delta < 0$ (and $|\mu| < 2|w|$), the XY chain, with an odd number of sites, becomes frustrated: the energy gap above the ground states closes (algebraically) in the thermodynamic limit [66, 70, 71, 73], the correlation functions acquire peculiar algebraic corrections [1, 71, 73], the entanglement entropy violates the area law [73], and, for $\mu = 0$, the AFM local order is replaced by the ferromagnetic mesoscopic order or by the AFM incommensurate modulated one, with a quantum phase transition separating the two (see chapters 3 and 4).

From a physical perspective, the main difference between the Kitaev and the XY chain is that only the former supports (symmetry protected) topological order. Given the close relation between the two models and the fact that the effects of frustration have already been established for the spin chain, we may wonder whether there is an even-odd effect also in the Kitaev chain

As presented in Appendix H.2, exploiting the approach illustrated in Ref. [56], we can diagonalize the Kitaev chain with periodic boundary conditions and odd N, obtaining

$$H = \sum_{q \in \Gamma} \varepsilon_q \left(a_q^\dagger a_q - \frac{1}{2} \right), \tag{8.25}$$

where a_q are Bogoliubov fermions, whose momenta q belong to the set $\Gamma = \{\frac{2\pi}{N} k\}$, with k running over integers between 0 and $N-1$. It is worth to note that, assuming N to be odd, $q = \pi$ is not an allowed momentum in this model. The dispersion

relation is given by

$$\varepsilon_q = \sqrt{(4w\cos q + \mu)^2 + 4\Delta^2 \sin^2 q}, \quad q \neq 0 \tag{8.26}$$

$$\varepsilon_0 = -2w - \mu, \tag{8.27}$$

Similarly to the Cluster-Ising model case, the mode $q = 0$ is special because it is the only one in which the energies can be negative. The eigenstates of the model are constructed by populating the vacuum state $|0\rangle$. Taking into account the dispersion relation, it is easy to see that the ground state of the Kitaev chain with periodic frustrated boundary conditions, is always non-degenerate, with a finite energy gap above it, except at the phase transition points $\mu = \pm 2w$, where the spectrum becomes gapless and relativistic. Similarly to the Cluster-Ising model, in the topologically ordered phase $|\mu| < 2|w|$, the ground state degeneracy, in the thermodynamic limit, is different from the one that characterizes the model with open boundary conditions. While the former is two-fold, with PBCs the ground state is unique. Nevertheless, the expectation values of bulk observables are the same, as we now show.

For this purpose, we define Majorana fermions using eq. (8.7). Then, similarly to the Cluster-Ising model, all operators acting on the Fock space generated by $c_j^\dagger$ can be expressed in terms of Majorana fermions, and using the Wick theorem it follows that the ground state expectation value of any observable is determined by the two-point correlators of Majorana fermions. As shown in Appendix H.1, the two-point correlators of Majorana fermions in the ground state, in all parameter regions of the model, are $\langle A_j A_l \rangle_g = \langle B_j B_l \rangle_g = \delta_{jl}$ and

$$\langle A_j B_l \rangle_g \overset{N\to\infty}{\simeq} \imath \int_0^{2\pi} \frac{2w\cos q + \mu + 2\Delta\imath \sin q}{|2w\cos q + \mu + 2\Delta\imath \sin q|} e^{-\imath q(j-l)} \frac{dq}{2\pi} \tag{8.28}$$

Hence, for large N, the expression of the Majorana correlation functions do not depend on the boundary conditions (the result for free boundary conditions follows from the equivalent spin chain[150]). Therefore, the expectation values of all bulk observables in the Kitaev chain with FBC are equal to those in other settings and no difference emerges when $w \pm \Delta < 0$. We conclude, in particular, that topological order in the Kitaev chain is, as in the Cluster-Ising model, not affected by frustrated boundary conditions.

8.5 Conclusions

We have presented an analysis of the effects of frustrated boundary conditions on (symmetry protected) topologically ordered phases of different one-dimensional models. At first, we have focused on the one-dimensional Cluster-Ising model with an odd number of spins and periodic boundary conditions. We have presented general arguments by which the symmetry protected topological order of the cluster phase is not expected to be affected by frustration, while the antiferromagnetic phase is. These speculative arguments have been confirmed by our analytic results. While in the antiferromagnetic phase FBC close the energy gap and destroy both the spin-correlations at large distances and the magnetization, the string order parameter in the cluster phase is not affected by FBC. The property that the effects of topological

frustration are lost when the cluster interactions start dominating over the antiferromagnetic ones is, in some extent, similar to the situation in the frustrated Ising model [66, 71, 73], where the effects of frustration are suppressed by increasing the magnetic field, resulting in the resilience of the paramagnetic phase to geometrical frustration.

Our results on the Cluster-Ising model are even more interesting if we observe that we can directly transfer our general arguments to the n-cluster Ising model, studied in Refs. [163, 170], which consists of n-body cluster interaction competing with the antiferromagnetic Ising pairing. It is known that for any odd n, the model is characterized by a symmetry protected topologically ordered phase, which is, by our general arguments, expected not to be affected by geometrical frustration. A question that arises naturally already at this point is whether FBC do not affect only models with cluster interactions or it is a general property of systems supporting topological order. For this reason, we have extended our analysis to two additional one-dimensional models that also exhibit SPT: the AKLT model and the Kitaev chain. In both cases, the topological phase is unaffected by FBC, as is also shown by the fact that a typical effect of frustration is the closing of the energy gap [66, 70, 71, 73] (see also previous chapters), which remains open in the topological phases of all the models analyzed. Since we have found in various models that the topologically ordered phases analyzed so far are not affected by FBC, we arrive naturally to the conjecture: Frustrated boundary conditions do not affect symmetry protected topological phases of one dimensional systems. One could also think that only Landau local orders are thus sensitive (and fragile) to topological frustration, but we have shown in Chapter 7 that this is not the case and that nematic order can be destroyed by FBC.

Chapter 9

Toeplitz determinants with a delta function singularity

In this chapter we find the asymptotic behaviors of Toeplitz determinants with symbols which are a sum of two contributions: one analytical and non-zero function in an annulus around the unit circle, and the other proportional to a Dirac delta function. The formulas are found by using the Wiener-Hopf procedure. The determinants of this type are found in computing the spin-correlation functions in low-lying excited states of some integrable models, mappable to free fermions, where the delta function represents a peak at the momentum of the excitation. In topologically frustrated models this type of determinants appears already in studying the ground state properties. As a concrete example of applications of our results, using the derived asymptotic formulas we compute the spin-correlation functions in the lowest energy band of the topologically frustrated quantum XY chain in zero field, and the ground state magnetization. In particular, we derive results presented in Chapter 3. This chapter is based on [3].

9.1 Introduction and Results

We consider Toeplitz determinants

$$\tilde{D}_n(\tilde{f}) = \det\left(\tilde{f}^{(n)}_{j-k}\right)_{j,k=1}^{n}, \qquad \tilde{f}^{(n)}_j = \frac{1}{2\pi}\int_0^{2\pi} \tilde{f}(\theta, n) e^{-\imath j\theta} d\theta \tag{9.1}$$

with a symbol

$$\tilde{f}(\theta, n) = f(e^{\imath\theta})\left[1 + 2\pi z_n\, \delta(\theta - \theta_0)\right] \tag{9.2}$$

Here δ is Dirac delta function, $\theta_0 \in [0, 2\pi)$, $(z_n)_{n\in\mathbb{N}}$ is an arbitrary sequence in $\mathbb{C}$ and f is a continuous function on the unit circle.

It follows that for $\theta_0 \neq 0$ the elements $\tilde{f}^{(n)}_j$ are equal to

$$\tilde{f}^{(n)}_j = f_j + z_n f(e^{\imath\theta_0}) e^{-\imath j\theta_0}, \tag{9.3}$$

where

$$f_j = \frac{1}{2\pi}\int_0^{2\pi} f(e^{\imath\theta}) e^{-\imath j\theta} d\theta\,. \tag{9.4}$$

For $\theta_0 = 0$ there is an ambiguity in the delta function integral. In this case we use (9.3) to define the coefficients $\tilde{f}^{(n)}_j$ and the Toeplitz matrix $\tilde{D}_n(\tilde{f})$.

We restrict ourselves to symbols f that are non-zero and analytic in an annulus including the unit circle. A general such symbol can be written as

$$f(z) = a(z)z^{\nu}, \tag{9.5}$$

where a is a function that is analytic and non-zero on the annulus and has zero winding number, while $\nu \in \mathbb{Z}$ is the winding number of the symbol f (see e.g. [193, 194]).

We are interested in asymptotic formulas for $\tilde{D}_n(\tilde{f})$ as $n \to \infty$. The asymptotic formulas for

$$D_n(f) = \det(f_{j-k})_{j,k=1}^{n} \tag{9.6}$$

for analytic non-zero symbols f are by now considered classical, and exist under much more general conditions. For $\nu = 0$ they are given by the strong Szegő limit theorem (originally proven in [195], for a review of later developments see [196–198]). The asymptotic formulas for nonzero ν have been first obtained in [199, 200], and later under different conditions and using different methods in [201, 202]. The delta function in the symbol (9.2) might also be considered, in a suitable limit, as a singularity of the symbol, different from the widely studied Fisher-Hartwig singularities (for a review see [203]).

We decided to solve this problem motivated by the appearance of determinants of type (9.1) in spin-correlation functions of certain low energy states in quantum spin chains mappable to free fermonic systems. In such instances, the determinant $D_n(f)$ reflects the ground state correlations (in absence of frustration) and the delta function of the symbol has a peak at the momentum of the fermionic excitation on the vacuum state. For chains with boundary frustration, the spin-correlation functions in the lowest admissible state are already determined by (9.1), where θ_0 emerges as the mode minimizing the energy and lying at the bottom of a band of states (in the thermodynamic limit) [1, 2, 71–73], as discussed in Chapter 3. The leading asymptotic term for particular determinants of the type (9.1) in the case $\nu = 0$ was found in [71] in the context of the frustrated quantum Ising chain, without discussion of the subleading terms and without rigor: providing a reliable proof has been the initial inspiration for this work, together with the possibility of extending the conditions of applicability.

To introduce the notation, we are first going to review some results on the asymptotics of the determinant $D_n(f)$ where f is non-zero and analytic in an annulus around the unit circle. The asymptotic formulas of [199, 200] are appropriate for this case. The function $a(z) = \sum_{k=-\infty}^{\infty} a_k z^k$, defined in (9.5), is analytic in an annulus including the unit circle so

$$\limsup_{k\to\infty} |a_{-k}|^{1/k} = \rho_- < 1 < \rho_+ = \liminf_{k\to\infty} |a_k|^{-1/k} . \tag{9.7}$$

An analytic logarithm of a on $\rho_- < |z| < \rho_+$ exists so we can introduce the Wiener-Hopf factorization (see e.g. [193, 204])

$$a_-(z) = \exp \sum_{k=1}^{\infty} (\log a)_{-k} z^{-k}, \quad a_+(z) = \exp \sum_{k=0}^{\infty} (\log a)_k z^k, \tag{9.8}$$

where $\log a(z) = \sum_{k=-\infty}^{\infty} (\log a)_k z^k$ and thus $a = a_- a_+$. We also introduce the functions

$$b = a_- a_+^{-1}, \quad c = a_+ a_-^{-1}, \qquad b\,c = 1 . \tag{9.9}$$

For expressing the subleading terms in the asymptotic formulas for $D_n(f)$ it is useful to define $\rho \in (0,1)$ by

$$\rho_- < \rho < 1 < \rho^{-1} < \rho_+ \,. \tag{9.10}$$

The function a is then analytic on $\rho \leq |z| \leq \rho^{-1}$ and $a_j = O(\rho^j)$, $a_{-j} = O(\rho^j)$, for $j \geq 0$, for all ρ satisfying (9.10). Analogous relations hold for the functions b and c.

The asymptotic behavior of $D_n(f)$ in the case of zero winding number of the symbol ($\nu = 0$) is given by the strong Szegő limit theorem. The version of [199, 200] in the case of analytic symbol reads

$$D_n(a) = \exp\left[n(\log a)_0 + \sum_{k=1}^{\infty} k(\log a)_k (\log a)_{-k} + O(\rho^{2n})\right] \quad \text{as } n \to \infty. \tag{9.11}$$

We note that in the same reference an explicit formula for the term $O(\rho^{2n})$ in (9.11) is given, up to corrections $O(\rho^{4n})$.

For $\nu \neq 0$ the asymptotic behavior of $D_n(f)$ is determined by the asymptotic behavior of $D_n(a)$ and the determinant of the $|\nu| \times |\nu|$ Toeplitz matrix, defined by

$$\Delta_{\nu,n} = \det\left(d^{(n)}_{j-k}\right)_{j,k=1}^{|\nu|}, \quad \text{where} \quad d^{(n)}_j = \begin{cases} b_{n+j} & \text{for } \nu < 0 \\ c_{-n-j} & \text{for } \nu > 0 \end{cases}. \tag{9.12}$$

The asymptotic formula is

$$D_n(f) = (-1)^{n\nu} D_{n+|\nu|}(a)\left[\Delta_{\nu,n} + O(\rho^{n(|\nu|+3)})\right]. \tag{9.13}$$

The formula (9.13) follows from the more precise result of [199, 200], given by Theorem 4 in [199] and Theorem 6 in [200].

We will extend these formulas to determinants of type (9.1). In order to do so, we first define the determinants $\tilde{\Delta}_{\nu,n}(l)$, for $l = 1, 2, ..., |\nu|$, for $\nu \neq 0$, as the determinants of the matrix $(d^{(n)}_{j-k})_{j,k=1}^{|\nu|}$ with the column l replaced by the vector $(1, e^{-\imath\theta_0}, e^{-\imath 2\theta_0}, \ldots, e^{-\imath(|\nu|-1)\theta_0})^{\mathrm{T}}$ for $\nu < 0$ and by $(1, e^{\imath\theta_0}, e^{\imath 2\theta_0}, ..., e^{\imath(\nu-1)\theta_0})^{\mathrm{T}}$ for $\nu > 0$. This definition can be written as

$$\tilde{\Delta}_{\nu,n}(l) = \det\left(\tilde{d}^{(l)}_{j,k}\right)_{j,k=1}^{|\nu|}, \quad \text{where } \tilde{d}^{(l)}_{j,k} = \begin{cases} (1-\delta_{k,l}) d^{(n)}_{j-k} + \delta_{k,l} e^{-\imath(j-1)\theta_0} & \text{for } \nu < 0 \\ (1-\delta_{k,l}) d^{(n)}_{j-k} + \delta_{k,l} e^{\imath(j-1)\theta_0} & \text{for } \nu > 0 \end{cases}. \tag{9.14}$$

Our main results are the following two theorems.

Theorem 3. *For $\nu = 0$ we have*

$$\tilde{D}_n(\tilde{f}) = D_n(a)\left\{1 + z_n\left[n + \imath\frac{d}{d\theta}\log b(e^{\imath\theta})\Big|_{\theta=\theta_0} + O(\rho^n)\right]\right\} \quad \text{as } n \to \infty, \tag{9.15}$$

where ρ is defined by (9.10).

Theorem 4 (not rigorous). *Let $\nu \neq 0$ and suppose $D_n(f) \neq 0$, $\Delta_{\nu,n} \neq 0$, for $n \geq n_0$, $n_0 \in \mathbb{N}$. If for sufficiently small ρ, satisfying (9.10), we have*

$$\lim_{n\to\infty} \frac{\tilde{\Delta}_{\nu,n}(j)}{\Delta_{\nu,n}} \rho^{2n} = 0 \quad \text{for all } j \in \{1, 2, ..., |\nu|\}\,, \tag{9.16}$$

where $\tilde{\Delta}_{\nu,n}(j)$ *are defined by* (9.14)*, then for* $n \geq n_0$

$$\tilde{D}_n(\tilde{f}) = D_n(f)\left\{1 + z_n\left[- b(e^{\iota\theta_0})e^{-\iota(n+1)\theta_0}\sum_{j=1}^{|\nu|}\frac{\tilde{\Delta}_{\nu,n}(j)}{\Delta_{\nu,n}}\left(e^{\iota j\theta_0} + O(\rho^n)\right) + n + O(1)\right]\right\}$$

if $\nu < 0$, (9.17)

$$\tilde{D}_n(\tilde{f}) = D_n(f)\left\{1 + z_n\left[- c(e^{\iota\theta_0})e^{\iota(n+1)\theta_0}\sum_{j=1}^{\nu}\frac{\tilde{\Delta}_{\nu,n}(j)}{\Delta_{\nu,n}}\left(e^{-\iota j\theta_0} + O(\rho^n)\right) + n + O(1)\right]\right\}$$

if $\nu > 0$. (9.18)

Compared to the usual behavior of Toeplitz determinants without delta-function singularities, in this case we see the emergence of algebraic contributions in the matrix rank n. The terms inside the sums in (9.17) an (9.18) are expected to be of the order of magnitude of the inverse of the coefficients $d_j^{(n)}$ for $|j| < |\nu|$. Therefore, since $d_j^{(n)} = O(\rho^n)$ as $n \to \infty$, they are expected typically to grow faster than ρ^{-n}, with exponentially suppressed subleading corrections.

We are going to derive these theorems by relating the determinant to a linear problem, which in turn can be expressed as a linear functional equation, whose solution can be obtained in the limit of large n. The leading contributions to this solution, obtained using the Wiener-Hopf procedure, provide the asymptotic formulas above for the determinant. The estimates on the order of magnitude of the corrections to the terms we have calculated explicitly rely on the intuitively clear property that a small perturbation to the functional equation yields a change to the solution of a similar order of magnitude. For the case of a zero winding number of the symbol we have also provided a rigorous proof of this statement, which makes Theorem 3 rigorous. For the case of a non-zero winding number we have not provided a rigorous proof, but the corrections are plausible for the same reasons and we have confirmed Theorem 4 numerically on a few relevant examples.

We derive the theorems in section 9.2. To give a concrete example of applications of these theorems (and to explicitly show the unusual behavior of these determinants) in section 9.3 we compute the spin-correlation functions in the lowest energy band of the frustrated quantum XY chain in zero magnetic field, and the ground state magnetization. In particular, results presented in Chapter 3 are derived.

9.2 Derivation of the Theorems

9.2.1 Linear Problem

The first step in the derivation of the theorems is to use (9.3) and the basic property that the determinant is an alternating mutilinear function of its columns, to expand $\tilde{D}_n(\tilde{f})$ as

$$\tilde{D}_n(\tilde{f}) = D_n(f) + z_n f(e^{\iota\theta_0})\sum_{j=1}^{n} e^{\iota(j-1)\theta_0} D_{n,j}(f), \tag{9.19}$$

where by $D_{n,j}(f)$ we denote the determinant obtained by replacing the column j in $D_n(f)$ by the column vector $(1, e^{-\iota\theta_0}, e^{-\iota 2\theta_0}, ..., e^{-\iota(n-1)\theta_0})^{\mathrm{T}}$.

We assume that there is $n_0 \in \mathbb{N}$ such that $D_n(f) \neq 0$ for $n \geq n_0$. In the case $\nu = 0$ this assumption is justified by the Szegő theorem, while for nonzero ν we restrict ourselves to symbols for which this assumption holds. This assumption implies that

there exists a unique solution $x_j^{(n)}$, $j = 0, 1, ..., n-1$, of the linear problem

$$\sum_{k=0}^{n-1} f_{j-k} x_k^{(n)} = e^{-\imath\theta_0 j}, \quad \text{for } j = 0, 1, ..., n-1, \tag{9.20}$$

that is by Cramer's rule given by

$$x_j^{(n)} = \frac{D_{n,j+1}(f)}{D_n(f)} \,. \tag{9.21}$$

This solution can be inserted in (9.19) to get

$$\tilde{D}_n(\tilde{f}) = D_n(f)\Big[1 + z_n f(e^{\imath\theta_0}) \sum_{j=0}^{n-1} e^{\imath\theta_0 j} x_j^{(n)}\Big]. \tag{9.22}$$

Defining the analytic function

$$X^{(n)}(z) = \sum_{j=0}^{n-1} x_j^{(n)} z^j \tag{9.23}$$

we have

$$\tilde{D}_n(\tilde{f}) = D_n(f)\Big(1 + z_n f(e^{\imath\theta_0}) X^{(n)}(e^{\imath\theta_0})\Big). \tag{9.24}$$

We are thus going to find an asymptotic formula for $X^{(n)}(z)$, and hence for $\tilde{D}_n(\tilde{f})$, by using the Wiener-Hopf procedure, similar to the one of [204, 205] used to compute the spin correlation functions of the Ising model. The prerequisites and details are given in the following sections.

Let us comment that the presented method of relating the determinant to a linear problem would not work with more than one delta function in the symbol (9.2). In arriving to expression (9.19) we have used the property that different column vectors resulting from the delta function in the symbol are one scalar multiple of the other. This has lead to many cancellations, since determinant is an alternating function. With more delta functions, column vectors arising from different delta functions could not anymore be related simply by scalar multiplication, which prevents cancellations.

9.2.2 Equivalent Problem

For a function $g(z) = \sum_{j=-\infty}^{\infty} g_j z^j$, defined and analytic in an annulus $\rho_- < |z| < \rho_+$ including the unit circle, we define its components

$$[g]_-(z) = \sum_{j=1}^{\infty} g_{-j} z^{-j}, \quad [g]_+(z) = \sum_{j=0}^{\infty} g_j z^j. \tag{9.25}$$

The function $[g]_-$ is analytic on $|z| > \rho_-$, while the function $[g]_+$ is analytic on $|z| < \rho_+$. For definiteness, in the following we are going to restrict the domain of these functions to the annulus $\rho_- < |z| < \rho_+$, where both are analytic.

As shown in Appendix I.1, defining the coefficients

$$y_j^{(n)} = \begin{cases} e^{-\imath j\theta_0}, & j \in \{0, 1, ..., n-1\} \\ 0, & j \in \mathbb{Z}\backslash\{0, 1, ..., n-1\} \end{cases} \tag{9.26}$$

and the analytic function

$$Y^{(n)}(z) = \sum_{j=0}^{n-1} y_j^{(n)} z^j \tag{9.27}$$

solving the linear problem (9.20) is equivalent to finding functions $X^{(n)}, U^{(n)}, V^{(n)}$, defined and analytic on an annulus including the unit circle, satisfying

$$fX^{(n)} = Y^{(n)} + U^{(n)} z^n + V^{(n)} \tag{9.28}$$

and having the properties

$$\left[X^{(n)}\right]_- = 0, \quad \left[X^{(n)} z^{-n}\right]_+ = 0, \quad \left[U^{(n)}\right]_- = 0, \quad \left[V^{(n)}\right]_+ = 0\,. \tag{9.29}$$

With $D_n(f) \neq 0$ the solution exists and is unique, with $X^{(n)}$ corresponding to (9.23). By solving this equivalent problem we find the asymptotic formula for $X^{(n)}(e^{\imath\theta_0})$ in (9.24).

9.2.3 Evaluating the components

Following the standard Wiener-Hopf approach, we seek the solution of (9.28) by exploiting the different analytical properties of the different components of the functions appearing in it. The components (9.25) can be evaluated as the following integrals. Let z belong to the annulus $\rho_- < |z| < \rho_+$, and let $\rho_1 \in (\rho_-, |z|), \rho_2 \in (|z|, \rho_+)$. Then

$$[g]_- (z) = \frac{1}{2\pi\imath} \oint_{|w|=\rho_1} \frac{g(w)}{z-w} dw, \qquad [g]_+ (z) = \frac{1}{2\pi\imath} \oint_{|w|=\rho_2} \frac{g(w)}{w-z} dw. \tag{9.30}$$

These formulas can be shown by summing, in accordance with definition (9.25), the Laurent series coefficients

$$g_k = \frac{1}{2\pi\imath} \oint_{|w|=\rho_1} g(w) \frac{dw}{w^{k+1}} = \frac{1}{2\pi\imath} \oint_{|w|=\rho_2} g(w) \frac{dw}{w^{k+1}} \tag{9.31}$$

and interchanging the sum and the integral, which is valid since the Laurent series is uniformly convergent on every closed subannulus in the interior of its annulus.

In the derivation of the theorems we are going to encounter functions G, analytic on the annulus $\rho_- < |z| < \rho_+$, that are of the form

$$G(z) = \frac{g(z) - g(e^{\imath\theta_0})}{z - e^{\imath\theta_0}} \quad \text{for } z \neq e^{\imath\theta_0}, \qquad G(e^{\imath\theta_0}) = \left.\frac{\mathrm{d}g(z)}{\mathrm{d}z}\right|_{z=e^{\imath\theta_0}}, \tag{9.32}$$

where g is analytic on the same annulus. For instance, the function (9.27) satisfies

$$Y^{(n)}(z) = e^{-\imath(n-1)\theta_0} \frac{z^n - e^{\imath n\theta_0}}{z - e^{\imath\theta_0}}, \quad Y^{(n)}(e^{\imath\theta_0}) = n = e^{-\imath(n-1)\theta_0} \left.\frac{\mathrm{d}z^n}{\mathrm{d}z}\right|_{z=e^{\imath\theta_0}}. \tag{9.33}$$

For $z \neq e^{\imath\theta_0}$, it will be convenient to consider the function G as a sum of two functions with a singularity on the unit circle, or, as we are about to show, the sum of two functions analytical inside/outside the unit circle. We thus need to introduce another structure. Let $\mathcal{G}$ be defined by the rule

$$\mathcal{G}(z) = \frac{g(z)}{z - e^{\imath\theta_0}} \qquad \text{for } \rho_- < |z| < \rho_+,\ z \neq e^{\imath\theta_0}, \tag{9.34}$$

with g being a function analytic on the annulus $\rho_- < |z| < \rho_+$. The function $\mathcal{G}$ is thus analytic on the annuli $\rho_- < |z| < 1$ and $1 < |z| < \rho_+$. Its Laurent series coefficients are different on two different annuli, let us denote them by

$$\mathcal{G}(z) = \sum_{j=-\infty}^{\infty} \mathcal{G}_j^{(<)} z^j \quad \text{for } \rho_- < |z| < 1, \qquad \mathcal{G}(z) = \sum_{j=-\infty}^{\infty} \mathcal{G}_j^{(>)} z^j \quad \text{for } 1 < |z| < \rho_+. \tag{9.35}$$

There are thus two ways of defining $+$ and $-$ components of the functions $\mathcal{G}$. We define

$$[\mathcal{G}]_-^{(<)}(z) = \sum_{j=1}^{\infty} \mathcal{G}_{-j}^{(<)} z^{-j}, \quad [\mathcal{G}]_+^{(<)}(z) = \sum_{j=0}^{\infty} \mathcal{G}_j^{(<)} z^j, \tag{9.36}$$

$$[\mathcal{G}]_-^{(>)}(z) = \sum_{j=1}^{\infty} \mathcal{G}_{-j}^{(>)} z^{-j}, \quad [\mathcal{G}]_+^{(>)}(z) = \sum_{j=0}^{\infty} \mathcal{G}_j^{(>)} z^j. \tag{9.37}$$

In this work we are going to make use of the functions $[\mathcal{G}]_-^{(<)}$ and $[\mathcal{G}]_+^{(>)}$, both of which are analytic on $\rho_- < |z| < \rho_+$. We are going to use the obvious notation

$$\left[\frac{g}{z - e^{\imath\theta_0}}\right]_-^{(<)} = [\mathcal{G}]_-^{(<)}, \quad \left[\frac{g}{z - e^{\imath\theta_0}}\right]_+^{(>)} = [\mathcal{G}]_+^{(>)}. \tag{9.38}$$

Analogously to (9.30) we have the integral representation

$$\begin{aligned} \left[\frac{g}{z - e^{\imath\theta_0}}\right]_-^{(<)}(z) &= \frac{1}{2\pi\imath} \oint_{|w|=\rho_1} \frac{g(w)}{(w - e^{\imath\theta_0})(z - w)} dw, \quad \text{where } \rho_1 \in \big(\rho_-, \min\{1, |z|\}\big), \\ \left[\frac{g}{z - e^{\imath\theta_0}}\right]_+^{(>)}(z) &= \frac{1}{2\pi\imath} \oint_{|w|=\rho_2} \frac{g(w)}{(w - e^{\imath\theta_0})(w - z)} dw, \quad \text{where } \rho_2 \in \big(\max\{1, |z|\}, \rho_+\big). \end{aligned} \tag{9.39}$$

Expanding $1/(w - e^{\imath\theta_0})$ under integrals into series and interchanging the series and the integral, we get the following representation:

$$\begin{aligned} \left[\frac{g}{z - e^{\imath\theta_0}}\right]_-^{(<)}(z) &= \sum_{j=0}^{\infty} e^{-\imath(j+1)\theta_0} \big[g z^j\big]_-(z), \\ \left[\frac{g}{z - e^{\imath\theta_0}}\right]_+^{(>)}(z) &= \sum_{j=0}^{\infty} e^{\imath j\theta_0} \big[g z^{-j-1}\big]_+(z). \end{aligned} \tag{9.40}$$

With the introduced definitions, for the function G defined by (9.32) we have

$$\begin{aligned} [G]_- &= \left[\frac{g - g(e^{\imath\theta_0})}{z - e^{\imath\theta_0}}\right]_-^{(<)} = \left[\frac{g}{z - e^{\imath\theta_0}}\right]_-^{(<)}, \\ [G]_+ &= \left[\frac{g - g(e^{\imath\theta_0})}{z - e^{\imath\theta_0}}\right]_+^{(>)} = \left[\frac{g}{z - e^{\imath\theta_0}}\right]_+^{(>)}, \end{aligned} \tag{9.41}$$

where the first equality follows immediately from the integral representations and the second is obtained using

$$\left[\frac{g(e^{\imath\theta_0})}{z - e^{\imath\theta_0}}\right]_-^{(<)} = 0, \quad \left[\frac{g(e^{\imath\theta_0})}{z - e^{\imath\theta_0}}\right]_+^{(>)} = 0, \tag{9.42}$$

which follows from (9.40). From (9.41) it follows

$$G = \left[\frac{g}{z - e^{\imath\theta_0}}\right]_-^{(<)} + \left[\frac{g}{z - e^{\imath\theta_0}}\right]_+^{(>)}. \tag{9.43}$$

We clearly have also the following linear property. Let h be a function analytic on the same annulus as g. Then

$$[hG]_- = \left[\frac{hg}{z - e^{\imath\theta_0}}\right]_-^{(<)} - \left[\frac{hg(e^{\imath\theta_0})}{z - e^{\imath\theta_0}}\right]_-^{(<)}, \qquad [hG]_+ = \left[\frac{hg}{z - e^{\imath\theta_0}}\right]_+^{(>)} - \left[\frac{hg(e^{\imath\theta_0})}{z - e^{\imath\theta_0}}\right]_+^{(>)}. \tag{9.44}$$

The definitions we have introduced are going to be useful because of the following two elementary lemmas that we state and prove.

Lemma 1. *Let g be a function analytic on an annulus $\rho_- < |z| < \rho_+$, that includes the unit circle. Then for $z \neq e^{\imath\theta_0}$ belonging to the annulus*

$$\left[\frac{g}{z - e^{\imath\theta_0}}\right]_-^{(<)}(z) = \frac{[g]_-(z) - [g]_-(e^{\imath\theta_0})}{z - e^{\imath\theta_0}}, \qquad \left[\frac{g}{z - e^{\imath\theta_0}}\right]_+^{(>)}(z) = \frac{[g]_+(z) - [g]_+(e^{\imath\theta_0})}{z - e^{\imath\theta_0}}. \tag{9.45}$$

Proof. Let us prove the first equality. From the representation (9.40) it follows

$$\left[\frac{[g]_+}{z - e^{\imath\theta_0}}\right]_-^{(<)} = 0, \tag{9.46}$$

which implies

$$\left[\frac{g}{z - e^{\imath\theta_0}}\right]_-^{(<)} = \left[\frac{[g]_-}{z - e^{\imath\theta_0}}\right]_-^{(<)}. \tag{9.47}$$

We now define a function $G^{(-)}$ as

$$\begin{aligned} G^{(-)}(z) &= \frac{[g]_-(z) - [g]_-(e^{\imath\theta_0})}{z - e^{\imath\theta_0}} \quad \text{for } z \neq e^{\imath\theta_0},\ \rho_- < |z| < \rho_+, \\ G^{(-)}(e^{\imath\theta_0}) &= \frac{\mathrm{d}}{\mathrm{d}z}[g]_-(z)\Big|_{z=e^{\imath\theta_0}}, \end{aligned} \tag{9.48}$$

and, using the decomposition (9.43) for this function, we have

$$G^{(-)} = \left[\frac{[g]_-}{z - e^{\imath\theta_0}}\right]_-^{(<)} + \left[\frac{[g]_-}{z - e^{\imath\theta_0}}\right]_+^{(>)} = \left[\frac{[g]_-}{z - e^{\imath\theta_0}}\right]_-^{(<)}, \tag{9.49}$$

where the last equality follows from (9.40). Combining (9.47) and (9.49) proves the first equality of the lemma. The second equality is proven in an analogous way. □

Lemma 2. *Let $(g_n)_{n\in\mathbb{N}}$ be a sequence of functions analytic on an annulus $\rho_- < |z| < \rho_+$, that includes the unit circle, and let $\rho_- < \rho_1 < 1 < \rho_2 < \rho_+$. Moreover, let $(s_n)_{n\in\mathbb{N}}$ be a sequence of positive numbers.*

(a) If $g_n = O(s_n)$ uniformly in z at the circle $|z| = \rho_1'$, for some $\rho_1' \in (\rho_-, \rho_1)$, then

$$[g_n]_-(z) = O(s_n), \quad \left[\frac{g_n}{z - e^{\imath\theta_0}}\right]_-^{(<)}(z) = O(s_n) \tag{9.50}$$

uniformly in z on $\rho_1 \le |z| \le \rho_2$.

(b) *If $g_n = O(s_n)$ uniformly in z at the circle $|z| = \rho_2'$, for some $\rho_2' \in (\rho_2, \rho_+)$, then*

$$[g_n]_+(z) = O(s_n), \quad \left[\frac{g_n}{z - e^{\imath\theta_0}}\right]_+^{(>)}(z) = O(s_n) \tag{9.51}$$

uniformly in z on $\rho_1 \le |z| \le \rho_2$.

Proof. Let us prove the first part of (a). By assumption there is $K > 0$ such that

$$|g_n(z)| \le K s_n \quad \text{for all } z \text{ on the circle } |z| = \rho_1'. \tag{9.52}$$

For $\rho_1 \le |z| \le \rho_2$ we have, from (9.30), the integral representation

$$[g]_-(z) = \frac{1}{2\pi\imath} \oint_{|w|=\rho_1'} \frac{g(w)}{z - w} dw. \tag{9.53}$$

Then from the assumption (9.52) and using $|z - w| \ge \rho_1 - \rho_1'$ it follows

$$\left|[g]_-(z)\right| \le \frac{K\rho_1'}{\rho_1 - \rho_1'} s_n, \tag{9.54}$$

which means that $[g]_-(z) = O(s_n)$ uniformly in z on $\rho_1 \le |z| \le \rho_2$. The other parts of the lemma are proven in an analogous way by using the integral representations (9.30) and (9.39). □

9.2.4 Solution for the zero winding number case

Having introduced the tools for the separation in components of the various functions, we can present the solutions. In the case $\nu = 0$, on the basis of a Wiener-Hopf procedure, presented in Appendix I.2, we construct the following functions, which are the specialization of (I.37), (I.32), and (I.25) and are defined and analytic on the annulus (9.7), given for $z \ne e^{\imath\theta_0}$ by

$$X_1^{(n)}(z) = e^{-\imath(n-1)\theta_0} a_+^{-1}(e^{\imath\theta_0}) a_+^{-1}(z) \frac{z^n c(z) - e^{\imath n\theta_0} c(e^{\imath\theta_0})}{z - e^{\imath\theta_0}}, \tag{9.55}$$

$$U_1^{(n)}(z) = -e^{-\imath(n-1)\theta_0} a_+(z) \frac{a_+^{-1}(z) - a_+^{-1}(e^{\imath\theta_0})}{z - e^{\imath\theta_0}}, \tag{9.56}$$

$$V_1^{(n)}(z) = e^{\imath\theta_0} a_-(z) \frac{a_-^{-1}(z) - a_-^{-1}(e^{\imath\theta_0})}{z - e^{\imath\theta_0}}, \tag{9.57}$$

and for $z = e^{\imath\theta_0}$ by continuity. It's easy to see that these functions satisfy the equation (9.28)

$$a X_1^{(n)} = Y^{(n)} + U_1^{(n)} z^n + V_1^{(n)}, \tag{9.58}$$

where, in this case, according to (9.5), $f = a$, and the function $a_\pm$ in (9.55) have been defined in (9.8) and we remind that $c = a_+ a_-^{-1}$.

Let ρ be defined by (9.10). A straightforward application of Lemma 1 and Lemma 2 yields the properties

$$[X_1^{(n)}]_- = O(\rho^n), \quad [X_1^{(n)} z^{-n}]_+ = O(\rho^n), \quad [U_1^{(n)}]_- = 0, \quad [V_1^{(n)}]_+ = 0, \tag{9.59}$$

where $O(\rho^n)$ holds on $\rho \le |z| \le \rho^{-1}$, uniformly in z. For example, let us show the first property. We have

$$\big[X_1^{(n)}\big]_- = e^{-\imath(n-1)\theta_0} a_+^{-1}(e^{\imath\theta_0}) \left[\frac{z^n a_-^{-1}}{z - e^{\imath\theta_0}}\right]_-^{(<)} - e^{\imath\theta_0} a_-^{-1}(e^{\imath\theta_0}) \left[\frac{a_+^{-1}}{z - e^{\imath\theta_0}}\right]_-^{(<)}. \tag{9.60}$$

Applying Lemma 2 on the first term, with $\rho_1' \in (\rho_-, \rho)$, $\rho_1 = \rho$, $\rho_2 = \rho^{-1}, s_n = \rho^n$, we see that it is equal to $O(\rho^n)$ on $\rho \le |z| \le \rho^{-1}$, uniformly in z. The second term is zero, by Lemma 1. The other properties in (9.59) are shown in an analogous way.

The properties (9.59) should be compared with (9.29). They imply that the function $X_1^{(n)}$ with the components $j < 0$ and $j \ge n$ removed, i.e. the function $X_2^{(n)} = X_1^{(n)} - [X_1^{(n)}]_- - z^n[X_1^{(n)} z^{-n}]_+$, is a solution of the problem

$$a X_2^{(n)} = Y_2^{(n)} + U_2^{(n)} z^n + V_2^{(n)} \tag{9.61}$$

$$\big[X_2^{(n)}\big]_- = 0, \quad \big[X_2^{(n)} z^{-n}\big]_+ = 0, \quad \big[U_2^{(n)}\big]_- = 0, \quad \big[V_2^{(n)}\big]_+ = 0\,, \tag{9.62}$$

where $[Y_2^{(n)}]_- = 0$, $[Y_2^{(n)} z^{-n}]_+ = 0$, and

$$Y_2^{(n)}(z) - Y^{(n)}(z) = O(\rho^n) \quad \text{uniformly in } z \text{ on the unit circle } |z| = 1. \tag{9.63}$$

Thus, we have constructed a linear problem whose corresponding functional equation is a $O(\rho^n)$ perturbation of the original one on the unit circle. It is intuitively clear that the solution $X^{(n)}$ will result into a $O(\rho^n)$ perturbation of $X_2^{(n)}$ on the unit circle. This passage is made rigorous by applying Lemma 3, stated and proven in Appendix I.3, on $X^{(n)}$ and $X_2^{(n)}$. It follows

$$X_2^{(n)}(z) - X^{(n)}(z) = O(\rho^n) \quad \text{uniformly in } z \text{ on the unit circle } |z| = 1 \tag{9.64}$$

and therefore, since $X_2^{(n)}(z) - X_1^{(n)}(z) = O(\rho^n)$ uniformly in z on the unit circle, we have

$$X^{(n)}(z) = X_1^{(n)}(z) + O(\rho^n) \quad \text{uniformly in } z \text{ on the unit circle } |z| = 1. \tag{9.65}$$

This, together with (9.55), gives

$$X^{(n)}(e^{\imath\theta_0}) = a_+^{-1}(e^{\imath\theta_0}) a_-^{-1}(e^{\imath\theta_0}) n + e^{\imath\theta_0} a_+^{-2}(e^{\imath\theta_0}) \frac{\mathrm{d}c(z)}{\mathrm{d}z}\bigg|_{z=e^{\imath\theta_0}} + O(\rho^n). \tag{9.66}$$

It follows

$$a(e^{\imath\theta_0}) X^{(n)}(e^{\imath\theta_0}) = n - \imath \frac{\mathrm{d}}{\mathrm{d}\theta} \log c(e^{\imath\theta})\bigg|_{\theta=\theta_0} + O(\rho^n). \tag{9.67}$$

Theorem 3 follows from (9.24) and (9.67). Let us comment here that the leading term in this solution was already determined in [71, 72], but without rigor, with a cavalier use of the component analysis and an improper analytical continuation. Most of all, the approach employed there does not allow to treat the non-zero winding number case.

9.2.5 Solution for the non-zero winding number case

Let us assume that $\nu > 0$. The result for $\nu < 0$ follows from this one by transposing the original Toeplitz matrix in (9.1) and doing the integral transformation $\theta \to -\theta$. On the basis of the Wiener-Hopf procedure presented in Appendix I.2, as a specialization of (I.37), (I.32) and (I.25) we construct the functions $X_1^{(n)}, U_1^{(n)}, V_1^{(n)}$, analytic on the annulus (9.7). For $z \neq e^{\imath\theta_0}$, $\rho_- < |z| < \rho_+$, they are defined by the rule

$$X_1^{(n)}(z)z^\nu = e^{-\imath(n+\nu-1)\theta_0}a_+^{-1}(z)a_+^{-1}(e^{\imath\theta_0})\frac{c(z)z^{n+\nu} - c(e^{\imath\theta_0})e^{\imath(n+\nu)\theta_0}}{z - e^{\imath\theta_0}}$$
$$+ e^{-\imath(n-1)\theta_0}a_-^{-1}(z)z^{n+\nu}\sum_{k=0}^{\nu-1}(a_+^{-1})_k\frac{z^{k-\nu} - e^{\imath(k-\nu)\theta_0}}{z - e^{\imath\theta_0}} + a_+^{-1}(z)\sum_{k=1}^{\nu}\alpha_k^{(n)}\left[c\, z^{n+\nu-k}\right]_+(z), \tag{9.68}$$

$$U_1^{(n)}z^{-\nu} = -e^{-\imath(n-1)\theta_0}a_+(z)\frac{[a_+^{-1}z^{-\nu}]_+(z) - [a_+^{-1}z^{-\nu}]_+(e^{\imath\theta_0})}{z - e^{\imath\theta_0}} + a_+(z)\sum_{k=1}^{\nu}\alpha_k^{(n)}z^{-k}, \tag{9.69}$$

$$V_1^{(n)}(z) = e^{\imath\theta_0}a_-(z)\frac{a_-^{-1}(z) - a_-^{-1}(e^{\imath\theta_0})}{z - e^{\imath\theta_0}} - a_-(z)\sum_{k=1}^{\nu}\alpha_k^{(n)}\left[c\, z^{n+\nu-k}\right]_-(z), \tag{9.70}$$

and for $z = e^{\imath\theta_0}$ by continuity. Here $\alpha_1^{(n)}, \alpha_2^{(n)}, ..., \alpha_\nu^{(n)} \in \mathbb{C}$ are for the moment unspecified, and it is simple to check that for any choice of them the functions above satisfy (9.28) as

$$az^\nu X_1^{(n)} = Y^{(n)} + U_1^{(n)}z^n + V_1^{(n)}. \tag{9.71}$$

Let ρ be defined by (9.10). As in the previous section, a straightforward application of Lemma 1 and Lemma 2 yields

$$\left[X_1^{(n)}z^\nu\right]_-(z) = O(\rho^n), \quad \left[U_1^{(n)}\right]_- = 0, \quad \left[V_1^{(n)}\right]_+ = 0, \tag{9.72}$$

where $O(\rho^n)$ holds on $\rho \leq |z| \leq \rho^{-1}$, uniformly in z. The coefficients $\alpha_1^{(n)}, \alpha_2^{(n)}, ..., \alpha_\nu^{(n)}$ are chosen to satisfy

$$\left(X_1^{(n)}z^\nu\right)_j = O(\rho^n) \quad \text{for } j = 0, 1, ..., \nu - 1, \tag{9.73}$$

thus extending (9.72) to also $\left[X_1^{(n)}\right]_- = O(\rho^n)$.

Thus, one computes the components $\left(X_1^{(n)}z^\nu\right)_j$ using (9.31), by integrating at the circle $|w| = \rho$, and imposes (9.73). As shown in Appendix I.2, this procedure results in

$$\alpha_k^{(n)} = -a_-^{-1}(e^{\imath\theta_0})e^{-\imath(\nu-1)\theta_0}\frac{\tilde{\Delta}_{\nu,n}(k)}{\Delta_{\nu,n}}, \tag{9.74}$$

where $\Delta_{\nu,n}$ is defined by (9.12) and $\tilde{\Delta}_{\nu,n}(k)$ by (9.14).

We have shown so far

$$\left[X_1^{(n)}\right]_- = O(\rho^n), \quad \left[U_1^{(n)}\right]_- = 0, \quad \left[V_1^{(n)}\right]_+ = 0, \tag{9.75}$$

which should be compared to (9.29). It remains to discuss $\left[X_1^{(n)} z^{-n}\right]_+$. Application of Lemmas 1 and 2 yields

$$\left[X_1^{(n)} z^{-n}\right]_+ = O(\rho^n) + \sum_{k=1}^{\nu} \alpha_k^{(n)} \left[a_+^{-1} z^{-(n+\nu)} \left[c z^{n+\nu-k}\right]_+\right]_+ . \tag{9.76}$$

We have further

$$\alpha_k^{(n)} \left[a_+^{-1} z^{-(n+\nu)} \left[c z^{n+\nu-k}\right]_+\right]_+ = -\alpha_k^{(n)} \left[a_+^{-1} z^{-(n+\nu)} \left[c z^{n+\nu-k}\right]_-\right]_+ = -\alpha_k^{(n)} O(\rho_1^n) \tag{9.77}$$

where in the last equality we have applied Lemma 2 two successive times for some $\rho_1 \in (\rho_-, \rho)$, and $O(\rho_1^{2n})$ holds on $\rho \le |z| \le \rho^{-1}$, uniformly in z. Now, assuming that the condition (9.16) of Theorem 4 holds, using (9.74) we get

$$\alpha_k^{(n)} O(\rho_1^{2n}) = O\big((\rho_1/\rho)^2\big) \tag{9.78}$$

Defining

$$\sigma = \max\{(\rho_1/\rho)^2, \rho\} \tag{9.79}$$

we have thus

$$\left[X_1^{(n)}\right]_-(z) = O(\sigma^n), \quad \left[X_1^{(n)} z^{-n}\right]_+ = O(\sigma^n), \quad \left[U_1^{(n)}\right]_- = 0, \quad \left[V_1^{(n)}\right]_+ = 0, \tag{9.80}$$

where $O(\sigma^n)$ holds on $\rho \le |z| \le \rho^{-1}$, uniformly in z. These properties should be compared with (9.29). Because of the same reasoning as for the zero winding number case we expect

$$X^{(n)}(z) = X_1(z) + O(\sigma^n) \tag{9.81}$$

on the unit circle $|z| = 1$. In this case we cannot provide a rigorous proof for this estimate, but we find it very natural and we have checked numerically that the final result, i.e. Theorem 4, holds in several relevant cases.

It follows

$$\begin{aligned} X^{(n)}(e^{\imath\theta_0}) e^{\imath\nu\theta_0} &= e^{-\imath(n+\nu-1)\theta_0} a_+^{-2}(e^{\imath\theta_0}) \frac{\mathrm{d}}{\mathrm{d}z}\Big(c(z) z^{n+\nu}\Big)\Big|_{z=e^{\imath\theta_0}} \\ &+ e^{\imath(\nu+1)\theta_0} a_-^{-1}(e^{\imath\theta_0}) \sum_{k=0}^{\nu-1} \big(a_+^{-1}\big)_k \frac{\mathrm{d}}{\mathrm{d}z} z^{k-\nu}\Big|_{z=e^{\imath\theta_0}} + a_+^{-1}(e^{\imath\theta_0}) \sum_{k=1}^{\nu} \alpha_k^{(n)} \left[c z^{n+\nu-k}\right]_+ (e^{\imath\theta_0}) + O(\sigma^n) \end{aligned} \tag{9.82}$$

from which we get

$$\begin{aligned} X^{(n)}(e^{\imath\theta_0}) e^{\imath\nu\theta_0} &= a_+^{-1}(e^{\imath\theta_0}) a_-^{-1}(e^{\imath\theta_0})(n+\nu) + e^{\imath\theta_0} a_+^{-2}(e^{\imath\theta_0}) \frac{\mathrm{d}c(z)}{\mathrm{d}z}\Big|_{z=e^{\imath\theta_0}} \\ &+ a_-^{-1}(e^{\imath\theta_0}) \sum_{k=0}^{\nu-1} (k-\nu) \big(a_+^{-1}\big)_k e^{\imath k\theta_0} + a_+^{-1}(e^{\imath\theta_0}) \sum_{k=1}^{\nu} \alpha_k^{(n)} \left[c z^{n+\nu-k}\right]_+ (e^{\imath\theta_0}) + O(\sigma^n). \end{aligned} \tag{9.83}$$

Lemma 2 gives a simplification

$$\left[c z^{n+\nu-k}\right]_+ (e^{\imath\theta_0}) = c(e^{\imath\theta_0}) e^{\imath(n+\nu-k)\theta_0} + O(\rho^n) \tag{9.84}$$

from which it follows

$$X^{(n)}(e^{\imath\theta_0})e^{\imath\nu\theta_0} = a_-^{-1}(e^{\imath\theta_0})\sum_{k=1}^{\nu}\alpha_k^{(n)}\left(e^{\imath(n+\nu-k)\theta_0}+O(\rho^n)\right)+a_+^{-1}(e^{\imath\theta_0})a_-^{-1}(e^{\imath\theta_0})n+O(1). \tag{9.85}$$

Theorem 4 follows directly from (9.24) and (9.85), where the result for the case $\nu<0$ descends from the one for $\nu>0$ by transposing the original Toeplitz matrix in (9.1) and making the integral transformation $\theta\to-\theta$.

9.3 Application of the results: Frustrated quantum XY chain in zero field

As an example of a concrete application of our results we compute the lowest energy band spin-correlation functions and the ground state magnetization for the frustrated quantum XY chain, studied in chapters 3 and 4, and defined by the Hamiltonian

$$H=\sum_{j=1}^{N}\left(\sigma_j^x\sigma_{j+1}^x-\lambda\sigma_j^y\sigma_{j+1}^y\right). \tag{9.86}$$

Here $\lambda\in(0,1)$ is the anisotropy parameter, $N=2M+1$ is the number of lattice sites, which is imposed to be odd, σ^α for $\alpha=x,y,z$, are Pauli matrices, and periodic boundary conditions are imposed ($\sigma_j^\alpha=\sigma_{j+N}^\alpha$). The notation used here can be related, up to multiplying the Hamiltonian by a positive constant, to the one in (3.1), by setting $\delta=0$ and $\lambda=-\tan\phi$. The one used here is simpler and shorter for the present purpose.

As discussed in Chapter 3 and Appendix C.2, in each sector of given z-parity, the XY chain can be mapped exactly, although non-locally, to a system of free fermions. This mapping allows to represent every state in a Fock space: one defines a vacuum $|0^\pm\rangle$ which is annihilated by fermionic operators a_q, with $q\in\Gamma^\pm$ belonging to a different set (of integers or half-integers) depending on the parity ($\Gamma^\pm=\left\{\frac{\pi}{N}\left(2j+\frac{1+\Pi^z}{2}\right):j=0,1,...,N-1\right\}$), $a_q|0^\pm\rangle=0$ for all $q\in\Gamma^\pm$, and applies the Bogoliubov creation operators $a_q^\dagger$ to create all other states. Only states with a number of excitations compatible with the parity are admissible in the Hilbert space of (9.86): assigning zero excitations to the vacua $|0^\pm\rangle$, each $a_q^\dagger$ adds one. Even excitation states belong to the positive z-parity sector, while odd excitation ones have negative z-parity. As a consequence of the symmetries, each eigenstate of the model is at least two-fold degenerate. Furthermore, for each state $|\psi\rangle$ in the $\Pi^z=-1$ sector we can construct the state $\Pi^x|\psi\rangle=(-1)^{(N-1)/2}\Pi^y|\psi\rangle$ with the same energy, but with opposite Π^z.

Due to the frustrated boundary conditions, the system is gapless with the energy gap above the ground state closing as $1/N^2$. The ground state is part of a band, spanned by the (single excitation) states $|q\rangle=a_q^\dagger|0^-\rangle$, which have negative z-parity $\Pi^z=-1$, and the states $\Pi^x|q\rangle=\imath(-1)^{(N-1)/2}\Pi^y|q\rangle$, with $\Pi^z=1$ and the same energy. The energy of the states $|q\rangle$ and $\Pi^x|q\rangle$ is equal and the index q is the momentum of the excitation, that can be related to lattice translations (see Appendix C.3). The ground state, in particular, has momentum $q=0$, and is two-fold degenerate. A generic ground state is, therefore, a superposition

$$|g\rangle=\cos\theta\,|g^-\rangle+\sin\theta\,e^{\imath\psi}\,|g^+\rangle\,, \tag{9.87}$$

where $|g^-\rangle = |q=0\rangle$, $|g^+\rangle = \Pi^x |g^-\rangle$, $\theta \in [0, 2\pi)$ and $\psi \in [0, 2\pi)$.

We are interested in the spin correlation functions $\langle q| \sigma_1^x \sigma_{1+n}^x |q\rangle$ and $\langle q| \sigma_1^y \sigma_{1+n}^y |q\rangle$, and in the ground state magnetizations $\langle g| \sigma_1^x |g\rangle$ and $\langle g| \sigma_1^y |g\rangle$. The spin correlation functions $\langle q| \sigma_1^z \sigma_{1+n}^z |q\rangle$ and the magnetization $\langle g| \sigma_1^z |g\rangle$ can be computed using simpler techniques, as done in Appendix C.5. As discussed throughout the thesis, as a consequence of the symmetries and of the exact degeneracies, it is possible to have a spontaneous finite magnetization even for finite N.

Spin-correlation functions

As shown in Appendix C.5, using the Majorana fermions representation of the spin operators and performing the Wick contractions as in [72], the spin correlation functions can be expressed in terms of Toeplitz determinants

$$\langle q| \sigma_1^\alpha \sigma_{1+n}^\alpha |q\rangle = (-1)^n \Big[\Big(\tilde{D}_n(\tilde{f}) + \text{c.c.} \Big) - D_n(f) \Big], \tag{9.88}$$

where c.c. stands for the complex conjugate and

$$\tilde{f}_j^{(n)} = f_j - \frac{1}{N} f(e^{\imath q}) e^{-\imath q j}, \tag{9.89}$$

$$f_j = \frac{1}{N} \sum_{\theta \in \Gamma^-} f(e^{\imath\theta}) e^{-\imath j\theta} \overset{N\to\infty}{\simeq} \frac{1}{2\pi} \int_0^{2\pi} f(e^{\imath\theta}) e^{-\imath j\theta} d\theta, \tag{9.90}$$

$$f(z) = a(z) z^\nu, \quad a(z) = \sqrt{\frac{1-\lambda z^{-2}}{1-\lambda z^2}}. \tag{9.91}$$

The winding number is $\nu = 0$ for $\alpha = x$ and $\nu = 2$ for $\alpha = y$. Comparing with (9.3) we see that $z_n = -1/N$, thus a constant with respect to n, although, from physical considerations, we must have $n < N/2$. We are going to neglect the difference between the sum and the integral in (9.90), and similarly later in computing the magnetization. We observe numerically that these differences are exponentially small in N. All the results are obtained within this approximation.

We see that a is analytic on $\lambda^{1/2} < |z| < \lambda^{-1/2}$ and by inspection we find

$$\begin{aligned} &a_+(z) = a_-^{-1}(z^{-1}) = (1-\lambda z^2)^{-1/2}, \\ &c(z) = b^{-1}(z) = a_+(z) a_-^{-1}(z) = \big[(1-\lambda z^2)(1-\lambda z^{-2}) \big]^{-1/2}. \end{aligned} \tag{9.92}$$

The determinant $D_n(f)$ has already been computed in [150] because it determines the ground state spin-correlation functions in absence of frustration. For $\nu = 0$ it is given by

$$\begin{aligned} &D_n(f) \\ &= (1-\lambda^2)^{1/2} \Big[1 + 4 \Big(\frac{\lambda}{1-\lambda^2} \Big)^2 \frac{\lambda^n}{\pi n^2} \big(1 + O(n^{-1}) \big) \Big], \quad \text{for } n = 2m \text{ as } m \to \infty, \end{aligned} \tag{9.93}$$

$$= (1-\lambda^2)^{1/2} \Big[1 + 2 \frac{1+\lambda^2}{\lambda} \Big(\frac{\lambda}{1-\lambda^2} \Big)^2 \frac{\lambda^n}{\pi n^2} \big(1 + O(n^{-1}) \big) \Big], \text{for } n = 2m+1 \text{ as } m \to \infty. \tag{9.94}$$

Applying Theorem 3, with the term

$$\frac{\mathrm{d}}{\mathrm{d}\theta}\log b(e^{\imath\theta})\Big|_{\theta=q} = \frac{2\lambda\sin q}{1+\lambda^2-2\lambda\cos 2q} \in \mathbb{R} \tag{9.95}$$

not contributing in (9.88), we find

$$\begin{aligned}&\langle q|\,\sigma_1^x\sigma_{1+n}^x\,|q\rangle\\ &= (1-\lambda^2)^{1/2}\Big[1+4\Big(\frac{\lambda}{1-\lambda^2}\Big)^2\frac{\lambda^n}{\pi n^2}\Big(1+O(n^{-1})\Big)\Big]\Big[1-\frac{2n}{N}\Big(1+O(\lambda^{\frac{n}{2}(1+\varepsilon)})\Big)\Big],\\ &\quad \text{for } n=2m \text{ as } m\to\infty,\end{aligned} \tag{9.96}$$

$$\begin{aligned}&= -(1-\lambda^2)^{1/2}\Big[1+2\frac{1+\lambda^2}{\lambda}\Big(\frac{\lambda}{1-\lambda^2}\Big)^2\frac{\lambda^n}{\pi n^2}\big(1+O(n^{-1})\big)\Big]\Big[1-\frac{2n}{N}\Big(1+O(\lambda^{\frac{n}{2}(1+\varepsilon)})\Big)\Big],\\ &\quad \text{for } n=2m+1 \text{ as } m\to\infty,\end{aligned} \tag{9.97}$$

where $\varepsilon>0$ is arbitrarily small.

To compute $\langle q|\,\sigma_1^y\sigma_{1+n}^y\,|q\rangle$ using Theorem 4 we need to find

$$c_{-n} = \frac{1}{2\pi\imath}\oint_{|w|=1}\frac{w^{n-1}}{[(1-\lambda z^2)(1-\lambda z^{-2})]^{1/2}}dw. \tag{9.98}$$

Integrals of this type have been computed in [90, 150, 204, 205], for the purpose of computing the ground state spin-correlation functions, using the properties of the hypergeometric functions. This one is given by

$$c_{-n} = \frac{2^{1/2}}{(1-\lambda^2)^{1/2}}\frac{\lambda^{\frac{n}{2}}}{\sqrt{\pi n}}\Big(1+O(n^{-1})\Big) \quad \text{for } n=2m \text{ as } m\to\infty. \tag{9.99}$$

$$c_{-n} = 0 \quad \text{for } n=2m+1. \tag{9.100}$$

Applying Theorem 4, where the condition (9.16) of the theorem is satisfied for ρ close to $\sqrt{\lambda}$, and using the result (9.13) for $D_n(f)$, we find

$$\begin{aligned}&\langle q|\,\sigma_1^y\sigma_{1+n}^y\,|q\rangle\\ &= \frac{2}{1-\lambda}\frac{\lambda^n}{\pi n}\Big(1+O(n^{-1})\Big)+2^{5/2}\frac{\cos nq}{(1+\lambda^2-2\lambda\cos 2q)^{1/2}}\frac{\lambda^{\frac{n}{2}}}{N\sqrt{\pi n}}\Big(1+O(n^{-1})\Big)\\ &\quad \text{for } n=2m \text{ as } m\to\infty.\end{aligned} \tag{9.101}$$

$$\begin{aligned}=&\frac{2}{1-\lambda}\frac{\lambda^n}{\pi n}\Big(1+O(n^{-1})\Big)\\ &+2^{3/2}\frac{\lambda^{-\frac{1}{2}}\cos[(n+1)q]+\lambda^{\frac{1}{2}}\cos[(n-1)q]}{(1+\lambda^2-2\lambda\cos 2q)^{1/2}}\frac{\lambda^{\frac{n}{2}}}{N\sqrt{\pi n}}\Big(1+O(n^{-1})\Big)\\ &\quad \text{for } n=2m+1 \text{ as } m\to\infty.\end{aligned} \tag{9.102}$$

In the ground state ($q=0$) terms proportional to $1/N$ in (9.96) and (9.101) are due to the delta-function singularity in the symbol and make the difference between the

frustrated model and the model without frustration (that is, periodic boundary conditions with $N = 2M$ or free boundary conditions). In this case, the difference is relevant only at distances n comparable to the system size N. Without these terms, the x correlation function would converge exponentially fast to a saturation value as the distance between sites is increased, while the y corrrelation decays to zero, reflecting a spontaneous magnetization developing only in the x direction. The dependence (9.96) implies, instead, that the correlations between the most distant spins, separated by $n = (N-1)/2$, decay as $1/N$ as we increase the (odd) system size N. This kind of behavior in frustrated quantum chains was first found in [67, 69] and later further discussed, and checked numerically, in [71–73]. We discuss it in details in Chapter 3.

9.3.1 The ground state magnetization

As discussed in Appendix C.5, the magnetization in the ground state is ferromagnetic, i.e. $\langle g|\,\sigma_1^\alpha\,|g\rangle = \langle g|\,\sigma_j^\alpha\,|g\rangle$ for $j = 2, 3, ..., N$ and $\alpha = x, y, z$, in a generic ground state $|g\rangle$ defined by (9.87). For $\alpha = x, y$ it is given by

$$\langle g|\,\sigma_1^x\,|g\rangle = \cos\psi \sin 2\theta\, \langle g^-|\,\sigma_1^x \Pi^x\,|g^-\rangle\,, \tag{9.103}$$

$$\langle g|\,\sigma_1^y\,|g\rangle = (-1)^{\frac{N-1}{2}} \sin\psi \sin 2\theta\, \langle g^-|\,\sigma_1^y \Pi^y\,|g^-\rangle\,. \tag{9.104}$$

The absolute values of the quantities $\langle g|\,\sigma_1^\alpha \Pi^\alpha\,|g\rangle$, for $\alpha = x, y$, are the maximal values of the magnetization on the ground state manifold, and it is shown in Appendix C.5 that these quantities can be expressed as Toeplitz determinants, as

$$\langle g^-|\,\sigma_1^\alpha \Pi^\alpha\,|g^-\rangle \overset{N\to\infty}{\simeq} (-1)^n \tilde{D}_n(\tilde{f}), \tag{9.105}$$

where

$$n = \frac{N-1}{2}, \quad \tilde{f}_j^{(n)} = f_j - \frac{2}{N}, \tag{9.106}$$

$$f_j = \frac{1}{2\pi}\int_0^{2\pi} f(e^{\imath\theta}) e^{-\imath j\theta} d\theta, \tag{9.107}$$

$$f(z) = a(z) z^\nu, \quad a(z) = \sqrt{\frac{1-\lambda z^{-1}}{1-\lambda z}}. \tag{9.108}$$

Here the winding number is $\nu = 0$ for $\alpha = x$ and $\nu = 1$ for $\alpha = y$. Theorems 3 and 4 can be applied with $z_n = -2/N = -2/(2n+1)$.

We proceed in a similar way to the previous section. The function $a(z)$ is analytic on $\lambda < |z| < \lambda^{-1}$, and by inspection we find

$$\begin{aligned} &a_+(z) = a_-^{-1}(z^{-1}) = (1-\lambda z)^{-1/2}, \\ &c(z) = b^{-1}(z) = a_+(z) a_-^{-1}(z) = \left[(1-\lambda z)(1-\lambda z^{-1})\right]^{-1/2}. \end{aligned} \tag{9.109}$$

The coefficients c_{-n} are given by

$$c_{-n} = \frac{1}{2\pi\imath}\oint_{|w|=1} \frac{w^{n-1}}{[(1-\lambda z)(1-\lambda z^{-1})]^{1/2}} dw = \frac{\lambda^n}{\sqrt{\pi n(1-\lambda^2)}}\Big(1 + O(n^{-1})\Big). \tag{9.110}$$

Applying Theorems 3 and 4 we find

$$\langle g^- | \sigma_1^x \Pi^x | g^- \rangle = (-1)^{\frac{N-1}{2}} \frac{1}{N} (1-\lambda^2)^{\frac{1}{4}} \Big(1 + O(\lambda^{\frac{N}{2}(1+\varepsilon)})\Big), \tag{9.111}$$

$$\langle g^- | \sigma_1^y \Pi^y | g^- \rangle = \frac{2}{N} \frac{(1+\lambda)^{\frac{1}{4}}}{(1-\lambda)^{\frac{3}{4}}} \Big(1 + O(\lambda^{\frac{N}{2}(1+\varepsilon)})\Big), \tag{9.112}$$

where $N = 2M+1$, as $M \to \infty$. Here $\varepsilon > 0$ is arbitrarily small.

We remark that without frustration (that is, without the delta-function in the symbol) the Toeplitz determinant in (9.111) would approach a constant exponentially fast, while the one in (9.112) would similarly decay to zero, while with the delta-function they both show an algebraic decay in the matrix rank. In particular, both magnetizations go to zero as $N = 2M+1, M \to \infty$. These results for the magnetization describe mesocopic ferromagnetic order, as discussed in Chapter 3.

Chapter 10

Conclusions

In this thesis we have studied the effects of topological frustration on low-energy properties of various quantum spin-1/2 chains with discrete symmetries, in which frustration is induced by imposing periodic boundary conditions and an odd number of lattice sites. To discuss the influence of frustration on the order parameter, we have developed a simple approach to symmetry breaking, which consists of the realization that many systems without external magnetic fields posses global anticommuting symmetries if the number of lattice sites is an odd number. This approach allows for a discussion of the order already in a finite system, and tracking it towards the thermodynamic limit afterwards. Moreover, in the studied exactly solvable models this approach allowed us to get exact analytical results.

While our symmetry breaking framework in ferromagnets yields the same results as the standard ones, namely the one with the ground state degeneracy only in the thermodynamic limit and the one with symmetry breaking fields, in topologically frustrated antiferromagnets different approaches can yield different results. This is in line with the general property of frustrated systems: the sensitivity to perturbations, due to large classical degeneracy [25]. In the studied topologically frustrated spin chains the classical point exhibits large degeneracy and different quantum perturbations can lift this degeneracy in a variety of different ways. The important realization is that, in general, this degeneracy is not lifted in a way to restore the standard staggered antiferromagnetic order, but different phenomenology arises.

Within our symmetry breaking framework, we have discovered that topological frustration can destroy local order, induce a site-dependent magnetization that varies in space, induce a first-order quantum phase transition and modify the nature of a second order quantum phase transition, by destroying local order parameters at both sides of the transition, so that the transition can be characterized only through non-local order parameters. We have discovered that topological frustration can affect also non-equilibrium properties of spin chains. Namely, the Loschmidt echo in a local quantum quench setup displays qualitatively and quantitatively different behavior for rings with an even and odd number of lattice sites, thus providing a simple out-of-equilibrium experiment to distinguish between the two, no matter how large they are.

All this phenomenology is due to a single interacting, frustrating, bond, intuitively negligible in a large system. The standard approach, based on the Ginzburg-Landau theory, that accepts this intuition and attempts to capture the properties of the system by taking the system size to infinity before computing the observables, cannot account for it. In topologically frustrated spin chains the chain length is a relevant scale. We hope, thus, that our results indicate the incompleteness of the standard approach, at least in the presence of topological frustration.

There are, of course, many properties of topologically frustrated spin chains left unexplored and nothing has been said about potential technological applications or

experimental realizations. We hope that the results presented in this thesis can raise the interest to discover more properties of these simple yet complex systems.

Appendix A

Quantum Ising Chain: Perturbative Analysis

This is the appendix related to Chapter 1. It includes the details of perturbative calculations. The different parts of the calculation in section A.1 were done by us in [1, 8], and in a similar form the calculation has already been done in [66, 67, 69], while the calculation in section A.2 is original content of this thesis.

A.1 Without symmetry breaking fields

Here, to the lowest order in perturbation theory in h we discuss the low energy physics of the Hamiltonian (1.2) with FBC and $J = 1$. For $h = 0$ the ground state manifold is $2N$-fold degenerate, spanned by the kink states $|j\rangle$ and $\Pi^z |j\rangle$, for $j = 1, 2, \ldots N$. These are the states with the ferromagnetic bond $\sigma_j^x = \sigma_{j+1}^x = 1$ and $\sigma_j^x = \sigma_{j+1}^x = -1$ respectively, and the remaining bonds antiferromagnetic. Note that the kink states are eigenstates of Π^x. The energy of the kink states is equal to $-(N-2)$. The excited states are separated by an energy gap of order unity and we neglect them in our perturbative treatment.

Making h non-zero the degenerate states split in energy. The eigenstates of the model are found by diagonalizing the perturbation $h\sum_j \sigma_j^z$. It's easy to see that we have the the matrix elements

$$\langle j| \sigma_k^z \Pi^z |l\rangle = \delta_{j,k}\delta_{l-j+1 \bmod N,0} + \delta_{l,k}\delta_{j-l+1 \bmod N,0}, \tag{A.1}$$

and, since σ_k^z anticommutes with Π^x, the matrix elements of σ_k^z between the states with the same Π^x vanish. Furthermore, from (A.1) we get

$$\mathbf{C}_{j,l} \equiv \langle j| \sum_{k=1}^{N} \sigma_k^z \, \Pi^z |l\rangle = \delta_{j-l-1 \bmod N,0} + \delta_{j-l+1 \bmod N,0}. \tag{A.2}$$

Thus, ordering the states as $|1\rangle, |2\rangle, \ldots, |N\rangle, \Pi^z |1\rangle, \Pi^z |2\rangle, \ldots, \Pi^z |N\rangle$, the perturbation can be written as a $2N \times 2N$ block matrix,

$$\sum_{k=1}^{N} \sigma_k^z = \begin{pmatrix} \mathbf{0} & \mathbf{C} \\ \mathbf{C} & \mathbf{0} \end{pmatrix}, \tag{A.3}$$

where $\mathbf{C}$ is an $N \times N$ matrix with the elements defined in (A.2).

To diagonalize the perturbation we note the following mathematical fact. If λ is an eigenvalue of an $n \times n$ matrix $\mathbf{M}$, then, denoting the corresponding (normalized)

eigenvector by $\mathbf{v}$, the (normalized) eigenvector of the block matrix

$$\begin{pmatrix} \mathbf{0} & \mathbf{M} \\ \mathbf{M} & \mathbf{0} \end{pmatrix} \tag{A.4}$$

corresponding to the eigenvalue $\pm\lambda$ can be constructed as $1/\sqrt{2}\begin{pmatrix}\mathbf{v} & \pm\mathbf{v}\end{pmatrix}^{\mathrm{T}}$. In this way all the eigenvectors of the block matrix can be constructed.

Now, the matrix $\mathbf{C}$ is a cyclic matrix,

$$\mathbf{C} = \begin{pmatrix} c_0 & c_{N-1} & \dots & c_2 & c_1 \\ c_1 & c_0 & \dots & c_3 & c_2 \\ \vdots & \vdots & \ddots & \vdots & \vdots \\ c_{N-2} & c_{N-1} & \dots & c_0 & c_{N-1} \\ c_{N-1} & c_{N-2} & \dots & c_1 & c_0 \end{pmatrix}, \tag{A.5}$$

with

$$c_j = \delta_{j,1} + \delta_{j,N-1}. \tag{A.6}$$

The diagonalization of the cyclic matrix is a standard problem (see e.g. [204]). Diagonalizing it and constructing the eigenvectors of the block matrix we find that to the lowest order in perturbation theory in h we have the eigenstates

$$|q,\pm\rangle = \frac{1 \pm \Pi^z}{\sqrt{2N}} \sum_{j=1}^{N} e^{\imath q j} |j\rangle \tag{A.7}$$

with the energies

$$E_{q,\pm} = -(N-2) \pm 2h\cos q. \tag{A.8}$$

Here q can assume any value from the set $\{2\pi k/N : k = 0, 1, \dots, N-1\}$. For $h > 0$ the ground state, in particular, is given by $|q = 0, -\rangle$ so we can write

$$|g\rangle = \frac{1}{\sqrt{N}} \sum_{j=1}^{N} \frac{1 - \Pi^z}{\sqrt{2}} |j\rangle . \tag{A.9}$$

The ground state is single and the system is gapless, with the gap above the ground state closing as $1/N^2$.

The spin correlation functions in the state $|q,\pm\rangle$, for any q, are equal to

$$\langle q,\pm| \sigma_j^x \sigma_{j+r}^x |q,\pm\rangle = \frac{1}{N} \sum_{l=1}^{N} \langle l| \sigma_j^x \sigma_{j+r}^x |l\rangle . \tag{A.10}$$

From the definition of the kink states it follows, as recognized in [1],

$$\langle l| \sigma_j^x |l\rangle = \begin{cases} (-1)^{l+j+1}, & l = 1, 2, \dots, j-1 \\ (-1)^{l+j}, & l = j, j+1, \dots, N \end{cases}. \tag{A.11}$$

From (A.11) we get

$$\langle \sigma_j^x \sigma_{j+r}^x \rangle_{q,\pm} = (-1)^r \left(1 - \frac{2r}{N}\right). \tag{A.12}$$

In particular, these are also the spin correlation functions in the ground state (A.9).

A.2 Local symmetry breaking field

Here, to the lowest order in perturbation theory in h we compute the ground state magnetization of the Hamiltonian (1.8) ,with FBC and $J = 1$, when the symmetry breaking field is localized at one site,

$$\lambda_j = \delta_{j,k}\lambda. \tag{A.13}$$

We focus on the case when the field is localized at the site $k = 1$ and then comment how the result for an arbitrary site k can be obtained from this one.

Let us assume $\lambda > 0$, while the opposite sign of λ just gives the opposite sign of the magnetization. For $h = 0$ the ground state manifold is N-fold degenerate. It is spanned by all the kink states that have $\sigma_1^x = -1$. These are the states $|j\rangle$, for $j = 2, 4, 6, \ldots, N-1$, and the states $\Pi^z |j\rangle$, for $j = 1, 3, 5, \ldots N$. Ordering the states in this way and using (A.2), we find that in this subspace the perturbation can be written as a block matrix

$$\sum_{k=1}^{N} \sigma_k^z = \begin{pmatrix} \mathbf{0} & \mathbf{D} \\ \mathbf{D}^{\mathrm{T}} & \mathbf{0} \end{pmatrix}, \tag{A.14}$$

where D is an $(N-1)/2 \times (N+1)/2$ matrix with the elements

$$\mathrm{D}_{j,k} = \delta_{j,k} + \delta_{j+1,k}, \tag{A.15}$$

for $j = 1, 2, \ldots (N-1)/2$ and $k = 1, 2, \ldots, (N+1)/2$. In the matrix form it reads

$$\mathrm{D} = \begin{pmatrix} 1 & 1 & 0 & 0 & \ldots & 0 & 0 & 0 \\ 0 & 1 & 1 & 0 & \ldots & 0 & 0 & 0 \\ \vdots & \vdots & \vdots & \vdots & \ddots & \vdots & \vdots & \vdots \\ 0 & 0 & 0 & 0 & \ldots & 1 & 1 & 0 \\ 0 & 0 & 0 & 0 & \ldots & 0 & 1 & 1 \end{pmatrix}. \tag{A.16}$$

To diagonalize the matrix (A.14) we simply guess the eigenvectors, based also on the similarity with some matrices in [69]. It's easy to check, using (A.15), and putting $n \equiv (N-1)/2$, that the normalized eigenvectors are

$$\mathbf{v}_{\pm}^{(\mathbf{m})} \equiv \frac{1}{\sqrt{n+1}} \begin{pmatrix} \pm \mathbf{v_1}^{(\mathbf{m})} \\ \mathbf{v_2}^{(\mathbf{m})} \end{pmatrix}, \tag{A.17}$$

for $m = 1, 2, \ldots, n+1$, where the components are given by

$$\begin{aligned} \left(\mathbf{v_1}^{(\mathbf{m})}\right)_j &= \sin\left[\frac{\pi m}{2(n+1)} 2j\right], \quad j = 1, 2, \ldots, n, \\ \left(\mathbf{v_2}^{(\mathbf{m})}\right)_j &= \sin\left[\frac{\pi m}{2(n+1)} (2j-1)\right], \quad j = 1, 2, \ldots, n+1. \end{aligned} \tag{A.18}$$

The corresponding eigenvalues are given by

$$\pm\, 2\cos\left[\frac{\pi m}{2(n+1)}\right]. \tag{A.19}$$

It follows that, to the lowest order in perturbation theory in h, the lowest energy states are

$$|a_m,\pm\rangle \equiv \sqrt{\frac{2}{N+1}}\Bigg\{ \pm \sum_{j=1}^{(N-1)/2} \sin\left[\frac{\pi m}{N+1}2j\right]|2j\rangle + \sum_{j=1}^{(N+1)/2} \sin\left[\frac{\pi m}{N+1}(2j-1)\right]\Pi^z|2j-1\rangle\Bigg\}, \tag{A.20}$$

for $m = 1, 2, \ldots (N+1)/2$, and the corresponding energies are

$$E_{m,\pm} = -(N-2) - \lambda \pm 2h\cos\left[\frac{\pi m}{N+1}\right]. \tag{A.21}$$

For $\lambda > 0$ the energy is minimized by taking $m = 1$ and the minus sign, so the ground state is given by $|g\rangle = |a_0, -\rangle$. The ground state is single and the system is gapless, with the gap above the ground state closing as $1/N^2$.

After a bit of algebra we obtain the ground state magnetization

$$\langle g|\,\sigma_j^x\,|g\rangle = (-1)^j\left\{1 - \frac{2}{N+1}\left(j-\frac{1}{2}\right) + \frac{1}{(N+1)\sin\left(\frac{\pi}{N+1}\right)}\sin\left[\frac{2\pi}{N+1}\left(j-\frac{1}{2}\right)\right]\right\}. \tag{A.22}$$

The obtained expression is valid for $j = 1, 2, \ldots, N$. The right hand side is not invariant under the transformation $j \to j+N$, but it takes the same value for $j = 1$ and $j = N+1$. The expression for the magnetization for the symmetry breaking field localized at the site $k = N$ can be obtained, thus, by making the transformation $j \to j+1$ on the r.h.s. of (A.22). More generally, for the field localized at an arbitrary site k the transformation $j \to (j-k)$ mod $N+1$ is required on the r.h.s. of (A.22).

Appendix B

Loschmidt Echo: Perturbative Analysis

This is the appendix for Chapter 2. Here we present the details of the perturbative analysis for the Loschmidt echo in the quantum Ising chain.

B.1 Diagonalization of the perturbed Hamiltonian

We start by finding the lowest energy states of the Hamiltonian

$$H_1 = \sum_{j=1}^{N} \left(\sigma_j^x \sigma_{j+1}^x + h\sigma_j^z \right) + \lambda \sigma_N^z. \tag{B.1}$$

for $h > 0$ and $\lambda > 0$, using the perturbation theory in h and λ. The perturbation theory for the model with $\lambda = 0$ has already been done in Appendix A.1.

First, we use the perturbation theory in λ for $h = 0$ and find how the $2N$ degenerate ground states of the classical point split. Then we treat the term $h\sum_j \sigma_j^z$ as a second-order correction and apply the perturbation theory in h to the degenerate states. Doing the perturbation theory in this way ensures the validity of the results in the regime $h \ll \lambda \ll 1$.

Thus, first we assume $h = 0$ and examine how the ground state degeneracy is lifted by turning $\lambda \neq 0$. Ordering the ground states as $|1\rangle, |2\rangle, \ldots, |N\rangle, \Pi^z |1\rangle, \Pi^z |2\rangle, \ldots, \Pi^z |N\rangle$, and using (A.1) we find that the operator σ_N^z in the ground space is given by the block matrix

$$\sigma_N^z = \begin{pmatrix} \mathbf{0} & \mathbf{C}^{(1)} \\ \mathbf{C}^{(1)} & \mathbf{0} \end{pmatrix}, \tag{B.2}$$

where $\mathbf{C}^{(1)}$ is an $N \times N$ matrix, given by

$$\mathbf{C}^{(1)} = \begin{pmatrix} 0 & \ldots & 0 & 0 & 0 \\ \vdots & \ddots & \vdots & \vdots & \vdots \\ 0 & \ldots & 0 & 0 & 0 \\ 0 & \ldots & 0 & 0 & 1 \\ 0 & \ldots & 0 & 1 & 0 \end{pmatrix}. \tag{B.3}$$

The diagonalization of $\mathbf{C}^{(1)}$ is trivial. Constructing the eigenvectors of the block matrix, as discussed around eq. (A.4), we find the eigenstates

$$\begin{aligned} |\psi_\pm\rangle &= \frac{1 \pm \Pi^z}{2}(|N-1\rangle \mp |N\rangle), \\ |\phi_\pm\rangle &= \frac{1 \pm \Pi^z}{2}(|N-1\rangle \pm |N\rangle), \end{aligned} \tag{B.4}$$

with the energies

$$\begin{aligned} E(\psi_\pm) &= -(N-2) - \lambda, \\ E(\phi_\pm) &= -(N-2) + \lambda. \end{aligned} \tag{B.5}$$

The remaining states are simply $|j\rangle$ and $\Pi^z|j\rangle$, for $j = 1, 2, \ldots, N-2$, with no change in energy. Thus, the presence of λ splits the $2N$ degenerate states into three parts. The two ground states, separated by an energy gap λ from $2N-4$ kink states, above which there are another two states.

Now we add the perturbation $h\sum_j \sigma_j^z$ to the Hamiltonian. We study separately three different degenerate subspaces. The ground space spanned by $|\psi_+\rangle$ and $|\psi_-\rangle$, the subspace spanned by $|j\rangle$ and $\Pi^z|j\rangle$ for $j = 1, 2, \ldots, N-2$, and the subspace spanned by $|\phi_+\rangle$ and $|\phi_-\rangle$. Using (A.2) it's easy to see that the perturbation is already diagonal in the subspace spanned by the states $|\psi_\pm\rangle$ and in the one spanned by $|\phi_\pm\rangle$. These states acquire only an energy shift,

$$E(\psi_\pm) = -(N-2) - (\lambda + h), \tag{B.6}$$

$$E(\phi_\pm) = -(N-2) + \lambda + h. \tag{B.7}$$

Also using (A.2) we find that in the subspace spanned by the states $|1\rangle$, $|2\rangle$, …, $|N-2\rangle$, $\Pi^z|1\rangle$, $\Pi^z|2\rangle$, …, $\Pi^z|N-2\rangle$, ordering the states in this way, we have the matrix representation

$$\sum_{k=1}^{N} \sigma_k^z = \begin{pmatrix} \mathbf{0} & \mathbf{C}^{(2)} \\ \mathbf{C}^{(2)} & \mathbf{0} \end{pmatrix}, \tag{B.8}$$

where $\mathbf{C}^{(2)}$ is an $(N-2)\times(N-2)$ matrix given by

$$\mathbf{C}^{(2)} = \begin{pmatrix} 0 & 1 & 0 & \ldots & 0 & 0 \\ 1 & 0 & 1 & \ldots & 0 & 0 \\ 0 & 1 & 0 & \ldots & 0 & 0 \\ \vdots & \vdots & \vdots & \ddots & \vdots & \vdots \\ 0 & 0 & 0 & \ldots & 0 & 1 \\ 0 & 0 & 0 & \ldots & 1 & 0 \end{pmatrix}. \tag{B.9}$$

The elements of the matrix in (B.9) are equal to 1 on the subdiagonal and superdiagonal, while they are zero elsewhere. The matrix of this type has already been diagonalized in Ref. [69], by writing a recursion relation for the characteristic polynomial. Using their results and constructing the eigenvectors of the block matrix we find the states

$$|\xi_\pm, m\rangle = \frac{1 \pm \Pi^z}{\sqrt{N-1}} \sum_{j=1}^{N-2} (-1)^j \sin\left(\frac{m\pi}{N-1} j\right) |j\rangle, \tag{B.10}$$

for $m = 1, 2, \ldots, N-2$, with the energies

$$E(\xi_\pm, m) = -(N-2) \mp 2h \cos\left(\frac{m\pi}{N-1}\right). \tag{B.11}$$

Therefore, the presence of non-zero h in addition to λ creates a band of states out of the degenerate states $|j\rangle$ and $\Pi^z |j\rangle$ for $j = 1, 2, \ldots, N-2$, while the remaining states acquire only an energy shift.

B.2 Computing the Loschmidt echo

Now we can compute the Loschmidt echo, using the perturbative results of the previous section. First, we express the ground state $|g\rangle$ of the model with $\lambda = 0$, given by (A.9), in terms of the eigenstates of the model with $\lambda \neq 0$.

From (B.10) we find

$$\frac{1 - \Pi^z}{\sqrt{2}} |j\rangle = (-1)^j \sqrt{\frac{2}{N-1}} \sum_{m=1}^{N-2} \sin\left(\frac{m\pi}{N-1} j\right) |\xi_-, m\rangle \,. \tag{B.12}$$

This representation, together with the definition (B.4) and the representation (A.9) of $|g\rangle$ enables us to express $|g\rangle$ in terms of the eigenstates of the model with perturbed magnetic field. We find

$$|g\rangle = \sqrt{\frac{2}{N(N-1)}} \sum_{j=1}^{N-2} (-1)^j \sum_{m=1}^{N-2} \sin\left(\frac{m\pi}{N-1} j\right) |\xi_-, m\rangle + \sqrt{\frac{2}{N}} |\psi_-\rangle \,. \tag{B.13}$$

Now it is easy to apply the time evolution operator,

$$\begin{aligned} e^{-\imath H_1 t} |g\rangle &= \sqrt{\frac{2}{N}} e^{-\imath t E(\psi_-)} |\psi_-\rangle \\ &+ \sqrt{\frac{2}{N(N-1)}} \sum_{j=1}^{N-2} (-1)^j \sum_{m=1}^{N-2} \sin\left(\frac{m\pi}{N-1} j\right) e^{-\imath t E(\xi_-, m)} |\xi_-, m\rangle \,. \end{aligned} \tag{B.14}$$

Multiplying from the left by $\langle g|$, performing a bit of algebra and using the expressions (B.11) and (B.5) for the energies we get

$$\begin{aligned} e^{-\imath(N-2)t} \langle g| e^{-\imath H_1 t} |g\rangle &= \frac{2}{N} \exp\left[\imath t(\lambda + h)\right] \\ &+ \frac{2}{N(N-1)} \sum_{k=1}^{(N-1)/2} \tan^2\left[\frac{(2k-1)\pi}{2(N-1)}\right] \exp\left\{ -\imath 2ht \cos\left[\frac{(2k-1)\pi}{N-1}\right]\right\} \end{aligned} \tag{B.15}$$

Finally, the Loschmidt echo is the squared absolute value of this quantity, given by (2.5).

Appendix C

Quantum XY Chain: Exact and Perturbative Analysis

This is the appendix related to chapters 3 and 4. Here we show in details how to compute different magnetizations and the spin-correlation functions for the antiferromagnetic XY chain in zero magnetic field, with frustrated boundary conditions. This appendix is based on the supplementary materials of [1] and [2].

C.1 The Model and its Symmetries

The XY chain is given by the Hamiltonian

$$H = \sum_{j=1}^{N} \left(\cos\phi \, \sigma_j^x \sigma_{j+1}^x + \sin\phi \, \sigma_j^y \sigma_{j+1}^y \right) , \tag{C.1}$$

where σ_j^α, with $\alpha = x, y, z$, are Pauli operators acting on the j-th spin, N is the number lattice sites and we assume frustrated boundary conditions (FBC), given by periodic boundary conditions $\sigma_j^\alpha = \sigma_{j+N}^\alpha$ and an odd number of lattice sites. We focus, without the loss of generality, on the region $\phi \in (-3\pi/4, \pi/4)$, while the rest of the phase diagram is related by rotations of the spins around the z-axis. For $\phi \in (-3\pi/4, -\pi/2)$ both couplings are ferromagnetic. For $\phi \in (-\pi/2, -\pi/4)$ only the larger coupling, in magnitude, is ferromagnetic, and the other is antiferromagnetic. For $\phi \in (-\pi/4, 0)$ only the larger is antiferromagnetic, while for $\phi \in (0, \pi/4)$ both are antiferromagnetic.

Since the model in eq. (C.1) does not include an external magnetic field, the Hamiltonian commutes with all three parity operators $\Pi^\alpha \equiv \bigotimes_{j=1}^{N} \sigma_j^\alpha$, $\alpha = x, y, z$, i.e. $[H, \Pi^\alpha] = 0$, $\forall \alpha$. However, assuming FBC and hence setting the number of sites to be an odd number, different parity operators anticommute, satisfying $\{\Pi^\alpha, \Pi^\beta\} = 2\delta_{\alpha,\beta}$. As explained in chapters 3 and 4, the fact that the different parity operators anticommute has an immediate relevant consequence: each eigenstate is at least two-fold degenerate. To explain this point, let us assume that $|\varphi\rangle$ is simultaneously an eigenstate of H and one of the three parity operators, for instance Π^z. Then, the image of $|\varphi\rangle$ under the action of one of the other parity operators, for example $\Pi^x |\varphi\rangle$, is still an eigenstate of both H and Π^z. But while $|\varphi\rangle$ and $\Pi^x |\varphi\rangle$ have the same energy, they have different z parity. As a consequence, for each eigenstate of the Hamiltonian in the even sector of one of the parities ($\Pi^\alpha = 1$), there will be a second eigenstate of the Hamiltonian, with the same energy but living in the odd sector ($\Pi^\alpha = -1$). Hence each eigenvalue of the Hamiltonian is, at least, two-fold degenerate.

However, other symmetry properties of the Hamiltonian will prove to be of extreme relevance in the following. Due to periodic boundary conditions, the model exhibits exact translational symmetry, which is expressed in the commutation of the Hamiltonian with the lattice translation operator T. The model also exhibits mirror symmetry with respect to any lattice site. Namely, for any lattice site k the Hamiltonian in eq. (C.1) is invariant under the mirror image with respect to it, achieved by the transformation $j \to 2k - j$ on spins, associated to the action of the mirror operator M_k.

C.2 Exact solution

As is well-known, the model in eq. (C.1) can be diagonalized exactly, using standard techniques of mapping spins to fermions [56, 91]. The Jordan-Wigner transformation defines the fermionic operators as

$$c_j = \left(\bigotimes_{l=1}^{j-1} \sigma_l^z\right) \otimes \sigma_j^+, \quad c_j^\dagger = \left(\bigotimes_{l=1}^{j-1} \sigma_l^z\right) \otimes \sigma_j^-, \tag{C.2}$$

where $\sigma_j^\pm = (\sigma_j^x \pm \imath \sigma_j^y)/2$ are spin raising and lowering operators. In this notation, not explicitly mentioning a lattice site in the tensor product corresponds to making a tensor product with an identity operator on that site. In terms of Jordan-Wigner fermionic operators, the Hamiltonian in eq. (C.1) reads

$$\begin{aligned} H = &\sum_{j=1}^{N-1} \left[(\sin\phi - \cos\phi) c_j c_{j+1} - (\cos\phi + \sin\phi) c_j c_{j+1}^\dagger + \text{h.c.}\right] \\ &- \Pi^z \left[(\sin\phi - \cos\phi) c_N c_1 - (\cos\phi + \sin\phi) c_N c_1^\dagger + \text{h.c.}\right] \end{aligned} \tag{C.3}$$

Due to the presence of the parity operator along z, the Hamiltonian given by eq. (C.3) is not in a quadratic form, but becomes quadratic in each of the two parity sector of Π^z, i.e.

$$H = \frac{1+\Pi^z}{2} H^+ \frac{1+\Pi^z}{2} + \frac{1-\Pi^z}{2} H^- \frac{1-\Pi^z}{2}, \tag{C.4}$$

where both H^+ and H^- are quadratic. Being quadratic, they can be brought to a form of free fermions, which is done conveniently in two steps. First, $H^\pm$ are written in terms of the Fourier transformed Jordan-Wigner fermions,

$$b_q = \frac{1}{\sqrt{N}} \sum_{j=1}^{N} c_j \, e^{-\imath q j}, \quad b_q^\dagger = \frac{1}{\sqrt{N}} \sum_{j=1}^{N} c_j^\dagger \, e^{\imath q j}, \tag{C.5}$$

for $q \in \Gamma^\pm$, where the two sets of quasi-momenta are given by $\Gamma^- = \{2\pi k/N\}$ and $\Gamma^+ = \{2\pi(k+\frac{1}{2})/N\}$ with k running on all integers between 0 and $N-1$. Then a Bogoliubov rotation

$$\begin{aligned} a_q &= \cos\theta_q \, b_q + \imath \sin\theta_q \, b_{-q}^\dagger, \quad q \neq 0, \pi \\ a_q &= b_q, \quad q = 0, \pi \end{aligned} \tag{C.6}$$

with a momentum-dependent Bogoliubov angle given by

$$\theta_q = \arctan \frac{|\sin\phi + \cos\phi \, e^{\imath 2q}| - (\sin\phi + \cos\phi)\cos q}{(\cos\phi - \sin\phi)\sin q} \tag{C.7}$$

is used to bring them to a form of free fermions. The Bogoliubov angle also satisfies

$$e^{\imath 2\theta_q} = e^{\imath q} \frac{\cos\phi + \sin\phi\, e^{-\imath 2q}}{|\cos\phi + \sin\phi\, e^{-\imath 2q}|}. \tag{C.8}$$

The right hand side is also defined for the mode $q = 0$, for which eq. (C.7) is undefined, and as such it is used later in eq. (C.30) and eq. (C.97). We end up with

$$H^{\pm} = \sum_{q\in\Gamma^{\pm}} \varepsilon(q) \left(a_q^\dagger a_q - \frac{1}{2} \right), \tag{C.9}$$

where the dispersion law is given by

$$\begin{aligned} \epsilon(q) &= 2\left|\sin\phi + \cos\phi\, e^{\imath 2q}\right|, \; q \neq 0, \pi\,, \\ \epsilon(0) &= -\epsilon(\pi) = 2(\sin\phi + \cos\phi)\,. \end{aligned} \tag{C.10}$$

The eigenstates of H are formed by populating the vacuum states $|0^{\pm}\rangle$ of Bogoliubov fermions a_q, $q \in \Gamma^{\pm}$, and by taking care of the parity requirements in (C.4). The parity-dependent vacuum states are given by

$$|0^{\pm}\rangle = \prod_{0<q<\pi,\, q\in\Gamma^{\pm}} \left(\cos\theta_q - \imath \sin\theta_q\, b_q^\dagger b_{-q}^\dagger \right) |0\rangle\,, \tag{C.11}$$

where $|0\rangle \equiv \bigotimes_{j=1}^{N} |\uparrow_j\rangle$ is the vacuum for Jordan-Wigner fermions, satisfying the relation $c_j |0\rangle = 0\ \forall j$. As it is easy to see from eq. (C.11), the vacuum states $|0^+\rangle$ and $|0^-\rangle$ by construction have even Π^z parity. Since each excitation $a_q^\dagger$ changes the parity of the state it follows that the eigenstates of H belonging to $\Pi^z = -1$ sector are of the form $a_{q_1}^\dagger a_{q_2}^\dagger ... a_{q_m}^\dagger |0^-\rangle$ with $q_i \in \Gamma^-$ and m odd, while $\Pi^z = +1$ sector eigenstates are of the same form but with $q_i \in \Gamma^+$, m even and the vacuum $|0^+\rangle$ used.

On the other hand, as we have discussed, from an eigenstate of one parity of Π^z we can, by applying Π^x, obtain a second eigenstate, with the same energy, but different Π^z parity. This implies that to each aforementioned odd parity state, for instance, there is a corresponding even parity state $\Pi^x a_{q_1}^\dagger a_{q_2}^\dagger ... a_{q_m}^\dagger |0^-\rangle$ with the same energy.

As we can see from eq. (C.10), for $\phi \in (-3\pi/4, -\pi/4)$ the energy of the mode $q = 0$ is negative. The consequence is that here the ground states are the states

$$\begin{aligned} |g^-\rangle &= a_0^\dagger |0^-\rangle\,, \quad \text{odd sector}, \\ |g^+\rangle &= \Pi^x a_0^\dagger |0^-\rangle\,, \quad \text{even sector}, \end{aligned} \tag{C.12}$$

where the latter is, up to a phase factor, equal to $|0^+\rangle$. Above the two ground states there is a finite energy gap, that does not close in the thermodynamic limit. On the other hand, for $\phi \in (-\pi/4, \pi/4)$ there is no momenta in the odd sector with a negative energy. Accordingly, the ground states in the odd parity sector of Π^z are constructed by exciting the lowest energy modes $q \in \Gamma^-$ and have the form $a_q^\dagger |0^-\rangle$. To each such state is associated an equivalent ground state in the even sector of the form $\Pi^x a_q^\dagger |0^-\rangle$. Similarly, the lowest lying excited states are obtained by exciting the other single modes. Therefore, the ground state is part of a band of $2N$ states. Due to the spectrum of the form eq. (C.10), the gap closes as $1/N^2$ and the system is gapless. The closing of the gap is a phenomenology analogous to Refs. [62–64, 66, 67, 71, 73].

In the region $\phi \in (-\pi/4, 0)$ the energy in eq. (C.10) for the momenta in the odd sector is minimized by $q = 0$, so the ground state manifold is two-fold degenerate, and, as in the phase $\phi \in (-3\pi/4, -\pi/4)$, it is spanned by the states (C.12).$a_0^\dagger |0^-\rangle$ and $\Pi^x a_0^\dagger |0^-\rangle$. Note that, although the expressions in eq. (C.12) describe the ground states both in the unfrustrated region, $\phi \in (-3\pi/4, -\pi/4)$, and the frustrated one, $\phi \in (-\pi/4, 0)$, they characterize quite different structures. In the frustrated case, since the GS is obtained as the lightest excitation on top of the lowest possible energy state, adding different excitations provides states with an almost continuum of energy, which becomes a dense, gapless band in the thermodynamic limit. On the other hand, in the unfrustrated case there is a finite energy gap above the two ground states.

For $\phi \in (0, \pi/4)$ the energy would be minimized assuming $q = \pm\pi/2$. However, for any finite system with odd N the momenta $q = \pm\pi/2$ are not allowed. As a consequence the modes in the odd sector with the lowest energy, that we denote as $\pm p \in \Gamma^-$, are given by

$$p = \begin{cases} \frac{\pi}{2}\left(1 - \frac{1}{N}\right) , & N \bmod 4 = 1 \\ \frac{\pi}{2}\left(1 + \frac{1}{N}\right) , & N \bmod 4 = 3 \end{cases} \tag{C.13}$$

Hence the two states $|\pm p\rangle \equiv a_{\pm p}^\dagger |0^-\rangle$ represent the two ground states in the odd parity sector. The ground state manifold is, therefore, four-fold degenerate and a generic ground state can be written as a superposition

$$|g\rangle = u_1 |p\rangle + u_2 |-p\rangle + u_3 \Pi^x |-p\rangle + u_4 \Pi^x |p\rangle , \tag{C.14}$$

where we have assumed that the normalization condition $\sum_i |u|^2 = 1$ is satisfied.

C.3 The Translation Operator

The lattice translation operator T is a linear operator that shifts cyclically all the spins in the lattice by one site. To define it, we choose a basis of the space and specify its action on the basis. One basis of the Hilbert space of N spins are the states

$$|\psi\rangle = \bigotimes_{k=1}^{N} (\sigma_k^-)^{n_k} |\uparrow_k\rangle , \tag{C.15}$$

where $n_1, n_2, ..., n_N \in \{0, 1\}$. The translation operator T can then be defined by

$$T |\psi\rangle = \bigotimes_{k=1}^{N} (\sigma_k^-)^{n_{k+1}} |\uparrow_k\rangle , \tag{C.16}$$

where we make the identification $n_{N+1} \equiv n_1$. From eq. (C.16) it follows immediately that, for each state $|\psi\rangle$, we have that $\langle\psi| T^\dagger T |\psi\rangle = 1$. Hence the translation operator is unitary, i.e. $T^\dagger T = \mathbb{1}$ and the adjoint $T^\dagger$ plays the role of the translation operator in the other direction. Moreover, applying the T operator N times translates the spins by the whole lattice and results in recovering the initial state, implying the idempotence of order N of T, i.e. $T^N = \mathbb{1}$. As a consequence, the only possible eigenvalues of the translation operator are the N-th roots of unity, given by $e^{iq}, q \in \Gamma^-$.

On the other hand, moving from the spin states to the operators, it is easy to see that the translation operator shifts the Pauli operators as

$$T^\dagger \sigma_j^\alpha T = \sigma_{j+1}^\alpha, \quad \alpha = x, y, z \,, \tag{C.17}$$

where $\sigma_{N+1}^\alpha = \sigma_1^\alpha$, and, consequently it commutes with both the Hamiltonian in eq. (C.1) ($[T, H] = 0$) and the parity operators ($[T, \Pi^\alpha] = 0$ for $\alpha = x, y, z$).

The fact that the Hamiltonian and the translation operator commute implies that they admit a complete set of common eigenstates. In the following we prove that such a complete set is made by the eigenstates introduced in the previous section. Let us start by proving the following theorem.

Theorem 5.

(a) The states $b_{q_1}^\dagger b_{q_2}^\dagger ... b_{q_m}^\dagger |0\rangle$, with m odd and $\{q_k\} \subset \Gamma^-$, are eigenstates of T with eigenvalue equal to $\exp\left[\imath \sum_{k=1}^m q_k\right]$.

(b) The states $b_{q_1}^\dagger b_{q_2}^\dagger ... b_{q_m}^\dagger |0\rangle$, with m even and $\{q_k\} \subset \Gamma^+$, are eigenstates of T with eigenvalue equal to $\exp\left[\imath \sum_{k=1}^m q_k\right]$.

Proof. We write $\prod_{k=1}^m b_{q_k}^\dagger$ to indicate the ordered product of fermionic operators $b_{q_1}^\dagger b_{q_2}^\dagger ... b_{q_m}^\dagger$. From the defining properties of T we know how it acts on spin states and how it transforms the spin operators. Hence to study its action on the fermionic states $\left(\prod_{k=1}^m b_{q_k}^\dagger\right)|0\rangle$ it is convenient to write them in terms of spin states. This can be done in two steps. At first, using the eq. (C.5), we can write our state in terms of the Jordan-Wigner fermions, obtaining

$$\left(\prod_{k=1}^m b_{q_k}^\dagger\right)|0\rangle = \frac{1}{N^{m/2}} \sum_{j_1,...,j_m=1}^N e^{\imath \sum_{k=1}^m q_k j_k} \prod_{k=1}^m \left(c_{j_k}^\dagger\right)|0\rangle \,. \tag{C.18}$$

Being the $c_{j_k}^\dagger$ operators fermionic, only the terms with all different j_k survive. The second step is to invert the Jordan-Wigner mapping to bring back the fermionic states to spin ones. To do this step we first sort the fermionic operators, after which it's easy to invert the Jordan-Wigner transformation. To provide an example we have

$$c_1^\dagger c_4^\dagger c_2^\dagger |0\rangle = -c_1^\dagger c_2^\dagger c_4^\dagger |0\rangle = -\sigma_1^- (\sigma_1^z)\sigma_2^- (\sigma_1^z \sigma_2^z \sigma_3^z)\sigma_4^- \bigotimes_{k=1}^N |\uparrow_k\rangle = -\sigma_1^- \sigma_2^- \sigma_4^- \bigotimes_{k=1}^N |\uparrow_k\rangle \,. \tag{C.19}$$

More generally we can write

$$\bigotimes_{k=1}^m \left(c_{j_k}^\dagger\right)|0\rangle = S[\{j_k\}] \bigotimes_{k=1}^m \left(\sigma_{j_k}^-\right) \bigotimes_{k'=1}^N |\uparrow_{k'}\rangle \,, \tag{C.20}$$

where $S[\{j_k\}]$ is the sign of the permutation that brings the tuple $\{j_k\}$ to normal order. Hence, the states (C.18) can be re-written in terms of spin operators as

$$\left(\prod_{k=1}^m b_{q_k}^\dagger\right)|0\rangle = \frac{1}{N^{m/2}} \sum_{j_1,...,j_m=1}^N S[(j_k)] e^{\imath \sum_{k=1}^m q_k j_k} \bigotimes_{k=1}^m \left(\sigma_{j_k}^-\right) \bigotimes_{k'=1}^N |\uparrow_{k'}\rangle \,.$$

Having the representation of the state in terms of spins, it is easy to see what is the result of the application of T. Using its discussed properties and taking into account

that that T leaves the state $\bigotimes_{k'=1}^{N} |\uparrow'_k\rangle$ unchanged we recover

$$T\left(\prod_{k=1}^{m} b^\dagger_{q_k}\right)|0\rangle = \frac{1}{N^{m/2}} \sum_{j_1,\dots,j_m=1}^{N} S[\{j_k\}] e^{\imath \sum_{k=1}^{m} q_k j_k} \bigotimes_{k=1}^{m} \left(\sigma^-_{j_k-1}\right) \bigotimes_{k'=1}^{N} |\uparrow_{k'}\rangle$$
$$= \frac{e^{\imath \sum_{k=1}^{m} q_k}}{N^{m/2}} \sum_{j_1,\dots,j_m=1}^{N} S[\{j_k\}] e^{\imath \sum_{k=1}^{m} q_k (j_k-1)} \bigotimes_{k=1}^{m} \left(\sigma^-_{j_k-1}\right) \bigotimes_{k'=1}^{N} |\uparrow_{k'}\rangle \ . \quad \text{(C.21)}$$

Let us focus now on part (a) of the Theorem. We have two different cases. If none of the elements in $\{j_k\}$ is equal to 1, then none of the elements in $\{j_k - 1\}$ is equal to zero, and trivially $S[\{j_k\}] = S[\{j_k - 1\}]$. On the contrary if one element of $\{j_k\}$ is equal to 1, then $j_k - 1$ becomes 0. However, the number m of the elements in $\{j_k\}$ is odd. Hence to move an element from the first to the last place requires an even number $m - 1$ of permutations and hence the sign of the permutation $S[\{j_k\}] = S[\{j_k - 1\}]$ remains the same if we replace $j_k - 1 = 0$ with N. From this and the fact that, since $\{q_k\} \subset \Gamma^-$, the exponential $e^{\imath q_k (j_k - 1)}$ remains the same if we replace $j_k - 1 = 0$ with N, it follows that we can write

$$T\left(\prod_{k=1}^{m} b^\dagger_{q_k}\right)|0\rangle = \frac{e^{\imath \sum_{k=1}^{m} q_k}}{N^{m/2}} \sum_{j_1,\dots,j_m=1}^{N} S[\{j_k - 1\}] e^{\imath \sum_{k=1}^{m} q_k (j_k-1)} \bigotimes_{k=1}^{m} \left(\sigma^-_{j_k-1}\right) \bigotimes_{k'=1}^{N} |\uparrow_{k'}\rangle \ , \quad \text{(C.22)}$$

where, if for some k we have $j_k - 1 = 0$, we can identify it with $j_k - 1 = N$. Because of this identification it's easy to write each term in the sum in terms of fermions:

$$T\left(\prod_{k=1}^{m} b^\dagger_{q_k}\right)|0\rangle = \frac{e^{\imath \sum_{k=1}^{m} q_k}}{N^{m/2}} \sum_{j_1,\dots,j_m=1}^{N} e^{\imath \sum_{k=1}^{m} q_k (j_k-1)} \prod_{k=1}^{m} \left(c^\dagger_{j_k-1}\right)|0\rangle \ . \quad \text{(C.23)}$$

In eq. (C.23) we can, again on the basis of the identification of 0 with N, rename the indices to get

$$T\left(\prod_{k=1}^{m} b^\dagger_{q_k}\right)|0\rangle = \frac{e^{\imath \sum_{k=1}^{m} q_k}}{N^{m/2}} \sum_{j_1,\dots,j_m=1}^{N} e^{\imath \sum_{k=1}^{m} q_k j_k} \prod_{k=1}^{m} \left(c^\dagger_{j_k}\right)|0\rangle = \exp\left(\imath \sum_{k=1}^{m} q_k\right) \left(\prod_{k=1}^{m} b^\dagger_{q_k}\right)|0\rangle \ , \quad \text{(C.24)}$$

which proves part (a) of Theorem 5. Part (b) is proven in a similar way. □

From Theorem 5 it follows immediately, by taking into account the definition of the Bogoliubov particles in eq. (C.6), the definition of the Bogoliubov vacua in eq. (C.11), and the linearity of the translation operator, that also the Hamiltonian eigenstates $\left(\prod_{k=1}^{m} a^\dagger_{q_k}\right)|0^\pm\rangle$ are eigenstates of T with eigenvalues equal to $\exp\left(\imath \sum_{k=1}^{m} q_k\right)$.

C.4 The Mirror Operator

As we have seen in the first section of this appendix, the Hamiltonian is invariant under the mirror transformation with respect to a generic site k that changes spin operators defined on the site j to ones defined on the site $2k - j$. Note that, with the odd number N of sites we work with, in a circular geometry, the line of mirror reflection crosses a site and a bond. Hence, only site k remains unchanged by the mirror action.

As we have done for translations, the mirror transformation can also be expressed by the action of a suitable operator. The mirror operator M_k, that makes

the mirror transformation of the states with respect to the k-th site, is defined by its action on the spin basis states $|\psi\rangle$, defined in eq. (C.15), as

$$M_k |\psi\rangle = M_k \bigotimes_{j=1}^{N} (\sigma_j^-)^{n_j} |\uparrow_j\rangle = \bigotimes_{j=1}^{N} (\sigma_j^-)^{n_{2k-j}} |\uparrow_j\rangle \ , \tag{C.25}$$

where, as always, $n_{j+N} \equiv n_j$. From eq. (C.25) it follows immediately that, for each state $|\psi\rangle$, we have that $\langle\psi| M_k^\dagger M_k |\psi\rangle = 1$. Hence, as the translation operator, also M_k is unitary, i.e. $M_k^\dagger M_k = \mathbb{1}$. Moreover, applying the mirror operator two times results in recovering the initial state, hence implying the idempotence of order 2 of the operator M_k, i.e. $M_k^2 = \mathbb{1}$. This implies that M_k is also Hermitian, i.e. $M_k^\dagger = M_k$, and that the only possible eigenvalues of M_k are ± 1. Moreover, different mirror operators are related by translations,

$$T^\dagger M_k T = M_{k+1} \tag{C.26}$$

From this relation it is also clear that the mirror operators do not commute with the translation operator ($[M_k, T] \neq 0$).

Since each of the mirror operators commutes with the Hamiltonian, the Hamiltonian shares a common basis with each one of them. The following theorem gives the relation between the eigenstates we have constructed and the mirror operators. Essentially, the mirror operators change the sign of the momenta of the excitations, up to a possible phase factor, depending on k. Since different mirror operators are related by eq. (C.26) we focus on the one with $k = N$ for which the phase factor is absent.

Theorem 6.

(a) The mirror operator M_N acts on the states $b^\dagger_{q_1} b^\dagger_{q_2} ... b^\dagger_{q_m} |0\rangle$, with m odd and $\{q_k\} \subset \Gamma^-$, as

$$M_N \, b^\dagger_{q_1} b^\dagger_{q_2} ... b^\dagger_{q_m} |0\rangle = b^\dagger_{-q_m} b^\dagger_{-q_{m-1}} ... b^\dagger_{-q_1} |0\rangle \tag{C.27}$$

(b) The mirror operator M_N acts on the states $b^\dagger_{q_1} b^\dagger_{q_2} ... b^\dagger_{q_m} |0\rangle$, with m even and $\{q_k\} \subset \Gamma^+$, as

$$M_N \, b^\dagger_{q_1} b^\dagger_{q_2} ... b^\dagger_{q_m} |0\rangle = b^\dagger_{-q_m} b^\dagger_{-q_{m-1}} ... b^\dagger_{-q_1} |0\rangle \tag{C.28}$$

The theorem is proven in a similar way as Theorem 5, and we omit the details. The other mirror operators M_k, with $k \neq N$, would introduce an additional phase factor by acting on the aforementioned eigenstates. The phase factor depends on the momentum of the state and can be reconstructed from eq. (C.26). The N-th site being special here is a consequence of its special position in the Jordan-Wigner transformation, which implicitly enters in the definition of the states we work on. In the proof of Theorem 6 the N-th site is special because for $k = N$ the exponentials of the type $e^{\imath q j}$ can be replaced by $e^{\imath(-q)(2k-j)}$, while for other k a compensating factor has to be introduced.

Similarly as after Theorem 5, but using also the property $\theta_{-q} = -\theta_q$ of the Bogoliubov angle, it follows from Theorem 6 that the mirror operator M_N acts on the Hamiltonian eigenstates $a^\dagger_{q_1} a^\dagger_{q_2} ... a^\dagger_{q_m} |0^\pm\rangle$ as $M_N \, a^\dagger_{q_1} a^\dagger_{q_2} ... a^\dagger_{q_m} |0^\pm\rangle = a^\dagger_{-q_m} a^\dagger_{-q_{m-1}} ... a^\dagger_{-q_1} |0^\pm\rangle$. Note that, as a consequence, only the states with the total momentum satisfying $\exp\left[\imath \sum_{j=1}^m q_j\right] = \pm 1$ can simultaneously be the eigenstates of T and M_N. Finally,

let us notice that mirroring does not change the parity and so the mirror operator commutes with the parity operators, i.e. $[M_N, \Pi^\alpha] = 0$, $\alpha = x, y, z$.

C.5 One Antiferromagnetic, One Ferromagnetic Coupling

Here we focus on the regions $\phi \in (-\pi/2, -\pi/4)$ (yFM) and $\phi \in (-\pi/4, 0)$ (xAFM), where one coupling in the Hamiltonian (C.1) is antiferromagnetic and the other ferromagnetic. Another part of the yFM region, given by $\phi \in (-3\pi, -\pi/2)$, where both couplings are ferromagnetic, can be treated in the same way as the former, with the same results. Different correlations and magnetizations can be computed by introducing the Majorana fermionic operators [91],

$$A_j \equiv \left(\bigotimes_{l=1}^{j-1} \sigma_l^z\right) \sigma_j^x \,, \quad B_j \equiv \left(\bigotimes_{l=1}^{j-1} \sigma_l^z\right) \sigma_j^y \,, \tag{C.29}$$

and exploiting Wick's Theorem [189–192]. From the exact solution we find the Majorana two-point correlation functions to be given by

$$\begin{aligned} &\langle g^- |\, A_{j+r} A_j \,| g^- \rangle = \langle g^- |\, B_{j+r} B_j \,| g^- \rangle = \delta_{r,0} \\ &G(r) \equiv -\imath \,\langle g^- |\, A_{j+r} B_j \,| g^- \rangle = \frac{1}{N} \sum_{q \in \Gamma^-} e^{\imath 2\theta_q} e^{-\imath q r} + \frac{2}{N} f(r) \,. \end{aligned} \tag{C.30}$$

Here the function $f(r)$ is zero for $-\pi/2 < \phi < -\pi/4$, while for $-\pi/4 < \phi < 0$ we have $f(r) = -1$.

C.5.1 Two–spins correlation function along the x and y directions:

Let us now move to analyze the behavior of the two–spin correlation functions along x and y directions as a function of r. Following the path traced in Ref. [90, 91], it is easy to express such correlations in terms of determinants of $r \times r$ Toeplitz matrices. More precisely, the two–spin correlation function along x at distance r, i.e. $C_{xx}(r) \equiv \langle g^\pm |\, \sigma_j^x \sigma_{j+r}^x \,| g^\pm \rangle$, is given by

$$C_{xx}(r) = (-1)^r \det \rho_{xx} \tag{C.31}$$

where the matrix ρ_{xx} is given by

$$\rho_{xx} \equiv \begin{pmatrix} G(1) & G(0) & G(-1) & \cdots & G(2-r) \\ G(2) & G(1) & G(0) & \cdots & G(3-r) \\ G(3) & G(2) & G(1) & \cdots & G(4-r) \\ \vdots & \vdots & \vdots & & \vdots \\ G(r) & G(r-1) & G(r-2) & \cdots & G(1) \end{pmatrix} . \tag{C.32}$$

At the same time the correlation function along y at distance r is given by

$$C_{yy}(r) = \langle g^\pm |\, \sigma_j^y \sigma_{j+r}^y \,| g^\pm \rangle = (-1)^r \det \rho_{yy} \tag{C.33}$$

where

$$\rho_{yy} \equiv \begin{pmatrix} G(-1) & G(0) & G(1) & \cdots & G(r-2) \\ G(-2) & G(-1) & G(0) & \cdots & G(r-3) \\ G(-3) & G(-2) & G(-1) & \cdots & G(r-4) \\ \vdots & \vdots & \vdots & & \vdots \\ G(-r) & G(1-r) & G(2-r) & \cdots & G(-1) \end{pmatrix}. \tag{C.34}$$

As we anticipated, the behavior of these two correlation functions is very different in the two phases of our system. In the ferromagnetic phase, the asymptotic behavior is well known from the literature [150]: $C_{xx}(r)$ exponentially decays to zero, while $C_{yy}(r)$ saturates exponentially fast to the square of the y-magnetization, that is to $\sqrt{1-\cot^2\phi}$.

In the xAFM phase, the evaluation of the asymptotic behaviors of the Toeplitz determinants is more complicated, but can also be done analytically, using the asymptotic formulas for such determinants, that we have derived in [3]. There, we have computed the spin correlation functions using another representation of them in terms of Toeplitz determinants, similar to the one found in [72], which can also be used for arbitrary definite-momentum state in the lowest energy band. We derive this representation now. The computation of the spin correlation functions is presented in Chapter 9, based on [3]. The results for the spin-correlations are given in the Chapter 3.

Let us consider the state $|p\rangle = a_p^\dagger |0^-\rangle$, for arbitrary $p \in \Gamma^-$. We start by noting that the spin correlation functions $\langle p| \sigma_j^x \sigma_{j+r}^x |p\rangle$ in any such state are independent of the site j and depend only on the distance r. To see this we recognize that $\sigma_j^x \sigma_{j+r}^x = (T^\dagger)^{j-1} \sigma_1^x \sigma_{1+r}^x T^{j-1}$, where T is the translation operator, introduced in section C.3. According to Theorem 5, the state $|p\rangle$ is an eigenstate of T with the eigenvalue $e^{\imath p}$, so the left and right eigenvalue in $\langle p| (T^\dagger)^{j-1} \sigma_1^x \sigma_{1+r}^x T^{j-1} |p\rangle$ cancel, and we are left with

$$\langle p| \sigma_j^x \sigma_{j+r}^x |p\rangle = \langle p| \sigma_1^x \sigma_{1+r}^x |p\rangle, \quad \forall j. \tag{C.35}$$

Next, we recognize that the spin correlation functions can be expressed as

$$\langle p| \sigma_1^x \sigma_{1+r}^x |p\rangle = (-1)^r \langle 0^-| a_p \prod_{k=1}^{r} (-\imath A_{k+1} B_k) a_p^\dagger |0^-\rangle \tag{C.36}$$

and then we make Wick contractions in the vacuum state $|0^-\rangle$. Adopting the short notation $\langle \cdot \rangle_0 = \langle 0^-| \cdot |0^-\rangle$, we have $\langle A_j A_k \rangle_0 = \langle B_j B_k \rangle_0 = \delta_{jk}$ and

$$-\imath \langle A_j B_k \rangle_0 = \frac{1}{N} \sum_{q \in \Gamma^-} e^{\imath 2\theta_q} e^{-\imath q(j-k)}. \tag{C.37}$$

Moreover, since for $\phi \in (-\pi/4, 0)$, as well as for $\phi \in (0, \pi/4)$, we can express the Majorana fermions as

$$\begin{aligned} A_j &= \frac{1}{\sqrt{N}} \sum_{q \in \Gamma^-} (a_q^\dagger + a_{-q}) e^{\imath \theta_q} e^{-\imath q j}, \\ -\imath B_j &= \frac{1}{\sqrt{N}} \sum_{q \in \Gamma^-} (a_q^\dagger - a_{-q}) e^{-\imath \theta_q} e^{-\imath q j}, \end{aligned} \tag{C.38}$$

we can easily obtain the contractions

$$\begin{aligned} -\imath \langle a_p A_j \rangle_0 \langle B_k a_p^\dagger \rangle_0 &= -\frac{1}{N} e^{\imath 2\theta_p} e^{-\imath p(j-k)}, \\ -\imath \langle a_p B_k \rangle_0 \langle A_j a_p^\dagger \rangle_0 &= \frac{1}{N} e^{-\imath 2\theta_p} e^{\imath p(j-k)}. \end{aligned} \tag{C.39}$$

Performing all the Wick contractions in eq. (C.36) and using the basic properties of determinants, the spin correlation functions can be expressed as

$$\langle p | \sigma_1^x \sigma_{1+r}^x | p \rangle = (-1)^r \left[\left(\det \tilde{\rho}_{xx}^{(p)} + \text{c.c.} \right) - \det \tilde{\rho}_{xx} \right], \tag{C.40}$$

where $\tilde{\rho}_{xx}^{(p)}$ and $\tilde{\rho}_{xx}$ are $r \times r$ matrices with the elements

$$\begin{aligned} \left(\tilde{\rho}_{xx} \right)_{j,k} &= -\imath \langle A_{j+1} B_k \rangle_0 , \\ \left(\tilde{\rho}_{xx}^{(p)} \right)_{j,k} &= \left(\tilde{\rho}_{xx} \right)_{j,k} - \frac{1}{N} e^{\imath 2\theta_p} e^{-\imath p(j-k+1)}, \end{aligned} \tag{C.41}$$

for $j, k \in \{1, 2, \ldots, r\}$, which give an alternative expression to eq. (C.31) for the evaluation of the spin correlation functions in the ground state. Here the vacuum expectation value is given simply by

$$-\imath \langle A_j B_k \rangle_0 = \frac{1}{N} \sum_{q \in \Gamma^-} e^{\imath 2\theta_q} e^{-\imath q(j-k)}. \tag{C.42}$$

In an analogous way we find

$$\langle p | \sigma_1^y \sigma_{1+r}^y | p \rangle = (-1)^r \left[\left(\det \tilde{\rho}_{yy}^{(p)} + \text{c.c.} \right) - \det \tilde{\rho}_{yy} \right], \tag{C.43}$$

where

$$\begin{aligned} \left(\tilde{\rho}_{yy} \right)_{j,k} &= -\imath \langle A_j B_{k+1} \rangle_0 , \\ \left(\tilde{\rho}_{yy}^{(p)} \right)_{j,k} &= \left(\tilde{\rho}_{yy} \right)_{j,k} - \frac{1}{N} e^{\imath 2\theta_p} e^{-\imath p(j-k-1)}. \end{aligned} \tag{C.44}$$

for $j, k \in \{1, 2, \ldots, r\}$.

C.5.2 Magnetizations along the x and y directions

In this section, we show how it is possible to exploit the particular symmetries of the model in eq. (C.3), to evaluate, for any odd N, the magnetization along the x and the y directions. For sake of simplicity, we limit ourselves to illustrate the method for the magnetization along the x direction and we report the results for both at the end.

In the region that we are analyzing, the ground state manifold has always dimension equal to two. An arbitrary ground state can be written as a superposition

$$|g\rangle = \left[\cos(\theta) + \sin(\theta) e^{\imath\psi} \Pi^x \right] |g^-\rangle \ , \tag{C.45}$$

for some real numbers θ and ϕ. Equivalently, it can be written using Π^y, since $\Pi^x |g^-\rangle$ and $\Pi^y |g^-\rangle$ only differ by a global phase factor.

Let us now choose a generic site j of the system. For the generic ground state in eq. (C.45) the magnetization along x on the j-th spin is

$$\begin{aligned} m_x(j) &= \langle g|\, \sigma_j^x \,|g\rangle \\ &= \cos^2(\theta)\, \langle g^-|\, \sigma_j^x \,|g^-\rangle + \sin^2(\theta)\, \langle g^-|\, \Pi^x \sigma_j^x \Pi^x \,|g^-\rangle \\ &+ \frac{1}{2}\sin(2\theta)\Big[e^{\imath\psi}\langle g^-|\sigma_j^x \Pi^x|g^-\rangle + e^{-\imath\psi}\langle g^-|\Pi^x\sigma_j^x|g^-\rangle\Big] \end{aligned} \tag{C.46}$$

Being both $|g^-\rangle$ and $\Pi^x\,|g^-\rangle$ eigenstates of Π^z, the two expectation values $\langle g^-|\,\sigma_j^x\,|g^-\rangle$ and $\langle g^-|\,\Pi^x\sigma_j^x\Pi^x\,|g^-\rangle$ vanish. On the contrary, because the number of spins in the system is odd, the operator $\Pi^x\sigma_j^x = \sigma_j^x\Pi^x$, that is equal to $\tilde{\Pi}_j^x = \bigotimes_{l\neq j}\sigma_l^x$, is an operator that commutes with Π^z and hence can have a non–vanishing expectation value on $|g^-\rangle$. Therefore we have

$$m_x(j) = \cos(\psi)\sin(2\theta)\langle g^-|\tilde{\Pi}_j^x\,|g^-\rangle\,. \tag{C.47}$$

which reaches the maximum for $\psi = 0$ and $\theta = \frac{\pi}{4}$, and this is the state on which we focus.

Hence, to evaluate the magnetization, we only need to determine the expectation value $\langle g^-|\tilde{\Pi}_j^x\,|g^-\rangle$. Since $[\tilde{\Pi}_j^x, \Pi^z] = 0$, the magnetization can be easily evaluated exploiting the representation of $\tilde{\Pi}_j^x$ in terms of the Majorana operators in eq. (C.29) and Wick's theorem. Now, it's important to notice that, since the translation operator T commutes with Π^x, the states $|g^-\rangle$ and $\Pi^x\,|g^-\rangle$ have the same eigenvalue of the translation operator (equal to zero). It follows that the magnetization $m_x(j)$ is independent of site j, i.e. ferromagnetic. We can, thus, without loss of generality, set $j = 1$.

From the definition of the Majorana operators in eq. (C.29), the operator $\tilde{\Pi}_1^x$ can be written as

$$\tilde{\Pi}_1^x = (-1)^{\frac{N-1}{2}}\prod_{l=1}^{\frac{N-1}{2}}(-\imath A_{2l+1}B_{2l})\,. \tag{C.48}$$

Exploiting Wick's theorem, we obtain that the expectation value $\langle g^-|\tilde{\Pi}_1^x\,|g^-\rangle$ is

$$\langle g^-|\tilde{\Pi}_1^x\,|g^-\rangle = (-1)^{\frac{N-1}{2}}\det\rho_x\,, \tag{C.49}$$

where ρ_x is an $\frac{N-1}{2}\times\frac{N-1}{2}$ Toeplitz matrix ρ_x, that reads

$$\rho_x = \begin{pmatrix} G(1) & G(-1) & G(-3) & \cdots & G(4-N) \\ G(3) & G(1) & G(-1) & \cdots & G(6-N) \\ G(5) & G(3) & G(1) & \cdots & G(8-N) \\ \vdots & \vdots & \vdots & & \vdots \\ G(N-2) & G(N-4) & G(N-6) & \cdots & G(1) \end{pmatrix}, \tag{C.50}$$

with G defined in (C.30). Similarly, the magnetization along y reads

$$m_y(1) = \cos(\psi)\sin(2\theta)\langle g^-|\tilde{\Pi}_1^y\,|g^-\rangle\,, \tag{C.51}$$

where $\tilde{\Pi}_1^y = \bigotimes_{l=2}^N \sigma_l^y$. Also in this case the maximum of the magnetization is equal to $\langle g^-|\tilde{\Pi}_1^y\,|g^-\rangle$, which in turn can be written as

$$\langle g^-|\tilde{\Pi}_1^y\,|g^-\rangle = (-1)^{\frac{N-1}{2}}\det\rho_y\,, \tag{C.52}$$

where ρ_y is an $\frac{N-1}{2} \times \frac{N-1}{2}$ Toeplitz matrix, that reads

$$\rho_y = \begin{pmatrix} G(-1) & G(-3) & G(-5) & \cdots & G(2-N) \\ G(1) & G(-1) & G(-3) & \cdots & G(4-N) \\ G(3) & G(1) & G(-1) & \cdots & G(6-N) \\ \vdots & \vdots & \vdots & & \vdots \\ G(N-4) & G(N-6) & G(N-6) & \cdots & G(-1) \end{pmatrix} . \tag{C.53}$$

C.5.3 Magnetizations in the ferromagnetic phase

If we are in the yFM phase the expressions for the magnetizations in the thermodynamic limit can be obtained analytically in the following way. We have in eq. (C.30) the function $f(r) = 0$ and hence $G(r)$ reads

$$G(r) = \frac{1}{N} \sum_{q \in \Gamma^-} \frac{\cos\phi + \sin\phi\, e^{-\imath 2q}}{|\cos\phi + \sin\phi\, e^{-\imath 2q}|} e^{-\imath q(r-1)} . \tag{C.54}$$

For large N we can approximate the sum with an integral, obtaining

$$G(r) = \frac{1}{2\pi} \int_0^{2\pi} \frac{\cos\phi + \sin\phi\, e^{-\imath 2q}}{|\cos\phi + \sin\phi\, e^{-\imath 2q}|} e^{-\imath q(r-1)} dq . \tag{C.55}$$

To evaluate the determinants $\det\rho_{x,y}$ of the Toeplitz matrices in eq. (C.50) and eq. (C.53) we introduce

$$D_n \equiv G(2n-1) = -\frac{1}{2\pi} \int_0^{2\pi} \frac{1 + \cot\phi\, e^{\imath q}}{|1 + \cot\phi\, e^{\imath q}|} e^{-\imath q n} dq , \tag{C.56}$$

and rewrite them as

$$\det\rho_x = \begin{vmatrix} D_1 & D_0 & \dots & D_{2-r} \\ D_2 & D_1 & \dots & D_{3-r} \\ \vdots & \vdots & \ddots & \vdots \\ D_r & D_{r-1} & \dots & D_1 \end{vmatrix} , \quad r = \frac{N-1}{2} , \tag{C.57}$$

and

$$\det\rho_y = \begin{vmatrix} D_0 & D_{-1} & \dots & D_{1-r} \\ D_1 & D_0 & \dots & D_{2-r} \\ \vdots & \vdots & \ddots & \vdots \\ D_{r-1} & D_{r-2} & \dots & D_0 \end{vmatrix} , \quad r = \frac{N-1}{2} . \tag{C.58}$$

The latter can be evaluated straightforwardly for large N using strong Szegö limit theorem [196], yielding, to leading order,

$$\langle g^- | \tilde{\Gamma}_1^y | g^- \rangle = (1 - \cot^2\phi)^{\frac{1}{4}} . \tag{C.59}$$

The magnetization in the x direction, instead, is more complicated, because the generating function of the corresponding Toeplitz matrix has a non–zero winding number. To overcome this problem, we proceed as in Ref. [205] and notice that the determinant $\det\rho_x(r)$ in eq. (C.57), where we have indicated the size r of the matrix, can be seen as the minor of $\rho_y(r+1)$ in eq. (C.58), obtained removing the first row and the last column. To calculate this minor, we use Cramer's rule and consider the

following linear problem:

$$\sum_{m=0}^{r} D_{n-m}\, x_m = \delta_{n,0}\,, \qquad n = 0, \ldots, r\,. \tag{C.60}$$

Then,

$$\det \rho_x(r) = (-1)^r x_r \det \rho_y(r+1)\,, \tag{C.61}$$

where $\det \rho_y(r+1)$ is a Toeplitz determinant satisfying the conditions for the Szegö theorem. For large r, x_r can be evaluated following the standard Wiener–Hopf procedure as in Ref. [205]. The result is

$$\begin{aligned} x_r &\overset{r\to\infty}{\simeq} -\frac{1}{2\pi\imath}\oint \frac{\xi^{r-1}\, d\xi}{\sqrt{(1+\cot\phi\,\xi)(1+\cot\phi\,\xi^{-1})}} \\ &= -\frac{1}{\pi}\int_0^{-\cot\phi} \frac{x^{r-1/2}\, dx}{\sqrt{(1+\cot\phi\, x)(-\cot\phi - x)}}\,, \end{aligned} \tag{C.62}$$

where we deformed the contour of integration around the branch cut. The integral in eq. (C.62) can be expressed in terms of hypergeometric functions,

$$x_r \overset{r\to\infty}{\simeq} -\frac{(-1)^r}{\sqrt{\pi}} \frac{\cot^r\phi}{\sqrt{1-\cot^2\phi}} \frac{\Gamma\left(r+\frac{1}{2}\right)}{\Gamma(r+1)}\, {}_2F_1\left(\frac{1}{2},\frac{1}{2}; r+1; \frac{\cot^2\phi}{\cot^2\phi - 1}\right)\,, \tag{C.63}$$

whose asymptotic behavior gives to the leading order

$$x_r \overset{r\to\infty}{\simeq} -\frac{(-1)^r}{\sqrt{\pi r}} \frac{\cot^r\phi}{\sqrt{1-\cot^2\phi}}\,, \tag{C.64}$$

since ${}_2F_1$ tends to 1 for large r. Combining eq. (C.64) with eq. (C.61) and eq. (C.59) we arrive at

$$\det \rho_x(r) \overset{r\to\infty}{\simeq} \frac{(-1)^r \cot^r\phi}{(1-\cot^2\phi)^{\frac{1}{4}}\sqrt{\pi r}}\,, \tag{C.65}$$

which means that the magnetization in the x direction decays exponentially with the system size,

$$\langle g^-|\, \tilde{\Pi}_1^x\, |g^-\rangle \overset{N\to\infty}{\simeq} \frac{\cot^{\frac{N-1}{2}}\phi}{(1-\cot^2\phi)^{\frac{1}{4}}\sqrt{\pi(N-1)/2}}. \tag{C.66}$$

Alternatively, the same result could be obtained using the theorem proven by Fisher and Hartwig in [199, 200], given by eq. (9.13). Note that, despite the x interaction being AFM, the corresponding magnetization is not staggered.

Finally, the magnetization in the z–direction is just equal to the Majorana two–point function in eq. (C.30) and thus its exponential decay to zero arises as the difference between the finite sum in eq. (C.30) and vanishing of the corresponding integral in the $N \to \infty$ limit.

C.5.4 Magnetizations in the frustrated phase

If we are in the xAFM phase we have that in eq. (C.30) the function $f(r) \neq 0$ and the function $G(r)$ becomes

$$G(r) = -\frac{2}{N} + \frac{1}{N}\sum_{q\in\Gamma^-} \frac{\cos\phi + \sin\phi\, e^{-\imath 2q}}{|\cos\phi + \sin\phi\, e^{-\imath 2q}|} e^{-\imath q(r-1)}\,, \tag{C.67}$$

in which, for large N, we can approximate the sum with an integral, hence obtaining

$$G(r) = -\frac{2}{N} + \frac{1}{2\pi}\int_0^{2\pi} \frac{\cos\phi + \sin\phi\, e^{-\imath 2q}}{|\cos\phi + \sin\phi\, e^{-\imath 2q}|} e^{-\imath q(r-1)} dq\,. \tag{C.68}$$

This function reflects the fact that, effectively, the ground states of the frustrated case have a single, delocalized excitation. Thus, in this phase, we write the Toeplitz determinants in eq. (C.50) and eq. (C.53) as

$$\det\rho_x = \begin{vmatrix} \tilde{D}_0 & \tilde{D}_{-1} & \dots & \tilde{D}_{1-r} \\ \tilde{D}_1 & \tilde{D}_0 & \dots & \tilde{D}_{2-r} \\ \vdots & \vdots & \ddots & \vdots \\ \tilde{D}_{r-1} & \tilde{D}_{r-2} & \dots & \tilde{D}_0 \end{vmatrix}, \quad r = \frac{N-1}{2}\,, \tag{C.69}$$

and

$$\det\rho_y = \begin{vmatrix} \tilde{D}_{-1} & \tilde{D}_{-2} & \dots & \tilde{D}_{-r} \\ \tilde{D}_0 & \tilde{D}_{-1} & \dots & \tilde{D}_{1-r} \\ \vdots & \vdots & \ddots & \vdots \\ \tilde{D}_{r-2} & \tilde{D}_{r-3} & \dots & \tilde{D}_{-1} \end{vmatrix}, \quad r = \frac{N-1}{2}\,, \tag{C.70}$$

where

$$\tilde{D}_n \equiv G(2n+1) = -\frac{2}{N} + \frac{1}{2\pi}\int_0^{2\pi} D\left(e^{\imath q}\right) e^{-\imath q n} dq, \tag{C.71}$$

with

$$D\left(e^{\imath q}\right) \equiv \frac{1+\tan\phi\, e^{-\imath q}}{|1+\tan\phi\, e^{-\imath q}|}\,. \tag{C.72}$$

Note that, compared to the definitions employed for the yFM phase, we changed the definition of the generating function by shifting its Fourier series, so that eq. (C.72) has zero winding number. Using these determinant representations the magnetizations can be computed analytically, similarly to the two-point correlation functions. We have done also this analytical computation in [3], and present it in Chapter 9. The result, for large (odd) N, is

$$\langle g^-|\,\tilde{\Pi}_1^x\,|g^-\rangle \overset{N\to\infty}{\simeq} (-1)^{\frac{N-1}{2}} \frac{1}{N}(1-\tan^2\phi)^{\frac{1}{4}}, \tag{C.73}$$

$$\langle g^-|\,\tilde{\Pi}_1^y\,|g^-\rangle \overset{N\to\infty}{\simeq} \frac{2}{N}\frac{(1-\tan\phi)^{\frac{1}{4}}}{(1+\tan\phi)^{\frac{3}{4}}}. \tag{C.74}$$

C.5.5 Two–spins correlation function and magnetization along the z direction in the frustrated phase

The correlation function along z is simply the determinant $\det \rho_{zz}$, where

$$\rho_{zz} \equiv \begin{pmatrix} G(0) & G(-r) \\ G(r) & G(0) \end{pmatrix}. \tag{C.75}$$

The integral in (C.68) can be studied by deforming the contour around the branch cuts and using the properties of hypergeometric functions, as in [90, 150, 205]. In this way we get

$$G(r) = -\frac{2}{N}, \qquad r = 2m\,, \tag{C.76}$$

$$G(r) \overset{r\to\infty}{\simeq} -\frac{2}{N} + \sqrt{2(1-\tan^2\phi)}\frac{(-\tan\phi)^{\frac{r-1}{2}}}{\sqrt{\pi r}} \qquad r = 2m+1\,, \tag{C.77}$$

$$G(-r) \overset{r\to\infty}{\simeq} -\frac{2}{N} - \sqrt{\frac{2}{1-\tan^2\phi}}\frac{(-\tan\phi)^{\frac{r+1}{2}}}{\sqrt{\pi r^3}} \qquad r = 2m+1\,. \tag{C.78}$$

Using these formulas we get the result in Chapter 3. Finally, the magnetization in the z direction is given by $G(0)$ so it is simply equal to $-\frac{2}{N}$.

C.6 Both Couplings Antiferromagnetic

C.6.1 The Spatial Dependence of the Magnetization

As we have shown in section C.2, in the region $\phi \in (0, \pi/4)$ the ground state manifold is four fold degenerate. Hence a large variety of possible ground states with different magnetic properties can be selected. Among them, the ground states at the center of Chapter 4 are of the form

$$|\tilde{g}\rangle = \frac{1}{\sqrt{2}}\big(\,|p\rangle + e^{\imath\theta}\,\Pi^x\,|-p\rangle\,\big), \tag{C.79}$$

where θ is a free phase. For such state the magnetization in the γ direction, with $\gamma = x, y$, shows the peculiar incommensurate antiferromagnetic order, that we have discussed in Chapter 4 and that we will elaborate on in the following. By definition, the magnetization in the γ direction is equal to

$$\langle\sigma_j^\gamma\rangle_{\tilde{g}} = \frac{1}{2}\big(e^{\imath\theta}\,\langle p|\,\sigma_j^\gamma\Pi^x\,|-p\rangle + \text{c.c.}\big)\,. \tag{C.80}$$

The magnetization is thus determined by the quantities $\langle p|\,\sigma_j^\gamma\Pi^x\,|-p\rangle$, which are matrix elements of the spin string operators σ_j^γ between the ground states vectors $|p\rangle$ and $\Pi^x\,|-p\rangle$. The matrix elements at any site j can be related to the ones at site N, using the translation operator. Using the relation $\sigma_k^\alpha = (T^\dagger)^k\sigma_N^\alpha(T)^k$ and knowing the eigenvalues of T we get

$$\langle p|\,\sigma_j^\gamma\Pi^x\,|-p\rangle = e^{-\imath 2pj}\,\langle p|\,\sigma_N^\gamma\Pi^x\,|-p\rangle\,. \tag{C.81}$$

The advantage of expressing the quantity $\langle p|\,\sigma_j^\gamma\Pi^x\,|-p\rangle$ in terms of the one at site $j = N$ is that this last one is real for $\gamma = x$ and purely imaginary for $\gamma = y$, as we

will now show. The reason why the N-th site is special is because the Jordan-Wigner transformation, which implicitly enters into the definition of the states, breaks the invariance under spatial translation by identifying the first (and the last) spin in the ring.

To show that the quantity $\langle p|\,\sigma_N^x\Pi^x\,|-p\rangle$ is real we resort to the mirror operator, which relates the states with opposite momentum as $M_N\,|p\rangle = |-p\rangle$, according to Theorem 6. Using this relation and taking into account that M_N is hermitian we get

$$\langle p|\,\sigma_N^x\Pi^x\,|-p\rangle = \langle -p|\,M_N\sigma_N^x\Pi^x M_N\,|p\rangle\ . \tag{C.82}$$

But, as we have said, Π^x commutes with the mirror operator, which together with the property $M_N\sigma_N^x M_N = \sigma_N^x$ gives

$$\langle p|\,\sigma_N^x\Pi^x\,|-p\rangle = \langle -p|\,\sigma_N^x\Pi^x\,|p\rangle = \big(\,\langle p|\,\sigma_N^x\Pi^x\,|-p\rangle\,\big)^*\,, \tag{C.83}$$

where the last equality holds because the operator $\sigma_N^x\Pi^x$ is hermitian. Hence $\langle p|\,\sigma_N^x\Pi^x\,|-p\rangle$ is equal to its conjugate and therefore real. To show that $\langle p|\,\sigma_N^y\Pi^x\,|-p\rangle$ is purely imaginary we can use the same method together with the property that $\sigma_N^y\Pi^x$ is antihermitian, or we can use the relation

$$\Pi^x = (-\imath)^N\Pi^y\Pi^z \tag{C.84}$$

and the eigenstate property $\Pi^z\,|\pm p\rangle = -\,|\pm p\rangle$, which give

$$\langle p|\,\sigma_N^y\Pi^x\,|-p\rangle = -(-\imath)^N\,\langle p|\,\sigma_N^y\Pi^y\,|-p\rangle\,. \tag{C.85}$$

The quantity $\langle p|\,\sigma_N^y\Pi^y\,|-p\rangle$ is real, by the same argument which shows that $\langle p|\,\sigma_N^x\Pi^x\,|-p\rangle$ is real and the factor in front, due to oddity of N, makes the whole quantity imaginary.

Taking these properties into account, we get the following spatial dependence for the magnetizations

$$\langle\sigma_j^x\rangle_{\tilde g} = \cos(2pj-\theta)\,\langle p|\,\sigma_N^x\Pi^x\,|-p\rangle\ , \tag{C.86}$$

$$\langle\sigma_j^y\rangle_{\tilde g} = \cos(2pj-\theta+N\frac{\pi}{2}+\pi)\,\langle p|\,\sigma_N^y\Pi^y\,|-p\rangle\ . \tag{C.87}$$

Inserting the exact value of the momentum (C.13), which is equal to $p = \frac{\pi}{2} + (-1)^{\frac{N+1}{2}}\frac{\pi}{2N}$, we get finally the dependence of the magnetizations on the position in the ring,

$$\langle\sigma_j^\gamma\rangle_{\tilde g} = (-1)^j\cos\left[\pi\frac{j}{N}+\lambda(\gamma,\theta,N)\right]\langle p|\,\sigma_N^\gamma\Pi^\gamma\,|-p\rangle\ , \tag{C.88}$$

where

$$\lambda(\gamma,\theta,N) \equiv \begin{cases}(-1)^{\frac{N-1}{2}}\theta, & \gamma = x\\ (-1)^{\frac{N-1}{2}}\theta+\frac{\pi}{2}, & \gamma = y\end{cases}. \tag{C.89}$$

The magnetization is antiferromagnetic, i.e. staggered, but its magnitude is modulated. Since the number of sites is odd, it is not possible to have every bond aligned antiferromagnetically, but there is necessarily at least a one ferromagnetic one. The magnetization is modulated in such a way to achieve the minimal absolute value at the ferromagnetic bond, thus minimizing the energy. The position of this ferromagnetic bond is determined by the phase θ. The position of the ferromagnetic bond of

the magnetization in the x direction is shifted by half of the ring with the respect to the ferromagnetic bond of the magnetization in the y direction.

C.6.2 Explicit evaluation of the magnetizations on the N-th site

We can evaluate the magnetization on the N-th spin of the lattice exploiting a method similar to the one for the other parameter region, described in section C.5. It consists of expressing the matrix elements $\langle p|\,\sigma_N^\gamma \Pi^x\,|-p\rangle$ in terms of expectation values of $\sigma_N^\gamma \Pi^x$ in a definite Π^z parity state, using the representation of $\sigma_N^\gamma \Pi^x$ in terms of Majorana fermions

$$A_j = \left(\bigotimes_{l=1}^{j-1} \sigma_l^z\right) \otimes \sigma_j^x\,, \quad B_j = \left(\bigotimes_{l=1}^{j-1} \sigma_l^z\right) \otimes \sigma_j^y\,, \tag{C.90}$$

using Wick's theorem [189–192] to express the expectation values as a determinant, and finally evaluating the determinant.

We express $\langle p|\,\sigma_N^\gamma \Pi^x\,|-p\rangle$ in terms of expectation values of $\sigma_N^\gamma \Pi^x$ on ground states living in the odd parity sector of Π^z. A general ground state belonging to the odd parity sector of Π^z can be written as in eq. (C.14) setting $u_3 = u_4 = 0$,

$$|u_1, u_2\rangle \equiv u_1\,|p\rangle + u_2\,|-p\rangle \tag{C.91}$$

It is immediate to see that

$$\langle \sigma_j^\gamma \Pi^x\rangle_{u_1=\frac{1}{\sqrt{2}},u_2=\frac{1}{\sqrt{2}}} - \langle \sigma_j^\gamma \Pi^x\rangle_{u_1=\frac{1}{\sqrt{2}},u_2=-\frac{1}{\sqrt{2}}} = \langle p|\,\sigma_j^\gamma \Pi^x\,|-p\rangle + \langle -p|\,\sigma_j^\gamma \Pi^x\,|p\rangle \tag{C.92}$$

Using the properties of the mirror operator, in the previous section we have shown that $\langle p|\,\sigma_N^x \Pi^x\,|-p\rangle = \langle -p|\,\sigma_N^x \Pi^x\,|p\rangle$, while in an analogous way we have also $\langle p|\,\sigma_N^y \Pi^x\,|-p\rangle = \langle -p|\,\sigma_N^y \Pi^x\,|p\rangle$. Using these relations we get, finally,

$$\langle p|\,\sigma_N^\gamma \Pi^x\,|-p\rangle = \frac{1}{2}\Big(\langle \sigma_N^\gamma \Pi^x\rangle_{u_1=\frac{1}{\sqrt{2}},u_2=\frac{1}{\sqrt{2}}} - \langle \sigma_N^\gamma \Pi^x\rangle_{u_1=\frac{1}{\sqrt{2}},u_2=-\frac{1}{\sqrt{2}}}\Big). \tag{C.93}$$

Now, $\sigma_N^x \Pi^x$ and $\sigma_N^y \Pi^x$, being products of spin operators, can be expressed in terms of Majorana fermions, as

$$\begin{aligned}
\sigma_N^x \Pi^x &= (-1)^{\frac{N-1}{2}} \prod_{l=1}^{\frac{N-1}{2}} (-\imath A_{2l} B_{2l-1}),\\
\sigma_N^y \Pi^x &= -\imath (-1)^{\frac{N-1}{2}} \left(\prod_{l=1}^{\frac{N-1}{2}} (-\imath A_{2l} B_{2l-1})\right) (-\imath A_N B_N)\,.
\end{aligned} \tag{C.94}$$

The expectation values of these operators in a definite z parity ground state can be expressed as a Pfaffian of the matrix of two-point correlators, using Wick's theorem.

To do so, we write the state (C.91) as a vacuum state for fermionic operators, in terms of which the Majorana fermions (C.90) are linear. These fermions are defined by

$$\alpha_p = u_1 a_p^\dagger + u_2 a_{-p}^\dagger, \quad \alpha_{-p} = u_2 a_p - u_1 a_{-p} \tag{C.95}$$

and by $\alpha_q = a_q$ for $q \neq p, -p$. It's easy to check that the operators α_q satisfy fermionic anticommutation relations and annihilate the state $|u_1, u_2\rangle = \alpha_p\,|0^-\rangle$, i.e. that we have $\alpha_q\,|u_1, u_2\rangle = 0$ for $q \in \Gamma^-$. Moreover, since the Majorana fermions in eq. (C.90)

can be written as a linear combination of Bogoliubov fermions $a_q, a_q^\dagger$, they can also be written as a linear combination of fermions $\alpha_q, \alpha_q^\dagger$. In this way, we are able to straightforwardly apply Wick's theorem to evaluate the string operators in eq. (C.94) over the chosen ground state vectors.

The two-point correlators of Majorana fermions are evaluated to be

$$\langle A_j A_l \rangle_{u_1,u_2} = \langle B_j B_l \rangle_{u_1,u_2} = \delta_{jl} - \frac{2\imath}{N}(|u_1|^2 - |u_2|^2)\sin\left[p(j-l)\right], \tag{C.96}$$

$$\begin{aligned} -\imath \langle A_j B_l \rangle_{u_1,u_2} =& \frac{1}{N}\sum_{q\in\Gamma^-} e^{\imath 2\theta_q} e^{-\imath q(j-l)} - \frac{2}{N}\cos\left[p(j-l) - 2\theta_p\right] \\ & - \frac{2}{N}\left(u_1^* u_2\, e^{-\imath p(j+l)} + \text{c.c.}\right), \end{aligned} \tag{C.97}$$

where the Bogoliubov angle θ_q is defined in eq. (C.7).

As a matter of fact, in the evaluation of the matrix elements we encounter only states of the type $|u_1| = |u_2| = 1/\sqrt{2}$, for which the correlators (C.96) vanish for $j \neq l$. This allows us to use the standard approach [91] on the basis of Wick's theorem to express the expectation value of (C.94) as a determinant. For $\langle \sigma_N^y \Pi^x \rangle_{u_1,u_2}$ we have that

$$\langle \sigma_N^y \Pi^x \rangle_{u_1,u_2} = -\imath(-1)^{\frac{N-1}{2}} \det \mathbf{C}\,, \tag{C.98}$$

with the $(N+1)/2 \times (N+1)/2$ correlation matrix $\mathbf{C}$ given by

$$\mathbf{C} = \begin{vmatrix} F(2,1) & F(2,3) & F(2,5) & \cdots & F(2,N-2) & F(2,N) \\ F(4,1) & F(4,3) & F(4,5) & \cdots & F(4,N-2) & F(4,N) \\ \vdots & \vdots & \vdots & \ddots & \vdots & \vdots \\ F(N-1,1) & F(N-1,3) & F(N-1,5) & \cdots & F(N-1,N-2) & F(N-1,N) \\ F(N,1) & F(N,3) & F(N,5) & \cdots & F(N,N-2) & F(N,N) \end{vmatrix}, \tag{C.99}$$

where $F(j,l) = -\imath \langle A_j B_l \rangle_{u_1,u_2}$. On the contrary

$$\langle \sigma_N^x \Pi^x \rangle_{u_1,u_2} = (-1)^{\frac{N-1}{2}} \det \mathbf{C}'\,, \tag{C.100}$$

where the $(N-1)/2 \times (N-1)/2$ correlation matrix $\mathbf{C}'$ is obtained from $\mathbf{C}$ by removing the last row and the last column.

The determinants we encounter have a more complicated form than those for which the standard analytical approach [90] applies, and than those in section C.5, so we have evaluated them numerically. The results are shown in Chapter 4.

C.7 Perturbative analysis

The discovered phenomenology in the quantum XY chain with FBC is captured well also by a simple perturbative analysis around the classical Ising point $\phi = 0$, similar to the one used in [67], that we have done in [1, 2]. In addition, the perturbative analysis provides analytical expressions for the matrix elements f_x discussed in Chapter 4, in the limit $\phi \to 0^+$.

At the classical Ising point $\phi = 0$ the model is diagonal in the basis where σ_j^x are diagonal. The ground state manifold is $2N$-fold degenerate and consists of kink states $|j\rangle$ and $\Pi^z |j\rangle$, for $j = 1, 2, ..., N$. Here, the kink state $|j\rangle$ is defined as the state

$$|j\rangle = |..., 1, -1, 1, 1, -1, 1, ...\rangle\,, \tag{C.101}$$

with the ferromagnetic bond $\sigma_j^x = \sigma_{j+1}^x = 1$ between sites j and $j+1$, and antiferromagnetic bonds between all other adjacent sites. The kink state $\Pi^z |j\rangle$, with all spins reversed, has the ferromagnetic bond $\sigma_j^x = \sigma_{j+1}^x = -1$ and all the other bonds antiferromagnetic. The parity of the states $|j\rangle$ is $\Pi^x = (-1)^{(N-1)/2}$, while $\Pi^z |j\rangle$ have, of course, the opposite parity. The higher energy states are separated by a finite gap and can be neglected in perturbation theory.

For small nonzero ϕ, the term $\sum_j \sigma_j^y \sigma_{j+1}^y$ kicks in, lifting the $2N$-fold ground state degeneracy. The corresponding eigenstates and the correction to the energies are found by diagonalizing the perturbation in the ground space. The excited states at $\phi = 0$ are separated by a finite gap and we neglect them in this perturbative approach. Since the matrix elements of the perturbation between two different Π^x sectors vanish (because the $\sigma_j^y \sigma_{j+1}^y$ terms still commute with all the parities Π^α), we can focus on each sector separately. In the $\Pi^x = (-1)^{(N-1)/2}$ sector they read

$$\langle l| \sum_{j=1}^{N} \sigma_j^y \sigma_{j+1}^y |k\rangle = \delta_{l-k+2 \bmod N,0} + \delta_{l-k-2 \bmod N,0} \,. \tag{C.102}$$

It follows that the perturbation in the subspace spanned by $|j\rangle$, $j = 1, ..., N$, is a cyclic matrix

$$\sum_{j=1}^{N} \sigma_j^y \sigma_{j+1}^y = \begin{pmatrix} c_0 & c_{N-1} & \dots & c_2 & c_1 \\ c_1 & c_0 & \dots & c_3 & c_2 \\ \vdots & \vdots & \ddots & \vdots & \vdots \\ c_{N-2} & c_{N-1} & \dots & c_0 & c_{N-1} \\ c_{N-1} & c_{N-2} & \dots & c_1 & c_0 \end{pmatrix}, \tag{C.103}$$

with

$$c_j = \delta_{j,2} + \delta_{j,N-2} \,. \tag{C.104}$$

Diagonalizing the cyclic matrix [204] we find the energies

$$E_q = -(N-2)\cos\phi + 2\sin\phi\cos(2q), \quad q \in \Gamma^-, \tag{C.105}$$

corresponding to the states

$$|s_q\rangle = \frac{1}{\sqrt{N}} \sum_{j=1}^{N} e^{\imath q j} |j\rangle \tag{C.106}$$

Clearly, the states with opposite Π^x corresponding to the same energies can be constructed as $\Pi^z |s_q\rangle$. The energies of the exact solution reduce, of course, to those of perturbative calculation when ϕ is close to 0.

It's easy to see that for $\phi < 0$ the energy is minimized by $q = 0$, while for $\phi > 0$ it is by $q = p$, where p is given by eq. (C.13), as in the exact solution. Evaluating the derivative of the ground state energy E_g we find a discontinuity at $\phi = 0$,

$$\left.\frac{dE_g}{d\phi}\right|_{\phi\to 0^-} - \left.\frac{dE_g}{d\phi}\right|_{\phi\to 0^+} = 2\Big(1 + \cos\frac{\pi}{N}\Big), \tag{C.107}$$

which goes to a constant non-zero value in the thermodynamic limit $N \to \infty$.

We can identify the states from the perturbation theory with those from the exact solution, in the limit $\phi \to 0$, by looking at the eigenstates of various operators. The translation operator shifts the kink as $T|j\rangle = |j-1\rangle$, from which it follows that the

states $|s_q\rangle$ are eigenstates of T with the eigenvalue $e^{\imath q}$. The mirror operator acts on the kink states as $M_N|j\rangle = |-j-1\rangle$, and therefore

$$M_N|s_q\rangle = e^{-\imath q}|s_{-q}\rangle \ . \tag{C.108}$$

Knowing that the eigenstates $|q\rangle = a_q^\dagger|0^-\rangle$ from the exact solution have parity $\Pi^z = -1$, are eigenstates of T with the eigenvalue $e^{\imath q}$ and that under mirroring behave as $M_N|q\rangle = |-q\rangle$, we can make the identification

$$|q\rangle = \frac{1-\Pi^z}{\sqrt{2}}|s_q\rangle \ , \quad |-q\rangle = \frac{1-\Pi^z}{\sqrt{2}}e^{-\imath q}|s_{-q}\rangle \ , \tag{C.109}$$

up to an irrelevant phase factor which is the same for the two states.

For $\phi < 0$ the energy is minimized by $q = 0$ and thus the ground state manifold is two-fold degenerate. From the identification (C.109) we have that the states in eq. (C.12) from the exact solution, in the limit $\phi \to 0^-$, are equal (up to a phase factor) to

$$|g^-\rangle = \frac{1}{\sqrt{2}}(1-\Pi^z)|s_{q=0}\rangle \, , \quad |g^+\rangle = \Pi^x|g^-\rangle \, . \tag{C.110}$$

The magnetization is determined by the element $\langle s_0|\sigma_j^x|s_0\rangle = \langle s_0|\sigma_N^x|s_0\rangle$. From the property of the kink states

$$\langle j|\sigma_N^x|j\rangle = \begin{cases} (-1)^j, & j = 1,2,...,N-1 \\ 1, & j = N \end{cases} \ , \tag{C.111}$$

that follows from their definition, we find

$$\langle s_{q=0}|\sigma_N^x|s_{q=0}\rangle = \frac{1}{N}\sum_{j=1}^{N}\langle j|\sigma_N^x|j\rangle = \frac{1}{N}. \tag{C.112}$$

It follows that in the generic ground state eq. (C.45) the magnetization is equal to

$$m_x(j) = (-1)^{(N-1)/2}\cos(\psi)\sin(2\theta)\frac{1}{N}, \tag{C.113}$$

describing mesoscopic ferromagnetic order. The two-point correlator can be computed, as in Appendix A, using the generalization of (C.111), given by (A.11). We get

$$\langle g^-|\sigma_j^x\sigma_{j+r}^x|g^-\rangle = (-1)^r\left(1-\frac{2r}{N}\right), \tag{C.114}$$

in agreement with the exact solution.

For $\phi > 0$ the energy is minimized by $q = \pm p$, where p is given by eq. (C.13) so the ground state manifold is four fold-degenerate. The magnetization in a generic ground state (C.14) is determined by the matrix elements $\langle p|\sigma_j^x\Pi^x|p\rangle$ and $\langle p|\sigma_j^x\Pi^x|-p\rangle$. While for any $q \in \Gamma^-$ we have, generalizing (C.112),

$$\langle q|\sigma_N^x\Pi^x|q\rangle = (-1)^{\frac{N-1}{2}}\frac{1}{N}, \tag{C.115}$$

where the factor $(-1)^{(N-1)/2}$ stems from the parity of the states $|s_q\rangle$, the matrix elements of the type $\langle q|\,\sigma_N^x\Pi^x\,|-q\rangle$ can have a different behavior. From the identification (C.109) we have

$$\langle q|\,\sigma_N^x\Pi^x\,|-q\rangle = (-1)^{\frac{N-1}{2}} e^{-\imath q}\,\langle s_q|\,\sigma_j^x\,|s_{-q}\rangle\ . \tag{C.116}$$

Using the definition of the states on the right we get

$$\langle q|\,\sigma_N^x\Pi^x\,|-q\rangle = (-1)^{\frac{N-1}{2}}\frac{1}{N}\sum_{j=1}^{N} e^{-\imath 2qj}\,\langle j|\,\sigma_N^x\,|j\rangle\ , \tag{C.117}$$

which can be evaluated using (C.111). We end up with

$$\langle q|\,\sigma_N^x\Pi^x\,|-q\rangle = (-1)^{\frac{N-1}{2}}\frac{1}{N\cos q}\ . \tag{C.118}$$

The matrix element for the ground state momentum $p = \pi/2 + (-1)^{(N+1)/2}\pi/2N$ becomes

$$\langle p|\,\sigma_N^x\Pi^x\,|-p\rangle = \frac{1}{N\sin\frac{\pi}{2N}}\ , \tag{C.119}$$

and in the limit $\phi \to 0^+$ determines the maximum value the magnetization achieves over the ring in the ground state $|\tilde{g}\rangle$, defined in eq. (C.79). For large N it becomes

$$\langle p|\,\sigma_N^x\Pi^x\,|-p\rangle = \frac{2}{\pi} + \frac{\pi}{12N^2} + O(N^{-4})\ , \tag{C.120}$$

which approaches quadratically the value $2/\pi \approx 0.64$ in the thermodynamic limit.

Appendix D

XY Chain with Bond Defects: Methods Details

This is the appendix for Chapter 5, based on the appendix in [4].

D.1 Numerical procedure

To diagonalize the Hamiltonian in eq. (5.1) we resort to the Jordan-Wigner transformation [56, 91, 149], that maps spin operators into fermionic ones

$$c_j = \left(\bigotimes_{k=1}^{j-1} \sigma_k^z\right) \otimes \sigma_j^+, \qquad c_j^\dagger = \left(\bigotimes_{k=1}^{j-1} \sigma_k^z\right) \otimes \sigma_j^-, \tag{D.1}$$

where $\sigma_j^\pm = (\sigma_j^x \pm \imath \sigma_j^y)/2$ are the Pauli ladder operators. Through eq. (D.1) the Hamiltonian in eq. (5.1) can be recast into the form

$$\begin{aligned} H = &\sum_{j=1}^{N-1} \Big[(\cos\phi - \sin\phi)\, c_j c_{j+1} - (\cos\phi + \sin\phi)\, c_j c_{j+1}^\dagger \Big] + \\ &- \Pi^z \Big[\big(\cos(\phi+\delta_x) - \sin(\phi+\delta_y)\big)\, c_N c_1 - \big(\cos(\phi+\delta_x) + \sin(\phi+\delta_y)\big)\, c_N c_1^\dagger \Big] + \text{h.c.} \end{aligned} \tag{D.2}$$

Since $[H, \Pi^z] = 0$ we can identify two different disconnected sectors corresponding respectively to the values $\Pi^z = \pm 1$. In the following we focus on the Hamiltonian of the odd sector, i.e. we fix $\Pi^z = -1$, since once the ground state $|g^-\rangle$ with $\Pi^z = -1$ is obtained, the other one with the same energy in the even sector is $\Pi^x |g^-\rangle$.

There, the Hamiltonian is quadratic in the fermionic operators, i.e. it can be rewritten as

$$H = \sum_{j=1}^{N-1} \left[c_j^\dagger S_{j,j+1} c_{j+1} + \frac{1}{2} \left(c_j^\dagger T_{j,j+1} c_{j+1}^\dagger + \text{h.c.} \right) \right], \tag{D.3}$$

where the matrices $\mathbf{S}^\dagger = \mathbf{S}$ and $\mathbf{T}^\dagger = -\mathbf{T}$ can be easily obtained by inspection from eq. (D.2). Following the standard approach [91] we introduce the linear transformation

$$\eta_k = \sum_i \left[\frac{\Phi_{ki} + \Psi_{ki}}{2} c_i + \frac{\Phi_{ki} - \Psi_{ki}}{2} c_i^\dagger \right], \tag{D.4}$$

$$\eta_k^\dagger = \sum_i \left[\frac{\Phi_{ki} + \Psi_{ki}}{2} c_i^\dagger + \frac{\Phi_{ki} - \Psi_{ki}}{2} c_i \right], \tag{D.5}$$

where the vectors Φ_k and Ψ_k are given by the solution of the problem

$$\Phi_k(\mathbf{S}-\mathbf{T})(\mathbf{S}+\mathbf{T}) = \Lambda_k^2\Phi_k, \tag{D.6}$$
$$\Phi_k(\mathbf{S}-\mathbf{T}) = \Lambda_k\Psi_k. \tag{D.7}$$

The Hamiltonian in eq. (D.3) can then be reduced to the form

$$H = \sum_k \Lambda_k \eta_k^\dagger \eta_k + \frac{1}{2}\left[\mathrm{Tr}\mathbf{S} - \sum_k \Lambda_k\right]. \tag{D.8}$$

For definiteness we take the energies Λ_k to be all positive.

At variance with the unperturbed model, in which the GS degeneracy depends on the type of interaction, tuned by the ϕ parameter, the GS of the perturbed one is two-fold degenerate, due to the breaking of the translational invariance of the system. The most general GS can be written in the form

$$|g\rangle = \left(\cos\theta + e^{\imath\psi}\sin\theta\,\Pi^x\right)|g^-\rangle\,, \tag{D.9}$$

where $|g^-\rangle$ is the (unique) GS of the system in the odd parity sector, and θ and ψ are real numbers.

The magnetization for the ground state in eq. (D.9) is given by

$$\langle g|\,\sigma_j^x\,|g\rangle = \cos\psi\sin(2\theta)\,\langle g^-|\,\sigma_j^x\Pi^x\,|g^-\rangle\,, \tag{D.10}$$

since the matrix elements of σ_j^x between different Π^z sectors vanish. Of interest is the maximal magnetization that can be obtained on the ground state manifold. It is achieved in the states with definite Π^x parity. This is

$$m_x(j) = \langle g^-|\,\sigma_j^x\Pi^x\,|g^-\rangle \tag{D.11}$$

for $\Pi^x = 1$ (achieved by $\psi = 0$, $\theta = \pi/4$) and

$$m_x(j) = -\langle g^-|\,\sigma_j^x\Pi^x\,|g^-\rangle \tag{D.12}$$

for $\Pi^x = -1$ (achieved by $\psi = 0$, $\theta = -\pi/4$). These are the magnetizations that we discuss in Chapter 5.

Eq. (D.11) can be evaluated expressing the operators on the r.h.s. in terms of Majorana fermions

$$A_j = c_j^\dagger + c_j = \left(\bigotimes_{l=1}^{j-1}\sigma_l^z\right)\otimes\sigma_j^x, \tag{D.13}$$
$$B_j = \imath(c_j^\dagger - c_j) = \left(\bigotimes_{l=1}^{j-1}\sigma_l^z\right)\otimes\sigma_j^y. \tag{D.14}$$

Furthermore, we can resort to Wick theorem to express the expectation values in eq. (D.11) in terms of the contractions $F(j,l) = -\imath\,\langle g^-|\,A_jB_l\,|g^-\rangle$.

Let us denote the vacuum state for fermions η_j by $|0^-\rangle$, i.e. we have $\eta_j\,|0^-\rangle = 0$ for $j = 1, 2, \ldots N$. We numerically verify, by direct computation, that the parity of the state $|0^-\rangle$ is $\Pi^z = 1$. On the other hand, the Hamiltonian without defects is also written in terms of free fermions with positive energy and the vacuum $|0^-\rangle$ has positive parity by construction there (see Appendix C.2).

Assuming the eigenvalue of the matrix appearing on the l.h.s. of eq. (D.6) are labeled in descending order, the GS is then $|g^-\rangle = \eta_N^\dagger |0^-\rangle$. From this identification a straightforward calculation gives

$$F(j,l) = \sum_{k=1}^{N-1} \Psi_{kj}\Phi_{kl}. \tag{D.15}$$

D.2 Perturbation theory

In this section we study perturbatively the Hamiltonian in eq. (5.1) with $\delta_y = 0$. Let us for the purpose of perturbation theory write the Hamiltonian as

$$H = \cos\phi \sum_{j=1}^{N} \sigma_j^x \sigma_{j+1}^x + \sin\phi \sum_{j=1}^{N} \sigma_j^y \sigma_{j+1}^y + \zeta \sigma_N^x \sigma_1^x, \tag{D.16}$$

so that $\zeta > 0$ corresponds to an antiferromagnetic defect, while $\zeta < 0$ is a ferromagnetic defect. The case $\zeta = 0$, of course, corresponds to FBC.

First, in section D.2.1 we are going to make the perturbation theory close to the classical point $\phi = 0$, which explains well our numerical results. Then, in section D.2.2 using the perturbation theory around $\zeta = 0$ we are going to find which of the four-fold degenerate ground states of the region $\phi \in (0, \pi/4)$, present without the defect, are selected by taking the limit of the small antiferromagnetic defect $\zeta \to 0^+$, which also explains well the order we have found numerically.

D.2.1 Perturbation theory around $\phi = 0$

The perturbation theory around $\phi = 0$ without the defect (for $\zeta = 0$) has already been done in Appendix C.7. Without the defect, exactly at the classical point $\phi = 0$ the ground state manifold is $2N$-fold degenerate and consists of kink states

$$|j\rangle = |..., 1, -1, 1, 1, -1, 1, ...\rangle\,, \tag{D.17}$$

for $j = 1, 2 \ldots N$, which have one ferromagnetic bond $\sigma_j^x = \sigma_{j+1}^x = 1$ and antiferromagnetic bonds between other adjacent sites, and the kink states obtained from $|j\rangle$ by reversing all spins, which have $\sigma_j^x = \sigma_{j+1}^x = -1$ and all the other bonds antiferromagnetic. The latter can be written as $\Pi^z |j\rangle$. Note that the states $|j\rangle$ have the parity $\Pi^x = (-1)^{(N-1)/2}$, while $\Pi^z |j\rangle$ have, of course, the opposite parity. By turning on $\phi \neq 0$, the term proportional to $\sum_j \sigma_j^y \sigma_{j+1}^y$ kicks in and the $2N$-fold degenerate ground state manifold splits, resulting in the two-fold ground state degeneracy for $\phi < 0$ and four fold for $\phi > 0$.

The new ground states and the corresponding energies are found by diagonalizing the perturbation in the basis of the kink states, while the other states are separated by a finite energy gap and can be neglected. The procedure is similar also with a defect, but not all the states will enter into the perturbation theory, because the defect will induce an energy gap between the kink states. Namely, the states which have a ferromagnetic bond between the sites $j = N$ and $j = 1$ have a different energy from the others. At $\phi = 0$, the states $|N\rangle$ and $\Pi^z |N\rangle$ have the energy

$$E_0 = -(N-2) + \zeta, \tag{D.18}$$

while the other kink states have the energy

$$E_0 = -(N-2) - \zeta. \tag{D.19}$$

Thus, for $\zeta < 0$ the ground states at $\phi = 0$ are only $|N\rangle$ and $\Pi^z |N\rangle$. The other kink states are separated by a gap 2ζ and can be neglected, so the perturbation theory is very simple. In fact, the perturbation, proportional to $\sum_j \sigma_j^y \sigma_{j+1}^y$, does not mix different Π^x sectors and is already diagonal in the basis $|N\rangle, \Pi^z |N\rangle$.

We conclude that for $\zeta < 0$ and small ϕ the ground states are (approximately) the states $|N\rangle$ and $\Pi^z |N\rangle$, with magnetization

$$\langle N| \sigma_j^x |N\rangle = (-1)^{j+1} \tag{D.20}$$

and the one with all spins reversed, respectively. This result explains well the magnetization at Fig. 5.2 in the bulk of the system, far from the defects.

For $\zeta > 0$ the ground state manifold at $\phi = 0$ is $2(N-1)$-fold degenerate. It consists of the states $|j\rangle$ and $\Pi^z |j\rangle$ for $j = 1, 2, \ldots N-1$. Turning on the perturbation the degeneracy splits. To get the new ground states and the corresponding energies we diagonalize the perturbation in the aforementioned states.

Since the perturbation, proportional to $\sum_j \sigma_j^y \sigma_{j+1}^y$, does not mix different Π^x sectors we can focus on just the states $|j\rangle$, for $j = 1, 2, \ldots N-1$. If we include also the state $|N\rangle$, the perturbation is an $N \times N$ cyclic matrix with the elements

$$\langle k| \sum_{j=1}^{N} \sigma_j^y \sigma_{j+1}^y |l\rangle = \delta_{(l-k+2) \bmod N,0} + \delta_{(l-k-2) \bmod N,0}. \tag{D.21}$$

Without the state $|N\rangle$ the perturbation is a matrix obtained by removing the last row and the last column of the cyclic matrix. It reads

$$\sum_{j=1}^{N} \sigma_j^y \sigma_{j+1}^y = \begin{pmatrix} 0 & 0 & 1 & 0 & \ldots & 0 & 0 & 1 \\ 0 & 0 & 0 & 1 & \ldots & 0 & 0 & 0 \\ 1 & 0 & 0 & 0 & \ldots & 0 & 0 & 0 \\ 0 & 1 & 0 & 0 & \ldots & 0 & 0 & 0 \\ \vdots & \vdots & \vdots & \vdots & & \vdots & \vdots & \vdots \\ 1 & 0 & 0 & 0 & \ldots & 1 & 0 & 0 \end{pmatrix}. \tag{D.22}$$

A similar matrix, obtained by deleting the last row and the last column of the $N \times N$ cyclic matrix with the elements

$$\delta_{(l-k+1) \bmod N,0} + \delta_{(l-k-1) \bmod N,0} \tag{D.23}$$

instead of eq. (D.21) was diagonalized analytically (as a special case) in [69], by writing a recursion relation in N for the characteristic polynomial. We diagonalize the matrix in (D.22) in a less dignified way. Based on the similarity with the aforementioned matrix of [69] we simply guess the eigenstates. As is easy to check, the normalized eigenstates of the matrix in eq. (D.22) are

$$|a_s\rangle = \sqrt{\frac{2}{N}} \sum_{j=1}^{N-1} (-1)^{sj} \sin\left(\frac{s\pi}{N} j\right) |j\rangle, \tag{D.24}$$

with the eigenvalues $a_s = 2\cos\left(\frac{2\pi s}{N}\right)$, and

$$|b_s\rangle = \begin{cases} \sqrt{\frac{2}{N}} \sum_{j=1}^{N-1} (-1)^{sj+\lfloor \frac{j-1}{2} \rfloor} \sin\left(\frac{s\pi}{N} j\right) |j\rangle\,, & N \bmod 4 = 1 \\ \sqrt{\frac{2}{N}} \sum_{j=1}^{N-1} (-1)^{sj+\lfloor \frac{j}{2} \rfloor} \sin\left(\frac{s\pi}{N} j\right) |j\rangle\,, & N \bmod 4 = 3 \end{cases} \tag{D.25}$$

with the eigenvalues $b_s = -2\cos\left(\frac{2\pi s}{N}\right)$. Here s takes values from the set $\{1, 2, \ldots (N-1)/2\}$. It follows that the energies associated to the eigenstates in eq. (D.24) and (D.25) are respectively

$$\begin{aligned} E_{a,s} &= -(N-2)\cos\phi - \zeta + 2\sin\phi\cos\left(\frac{2\pi s}{N}\right), \\ E_{b,s} &= -(N-2)\cos\phi - \zeta - 2\sin\phi\cos\left(\frac{2\pi s}{N}\right). \end{aligned} \tag{D.26}$$

The parity of the states in eq. (D.24) and (D.25) is equal to $\Pi^x = (-1)^{(N-1)/2}$. The states of the opposite parity are constructed, of course, by applying the Π^z operator.

Thus, the $2N$-fold degenerate ground state manifold splits, for small ϕ, into a band of states, with a two-fold degenerate ground state manifold and an energy gap between the states that closes as $1/N^2$. For $\phi > 0$ the ground states are $|g\rangle = |a_s\rangle$ for $s = (N-1)/2$ and $\Pi^z |g\rangle$, while for $\phi < 0$ the ground states are $|g\rangle = |b_s\rangle$ for $s = (N-1)/2$ and $\Pi^z |g\rangle$. After a bit of straightforward algebra, using

$$\langle l | \sigma_j^x | l \rangle = \begin{cases} (-1)^{l+j+1}, & l = 1, 2 \ldots, j-1 \\ (-1)^{l+j}, & l = j, j+1, \ldots N \end{cases}, \tag{D.27}$$

we find that the magnetization in the ground state $|g\rangle$ is, for both signs of ϕ,

$$\langle g | \sigma_j^x | g \rangle = \frac{(-1)^j \sin\left[\frac{\pi}{N}\left(j - \frac{1}{2}\right)\right]}{N \sin\left(\frac{\pi}{2N}\right)} + \frac{1}{N}. \tag{D.28}$$

In the ground state $\Pi^z |g\rangle$ the magnetization acquires, of course, an additional minus sign. The obtained order is in agreement with the numerical results on the magnetization in the presence of an antiferromagnetic defect, presented in Fig. 5.2. Note that, for large N, the magnetization in eq. (D.28) is approximated by

$$\langle \sigma_j^x \rangle_g = (-1)^j \frac{2}{\pi} \sin\left(\frac{\pi}{N} j\right), \tag{D.29}$$

which is the incommensurate AFM order present for $\phi \in (0, \pi/4)$ in the absence of the defect (see Chapter 4). The magnetization is modulated in such a way to achieve zero value where the defect is placed.

D.2.2 Perturbation theory around $\zeta = 0$

In this section by using perturbation theory around $\zeta = 0$ we find which of the four-fold degenerate ground states of the region $\phi \in (0, \pi/4)$ are selected in the limit of a small antiferromagnetic defect $\zeta \to 0^+$. For this task we treat the term $\zeta \sigma_N^x \sigma_1^x$ in eq. (D.16) as a perturbation. The model with $\zeta = 0$ has been solved in details in Chapter 4 and Appendix C, and we use the same notation. Thus, while before we

used the kink states as basis for the perturbation, here we employ the four ground states states determined in Chapter 4.

For $\zeta = 0$ the ground state manifold is spanned by states $|p\rangle, |-p\rangle, \Pi^x |p\rangle, \Pi^x |-p\rangle$ which are simultaneous eigenstates of the Hamiltonian in eq. (D.16), with $\zeta = 0$, the parity operator Π^z (with eigenvalues, respectively $\Pi^z = -1, -1, 1, 1$) and the translation operator T (with eigenvalues, respectively $T = e^{\imath p}, e^{-\imath p}, e^{\imath p}, e^{-\imath p}$). Here $p = \pi/2 + (-1)^{(N+1)/2}\pi/2N$ is the momentum of the states. Above the ground states there is a band of states, with the energy gap closing as $1/N^2$.

To find which ground state vectors are selected in the limit of a small defect we diagonalize the perturbation $\zeta\sigma_N^x\sigma_1^x$ in the basis of the four ground states above. We are going to neglect all the excited states of the model, including those belonging to the lowest-energy band. This is not justified in general, because of the gapless nature of the system, but the procedure is going to yield the results in agreement with numerics, as we comment in the end. Since the perturbation does not mix different Π^x sectors it is sufficient to focus on the subspace spanned by $|p\rangle, |-p\rangle$. Thus, we need to compute and diagonalize the matrix

$$\sigma_N^x\sigma_1^x = \begin{pmatrix} \langle p| \sigma_N^x\sigma_1^x |p\rangle & \langle p| \sigma_N^x\sigma_1^x |-p\rangle \\ \langle -p| \sigma_N^x\sigma_1^x |p\rangle & \langle -p| \sigma_N^x\sigma_1^x |-p\rangle \end{pmatrix}. \tag{D.30}$$

The elements of the perturbation matrix are computed using the Majorana fermions representation of the spin operators, in terms of which

$$\sigma_N^x\sigma_1^x = \Pi^z(-\imath A_1 B_N), \tag{D.31}$$

and using the representation of the Majorana fermions in terms of Bogoliubov fermions a_q, that can be obtained from the exact solution presented in Appendix C.2. We have

$$\begin{aligned} A_j &= \frac{1}{\sqrt{N}} \sum_{q\in\Gamma^-} (a_q^\dagger + a_{-q}) e^{\imath\theta_q} e^{-\imath qj}, \\ B_j &= \frac{1}{\sqrt{N}} \sum_{q\in\Gamma^-} \imath(a_q^\dagger - a_{-q}) e^{-\imath\theta_q} e^{-\imath qj}, \end{aligned} \tag{D.32}$$

where $\Gamma^- = \{2\pi k/N : k = 0, 1, \ldots N-1\}$, and the Bogoliubov angle θ_q is defined by (C.7) for $q \neq 0$ and $\theta_0 = 0$. In terms of Bogoliubov fermions the ground states are given by $|\pm p\rangle = a_{\pm p}^\dagger |0^-\rangle$, where $|0^-\rangle$ is the vacuum state, satisfying $a_q |0^-\rangle = 0$, $q \in \Gamma^-$. Using eq. (D.31), (D.32) and this ground states representation we get the matrix elements of the perturbation. For $\langle p| \sigma_N^x\sigma_1^x |p\rangle = \langle -p| \sigma_N^x\sigma_1^x |-p\rangle$ we recover

$$\langle p| \sigma_N^x\sigma_1^x |p\rangle = \frac{2}{N}\cos(2\theta_p - p) - \frac{1}{N}\sum_{q\in\Gamma^-} e^{\imath(2\theta_q - q)} \tag{D.33}$$

while for $\langle p| \sigma_N^x\sigma_1^x |-p\rangle$

$$\langle p| \sigma_N^x\sigma_1^x |-p\rangle = \frac{2}{N} e^{-\imath p}. \tag{D.34}$$

Then, diagonalizing the perturbation matrix we obtain the eigenstates

$$|\xi_\pm\rangle = \frac{1}{\sqrt{2}}(|p\rangle \pm e^{\imath p} |-p\rangle), \tag{D.35}$$

which are also even/odd under the mirror symmetry crossing the site $\frac{N+1}{2}$ (see Appendix C.4). These states have energies

$$E_\pm = E_0 - \zeta\frac{1}{N}\sum_{q\in\Gamma^-} e^{\imath(2\theta_q - q)} + \zeta\frac{2}{N}\cos(2\theta_p - p) \pm \zeta\frac{2}{N}, \tag{D.36}$$

where E_0 is the ground state energy of the unperturbed model. For the antiferromagnetic defect $\zeta > 0$ the state $|g^-\rangle \equiv |\xi_-\rangle$ is lower in energy and, therefore, (approximately) the new ground state, belonging to $\Pi^z = -1$ sector. Of course, the ground state belonging to $\Pi^z = +1$ sector is $|g^+\rangle = \Pi^x |\xi_-\rangle$.

The magnetization can be computed using the same techniques as in Chapter 4, that employ the translation operator. Denoting $|g\rangle = \frac{1}{\sqrt{2}}(1+\Pi^x)|g^-\rangle$, we get

$$\begin{aligned}\langle\sigma_j^x\rangle_g &= \langle g^-|\,\sigma_j^x\Pi^x\,|g^-\rangle \\ &= (-1)^j(-1)^{\frac{N-1}{2}}\sin\left[\frac{\pi}{N}\left(j-\frac{1}{2}\right)\right]\langle p|\,\sigma_N^x\Pi^x\,|-p\rangle + \langle p|\,\sigma_N^x\Pi^x\,|p\rangle\,,\end{aligned} \tag{D.37}$$

where we have used $\langle p|\,\sigma_j^x\Pi^x\,|-p\rangle = e^{-\imath 2pj}\langle p|\,\sigma_N^x\Pi^x\,|-p\rangle$ and $\langle p|\,\sigma_N^x\Pi^x\,|-p\rangle = \langle -p|\,\sigma_N^x\Pi^x\,|p\rangle$ from Chapter 4 and Appendix C.6.1. The matrix elements encountered in this expression have also been computed in Chapter 4. It has been found numerically that in the thermodynamic limit $N\to\infty$ we have

$$\langle p|\,\sigma_N^x\Pi^x\,|-p\rangle = \frac{2}{\pi}(1-\tan^2\phi)^{1/4}, \tag{D.38}$$

$$\langle p|\,\sigma_N^x\Pi^x\,|p\rangle = 0, \tag{D.39}$$

which gives the magnetization

$$\langle\sigma_j^x\rangle_g = \frac{2(-1)^{\frac{N-1}{2}+j}}{\pi}(1-\tan^2\phi)^{\frac{1}{4}}\sin\left[\frac{\pi}{N}\left(j-\frac{1}{2}\right)\right] \tag{D.40}$$

The obtained magnetization generalizes eq. (D.29) to the whole region $\phi\in(0,\pi/4)$ (the factor $(-1)^{(N-1)/2}$ of difference arises because of the different parities of the involved states) and describes well our numerical results. Note that, since the states in eq. (D.35) are eigenstates of the mirror symmetry across the site $\frac{N+1}{2}$, the magnetization pattern they generate must be even under such transformation, a property present in that is in eq. (D.40) and (D.28), but not in eq. (D.29).

Since we have performed two different perturbation theories, we can check their agreement in the regime where both applies and at finite sizes. From Appendix C.7 we know that in the limit $\phi\to 0^+$ we have

$$\langle p|\,\sigma_N^x\Pi^x\,|-p\rangle = \frac{1}{N\sin\left(\frac{\pi}{2N}\right)}, \tag{D.41}$$

$$\langle p|\,\sigma_N^x\Pi^x\,|p\rangle = (-1)^{\frac{N-1}{2}}\frac{1}{N}. \tag{D.42}$$

Sticking this into eq. (D.37) gives us exactly eq. (D.28), up to factor $(-1)^{(N-1)/2}$ that arises from the parities of the involved states. The two perturbation theories are, thus, in agreement.

The perturbation theory done in this section describes well our numerical results in the region $\phi\in(0,\pi/4)$ in the case of an antiferromagnetic defect and shows to

which ground states out of the four-fold degenerate manifold the discovered order corresponds. The same perturbation theory would not be successful in describing the order in all cases of ϕ and ζ. The reason is that due to the gapless nature of the system it is not justified to neglect the low-lying states of the model in the perturbation theory, so the procedure does not have to give the right results in general.

Appendix E

Matrix Elements of Local Operators Between Kink States

In this appendix we prove theorems 1 and 2 from Chapter 6, on matrix elements of local operators between translationally invariant states formed from states with one or more kinks. This appendix is based on [6].

E.1 Proof of Theorem 1

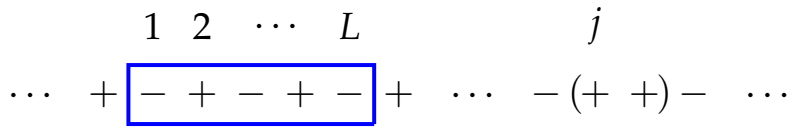

FIGURE E.1: Graphical representation of a kink state $|j\rangle$, where the kink is far on the right. Away from the kink, there is the standard antiferromagnetic order. Let the blue rectangle represent the portion of the lattice where A has the support. Flipping any state in the rectangle will necessarily create a second kink.

For any $A = \sigma_1^{\alpha_1}\sigma_2^{\alpha_2}\dots\sigma_L^{\alpha_L}$ we have

$$\begin{aligned}\langle g_1|\, A\, |g_2\rangle =& u_1^* u_2 \langle s_{p_1}|\, A\, |s_{p_2}\rangle + u_1^* v_2 \langle s_{p_1}|\, A\Pi^z\, |s_{p_2}\rangle \\ &+ v_1^* u_2 \langle s_{p_1}|\, \Pi^z A\, |s_{p_2}\rangle + v_1^* v_2 \langle s_{p_1}|\, \Pi^z A\Pi^z\, |s_{p_2}\rangle .\end{aligned} \tag{E.1}$$

Now, since the kink states $|j\rangle$ are eigenstates of Π^x, with the eigenvalue $(-1)^{(N-1)/2}$, the states $|s_p\rangle$ are also eigenstates of Π^x, with the same eigenvalue. From this fact and the property that A either commutes or anticommutes with Π^x we have that two out of four terms in (E.1) necessarily vanish. If A commutes with Π^x ($[A, \Pi^x] = 0$) then the second and the third term in (E.1) vanish. Using the Cauchy-Schwarz inequality we get

$$|\langle g_1|\, A\, |g_2\rangle| \leq |\langle s_{p_1}|\, A\, |s_{p_2}\rangle|. \tag{E.2}$$

Similarly, if A anticommutes with Π^x ($\{A, \Pi^x\} = 0$) then the first and the fourth term vanish and we have

$$|\langle g_1|\, A\, |g_2\rangle| \leq |\langle s_{p_1}|\, A\Pi^z\, |s_{p_2}\rangle|. \tag{E.3}$$

Thus we focus our analysis on elements $\langle s_{p_1}| A |s_{p_2}\rangle$ and $\langle s_{p_1}| A\Pi^z |s_{p_2}\rangle$. In terms of kink states they read

$$\langle s_{p_1}| A |s_{p_2}\rangle = \frac{1}{N}\sum_{j,l=1}^{N} e^{-\imath(p_1 j - p_2 l)} \langle j| A |l\rangle , \tag{E.4}$$

$$\langle s_{p_1}| A\Pi^z |s_{p_2}\rangle = \frac{1}{N}\sum_{j,l=1}^{N} e^{-\imath(p_1 j - p_2 l)} \langle j| A\Pi^z |l\rangle . \tag{E.5}$$

Case a): In case a), A commutes with Π^x so (E.2) holds. Moreover, A acts only as a phase factor on the kink states, so $\langle j| A |l\rangle = 0$ for $j \neq l$. Since far from the kink we have simply staggered antiferromagnetic order (see Figure E.1) we conclude that for all $j \geq L$ we have

$$\langle j| A |j\rangle = c(-1)^j \quad \text{for some constant } c \in \{-1, 1\}. \tag{E.6}$$

Putting this into (E.4) we get

$$\langle s_{p_1}| A |s_{p_2}\rangle = \frac{c}{N}\sum_{j=1}^{N}(-1)^j e^{-\imath(p_1-p_2)j} + \xi_N, \tag{E.7}$$

where ξ_N is a correction coming from the terms $1 \leq j < L$ in (E.4) for which (E.6) does not have to hold. It is equal to

$$\xi_N = \frac{1}{N}\sum_{j=1}^{L-1} e^{-\imath(p_1-p_2)j}\left[\langle j| A |j\rangle - c(-1)^j\right] \tag{E.8}$$

and, clearly, satisfies

$$|\xi_N| \leq \frac{2(L-1)}{N}. \tag{E.9}$$

Performing the sum in (E.7) we are left with

$$\langle s_{p_1}| A |s_{p_2}\rangle = -ce^{-\imath(p_1-p_2)/2}\frac{1}{N\cos\frac{p_1-p_2}{2}} + \xi_N. \tag{E.10}$$

Taking the absolute value we get

$$|\langle s_{p_1}| A |s_{p_2}\rangle| \leq \frac{1}{N|\cos\frac{p_1-p_2}{2}|} + \frac{2(L-1)}{N}. \tag{E.11}$$

Using (E.2) proves this part of the theorem. We can take for the theorem the constant $C_1 = 1 + 2(L-1) = 2L - 1$.

Case b): The case b) is even simpler. Here A does not act only as a phase on the kink states, but it flips some spins. Flipping any state far from the kink will necessarily create a second kink (see Figure E.1), so all the elements $\langle j| A |l\rangle$ and $\langle j| A\Pi^z |l\rangle$ vanish for $L < j < N$ or $L < l < N$. There are thus at most $(L+1)^2$ non-zero elements in the sums (E.4) and (E.5). It follows

$$|\langle s_{p_1}| A |s_{p_2}\rangle| \leq \frac{(L+1)^2}{N}, \quad |\langle s_{p_1}| A\Pi^z |s_{p_2}\rangle| \leq \frac{(L+1)^2}{N}. \tag{E.12}$$

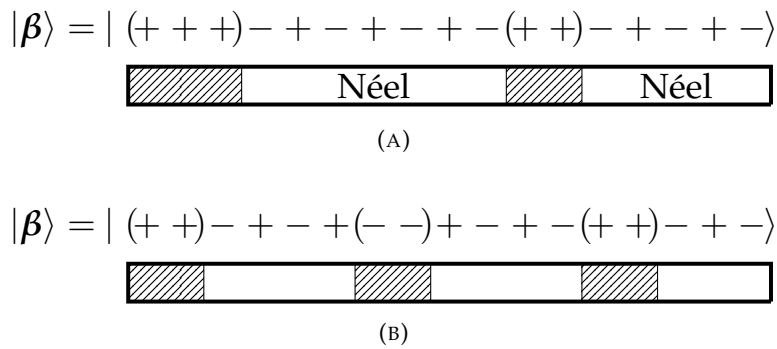

FIGURE E.2: Examples of the first excited states of H at the classical point $\lambda = 0$, and their symbolical representation. The white regions represent the Néel order, while the shaded ones include spins that participate in ferromagnetic bonds (kinks).

Now, using (E.2) and (E.3) proves this part of the theorem.

E.2 Proof of Theorem 2

To prove the theorem it is convenient to we write the matrix elements of interest as

$$\langle \boldsymbol{\beta}_1, p_1 | A | \boldsymbol{\beta}_2, p_2 \rangle = \frac{1}{N} \sum_{j,l=0}^{N-1} e^{-\imath(p_1 j - p_2 l)} \langle \boldsymbol{\beta}_1 | (T^\dagger)^j A T^l | \boldsymbol{\beta}_2 \rangle . \tag{E.13}$$

It is also convenient to introduce a symbolical representation of the structure of the states $|\boldsymbol{\beta}\rangle$, in terms of white and shaded regions, as in Figure E.2. We define the shaded regions to consist of all spins participating in a ferromagnetic bond (kink) with some of its neighbors, and the white regions to consists of the remaining spins, that participate only in antiferromagnetic bonds. Clearly, the number of white regions in a state $|\boldsymbol{\beta}\rangle$ is equal to the number of shaded regions. Let us denote the number of shaded regions in $|\boldsymbol{\beta}_1\rangle$ and $|\boldsymbol{\beta}_2\rangle$ by $\tilde{N}_1$ and $\tilde{N}_2$ respectively. Let us denote the number of kinks by N_1 and N_2 respectively. We have then, clearly, $\tilde{N}_1 \leq N_1$ and $\tilde{N}_2 \leq N_2$. Let us also introduce the concept of the size of a region. We will say that a particular region is of size R if there are R spins inside. For example, in the part a) of Figure E.2 there are two shaded regions, of size $R_1 = 3$ and $R_2 = 2$.

Case a): In case a) the matrix elements $\langle \boldsymbol{\beta}_1 | (T^\dagger)^j A T^l | \boldsymbol{\beta}_2 \rangle$ can be non-zero only if $\boldsymbol{\beta}_1 = \boldsymbol{\beta}_2$ and $j = l$, since A acts then only as a phase factor on the eigenstates of σ_j^x. For $\boldsymbol{\beta}_1 \neq \boldsymbol{\beta}_2$ the elements (E.13) are thus zero, while for $\boldsymbol{\beta}_1 = \boldsymbol{\beta}_2$ we are left with

$$\langle \boldsymbol{\beta}_1, p_1 | A | \boldsymbol{\beta}_1, p_2 \rangle = \frac{1}{N} \sum_{j=0}^{N-1} e^{-\imath(p_1 - p_2) j} \langle \boldsymbol{\beta}_1 | (T^\dagger)^j A T^j | \boldsymbol{\beta}_1 \rangle . \tag{E.14}$$

Let us focus now on a particular white region in $|\boldsymbol{\beta}_1\rangle$, exhibiting Néel order, and suppose it extends from site $j = r$ to site $j = r + R - 1$. This region has a contribution

$$S \equiv \frac{1}{N} \sum_{j=r}^{r+R-1} e^{-\imath(p_1 - p_2) j} \langle \boldsymbol{\beta}_1 | (T^\dagger)^j A T^j | \boldsymbol{\beta}_1 \rangle \tag{E.15}$$

in the sum (E.13). If $R > L$ then we have necessarily the staggered dependence

$$\langle \boldsymbol{\beta}_1 | \, (T^\dagger)^j A T^j \, | \boldsymbol{\beta}_1 \rangle = c(-1)^j \tag{E.16}$$

for $r \leq j \leq r + R - L$, i.e. before the support of $(T^\dagger)^j A T^j$ starts overlapping with the next shaded region, and with the constant $c \in \{-1, 1\}$ given explicitly by $c = (-1)^r \langle \boldsymbol{\beta}_1 | \, (T^\dagger)^r A T^r \, | \boldsymbol{\beta}_1 \rangle$. We have thus

$$S = \frac{1}{N} \sum_{j=r}^{r+R-1} e^{-\imath(p_1-p_2)j} c(-1)^j + \xi, \tag{E.17}$$

where the correction is given by

$$\xi = \frac{1}{N} \sum_{j=r+R-L+1}^{r+R-1} e^{-\imath(p_1-p_2)j} \left[\langle \boldsymbol{\beta}_1 | \, (T^\dagger)^j A T^j \, | \boldsymbol{\beta}_1 \rangle - c(-1)^j \right]. \tag{E.18}$$

Clearly, the correction satisfies

$$|\xi| \leq \frac{2(L-1)}{N}. \tag{E.19}$$

Performing the sum in in (E.17) we are left with

$$S = c e^{\imath(p_2-p_1)(r-\frac{1}{2})} \frac{(-1)^{R+1} e^{\imath(p_2-p_1)R} + 1}{2N \cos \frac{p_1-p_2}{2}} + \xi. \tag{E.20}$$

Taking the absolute value we get

$$|S| \leq \frac{1}{N |\cos \frac{p_1-p_2}{2}|} + \frac{2(L-1)}{N}. \tag{E.21}$$

In the other case, $R \leq L$, this bound holds trivially. To obtain the bound for the total contribution of the white regions we have to multiply (E.21) by the number of white regions in $|\boldsymbol{\beta}_1\rangle$, which is not greater than the number of kinks N_1.

We have thus obtained the bound for the contribution of white regions. We can obtain the bound for the contribution of the shaded regions in (E.14) by recognizing that the total number of spins in the shaded regions is not greater than $2N_1$, where N_1 is the number of kinks. Altogether, we get

$$| \langle \boldsymbol{\beta}_1, p_1 | \, A \, | \boldsymbol{\beta}_1, p_2 \rangle | \leq \frac{N_1}{N |\cos \frac{p_1-p_2}{2}|} + \frac{2(L-1)N_1}{N} + \frac{2N_1}{N}, \tag{E.22}$$

so we can take for the theorem the constant

$$C_1 = 3N_1 + 2(L-1)N_1. \tag{E.23}$$

Case b): We examine the elements $\langle \boldsymbol{\beta}_1 | \, (T^\dagger)^j A T^l \, | \boldsymbol{\beta}_2 \rangle$ and what are the necessary conditions for them to be nonzero. Let us suppose, without loss of generality, that $\tilde{N}_1 \leq \tilde{N}_2$, i.e. the number of shaded regions in $|\boldsymbol{\beta}_2\rangle$ is greater than or equal to the number of shaded regions in $|\boldsymbol{\beta}_1\rangle$.

First we notice that all the states $A T^l \, | \boldsymbol{\beta}_2 \rangle$ where l is such that A creates a new shaded region have necessarily zero product with the states $T^j \, | \boldsymbol{\beta}_1 \rangle$, for all j, because

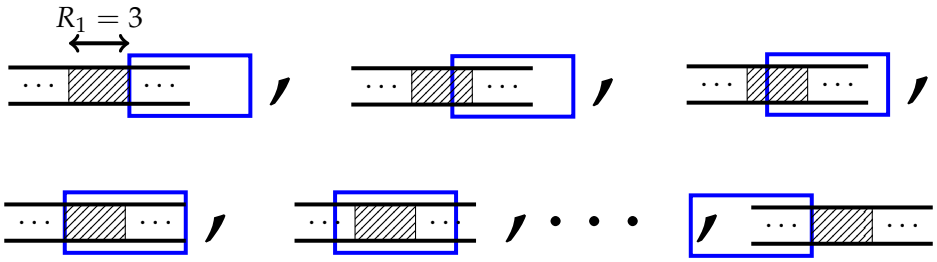

FIGURE E.3: The states $T^l |\beta_2\rangle$ for different values of l, where we focus on one shaded region of $|\beta_2\rangle$ and its translations. The blue rectangle represents the sites $1 \leq j \leq L$, where the support of A is found. All values of l for which the range $1 \leq j \leq L$ either borders or overlaps the shaded region are represented. See the proof of case b) of Theorem 2.

of a strictly greater number of shaded regions in $AT^l |\beta_2\rangle$ in that case. Thus, first we bound the number of states $T^l |\beta_2\rangle$ in which A does not create a new shaded region. The only states for which this is is a possibility are the states in which the shaded regions overlap or border the range $1 \leq j \leq L$, where the support of A is placed, since A creates kinks when acting on a white region. These states are represented in Figure E.3.

For a particular shaded region in $|\beta_2\rangle$, of size R, there is at most $R + L + 1$ states $T^l |\beta_2\rangle$ which place the shaded region to overlap or border with the the range $1 \leq j \leq L$ (see Figure E.3). Denoting the sizes of different shaded regions in $|\beta_2\rangle$ by $R_1, R_2, \ldots, R_{\tilde{N}_2}$ we have that there is at most

$$(R_1 + L + 1) + (R_2 + L + 1) + \ldots + (R_{\tilde{N}_2} + L + 1) \tag{E.24}$$

such states. Recognizing that the total size of the shaded regions is bounded as

$$R_1 + R_2 + \ldots + R_{\tilde{N}_2} \leq 2N_2, \tag{E.25}$$

where N_2 is the number of kinks in $|\beta_2\rangle$, and that $\tilde{N}_2 \leq N_2$, we can bound (E.24) by the number $N_2(L + 3)$. Thus, there is at most $N_2(L + 3)$ different values of l for which the product of $AT^l |\beta_2\rangle$ with $T^j |\beta_1\rangle$ is nonzero for some j..

The next step is to bound the number of states $T^j |\beta_1\rangle$ which have a nonzero product with a given state $AT^l |\beta_2\rangle$, for fixed l. There are two cases to consider. The first one is if there is a shaded region in $T^l |\beta_2\rangle$ that is outside the range $1 \leq j \leq L$, or at least a part of size 2 of the shaded region. In this case the necessary condition for a nonzero value of the elements $\langle\beta_1| (T^\dagger)^j AT^l |\beta_2\rangle$ is that some shaded region of $T^j |\beta_1\rangle$ coincides exactly with the aforementioned shaded region of $T^l |\beta_2\rangle$. There is at most one such state $T^j |\beta_1\rangle$ for each shaded region of $|\beta_1\rangle$. Thus the number of states $T^j |\beta_1\rangle$ which have a nonzero product with a given state $AT^l |\beta_2\rangle$ is at most $\tilde{N}_1$ in this case. The second case is if in $T^l |\beta_2\rangle$ there is no shaded region, or a part of size 2, outside the range $1 \leq j \leq L$. In this case there is at most $L + 1$ states $T^j |\beta_1\rangle$ that give a nonzero product, since the translation of any state by $L + 1$ sites will necessarily create a shaded region outside the support of A. We can include both cases by taking the sum of the bounds from each one, i.e. the number $L + 1 + \tilde{N}_1$.

Therefore, there is at most $N_2(L + 3)$ values of l which give a nonzero product of $AT^l |\beta_2\rangle$ with some of the states $T^j |\beta_1\rangle$ and each of these $N_2(L + 3)$ states has a

nonzero product with at most $L+1+\tilde{N}_1$ states $T^j|\boldsymbol{\beta}_1\rangle$. We conclude

$$|\langle \boldsymbol{\beta}_1, p_1| A |\boldsymbol{\beta}_2, p_2\rangle| \leq \frac{(L+1+\tilde{N}_1)(L+3)N_2}{N}. \tag{E.26}$$

We prefer to express the bound in terms of the number of kinks N_1, which satisfies $N_1 \geq \tilde{N}_1$, so we can take for the theorem the constant

$$C_2 = (L+1+N_1)(L+3)N_2. \tag{E.27}$$

Appendix F

n-Cluster-Ising Models: Diagonalization, Symmetries

Here we diagonalize the exactly solvable n-Cluster-Ising models

$$H = \sum_{j=1}^{N} \sigma_j^x \sigma_{j+1}^x + \lambda \sum_{j=1}^{N} \sigma_j^y \left(\sigma_{j+1}^z \sigma_{j+2}^z \dots \sigma_{j+n}^z\right) \sigma_{j+n+1}^y, \tag{F.1}$$

with frustrated boundary conditions (given by periodic boundary conditions $\sigma_{j+N}^\alpha = \sigma_j^\alpha$, for $\alpha = x, y, z$, and odd system size $N = 2M + 1$) and discuss the symmetries of the models. We consider the Cluster Ising models with an even number n, since they belong to the symmetry class considered in Chapter 6, i.e. they posses anticommuting parity symmetries for odd N. Moreover, we focus on the parameter region $\lambda \in (-1, 1)$, where the Ising coupling is larger than (and dominating over) the cluster one.

It is known [161, 170] that the models described by Hamiltonian (F.1) can be solved through an exact mapping to a system of free fermions, employing the same techniques as in the diagonalization of the quantum XY chain [56, 91], which can be considered the special case $n = 0$. The diagonalization is thus similar to the diagonalization of the XY chain with FBC, presented in details in Appendix C. This appendix is based on [6].

F.1 Diagonalization of the n-Cluster-Ising models

We are now diagonalizing Hamiltonian (F.1), when n is an even number. Let us note that the procedure works for odd n as well, the difference being in the expression for the energy of the π-mode in (F.10) later. The Hamiltonian commutes with Π^z and we split the diagonalization in two sectors of Π^z,

$$H = \frac{1+\Pi^z}{2} H^+ \frac{1+\Pi^z}{2} + \frac{1-\Pi^z}{2} H^- \frac{1-\Pi^z}{2}. \tag{F.2}$$

In each sector the Hamiltonian is quadratic in terms of Jordan-Wigner fermions

$$c_j = \left(\bigotimes_{l=1}^{j-1} \sigma_l^z\right) \frac{\sigma_j^x + \imath \sigma_j^y}{2}, \quad c_j^\dagger = \left(\bigotimes_{l=1}^{j-1} \sigma_l^z\right) \frac{\sigma_j^x - \imath \sigma_j^y}{2}. \tag{F.3}$$

It reads

$$H^\pm = -\sum_{j=1}^{N} (c_j c_{j+1} + c_j c_{j+1}^\dagger + \text{h.c.}) + \lambda \sum_{j=1}^{N} (c_j c_{j+n+1} - c_j c_{j+n+1}^\dagger + \text{h.c.}), \tag{F.4}$$

where $c_{j+N} = \mp c_j$ in the sector $\Pi^z = \pm 1$.

The Hamiltonian in each sector is quadratic so it can be brought to a form of free fermions. To achieve this, first $H^{\pm}$ are written in terms of the Fourier transformed Jordan-Wigner fermions,

$$b_q = \frac{1}{\sqrt{N}} \sum_{j=1}^{N} c_j \, e^{-\imath q j}, \quad b_q^\dagger = \frac{1}{\sqrt{N}} \sum_{j=1}^{N} c_j^\dagger \, e^{\imath q j}, \tag{F.5}$$

for $q \in \Gamma^{\pm}$, where the two sets of quasi-momenta are given by $\Gamma^- = \{2\pi k/N\}$ and $\Gamma^+ = \{2\pi(k+\frac{1}{2})/N\}$ with k running over all integers between 0 and $N-1$. The Bogoliubov rotation

$$\begin{aligned} a_q &= \cos\theta_q \, b_q + \imath \sin\theta_q \, b_{-q}^\dagger, \quad q \neq 0, \pi \\ a_q &= b_q, \quad q = 0, \pi \end{aligned} \tag{F.6}$$

with the Bogoliubov angle

$$\theta_q = \arctan \frac{|1 + \lambda \, e^{\imath(n+2)q}| - \lambda \cos\left[(n+1)q\right] - \cos q}{-\lambda \sin\left[(n+1)q\right] + \sin q} \tag{F.7}$$

then brings $H^{\pm}$ to a free fermionic form. The Bogoliubov angle also satisfies

$$e^{\imath 2\theta_q} = e^{\imath q} \frac{1 + \lambda \, e^{-\imath(n+2)q}}{|1 + \lambda \, e^{-\imath(n+2)q}|}. \tag{F.8}$$

After these sets of transformations, the original Hamiltonian is mapped into

$$H^{\pm} = \sum_{q \in \Gamma^{\pm}} \varepsilon_q \left(a_q^\dagger a_q - \frac{1}{2} \right), \tag{F.9}$$

where the quasi-particle energies are given by

$$\begin{aligned} \varepsilon_q &= 2|1 + \lambda \, e^{\imath(n+2)q}| = 2\sqrt{1 + \lambda^2 + 2\lambda \cos\left[(n+2)q\right]} && \forall \, q \neq 0, \pi, \\ \varepsilon_0 &= 2(1+\lambda) && q = 0 \in \Gamma^-, \\ \varepsilon_\pi &= -2(1+\lambda) && q = \pi \in \Gamma^+. \end{aligned} \tag{F.10}$$

Before proceeding, let us note one technical subtlety in the diagonalization of the model. The Bogoliubov angle θ_q, defined by (F.7) can become undefined for some modes $q \neq 0, \pi$ also point-wise, by fine–tuning of the parameters n, N, and λ. This problem can be circumvented by using (F.8) to define the Bogoliubov angle and such points can be neglected.

F.2 Eigenstates construction for the n-Cluster-Ising models

The eigenstates of H are formed by applying Bogoliubov fermions creation operators on the vacuum states $|0^{\pm}\rangle$, which satisfy $a_q \, |0^{\pm}\rangle = 0$ for $q \in \Gamma^{\pm}$ and taking care of the parity requirements in (F.2). The vacuum states are given by

$$|0^{\pm}\rangle = \prod_{0<q<\pi, \, q \in \Gamma^{\pm}} \left(\cos\theta_q - \imath \sin\theta_q \, b_q^\dagger b_{-q}^\dagger \right) |0\rangle, \tag{F.11}$$

where $|0\rangle = |\uparrow\uparrow ... \uparrow\rangle$ is the state of all spin up and the vacuum for Jordan-Wigner fermions, satisfying $c_j |0\rangle = 0$. The vacuum states $|0^+\rangle$ and $|0^-\rangle$ both have, by construction, parity $\Pi^z = +1$. The parity requirements in (F.2) imply that the eigenstates of H belonging to the $\Pi^z = -1$ sector are of the form $a^\dagger_{q_1} a^\dagger_{q_2} ... a^\dagger_{q_m} |0^-\rangle$ with $q_i \in \Gamma^-$ and m odd, while $\Pi^z = +1$ eigenstates are of the same form but with $q_i \in \Gamma^+$, m even and the vacuum $|0^+\rangle$ used. It is important to stress that the total quasi-momentum of these Hamiltonian eigenstates is also the momentum of the states that generates lattice translations, i.e. the action of translation operator T on these states acts as a phase factor

$$T = \exp\left(\imath \sum_{q \in \Gamma^\pm} q a^\dagger_q a_q\right), \tag{F.12}$$

which follows from Theorem 5 from Appendix C.3. The identification of the quasi-momentum from the exact solution with the momentum that generates lattice translations allows us to draw a connection between the general results of Chapter 6 and the exactly solvable cluster models.

Because of the anticommuting parity symmetries of the model, having constructed the states of one sector, say $\Pi^z = -1$, the states of the other sector can be constructed also by applying the parity operator Π^x (or Π^y). Namely, if $|\psi\rangle$ is the eigenstate of H with $\Pi^z = -1$ then $\Pi^x |\psi\rangle$ is also the eigenstate, with the same energy, but with $\Pi^z = +1$.

From our construction of the eigenstates we see, in particular, that the ground states of the model (F.1) are the states $a^\dagger_q |0^-\rangle$ and $\Pi^x a^\dagger_q |0^-\rangle$ for all momenta $q \in \Gamma^-$ that minimize the energy (F.10). Note that in the studied parameter region $\lambda \in (-1, 1)$ the energy of every mode $q \in \Gamma^-$ is positive. A consequence of this fact is that the system is gapless, with the energy gap above the ground state closing as $1/N^2$, a phenomenology analogous to that of Refs. [1, 2, 66, 71, 73].

Determining the ground states, their momenta and the ground state degeneracy becomes, thus, a matter of finding the modes $q \in \Gamma^-$ with minimal energy. From (F.10) we see that the modes $q \in \Gamma^-$ with minimal energy are, for $\lambda \in (0, 1)$, those that minimize $\cos[(n+2)q]$, and, for $\lambda \in (-1, 0)$, those that maximize $\cos[(n+2)q]$. The number of such momenta is given by the theorem which is the subject of the next section. Denoting by $g = \gcd(N, n+2)$ the greatest common divisor of N and $n+2$, from the theorem it follows that the number of modes minimizing the energy is $2g$ and g for $\lambda \in (0, 1)$ and $\lambda \in (-1, 0)$ respectively. Taking into account the two-fold degeneracy between different parity sectors, we conclude that the ground state degeneracy is $4g$ and $2g$ for $\lambda \in (0, 1)$ and $\lambda \in (-1, 0)$ respectively.

Let us determine explicitly some of the ground state momenta. We are going to focus on the example presented in Chapter 6, given by $n = 4$ and $\lambda \in (0, 1)$. From part b) of the theorem in the next section we see that the ground state momenta $q \in \Gamma^-$ are those that satisfy

$$\cos(6q) = -\cos\left(\pi \frac{g}{N}\right), \tag{F.13}$$

where $g = \gcd(N, 6)$. We are going to focus on the cases $N \bmod 12 = 1$ and $N \bmod 12 = 3$, that illustrate our points in Chapter 6, while the other cases can be treated in an analogous way. In the case $N \bmod 12 = 1$ we have $g = 1$ so the ground space is four-fold degenerate (corresponding to two different momenta). It is easy to see that momenta

$$q = \frac{2\pi}{N} \frac{N-1}{12}, \ \frac{2\pi}{N} \frac{11N+1}{12} \tag{F.14}$$

indeed belong to Γ^- and satisfy the relation (F.13), and are thus the ground state momenta. In the case $N \bmod 12 = 3$ we have, on the other hand, $g = 3$ so the ground space is 12-fold degenerate (corresponding to six different momenta). The ground state momenta are in this case

$$q = \frac{2\pi}{N}\frac{N-3}{12}, \frac{2\pi}{N}\frac{3N+3}{12}, \frac{2\pi}{N}\frac{5N-3}{12}, \frac{2\pi}{N}\frac{7N+3}{12}, \frac{2\pi}{N}\frac{9N-3}{12}, \frac{2\pi}{N}\frac{11N+3}{12}. \tag{F.15}$$

F.3 Extremization of the energy spectrum for the n-Cluster-Ising models

In this section we prove the following theorem, that enables to find the ground state degeneracy of the n-Cluster-Ising model setting $m = n + 2$.

Theorem 7. *Let m and N be positive integers, such that $m < N$ and N is odd. Let us denote their greatest common divisor by $g = \gcd(N, m)$. Consider the function $f(j) = \cos\left(\frac{2\pi m}{N} j\right)$ defined for $j \in \{0, 1, \dots N-1\}$.*

(a) The function f has g maxima on the set $\{0, 1, \dots N-1\}$, where the function reaches value 1.

(b) The function f has $2g$ minima on the set $\{0, 1, \dots N-1\}$, where the function reaches value $-\cos(\pi g/N)$.

For the proof we will use the concept of a *multiset*, i.e. a set in which elements can repeat. Two multisets are equal if they contain the same elements, with the same multiplicities. We define the multiplication of the multiset of numbers by a constant: If $A = \{\alpha : \alpha \in A\}$ is a multiset of (complex) numbers and c a (complex) number we define the multiplication in the obvious way, by multiplying each element of the multiset by c,

$$cA = \{c\alpha : \alpha \in A\}. \tag{F.16}$$

We also introduce the distance of a number from a set, or a multiset, of numbers. Let β be a (complex) number and A a set, or a multiset. Then the distance of β from A is

$$d(\beta; A) = \min\{|\alpha - \beta| : \alpha \in A\}. \tag{F.17}$$

More generally inf should be used instead of min, of course, but for our purposes it is going to be the same.

Now we introduce a definition about modular arithmetic and multisets. Suppose we have two multisets of integers, A and B, and let m also be an integer. We say that $A = B \pmod m$ if

$$\{\alpha \bmod m : \alpha \in A\} = \{\beta \bmod m : \beta \in B\}, \tag{F.18}$$

i.e. if looking at equalities modulo m the elements and multiplicities are the same.

With these notions introduced we can prove the theorem.

Proof. (a) If we expand the domain $j \in \{0, 1, \dots N-1\}$ of function f to real values $j \in \mathbb{R}$ then it is easy to see that the function is maximized for $j \in \frac{N}{m}\mathbb{Z}$, with value $f(j) = 1$. Within our restricted domain of integers, the elements j that

minimize the function $f(j)$ are simply those that satisfy both $j \in \{0, 1, \dots N-1\}$ and $j \in \frac{N}{m}\mathbb{Z}$, i.e. those $j \in \{0, 1, \dots N-1\}$ satisfying

$$d\Big(j; \frac{N}{m}\mathbb{Z}\Big) = 0. \tag{F.19}$$

Since $0 \leq j \leq N-1$ the condition (F.19) is equivalent to

$$d\Big(j; \frac{N}{m}\{0, 1, 2 \dots, m-1\}\Big) = 0. \tag{F.20}$$

Clearly, there are as many minimizing values j as there are integers in the set

$$\frac{N}{m}\{0, 1, 2 \dots, m-1\}, \tag{F.21}$$

and this number is, further, equal to the number of zeroes in the multiset

$$A \equiv \Big\{Nl \bmod m : l = \{0, 1, 2, \dots m-1\}\Big\}. \tag{F.22}$$

We proceed by exploring the properties of the multiset A. Bringing N out of the multiset we get

$$A = N\{0, 1, 2 \dots, m-1\} \pmod m. \tag{F.23}$$

Introducing the greatest common divisor of N and m, denoted by $g = \gcd(N, m)$, and defining

$$B = g\{0, 1, 2, \dots m-1\} \tag{F.24}$$

we can write

$$A = \frac{N}{g}B \pmod m. \tag{F.25}$$

The first step is to show that B consists of repeating blocks, if we look at equalities $\pmod m$. Multiplying with g in (F.24) we get trivially

$$B = \{0, g, 2g \dots, (m-1)g\} \pmod m. \tag{F.26}$$

But notice

$$g(m-1) \overset{(\mathrm{mod}\ m)}{=} m - g = \Big(\frac{m}{g} - 1\Big)g. \tag{F.27}$$

This means that the multiset B consists mod m of repeating blocks

$$0, g, 2g, \dots, \Big(\frac{m}{g} - 1\Big)g. \tag{F.28}$$

We know that the number of elements in the multiset is m, while we see that the number of elements in the block is m/g. We conclude that the total number of blocks that form the multiset B must be g.

The next step is to examine each block as a multiset and show that it is unaffected by multiplication by N/g, i.e. that

$$\frac{N}{g}\{0, g, 2g, \dots \Big(\frac{m}{g} - 1\Big)g\} = \{0, g, 2g, \dots \Big(\frac{m}{g} - 1\Big)g\} \pmod m. \tag{F.29}$$

For this purpose, it is sufficient to show that all elements on the left are different. It is simple to see that this is the case by assuming the contrary and reducing to contradiction. We assume, thus, that there are two elements which are equal,

$$\frac{N}{g}(l_1 g) = \frac{N}{g}(l_2 g) \pmod{m}, \tag{F.30}$$

for some $l_1, l_2 \in \{0, 1, \ldots, m/g - 1\}$ such that $l_1 < l_2$. The assumed equality implies

$$N(l_2 - l_1) = 0 \pmod{m}, \tag{F.31}$$

so that $N(l_2 - l_1)$ is divisible by m, and $(l_2 - l_1)N/g$ is divisible by m/g. But since $l_2 - l_1 \in \{0, 1, \ldots m/g - 1\}$ we have that $l_2 - l_1$ is not divisible by m/g. It follows that N/g must have common divisors with m/g, which is in contradiction with the property of g being the greatest common divisor of N and m. Thus, we have shown that each block is unaffected by multiplication by N/g.

The last step is to conclude from (F.25) that the set A consists of g repeating blocks (F.28). In particular, A contains g zeroes, which proves part (a) of the theorem.

(b) If we expand the domain $j \in \{0, 1, \ldots N - 1\}$ of function f to real values $j \in \mathbb{R}$ then it is easy to see that $f(j)$ is minimized for $j = \frac{N}{2m}(2l + 1)$, $l \in \mathbb{Z}$, with value $f(j) = -1$. However, since for odd N these values of j are never integers, they do not coincide with our restricted domain $j \in \{0, 1, \ldots, N - 1\}$, and we have to find how close to these values we can get. The minimum of f is achieved by those values $j \in \{0, 1, \ldots, N - 1\}$ that minimize the distance

$$d\Big(j; \frac{N}{2m}\{2l + 1 : l \in \mathbb{Z}\}\Big) = d\Big(j; \frac{N}{2m}\{2l + 1 : l \in \{0, 1, \ldots, m - 1\}\Big), \tag{F.32}$$

where the equality holds since $0 \leq j \leq N - 1$. To count all j that minimize the distance we take the following approach. Let us denote the minimal distance by $d_{\min}$. We first count how many values of $l \in \{0, 1, \ldots, m - 1\}$ have

$$d\Big(\frac{N}{2m}(2l + 1); \{0, 1, \ldots, N - 1\}\Big) = d_{\min}, \tag{F.33}$$

and then for each such minimizing l we count all $j \in \{0, 1, \ldots, N - 1\}$ with

$$\Big|\frac{N}{2m}(2l + 1) - j\Big| = d_{\min}, \tag{F.34}$$

To each such l there can be associated one or two values of j, depending on whether $d_{\min} < 1/2$ or $d_{\min} = 1/2$ respectively. It is easy to see that, since $m < N$, the same value of j cannot be associated to different values of l.

We will now use a similar procedure as in part (a) and explore the multiset

$$C \equiv \Big\{N(2l + 1) \bmod (2m) : l = \{0, 1, 2, \ldots m - 1\}\Big\}, \tag{F.35}$$

which determines the distances of interest. Bringing N out we have

$$C = N\{1, 3, \ldots 2m - 1\} \pmod{2m}. \tag{F.36}$$

Now we introduce the greatest common divisor $g = \gcd(N, m) = \gcd(N, 2m)$, where the last equality holds since N is odd, and define the multiset

$$D = g\{1, 3, \ldots, 2m-1\}. \tag{F.37}$$

Then we can write

$$C = \frac{N}{g} D \pmod{2m}. \tag{F.38}$$

The first step is to show that D consists of repeating blocks, if we look at equalities $(\mathrm{mod}\ 2m)$. Multiplying with g in (F.37) we get trivially

$$B = \{g, 3g \ldots, (2m-1)g\} \pmod{2m}. \tag{F.39}$$

But notice

$$g(2m-1) \overset{(\mathrm{mod}\ 2m)}{=} 2m - g = \Big(2\frac{m}{g} - 1\Big)g. \tag{F.40}$$

This means that the multiset D consists $(\mathrm{mod}\ 2m)$ of repeating blocks

$$g, 3g, \ldots, \Big(2\frac{m}{g} - 1\Big)g. \tag{F.41}$$

We know that the number of elements in the multiset is m, while we see that the number of elements in the block is m/g. We conclude that the total number of blocks that forms the multiset D must be g.

The next step is to examine each block as a multiset and show that it is unaffected by multiplication by N/g, i.e. that

$$\frac{N}{g}\{g, 3g, \ldots \Big(2\frac{m}{g} - 1\Big)g\} = \{g, 3g, \ldots \Big(2\frac{m}{g} - 1\Big)g\} \pmod{2m}. \tag{F.42}$$

Since N/g is odd, for this it is sufficient to show that all elements on the left are different. It is simple to see that this is the case by assuming the contrary and reducing to contradiction. We assume, thus, that there are two elements which are equal,

$$\frac{N}{g}(2l_1 + 1)g = \frac{N}{g}(2l_2 + 1)g \pmod{2m}, \tag{F.43}$$

for some $l_1, l_2 \in \{0, 1, \ldots, m/g - 1\}$ such that $l_1 < l_2$. The assumed equality implies (F.30), and by the same argument as in part (a) we conclude there is a contradiction. Thus, blocks are unaffected by multiplication by N/g. It follows that C consists of g repeating blocks (F.41)

The last step is to conclude from the block structure of C about the number of minima. We look separately at two cases, $g = m$ and $g < m$. In the first case, $g = m$, we have $2m - g = g$ so C consists only of elements $g = m$, implying the distance

$$d\Big(\frac{N}{2m}(2l+1); \{0, 1, \ldots, N-1\}\Big) = \frac{1}{2}. \tag{F.44}$$

for all $l \in \{0, 1, \ldots m-1\}$. For each l there is necessarily $j \in \{0, 1 \ldots, N-1\}$ such that

$$\Big|\frac{N}{2m}(2l+1) - j\Big| = \Big|\frac{N}{2m}(2l+1) - (j+1)\Big| = \frac{1}{2}. \tag{F.45}$$

Counting all corresponding j and $j+1$ it follows that f has $2g$ minima on the set $\{0,1,\dots N-1\}$.

In the second case, $g<m$, the values l with

$$N(2l+1) \overset{(\mathrm{mod}\ 2m)}{=} g \quad \text{and} \quad N(2l+1) \overset{(\mathrm{mod}\ 2m)}{=} 2m-g \tag{F.46}$$

minimize the distance (F.33), with

$$d_{\min} = \frac{g}{2m} \tag{F.47}$$

Since $d_{\min} < 1/2$ in this case, for each such l there is only one value $j \in \{0,1,\dots,N-1\}$ with

$$\left|\frac{N}{2m}(2l+1) - j\right| = d_{\min}. \tag{F.48}$$

Due to block structure of C, there is g values of l satisfying the first and g values satisfying the second equation in (F.46). It follows that the number of minima of f is again $2g$. Both in the case $m=g$ and $m<g$ the value of the minimum is

$$\cos\left[\frac{2\pi m}{N}\left(\frac{N(2l+1)}{2m} \pm \frac{g}{2m}\right)\right] = -\cos\left(\frac{\pi g}{N}\right). \tag{F.49}$$

□

In fact, in the proof of part (a) of the theorem the property of N being odd was nowhere used, and the same statement holds for the case of even N. The part (b) would be different in the case of even N, since then, in general, $N(2l+1)/(2m)$ could achieve integer values and belong to the domain $\{0,1,\dots,N-1\}$.

F.4 Ground state degeneracy from the symmetries

Here we explain the ground state degeneracy of the n-Cluster-Ising chain based on the symmetries, in details. We denote $g \equiv \gcd(N, n+2)$. Let us introduce the shorthand notation

$$R_j \equiv \sigma^x_{j-1}\sigma^x_j + \lambda\sigma^y_j\left(\sigma^z_{j+1}\sigma^z_{j+2}\dots\sigma^z_{j+n}\right)\sigma^y_{j+n+1} \tag{F.50}$$

so that $H = \sum_{j=1}^{N} R_j$. The Hamiltonian can then be decomposed as

$$H = \sum_{k=1}^{g} H^{(k)}, \tag{F.51}$$

where

$$H^{(g)} = R_g + R_{2g} + R_{3g} + \ldots + R_N \tag{F.52}$$

and

$$H^{(k)} = \left(T^\dagger\right)^k H^{(g)} T^k \tag{F.53}$$

for $k = 1,2,\dots,g-1$. All the Hamiltonians $H^{(k)}$ commute with T^g. Crucially, we find that all these Hamiltonians mutually commute ($[H^{(k)}, H^{(l)}] = 0$). Since different cluster terms, i.e. $\sigma^y_j\left(\sigma^z_{j+1}\sigma^z_{j+2}\dots\sigma^z_{j+n}\right)\sigma^y_{j+n+1}$ for different j, mutually commute, to show the latter it is sufficient to show that all the terms $\sigma^x_{j-1}\sigma^x_j$ appearing in $H^{(k)}$ for $k \neq g$ commute with all the cluster terms $\sigma^y_j\left(\sigma^z_{j+1}\sigma^z_{j+2}\dots\sigma^z_{j+n}\right)\sigma^y_{j+n+1}$ appearing in

$H^{(g)}$. This follows simply from the observation that $\sigma_0^y(\sigma_1^z\sigma_2^z\dots\sigma_n^z)\sigma_{n+1}^y$ commutes with $\sigma_{j-1}^x\sigma_j^x$ for $j \in \{0,1,2,\dots,n+2\} - \{0,g,2g,\dots,n+2\}$, where the minus sign stands for the exclusion.

Thus, different Hamiltonians $H^{(k)}$ mutually commute and they commute with the total Hamiltonian H. Moreover all these operators commute with T^g. Since all these operators mutually commute they can be diagonalized simultaneously. Suppose then that the state $|\psi\rangle$ is a common eigenstate of H, T^g and $H^{(k)}$ for $k = 0,1,\dots g-1$. Due to topological frustration the ground state of H does not coincide with the ground state of $H^{(k)}$ for all k, but it is the first excited state for a particular k and the ground state for the other (it is easy to see for $\lambda = 0$, while for general $\lambda \in (-1,1)$ this can be seen in the fermionic picture of the exact solution). This implies that the states $T^k|\psi\rangle$ for $k = 0,1,\dots g-1$ are mutually orthogonal and that the ground state manifold is at least g-fold degenerate.

We can relate this degeneracy to the momentum shift. Suppose that $|\psi\rangle$ is an eigenstate of T^g with the eigenvalue $e^{\imath gp}$ for some momentum $p \in \frac{2\pi}{N}\mathbb{Z}$. Any eigenvalue of T^g can be written in this form. It follows that the (normalized) state

$$\frac{1}{\sqrt{g}}\left[1 + e^{-\imath p}T + \left(e^{-\imath p}T\right)^2 + \dots + \left(e^{-\imath p}T\right)^{g-1}\right]|\psi\rangle \tag{F.54}$$

is an eigenstate of T with the eigenvalue $e^{\imath p}$. However, since the transformation $p \to p + 2\pi/g$ does not change the value of $e^{\imath gp}$, the state obtained from (F.54) by this transformation is also an eigenstate of T. Thus, if there is a ground state with momentum p, there is also a ground state with momentum $p + 2\pi/g$.

The ground state degeneracy of the model, $2g$ or $4g$, now follows from the parity symmetry and the mirror symmetry, as discussed in Chapter 6.

Appendix G

2-Cluster-Ising Chain: Exact Methods, Bond Defect

This is the appendix for Chapter 7, based on [7].

G.1 Diagonalization of the Hamiltonian:

The n-Cluster Ising model for arbitrary even n has been already diagonalized in Appendix E. The Hamiltonian (7.1) can be obtained from Hamiltonian (F.1) by multiplying the latter by $\cos\phi$ and setting $\lambda = \tan\phi$, $n = 2$.

It follows that decomposing the Hamiltonian of the 2-Cluster Ising Model eq. (7.1) in two Π^z sectors as

$$H = \frac{1+\Pi^z}{2} H^+ \frac{1+\Pi^z}{2} + \frac{1-\Pi^z}{2} H^- \frac{1-\Pi^z}{2}, \tag{G.1}$$

in each one it can be brought to a form of free fermions

$$H^\pm = \sum_{q\in\Gamma^\pm} \varepsilon_q \left(a_q^\dagger a_q - \frac{1}{2} \right). \tag{G.2}$$

The Bogoliubov fermions a_q are defined by (F.6), with the Bogoliubov angle

$$\theta_q = \tan^{-1} \frac{|\sin\phi + \cos\phi\, e^{\imath 4q}| - \sin\phi\cos(3q) - \cos\phi\cos q}{-\sin\phi\sin(3q) + \cos\phi\sin q} \tag{G.3}$$

for $q \neq 0, \pi$ and by $\theta_0 = \theta_\pi = 0$. The Bogoliubov angle also satisfies

$$e^{\imath 2\theta_q} = e^{\imath q} \frac{\cos\phi + \sin\phi\, e^{-\imath 4q}}{|\cos\phi + \sin\phi\, e^{-\imath 4q}|}. \tag{G.4}$$

The energies ε_q associated to each mode with momentum $q \in \Gamma^\pm$ are given by

$$\begin{aligned} \varepsilon_q &= 2|\cos\phi + \sin\phi\, e^{\imath 4q}| \quad \forall\, q \neq 0, \pi\,; \\ \varepsilon_0 &= 2(\cos\phi + \sin\phi) \qquad\quad q = 0 \in \Gamma^-\,; \\ \varepsilon_\pi &= -2(\cos\phi + \sin\phi) \qquad q = \pi \in \Gamma^+\,. \end{aligned} \tag{G.5}$$

Depending on the value of ϕ, the energies of the modes with $q = 0 \in \Gamma^-$ and $q = \pi \in \Gamma^+$ are different from the others because they can become negative. Without frustration, these negative energy modes are responsible for the ground state degeneracy that allows for the spontaneous symmetry breaking mechanism, while

in presence of frustration they play a different and pivotal role in the emerging phenomenolgy. Indeed, for each ϕ the ground states of the system can be determined starting from the vacuum of Bogoliubov fermions in the two sectors ($|0^{\pm}\rangle$), which, by construction, have positive parity $\Pi^z = 1$, and taking into account both the presence of modes with negative energy and the parity constrains.

When $\phi \in (-\pi, -\frac{\pi}{2})$ (both interactions are "ferromagnetic"), we have $\varepsilon_\pi > 0$ while $\varepsilon_0 < 0$ and hence, in each parity sector, the state with the lowest energy, respectively $|0^+\rangle$ and $a_0^\dagger |0^-\rangle$, fulfills the parity requirement. They are separated from the other states by a finite energy gap that, in the thermodynamic limit becomes equal to $-2\varepsilon_0 = 2\varepsilon_\pi \neq 0$. This is the same physical picture that can be found also assuming open boundary conditions [170] and hence also the thermodynamic behavior is the same. A quantum phase transition at $\phi = -3\frac{\pi}{4}$ separates two different ordered phases. When the Ising interaction prevails over the cluster one, i.e. for $\phi \in (-\pi, -3\frac{\pi}{4})$, the system shows a ferromagnetic phase characterized by a non-zero value of the magnetization along x. On the other side of the critical point, when $\phi \in (-3\frac{\pi}{4}, -\frac{\pi}{2})$, we have that the system is in a nematic phase identified by the zeroing of the magnetization in all directions and the simultaneous setting up of a non-vanishing value of the expectation value of the nematic operator O_j.

On the contrary, when $\phi \in (0, \frac{\pi}{2})$, both the cluster and Ising interaction are "antiferromagnetic", and hence we have topological frustration (TF) in the system: in this region $\varepsilon_0 > 0$ while $\varepsilon_\pi < 0$. As a consequence of this, the two states with the lowest energy are, respectively, $a_\pi^\dagger |0^+\rangle$ in the even sector and $|0^-\rangle$ in the odd one. Both of them violate the parity requirements in (G.1) and, therefore, cannot be eigenstates of the the Hamiltonian in eq. (7.1). Instead, the ground-states belong to a four-fold degenerate manifold spanned by the states $|\pm p\rangle \equiv a_{\pm p}^\dagger |0^-\rangle$ in the odd sector and $\Pi^x |\pm p\rangle$ in the even one, where the momentum p obeys

$$p = \begin{cases} \frac{\pi}{4} - \frac{\pi}{4N}, & \text{N mod 8=1} \\ \frac{3\pi}{4} - \frac{\pi}{4N}, & \text{N mod 8=3} \\ \frac{3\pi}{4} + \frac{\pi}{4N}, & \text{N mod 8=5} \\ \frac{\pi}{4} + \frac{\pi}{4N}, & \text{N mod 8=7.} \end{cases} \tag{G.6}$$

These states are surmounted by a band states, with the gap above the ground state closing as $1/N^2$ for large N.

G.1.1 The order parameters and their representation as determinants:

In evaluating the order parameters it is useful to first define the Majorana fermions

$$A_j = \Big(\bigotimes_{l=1}^{j-1} \sigma_l^z\Big)\sigma_j^x \,, \quad B_j = \Big(\bigotimes_{l=1}^{j-1} \sigma_l^z\Big)\sigma_j^y \,. \tag{G.7}$$

The expectation values of interest will be expressed in terms of determinants of Majorana correlation matrices, employing techniques similar to the ones used in Chapter 4 for the magnetization. Among the states in the ground space manifold a special role is played by two of them, defined as

$$|g_\pm\rangle \equiv \frac{1}{\sqrt{2}} \left(|p\rangle \pm |-p\rangle\right), \tag{G.8}$$

which are eigenstates of Π^z with eigenvalue -1 and of the mirror operator with respect to site N, denoted by M_N, (see Appendix C.4) with eigenvalue ± 1 (respectively). Note that the site N is defined with respect to the beginning of the Jordan-Wigner string in eq. (F.3).

As discussed in Chapter 7, for an operator K_N, that commutes with Π^x and anticommutes with Π^z, the ground state expectation values depend on the matrix elements $F_1(K_N) = \langle p| \Pi^x K_N |p\rangle$ and $F_2(K_N) = \langle -p| \Pi^x K_N |p\rangle$. Assuming $M_N K_N M_N = K_N$, we have both $\langle p| K_N \Pi^x |p\rangle = \langle -p| K_N \Pi^x |-p\rangle$ and $\langle -p| K_N \Pi^x |p\rangle = \langle p| K_N \Pi^x |-p\rangle$, so the matrix elements can be expressed through the expectation values of the states in eq. (G.8) as

$$\begin{aligned} F_1(K_N) &= \tfrac{1}{2}(\langle g_+|K_N\Pi^x|g_+\rangle + \langle g_-|K_N\Pi^x|g_-\rangle)\,, \\ F_2(K_N) &= \tfrac{1}{2}(\langle g_+|K_N\Pi^x|g_+\rangle - \langle g_-|K_N\Pi^x|g_-\rangle)\,. \end{aligned} \tag{G.9}$$

Now, because the operator $K_N\Pi^x$ commutes with Π^z, the expectation values $\langle g_\pm|K_N\Pi^x|g_\pm\rangle$ can be obtained following a well known approach that applies to all operators that commute with Π^z and all ground states of well-defined parity [90, 91].

The first step is to express $K_N\Pi^x$ as a product of Majorana fermions. The second step is to use Wick theorem (the same argument as in Appendix C can be used to justify the validity of Wick theorem in these states) to express the expectation values as determinants of matrices of two-point Majorana correlators. Adopting the short notation $\langle\cdot\rangle_\pm = \langle g_\pm|\cdot|g_\pm\rangle$, we have that $\langle A_j A_k\rangle_\pm = \langle B_j B_k\rangle_\pm = \delta_{jk}$ and

$$-\imath\,\langle A_j B_k\rangle_\pm = \frac{1}{N}\sum_{q\in\Gamma^-} e^{\imath 2\theta_q} e^{-\imath q(j-k)} - \frac{2}{N}\cos\left[p(j-k) - 2\theta_p\right] \mp \frac{2}{N}\cos\left[(j+k)p\right]. \tag{G.10}$$

Local Order Parameter

Following this approach, for $K_N = \sigma^x_N$ we get

$$\langle \sigma^x_N \Pi^x\rangle_\pm = (-1)^{\frac{N-1}{2}} \det \mathbf{C^{(1)}}, \tag{G.11}$$

where the elements of the $\frac{N-1}{2}\times\frac{N-1}{2}$ matrix $\mathbf{C^{(1)}}$ are equal to $\mathbf{C^{(1)}}_{\alpha,\beta} = -\imath\langle A_{2\alpha}B_{2\beta-1}\rangle_\pm$, for $\alpha,\beta\in\{1,2,\dots(N-1)/2\}$. Similarly, for $K_N = O_N$ we obtain

$$\langle O_N \Pi^x\rangle_\pm = (-1)^{\frac{N-1}{2}} \det \mathbf{C^{(2)}}, \tag{G.12}$$

where $\mathbf{C^{(2)}}$ is an $\frac{N+1}{2}\times\frac{N+1}{2}$ matrix. Its elements are given by $\mathbf{C^{(2)}}_{\alpha,\beta} = -\imath\langle A_{f(\alpha)}B_{f'(\beta)}\rangle_\pm$, where as α,β go over $1,2,\dots(N+1)/2$ we have that $f(\alpha)$ and $f'(\beta)$ assume the values $f(\alpha) = 1,3,5,\dots,N-4,N-2,N-1$ and $f'(\beta) = 1,2,4,6,\dots,N-3,N-1$.

String Order Parameters

To define string operators that can be exploited to characterize the quantum phase transition at $\phi = \pi/4$ we started from an observation made in Ref. [161]. In that work, the authors prove that in the thermodynamic limit of the unfrustrated cluster-Ising model, the only Majorana correlation functions that are not zero are those for which the site indices satisfy the relation $i - j = 3k - 1$ where k is an integer. Even if this observation was made for a different model and in the absence of frustration,

from the expression of the Majorana functions it is easy to observe that a similar property holds also in our case. In fact, it is possible to see that, in our case, all the Majorana correlation functions that do not satisfy the property $i - j = 4k - 1$ vanish in the limit of large N. The presence of TF adds $1/N$ corrections to Majorana fermions so it does not affect these properties, but it can affect the values of order parameters because they are expressed in terms of determinants of Majorana correlation matrices whose size grows with N. Hence, we tried to see if string operators, whose expectation value depends only on Majorana correlators that do not become zero in the thermodynamic limit, are able to characterize the quantum phase transition. Among all the possibilities we focus on two of them that are one the image of the other after the duality transformation, namely

$$\mathcal{M} = \prod_{k=1}^{I(N)} \left(\sigma^x_{4k-2}\sigma^x_{4k-1}\right); \quad \mathcal{N} = \prod_{k=1}^{I(N)} \left(O_{4k-2}O_{4k-1}\right), \tag{G.13}$$

where $I(N) = \frac{N-1}{4}$ for $N \bmod 4 = 1$ and $I(N) = \frac{N+1}{4} - 1$ for $N \bmod 4 = 3$.

We can use the same approach as for the local operators for the evaluation of the expectation values for two string order parameters, $\mathcal{F}_1(\mathcal{M})$ and $\mathcal{F}_1(\mathcal{N})$, in terms of determinants. With respect to the states $|g_\pm\rangle$ they read

$$\mathcal{F}_1(\mathcal{K}) \;=\; \frac{1}{2}\Big(\langle \mathcal{K} \rangle_+ + \langle \mathcal{K} \rangle_- \Big), \tag{G.14}$$

with $\mathcal{K} = \mathcal{N}, \mathcal{M}$. In this case we have the determinant representation

$$\begin{aligned} \langle \mathcal{M} \rangle_\pm &= (-1)^{I(N)} \det \mathbf{C}^{(\mathbf{3})}, \\ \langle \mathcal{N} \rangle_\pm &= (-1)^{I(N)} \det \mathbf{C}^{(\mathbf{4})}, \end{aligned} \tag{G.15}$$

where $\mathbf{C}^{(\mathbf{3})}$ and $\mathbf{C}^{(\mathbf{4})}$ are $I(N) \times I(N)$ matrices, with $I(N) = \frac{N-1}{4}$ for $N \bmod 4 = 1$ and $I(N) = \frac{N+1}{4} - 1$ for $N \bmod 4 = 3$. Their elements are given by $\mathbf{C}^{(\mathbf{3})}{}_{\alpha,\beta} = -\imath \langle A_{4\alpha-1} B_{4\beta-2} \rangle_\pm$ and $\mathbf{C}^{(\mathbf{4})}{}_{\alpha,\beta} = -\imath \langle A_{4\alpha} B_{4\beta-3} \rangle_\pm$, for $\alpha, \beta \in \{1, 2, \ldots, I(N)\}$.

Analytic evaluation of the string order parameter

The expressions in eq. (G.14) are efficient for the numerical evaluation of the string order parameters. Here we show how to analytically evaluate the value that the string order parameter $\mathcal{F}_1(\mathcal{M})$ assumes in the thermodynamic limit. To do so we express it in terms of Toeplitz determinants, using an approach similar to the one used in [3, 72] (see Appendix C.5.1) for the two-point spin correlation functions. The string order parameter $\mathcal{F}_1(\mathcal{N})$ can be studied in an analogous way.

We start by noting that the string order parameter is equal to

$$\mathcal{F}_1(\mathcal{M}) = (-1)^{I(N)} \langle 0^- | \, a_p \prod_{k=1}^{I(N)} (-\imath A_{4k-1} B_{4k-2}) a_p^\dagger \, |0^-\rangle \tag{G.16}$$

and then we make Wick contractions in the vacuum state $|0^-\rangle$. Adopting the short notation $\langle \cdot \rangle_0 = \langle 0^- | \cdot |0^-\rangle$, we have $\langle A_j A_k \rangle_0 = \langle B_j B_k \rangle_0 = \delta_{jk}$ and

$$-\imath \, \langle A_j B_k \rangle_0 = \frac{1}{N} \sum_{q \in \Gamma^-} e^{\imath 2\theta_q} e^{-\imath q(j-k)}. \tag{G.17}$$

Moreover, since we can express the Majorana fermions as

$$\begin{aligned} A_j &= \frac{1}{\sqrt{N}} \sum_{q\in\Gamma^-} (a_q^\dagger + a_{-q}) e^{\imath\theta_q} e^{-\imath qj}, \\ -\imath B_j &= \frac{1}{\sqrt{N}} \sum_{q\in\Gamma^-} (a_q^\dagger - a_{-q}) e^{-\imath\theta_q} e^{-\imath qj}, \end{aligned} \tag{G.18}$$

we can easily find the contractions

$$\begin{aligned} -\imath \left\langle a_p A_j \right\rangle_0 \left\langle B_k a_p^\dagger \right\rangle_0 &= -\frac{1}{N} e^{\imath 2\theta_p} e^{-\imath p(j-k)}, \\ -\imath \left\langle a_p B_k \right\rangle_0 \left\langle A_j a_p^\dagger \right\rangle_0 &= \frac{1}{N} e^{-\imath 2\theta_p} e^{\imath p(j-k)}. \end{aligned} \tag{G.19}$$

Performing all the Wick contractions in eq. (G.16) and using the basic properties of determinants, the string order parameter can be expressed as

$$\mathcal{F}_1(\mathcal{M}) = (-1)^{I(N)} \left[\left(\det \tilde{\mathbf{C}} + \text{c.c.} \right) - \det \mathbf{C} \right], \tag{G.20}$$

where $\tilde{\mathbf{C}}$ and $\mathbf{C}$ are $I(N) \times I(N)$ matrices with the elements

$$\begin{aligned} \mathbf{C}_{\alpha,\beta} &= -\imath \left\langle A_{4\alpha-1} B_{4\beta-2} \right\rangle_0, \\ \tilde{\mathbf{C}}_{\alpha,\beta} &= \mathbf{C}_{\alpha,\beta} - \frac{1}{N} e^{\imath(2\theta_p - p)} e^{-\imath 4p(\alpha-\beta)}, \end{aligned} \tag{G.21}$$

for $\alpha, \beta \in \{1, 2, \ldots, I(N)\}$, which give an alternative expression to eq. (G.14) for its analytical evaluation.

Using eq. (G.4), approximating the sum in eq. (G.17) by an integral, and doing some simple manipulations we get

$$\mathbf{C}_{\alpha,\beta} \overset{N\to\infty}{\simeq} \int_0^{2\pi} f(e^{\imath\theta}) e^{-\imath\theta(\alpha-\beta)} \frac{d\theta}{2\pi}, \tag{G.22}$$

where

$$f(e^{\imath\theta}) = \frac{1 + \tan\phi\, e^{-\imath\theta}}{|1 + \tan\phi\, e^{-\imath\theta}|}. \tag{G.23}$$

With this definition we can also write

$$\tilde{\mathbf{C}}_{\alpha,\beta} = \mathbf{C}_{\alpha,\beta} - \frac{1}{N} f(e^{\imath\theta_0}) e^{-\imath\theta_0(\alpha-\beta)}, \tag{G.24}$$

where $\theta_0 = 4p$.

Thus for $\phi \in (0, \pi/4)$ the matrix $\mathbf{C}$ is a standard Toeplitz matrix, whose symbol is a non-zero analytic function in an annulus around the unit circle, with zero winding number. Its determinant can be computed in the standard way using strong Szegő limit theorem (see [196]) and we get

$$\det \mathbf{C} \overset{N\to\infty}{\simeq} (1 - \tan^2\phi)^{\frac{1}{4}}. \tag{G.25}$$

To compute the determinant of $\tilde{\mathbf{C}}$ we need to use Theorem 1 from [3] (Theorem 3 from Chapter 9), which gives a correction to Szegő theorem for this type of Toeplitz

matrices. We get

$$\det \tilde{\mathbf{C}} \overset{N\to\infty}{\simeq} \left(1 - \frac{I(N)}{N}\right) \det \mathbf{C} \overset{N\to\infty}{\simeq} \frac{3}{4}(1-\tan^2\phi)^{\frac{1}{4}}. \tag{G.26}$$

Finally, from eq. (G.20) we get the string order parameter

$$\mathcal{F}_1(\mathcal{M}) \overset{N\to\infty}{\simeq} (-1)^{I(N)} \frac{1}{2}(1-\tan^2\phi)^{\frac{1}{4}}. \tag{G.27}$$

For $\phi \in (\pi/4, \pi/2)$ the symbol f has a non-zero winding number. It follows immediately from Theorem 2 from [3] (Theorem 4 from Chapter 9) that the string order parameter is zero in the thermodynamic limit,

$$\mathcal{F}_1(\mathcal{M}) \overset{N\to\infty}{\simeq} 0. \tag{G.28}$$

G.1.2 Effects of the presence of a defect

The scenario that we have depicted for the 2-cluster-Ising model is very peculiar, and it is normal to wonder whether it is resilient to the presence of noise, or it is the result of fine-tuning in the system parameters. Obviously, a complete analysis of the effects of the presence of defects in our model is far beyond the scope of Chapter 7 and has been the subject of analysis in Chapter 5, but for a different model. Here we discuss a simple example that shows that the phenomenology that we have depicted in the main body of this work is quite resilient.

Hence let us take into account the Hamiltonian

$$H' = \sin\phi \sum_{j=1}^{N} \sigma^y_{j-1}\sigma^z_j\sigma^z_{j+1}\sigma^y_{j+2} + \; + \cos\phi \sum_{j=1}^{N-1} \sigma^x_j\sigma^x_{j+1} + \cos(\phi+\delta_x)\; \sigma^x_N\sigma^x_1,$$

that coincides with the Hamiltonian in eq. (7.1) except for the presence of a defect in the Ising interaction, localized between the first and the last spin of the model. Such a presence implies that the new Hamiltonian in eq. (G.29) is neither translationally invariant nor preserves the mirror symmetries, except the one with respect to the $(N+1)/2$-th spin, while it continues to commute with all the parity operators. As a consequence, the ground state degeneracy of H' is reduced to two, even in the region where H, without the defect, presents a four dimensional manifold. However, independently of the parameters, H' always includes states of both parities so we can continue to use the already described approach to evaluate directly the order parameter.

Since H' is no more translationally invariant, it is now impossible to find an exact analytical expression for the ground states. We are then forced to resort to an efficient numerical procedure based on the fact that the Hamiltonian is, in each Π^z sector, still quadratic in terms of the fermionic operators and hence its eigenstates can be found following Ref. [4, 91] (see Appendix D). We focus on the odd sector ($\Pi^z = -1$), since having the ground state $|g'_-\rangle$ of H' belonging to the odd sector we can construct the ground state of H' belonging to the even sector as $|g'_+\rangle = \Pi^x |g'_-\rangle$. We write H' in the odd sector as

$$H' = \sum_{j,k=1}^{N} \left[c^\dagger_j S_{j,k} c_k + \frac{1}{2}\left(c^\dagger_j T_{j,k} c^\dagger_k + \text{h.c.}\right)\right], \tag{G.29}$$

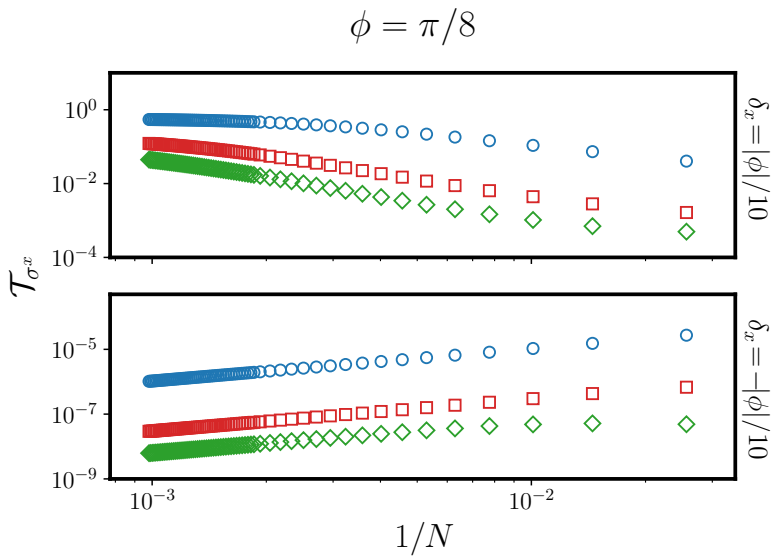

FIGURE G.1: Absolute value of the Discrete Fourier transform (DFT) of the magnetization $\langle g'| \sigma_j^x |g'\rangle$ at $\phi = \frac{\pi}{8}$, as a function of the inverse chain length, for chain lengths up to $N = 1019$. Data corresponds to the following different momenta: green diamonds $k = \frac{N\pm5}{2}$, red squares $k = \frac{N\pm3}{2}$, and blue circles $k = \frac{N\pm1}{2}$. A ferromagnetic type defect (upper panel) yields a staggered AFM order, while the presence of an antiferromagnetic one (lower panel) gives rise to an algebraic decay of the magnetization, characteristic to the presence of TF (see the text for discussion).

where the matrices $\mathbf{S} = \mathbf{S}^\dagger$ and $\mathbf{T}^\dagger = -\mathbf{T}$ can be easily obtained by inspection from eq. (G.29). In this approach, the ground state $|g'_-\rangle$ can be expressed in terms of the vectors Φ_k and Ψ_k, that are the solution of the problem:

$$\Phi_k(\mathbf{S}-\mathbf{T})(\mathbf{S}+\mathbf{T}) = \Lambda_k^2 \Phi_k, \tag{G.30}$$
$$\Phi_k(\mathbf{S}-\mathbf{T}) = \Lambda_k \Psi_k, \tag{G.31}$$

with the eigenvalues Λ_k^2 sorted in descending order. From the knowledge of Φ_k and Ψ_k it is easy to recover the correlation functions of the Majorana operators. With respect to the odd-sector ground state we have $\langle g'_-| A_j A_k |g'_-\rangle = \langle g'_-| B_j B_k |g'_-\rangle = \delta_{jk}$ and

$$-\imath \langle g'_-| A_j B_k |g'_-\rangle = \sum_{l=1}^{N-1} \Psi_{lj}\Phi_{lk}. \tag{G.32}$$

If we consider the ground state choice

$$|g'\rangle = \frac{1}{\sqrt{2}}(|g'_-\rangle + |g'_+\rangle) = \frac{1}{\sqrt{2}}(|g'_-\rangle + \Pi^x |g'_-\rangle), \tag{G.33}$$

we obtain that the site dependent expectation values of the magnetization and the nematic order parameter are

$$\begin{aligned} \langle g'| \sigma_j^x |g'\rangle &= \langle g'_-| \Pi^x \sigma_j^x |g'_-\rangle, \\ \langle g'| O_j |g'\rangle &= \langle g'_-| \Pi^x O_j |g'_-\rangle. \end{aligned} \tag{G.34}$$

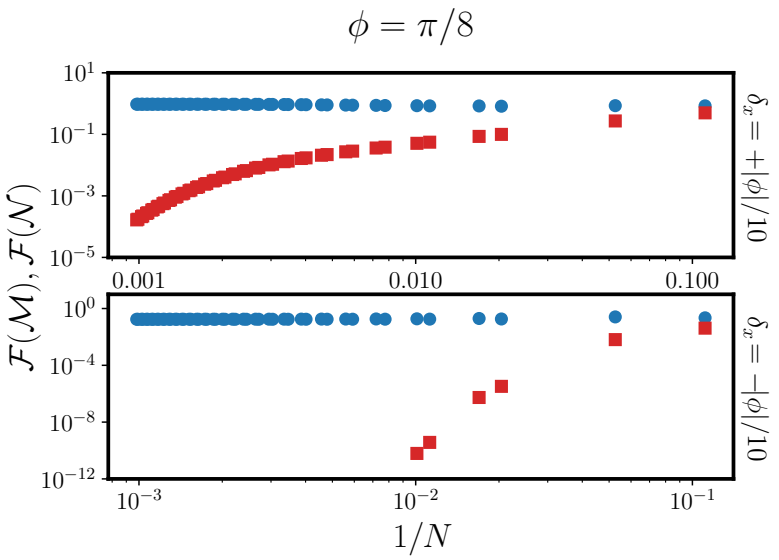

FIGURE G.2: Dependence of the absolute value of the ground state expectation values $\mathcal{F}(\mathcal{M})$ (blue circles) and $\mathcal{F}(\mathcal{N})$ (red squares), for the string operators defined in eq. (G.13), on the inverse chain length, for chain lengths up to $N = 1019$, at $\phi = \frac{\pi}{8}$. We observe that, while $\mathcal{F}(\mathcal{M})$ tends to a finite value, $\mathcal{F}(\mathcal{N})$ goes to zero. For both types of defects we have thus qualitatively a behavior as in Fig. 7.4. The exact asymptotic value for large N depends on δ_x: $\mathcal{F}(\mathcal{M}) \simeq 0.95$ and $\mathcal{F}(\mathcal{M}) \simeq 0.17$ in the upper and lower panel respectively.

These site dependent expectation values can present a complex pattern, from which the behavior in the thermodynamic limit might not be obvious. Hence, following [4] (see Appendix D) we resort to their Discrete Fourier Transform (DFT)

$$\mathcal{T}_K \equiv \frac{1}{N} \sum_{j=1}^{N} \langle g' | K_j | g' \rangle \, e^{\frac{2\pi i}{N} kj}, \quad k = 1, \ldots, N, \tag{G.35}$$

that allows a quantitative analysis of their behavior in the thermodynamic limit.

In Fig. G.1 we focus on the analysis of the magnetization, presenting the results obtained for its DFT $\mathcal{T}_{\sigma^x}$ as a function of the inverse chain length. We see that for $\delta_x > 0$ (upper panel) all sampled values go towards finite values in the thermodynamic limit, hence reproducing the typical behavior of the DFT of the staggered AFM order [4]. On the contrary, changing the sign of δ_x, the DFT goes to zero for all k, hence signaling zeroing of the magnetization independently of the site taken into account. The effect of a negative defect ($\delta_x < 0$) for $\phi > 0$ is to strengthen the AFM interaction, so reinforcing the topological frustration, while a positive defect ($\delta_x > 0$) weakens the Ising term, so reducing the effect of the frustration and, as a consequence, allowing the existence of a macroscopic phase characterized by a local magnetic order parameter. Note that the property that changing the sign of the defect yields different properties is a similar phenomenology to the quantum phase transition driven by the defect in the quantum Ising chain [67] and the XY chain [4] (see Chapter 5).

Our results imply that, while it is possible to remove the peculiar phase that we have found by the presence of a localized defect as the one we have considered, this fact depends on its sign and hence our results are, at least partially, resilient

to the presence of a defect. To further strengthen this result in Fig. G.2 we have also analyzed the behavior of the ground state expectation values of the two string order operators, $\mathcal{F}(\mathcal{M}) \equiv \langle g' | \mathcal{M} | g' \rangle = \langle g'_- | \mathcal{M} | g'_- \rangle$ and $\mathcal{F}(\mathcal{N}) \equiv \langle g' | \mathcal{N} | g' \rangle = \langle g'_- | \mathcal{N} | g'_- \rangle$, as a function of $1/N$. In the figure we can appreciate that, regardless of the sign of the defect, $\mathcal{F}(\mathcal{M})$ remains finite in the thermodynamic limit. This result is in strong agreement with the fact that the phases discovered in the 2-Cluster-Ising model are partially resilient to the presence of a localized defect.

Appendix H

Cluster-Ising Chain and Kitaev Chain: Exact Solution

This is the appendix for Chapter 8, based on the Supplementary Information for [5].

H.1 Cluster-Ising Chain

H.1.1 Diagonalization

The diagonalization of the Cluster-Ising chain is analogous to the diagonalization of the XY chain, presented in details in Appendix C.2. The Cluster-Ising Hamiltonian

$$H = \cos\phi \sum_{j=1}^{N} \sigma_j^x \sigma_{j+1}^x + \sin\phi \sum_{j=1}^{N} \sigma_{j-1}^y \sigma_j^z \sigma_{j+1}^y \tag{H.1}$$

in terms of Jordan-Wigner fermions

$$c_j = \Big(\bigotimes_{l=1}^{j-1} \sigma_l^z\Big) \frac{\sigma_j^x + \imath\sigma_j^y}{2}, \quad c_j^\dagger = \Big(\bigotimes_{l=1}^{j-1} \sigma_l^z\Big) \frac{\sigma_j^x - \imath\sigma_j^y}{2}, \tag{H.2}$$

reads

$$\begin{aligned} H = &- \cos\phi \left[\sum_{j=1}^{N-1} (c_j c_{j+1} + c_j c_{j+1}^\dagger) - \Pi^z (c_N c_1 + c_N c_1^\dagger) + \text{h.c.} \right] \\ &+ \sin\phi \left[\sum_{j=2}^{N-1} (c_{j-1} c_{j+1} - c_{j-1} c_{j+1}^\dagger) - \Pi^z (c_{N-1} c_1 + c_N c_2 - c_{N-1} c_1^\dagger - c_N c_2^\dagger) + \text{h.c.} \right]. \end{aligned} \tag{H.3}$$

Because of the presence of Π^z, the Hamiltonian is not quadratic in the fermions, but becomes such in each Π^z parity sector. Namely, we can split the Hamiltonian as

$$H = \frac{1+\Pi^z}{2} H^+ \frac{1+\Pi^z}{2} + \frac{1-\Pi_z}{2} H^- \frac{1-\Pi_z}{2}, \tag{H.4}$$

where both H^+ and H^- are quadratic. As such, they can be brought to a form of free fermions.

This is achieved by first writing $H^{\pm}$ in terms of the Fourier transformed Jordan-Wigner fermions,

$$b_q = \frac{1}{\sqrt{N}} \sum_{j=1}^{N} c_j \, e^{-\imath q j}, \quad b_q^\dagger = \frac{1}{\sqrt{N}} \sum_{j=1}^{N} c_j^\dagger \, e^{\imath q j}, \tag{H.5}$$

for $q \in \Gamma^{\pm}$, where the two sets of momenta are given by $\Gamma^- = \{2\pi k/N\}$ and $\Gamma^+ = \{2\pi(k+\frac{1}{2})/N\}$ with k running over all integers between 0 and $N-1$. Then the Bogoliubov rotation

$$\begin{aligned} a_q &= \cos\theta_q \, b_q + \imath \sin\theta_q \, b_{-q}^\dagger, \quad q \neq 0, \pi \\ a_q &= b_q, \quad q = 0, \pi \end{aligned} \tag{H.6}$$

with the Bogoliubov angle

$$\theta_q = \arctan \frac{|\sin\phi + \cos\phi \, e^{\imath 3q}| + \cos\phi\cos q - \sin\phi\cos 2q}{\cos\phi \sin q - \sin\phi \sin 2q} \tag{H.7}$$

brings $H^{\pm}$ to a free fermionic form. We end up with

$$H^{\pm} = \sum_{q \in \Gamma^{\pm}} \varepsilon_q \left(a_q^\dagger a_q - \frac{1}{2} \right), \tag{H.8}$$

where the energies are given by

$$\begin{aligned} \varepsilon_q &= 2\sqrt{1 + \sin 2\phi \cos 3q} && \forall \, q \neq 0, \pi, \\ \varepsilon_0 &= 2(\sin\phi + \cos\phi) && q = 0 \in \Gamma^-, \\ \varepsilon_\pi &= 2(\sin\phi - \cos\phi) && q = \pi \in \Gamma^+. \end{aligned} \tag{H.9}$$

The eigenstates of H are formed starting from the vacuum states $|0^{\pm}\rangle$, which satisfy $a_q |0^{\pm}\rangle = 0$ for $q \in \Gamma^{\pm}$, and applying Bogoliubov fermions creation operators, while taking care of the parity requirements in (H.4). The vacuum states are given by

$$|0^{\pm}\rangle = \prod_{0<q<\pi, \, q \in \Gamma^{\pm}} \left(\cos\theta_q - \imath \sin\theta_q \, b_q^\dagger b_{-q}^\dagger \right) |0\rangle, \tag{H.10}$$

where $|0\rangle$ is the vacuum for Jordan-Wigner fermions, satisfying $c_j |0\rangle = 0$. In particular, $|0\rangle = |\uparrow\uparrow \ldots \uparrow\rangle$ is the state of all spin up. The vacuum states $|0^+\rangle$ and $|0^-\rangle$ both have parity $\Pi^z = +1$ by construction. The parity requirements in (H.4) imply that the eigenstates of H belonging to $\Pi^z = -1$ sector are of the form $a_{q_1}^\dagger a_{q_2}^\dagger \ldots a_{q_m}^\dagger |0^-\rangle$ with $q_i \in \Gamma^-$ and m odd, while $\Pi^z = +1$ sector eigenstates are of the same form but with $q_i \in \Gamma^+$, m even and the vacuum $|0^+\rangle$ used. The ground states are given explicitly in Chapter 8.

Let us also note one technical subtlety of the model. The Bogoliubov angle θ_q, defined by (H.7) can become undefined for some modes $q \neq 0, \pi$ also point-wise, by fine–tuning of the parameters N and ϕ. The Bogoliubov angle for these modes θ_q can be defined in the same way as for modes $q = 0, \pi$ in the next section and the problem with them can be circumvented. These points do not have different expectation values of observables and can be neglected.

H.1.2 Majorana correlators

We are going to present the computation of two-point correlators of Majorana fermions

$$A_j = c_j^\dagger + c_j, \quad B_j = \imath(c_j^\dagger - c_j), \tag{H.11}$$

in the cluster phase in some details, because essentially the same reasoning is valid also for the Kitaev chain. For this computation it is convenient to write the Hamiltonians $H^\pm$ in terms of positive energy fermions d_q, that we now define. For $q \neq 0, \pi$ we put simply

$$d_q = a_q. \tag{H.12}$$

For the modes $q = 0, \pi$ the Bogoliubov angle (H.7) is undefined. We are going to define it also for these modes and use the analogoue of (H.6) to define d_q. First, we note that the Bogoliubov angle defined by (H.7) for $q \neq 0, \pi$ satisfies

$$e^{\imath 2\theta_q} = e^{-\imath 2q} \frac{\sin\phi + \cos\phi\, e^{\imath 3q}}{|\sin\phi + \cos\phi\, e^{\imath 3q}|}\,. \tag{H.13}$$

Although for modes $q = 0, \pi$ the expression (H.7) is undefined, there is no problems with expression (H.13). We exploit this property and define

$$\theta_q \equiv \frac{1}{2\imath} \log e^{\imath 2\theta_q}, \quad q = 0, \pi, \tag{H.14}$$

where by $e^{\imath 2\theta_q}$ the expression on the right hand side of (H.13) is understood. Having θ_q we define, as in (H.6),

$$d_q = \cos\theta_q\, b_q + i \sin\theta_q\, b_{-q}^\dagger, \quad q = 0, \pi. \tag{H.15}$$

Since for $q = 0, \pi$ we have

$$e^{\imath 2\theta_q} = \mathrm{sgn}(\varepsilon_q) \tag{H.16}$$

these definitions will result in the property that all fermions d_q have positive energies, i.e. we can write

$$H^\pm = \sum_{q \in \Gamma^\pm} |\varepsilon_q| \left(d_q^\dagger d_q - \frac{1}{2} \right). \tag{H.17}$$

With these definitions the ground state of H^- (H^+), let's denote it by $|g, H^-\rangle$ ($|g, H^+\rangle$) is the state that is annihilated by all d_q for $q \in \Gamma^-$ (Γ^+), i.e. $d_q\, |g, H^-\rangle = 0$.

It is easy to see from the exact solution that the ground state $|g\rangle$ of the Cluster-Ising Hamiltonian H, coincides with $|g, H^+\rangle$ for $\phi \in (\pi/4, 3\pi/4)$ and with $|g, H^-\rangle$ for $\phi \in (-3\pi/4, -\pi/4)$. We note that a typical effect of topological frustration [1, 2, 71, 73] is that $|g\rangle$ does not coincide with either of them, because of the parity requirements in (H.4), which is not the case here.

Let us thus compute the Majorana correlation functions in the state $|g, H^-\rangle$, while an identical analysis can be made also for $|g, H^+\rangle$.

From the definitions (H.12) and (H.15), we obtain

$$b_q = \cos\theta_q d_q + \imath \sin\theta_q d_{-q}^\dagger. \tag{H.18}$$

Now, using the definition (H.5) we get

$$c_j = \frac{1}{\sqrt{N}} \sum_{q\in\Gamma^-} (\cos\theta_q d_q - \imath \sin\theta_q d^\dagger_{-q}) e^{\imath qj}, \tag{H.19}$$

from which we get easily the correlation functions

$$\langle c_j c_l \rangle_{g,H^-} = \frac{\imath}{2N} \sum_{q\in\Gamma^-} \sin 2\theta_q e^{\imath q(j-l)}, \tag{H.20}$$

$$\langle c_j c^\dagger_l \rangle_{g,H^-} = \frac{1}{2N} \sum_{q\in\Gamma^-} (1+\cos 2\theta_q) e^{\imath q(j-l)}, \tag{H.21}$$

Finally, from the definition (H.11) of Majorana fermions we get

$$\langle A_j A_l \rangle_{g,H^-} = \langle B_j B_l \rangle_{g,H^-} = \delta_{jl}, \tag{H.22}$$

$$-\imath \langle A_j B_l \rangle_{g,H^-} = \frac{1}{N} \sum_{q\in\Gamma^-} e^{\imath 2\theta_q} e^{-iq(j-l)}. \tag{H.23}$$

The only difference in the ground state $|g, H^+\rangle$ is that the sum in (H.23) would be over Γ^+ instead of Γ^-. In the limit of a large system the results are the same since the sum becomes an integral, exponentially fast. We have

$$\langle A_j A_l \rangle_{g,H^\pm} = \langle B_j B_l \rangle_{g,H^\pm} = \delta_{jl}, \tag{H.24}$$

$$-\imath \langle A_j B_l \rangle_{g,H^\pm} \overset{N\to\infty}{\simeq} \int_0^{2\pi} e^{\imath 2\theta_q} e^{-iq(j-l)} \frac{dq}{2\pi}. \tag{H.25}$$

In the antiferromagnetic phase the ground state of the Cluster-Ising chain with FBCs is not anymore a vacuum state for positive energy fermions, i.e. the ground state coincides neither with the ground state of H^+ nor with the one of H^-. Instead, it corresponds to the vacuum state with one excitation on top of it. Correspondingly, the Majorana correlation functions acquire corrections of order $1/N$. For the ground state for $\phi \in (-\pi/4, 0)$ when N is divisible by 3, presented in Chapter 8, and given by

$$|g\rangle = (u_1 a^\dagger_0 + u_2 a^\dagger_{\frac{2\pi}{3}} + u_3 a^\dagger_{-\frac{2\pi}{3}}) |0^-\rangle, \tag{H.26}$$

after some algebra we get

$$\begin{aligned}\langle A_j A_l \rangle_g =& \delta_{jl} - \frac{2\imath}{N}(|u_2|^2 - |u_3|^2) \sin\left[\frac{2\pi}{3}(j-l)\right] \\ &- \frac{2\imath}{N}\left[(u_1^* u_2 - u_3^* u_1) e^{\imath\frac{\pi}{3}(j+l-1)} + \text{c.c.}\right] \sin\left[\frac{\pi}{3}(j-l)\right],\end{aligned} \tag{H.27}$$

$$\begin{aligned}\langle B_j B_l \rangle_g =& \delta_{jl} - \frac{2\imath}{N}(|u_2|^2 - |u_3|^2) \sin\left[\frac{2\pi}{3}(j-l)\right] \\ &- \frac{2\imath}{N}\left[(u_1^* u_2 - u_3^* u_1) e^{\imath\frac{\pi}{3}(j+l+1)} + \text{c.c.}\right] \sin\left[\frac{\pi}{3}(j-l)\right],\end{aligned} \tag{H.28}$$

$$\begin{aligned}-\imath \langle A_j B_l \rangle_g =& \frac{1}{N} \sum_{q\in\Gamma^-} e^{\imath 2\theta_q} e^{-\imath q(j-l)} - \frac{2}{N}\left\{|u_1|^2 + (|u_2|^2 + |u_3|^2)\cos\left[\frac{2\pi}{3}(j-l-1)\right]\right\} \\ &- \frac{2}{N}\left[(u_1^* u_2 + u_3^* u_1) e^{\imath\frac{\pi}{3}(j+l)} + \text{c.c.}\right] \cos\left[\frac{\pi}{3}(j-l-1)\right] - \frac{2}{N}\left[u_2^* u_3\, e^{-\imath\frac{2\pi}{3}(j+l)} + \text{c.c.}\right].\end{aligned} \tag{H.29}$$

The ground state and the correlators when N is not divisible by 3 can be reproduced from these expressions by taking formally $u_2 = u_3 = 0$.

H.1.3 Spin-correlation functions

In this section we compute the spin-correlation functions $\langle \sigma_1^x \sigma_{1+r}^x \rangle_g$ in the ground state $|g\rangle$ in the antiferromagnetic phase of the model, given in Chapter 8. We start from the relation

$$\sigma_1^x \sigma_{1+r}^x = (-1)^r \prod_{j=1}^{r} (-iA_{j+1}B_j) \tag{H.30}$$

and use the Wick theorem [189–192] to reduce the spin-correlation functions to the pfaffian of the Majorana correlation matrix.

Let us first discuss the applicability of the Wick theorem. When N is not divisible by 3, or when N is divisible by 3 and $u_j = 1$ for some $j \in \{1,2,3\}$, it's easy to write the ground state as a vacuum state for some fermionic operators, so the Wick theorem can be applied. In a more general case when N is divisible by 3 it's a bit more complicated. If some coefficient u_j is equal to zero then the same argument as in Appendix C.6.2 can be given for the applicability. If all of them are non-zero we proceed in the following way. First, similarly to Appendix C.6.2, we define the fermions α_q by

$$\alpha_p = \frac{1}{(|u_2|^2 + |u_3|^2)^{1/2}} \left(u_2 a_p^\dagger + u_3 a_{-p}^\dagger \right), \quad \alpha_{-p} = \frac{1}{(|u_2|^2 + |u_3|^2)^{1/2}} \left(u_3 a_p - u_2 a_{-p} \right), \tag{H.31}$$

for $p \equiv 2\pi/3$, and by $\alpha_q = a_q$ for $q \neq p, -p$. Then we make another similar step and define the fermions β_q by

$$\beta_0 = \alpha_{-p}, \quad \beta_p = u_1 a_0^\dagger + (|u_2|^2 + |u_3|^2)^{1/2} \alpha_p, \quad \beta_{-p} = (|u_2|^2 + |u_3|^2)^{1/2} a_0 - u_1 \alpha_p^\dagger,$$

and by $\beta_q = \alpha_q$ for $q \neq 0, p, -p$. Then the state (H.26) satisfies $|g\rangle = \beta_p |0^-\rangle$ and it's easy to see that it is annihilated by all β_q, i.e. we have $\beta_q |g\rangle = 0$ for all $q \in \Gamma^-$. Thus, we have expressed the ground state as the vacuum for fermions β_q. Moreover, since Majorana fermions A_j, B_j can be expressed as a linear combination of fermions $a_q, a_q^\dagger$, they can also be expressed as a linear combination of $\beta_q, \beta_q^\dagger$. Therefore, Wick theorem can be applied.

Applying the Wick theorem, we express the spin-correlation function as a pfaffian

$$\langle \sigma_1^x \sigma_{1+r}^x \rangle_g = (-1)^{r + \lfloor \frac{r}{2} \rfloor} \operatorname{pf} \begin{pmatrix} \mathbf{A} & \mathbf{C} \\ -\mathbf{C}^{\mathrm{T}} & -\mathbf{B} \end{pmatrix}. \tag{H.32}$$

Here $\mathbf{A}$ and $\mathbf{B}$ are antisymmetric $r \times r$ matrices, defined by the elements $\mathbf{A}_{j,l} = \langle A_{j+1} A_{l+1} \rangle_g$ and $\mathbf{B}_{j,l} = \langle B_j B_l \rangle_g$ for $j < l$, while $\mathbf{C}$ is an $r \times r$ matrix with the elements $\mathbf{C}_{j,l} = -\imath \langle A_{j+1} B_l \rangle_g$ (j and l range from 1 to r). In a more simple special case when the correlators $\langle A_j A_l \rangle_g$ and $\langle B_j B_l \rangle_g$ in the ground state $|g\rangle$ are zero for $j \neq l$, the spin correlations become simply the determinant

$$\langle \sigma_1^x \sigma_{1+r}^x \rangle_g = (-1)^r \det \mathbf{C}, \tag{H.33}$$

as in ref. [91].

Now let us compute the spin-correlation functions. When N is not divisible by 3 the correlators $\langle A_j A_l \rangle_g$ and $\langle B_j B_l \rangle_g$ are zero so we can use (H.33). Approximating

the sum in (H.29) by integral we get

$$\mathbf{C}_{j,l} \overset{N\to\infty}{\simeq} \int_0^{2\pi} \frac{1+\tan\phi\, e^{-\imath 3q}}{|1+\tan\phi\, e^{-\imath 3q}|} e^{-\imath q(j-l)} \frac{dq}{2\pi} - \frac{2}{N}, \tag{H.34}$$

Without the second term, that stems from frustration, we would be able to apply strong Szegő limit theorem [196, 204] to find the asymptotics of the Toeplitz determinant, and, therefore, of the spin-correlation functions. The second term is a correction, which can be understood as resulting from the part proportional to the delta function $\delta(q)$ in the symbol of the Toeplitz matrix $\mathbf{C}$. The asymptotics of such determinants has been studied in ref. [3], presented in Chapter 9. The correction to the elements of the Toeplitz matrix results in a multiplicative correction to the determinant. Using Theorem 3, from Chapter 9, in combination with the strong Szegő limit theorem [196, 204], we get

$$\langle \sigma_1^x \sigma_{1+r}^x \rangle_g \overset{r\to\infty}{\simeq} (-1)^r (1-\tan^2\phi)^{3/4} \left(1 - \frac{2r}{N}\right). \tag{H.35}$$

For a three-fold degenerate ground state when N is divisible by 3 the calculation is more complicated. Then we use directly (H.32) and resort to the numerical evaluation of pfaffians. However, we find that the result is the same, given by (H.35).

H.1.4 Expectation value of the String operator

For completeness we also compute the ground state expectation value of the string operator

$$O(r) = \sigma_1^y \sigma_2^x \Big(\bigotimes_{j=3}^{r} \sigma_j^z \Big) \sigma_{r+1}^x \sigma_{r+2}^y. \tag{H.36}$$

In terms of Majorana fermions (H.11) the operator reads

$$O(r) = \prod_{j=1}^{r} (-\imath A_j B_{j+2}). \tag{H.37}$$

Let us focus on the region $\phi \in (\pi/4, 3\pi/4)$. Since the correlators $\langle A_j A_l \rangle_g$ and $\langle B_j B_l \rangle_g$ vanish for $j \neq l$, the expectation value of the string operator can be expressed, using Wick theorem, as a determinant

$$\langle O(r) \rangle_g = \det \mathbf{D}, \tag{H.38}$$

where $\mathbf{D}$ is an $r \times r$ correlation matrix with the elements

$$\mathbf{D}_{j,l} = -\imath \langle A_j B_{l+2} \rangle_g \overset{N\to\infty}{\simeq} \int_0^{2\pi} \frac{1+\cot\phi\, e^{\imath 3q}}{|1+\cot\phi\, e^{\imath 3q}|} e^{-\imath q(j-l)} \frac{dq}{2\pi}. \tag{H.39}$$

For $\phi \in (-3\pi/4, -\pi/4)$ the only difference is that there is an additional factor $(-1)^r$ in front of the determinant in (H.38), because in this case $\sin\phi < 0$ in (H.13). The asymptotic behavior as $r \to \infty$ of the Toeplitz determinant $\det \mathbf{D}$ is obtained using

the Strong Szegő limit theorem [196, 204]. The result is

$$\langle O(r)\rangle_g \overset{r\to\infty}{\simeq} \begin{cases} (1-\cot^2\phi)^{\frac{3}{4}}, & \phi\in(\frac{\pi}{4},\frac{3\pi}{4}) \\ (-1)^r(1-\cot^2\phi)^{\frac{3}{4}}, & \phi\in(-\frac{3\pi}{4},-\frac{\pi}{4}) \end{cases} \tag{H.40}$$

H.2 Kitaev chain

The diagonalization of the Kitaev chain Hamiltonian

$$H=-\mu\sum_{j=1}^{N}\left(c_j^\dagger c_j-\frac{1}{2}\right)-\sum_{j=1}^{N}\left[w\left(c_j^\dagger c_{j+1}+\text{h.c.}\right)-\Delta\left(c_j c_{j+1}+\text{h.c.}\right)\right] \tag{H.41}$$

with periodic BC is very similar to the diagonalization of H^- of the Cluster-Ising chain, discussed in section H.1.1. The Hamiltonian is brought to a form of free fermions

$$H=\sum_{q\in\Gamma^-}\varepsilon_q\left(a_q^\dagger a_q-\frac{1}{2}\right), \tag{H.42}$$

where a_q are, again, Bogoliubov fermions, and the dispersion is now given by

$$\varepsilon_q=\sqrt{(4w\cos q+\mu)^2+4\Delta^2\sin^2 q}, \quad q\neq 0,\pi \tag{H.43}$$

$$\varepsilon_0=-2w-\mu, \tag{H.44}$$

$$\varepsilon_\pi=2w-\mu. \tag{H.45}$$

The Bogoliubov angle satisfies

$$\tan\theta_q=-\frac{|2w\cos q+\mu+2\Delta\sin q|+2w\cos q+\mu}{2\Delta\sin q} \tag{H.46}$$

and

$$e^{\imath 2\theta_q}=-\frac{2w\cos q+\mu+2\Delta\imath\sin q}{|2w\cos q+\mu+2\Delta\imath\sin q|} \tag{H.47}$$

for $q\neq 0,\pi$. Note that the mode $q=\pi$ does not exist with FBC, since N is odd and momenta are quantized as integers.

Since in the Kitaev chain we do not have parity restrictions like in (H.4), the ground state can always be written as a state annihilated by all positive energy fermions d_q, defined in section (H.1.2). This also implies that the Majorana correlation functions in the ground state are given by (H.24) and (H.25), with $e^{\imath 2\theta_q}$ given by (H.47). This is valid both for N odd and N even.

Appendix I

Toeplitz determinants with a delta function singularity

This is the appendix for Chapter 9, based on the appendix in [3].

I.1 Existence and uniqueness of the solution

For all $n \geq n_0$ we have $D_n(f) \neq 0$ so there exists a unique solution $x_j^{(n)}$, for $j = 0, 1, ..., n-1$, of the linear problem

$$\sum_{k=0}^{n-1} f_{j-k} x_k^{(n)} = y_j^{(n)}, \quad \text{for } j = 0, 1, ..., n-1, \tag{I.1}$$

for arbitrary complex numbers $y_j^{(n)}$, $j = 0, 1, \dots n-1$. We define the coefficients

$$\begin{aligned} u_j^{(n)} &= \begin{cases} \sum_{k=0}^{n-1} f_{j-k+n} x_k^{(n)}, & \text{for } j = 0, 1, 2, ... \\ 0, & \text{for } j = -1, -2, ... \end{cases}, \\ v_j^{(n)} &= \begin{cases} 0, & \text{for } j = 0, 1, 2, ... \\ \sum_{k=0}^{n-1} f_{j-k} x_k^{(n)}, & \text{for } j = -1, -2, ... \end{cases} \end{aligned} \tag{I.2}$$

and the functions

$$U^{(n)} = \sum_{j=0}^{\infty} u_j^{(n)} z^j, \qquad V^{(n)} = \sum_{j=1}^{\infty} v_{-j}^{(n)} z^{-j}. \tag{I.3}$$

The functions $U^{(n)}$ and $V^{(n)}$ are well defined, and therefore analytic, on the same annulus as $f(z)$, the one defined by (9.7). To see this pick some z from the annulus. We have

$$\begin{aligned} \sum_{j=1}^{\infty} |v_{-j}^{(n)}||z|^{-j} &\leq \sum_{j=1}^{\infty} \sum_{k=0}^{n-1} |f_{-j-k}||x_k^{(n)}||z|^{-j} = \sum_{k=0}^{n-1} |x_k^{(n)}||z|^k \sum_{j=1}^{\infty} |f_{-j-k}||z|^{-j-k} \\ &\leq \Big(\sum_{j=-\infty}^{\infty} |f_j||z|^j \Big) \Big(\sum_{k=0}^{n-1} |x_k^{(n)}||z|^k \Big) < \infty \,, \end{aligned} \tag{I.4}$$

where the last inequality holds because Laurent series is absolutely convergent in the interior of its annulus. In an analogous way it is shown that $U^{(n)}$ is well defined.

It follows from definition (I.2) that the equation

$$\sum_{k=0}^{n-1} f_{j-k} x_k^{(n)} = y_j^{(n)} + u_{j-n}^{(n)} + v_j^{(n)}, \tag{I.5}$$

with $y_j^{(n)}$ defined to be zero for $j < 0$ and $j \geq n$, holds for all $j \in \mathbb{Z}$. Multiplying the equation by z^j, with z belonging to the annulus (9.7), and summing from $j = -\infty$ to $j = \infty$ it follows

$$f(z)X^{(n)}(z) = Y^{(n)}(z) + U^{(n)}(z)z^n + V^{(n)}(z)\ , \tag{I.6}$$

where

$$X^{(n)}(z) = \sum_{j=0}^{n-1} x_j^{(n)} z^j, \quad Y^{(n)}(z) = \sum_{j=0}^{n-1} y_j^{(n)} z^j. \tag{I.7}$$

Thus we have shown that, for arbitrary polynomials $Y^{(n)}$ of degree not greater than $n-1$, i.e. analytic functions with the properties

$$\left[Y^{(n)}\right]_- = 0, \quad \left[Y^{(n)} z^{-n}\right]_+ = 0, \tag{I.8}$$

that the functions $X^{(n)}, U^{(n)}, V^{(n)}$ are the solution of the functional equation

$$fX^{(n)} = Y^{(n)} + U^{(n)} z^n + V^{(n)} \tag{I.9}$$

on the annulus and by construction they have the properties

$$\left[X^{(n)}\right]_- = 0, \quad \left[X^{(n)} z^{-n}\right]_+ = 0, \quad \left[U^{(n)}\right]_- = 0, \quad \left[V^{(n)}\right]_+ = 0\ . \tag{I.10}$$

The uniqueness of the solution of (I.1) implies the uniqueness of the solution of (I.9) under constraint (I.10).

I.2 Wiener-Hopf procedure

I.2.1 Wiener-Hopf equations

We assume $\nu \geq 0$. The determinant (9.1) for $\nu < 0$ can be obtained simply by transposing the Toeplitz matrix for the opposite sign of ν and making the integral transformation $\theta \to -\theta$. From (I.9) it follows, separating the components,

$$a_+ z^\nu X^{(n)} - \left[a_-^{-1} Y^{(n)}\right]_+ - \left[a_-^{-1} U^{(n)} z^n\right]_+ = a_-^{-1} V^{(n)} + \left[a_-^{-1} Y^{(n)}\right]_- + \left[a_-^{-1} U^{(n)} z^n\right]_-, \tag{I.11}$$

where $a_\pm$ have been defined in (9.8). We now use the standard Wiener-Hopf argument [204]. Namely, the properties (I.10) imply that through it's Laurent series the left-hand side defines a function analytic on $|z| < \rho_+$, while the right-hand side defines a function analytic on $|z| > \rho_-$, that goes to zero for $|z| \to \infty$. The two sides together define a function analytic on the whole plane and zero at infinity, thus, by Liouville's theorem, zero on the whole plane. It follows

$$X^{(n)} z^\nu = a_+^{-1}\left(\left[a_-^{-1} Y^{(n)}\right]_+ + \left[a_-^{-1} U^{(n)} z^n\right]_+\right), \tag{I.12}$$

$$V^{(n)} = -a_-\left(\left[a_-^{-1} Y^{(n)}\right]_- + \left[a_-^{-1} U^{(n)} z^n\right]_-\right). \tag{I.13}$$

Similarly, denoting

$$\alpha_k^{(n)} = \left(a_+^{-1} U^{(n)} z^{-\nu}\right)_{-k}, \tag{I.14}$$

and multiplying (I.9) by $a_+^{-1} z^{-(n+\nu)}$, we can make the separation

$$\begin{aligned}\left(a_+^{-1} U^{(n)} z^{-\nu} - \sum_{k=1}^{\nu} \alpha_k^{(n)} z^{-k}\right) + \left[a_+^{-1} Y^{(n)} z^{-(n+\nu)}\right]_+ + \left[a_+^{-1} V^{(n)} z^{-(n+\nu)}\right]_+ \\ = a_- X^{(n)} z^{-n} - \left[a_+^{-1} Y^{(n)} z^{-(n+\nu)}\right]_- - \left[a_+^{-1} V^{(n)} z^{-(n+\nu)}\right]_- - \sum_{k=1}^{\nu} \alpha_k^{(n)} z^{-k}.\end{aligned} \tag{I.15}$$

It follows

$$U^{(n)} z^{-\nu} = -a_+\left(\left[a_+^{-1} Y^{(n)} z^{-(n+\nu)}\right]_+ + \left[a_+^{-1} V^{(n)} z^{-(n+\nu)}\right]_+\right) + a_+ \sum_{k=1}^{\nu} \alpha_k^{(n)} z^{-k}, \tag{I.16}$$

$$X^{(n)} z^{-n} = a_-^{-1}\left(\left[a_+^{-1} Y^{(n)} z^{-(n+\nu)}\right]_- + \left[a_+^{-1} V^{(n)} z^{-(n+\nu)}\right]_-\right) + a_-^{-1} \sum_{k=1}^{\nu} \alpha_k^{(n)} z^{-k}. \tag{I.17}$$

This result is also valid for $\nu = 0$ adopting the convention $\sum_{k=1}^{0} = 0$.

The solution of the set of equations (I.12), (I.13), (I.16) and (I.17), together with the requirement

$$\left(X^{(n)} z^{\nu}\right)_j = 0 \quad \text{for } j = 0, 1, ..., \nu - 1, \tag{I.18}$$

that fixes the coefficients $\alpha_1^{(n)}, \alpha_2^{(n)}, ..., \alpha_\nu^{(n)}$, is the solution of (I.9) with the desired properties (I.10).

I.2.2 The solution

In this section we solve asymptotically the functional equation (I.9) with $Y^{(n)}$ defined by (9.26) and (9.27). For the set of equations (I.12), (I.13), (I.16) and (I.17) a solution in the closed form might not exist so we follow the standard approach [204, 205] and we look for the solution by making an assumption on the function $U^{(n)}$ and then checking whether the final solution we obtain is consistent with this assumption.

We assume that

$$\begin{aligned}&U^{(n)} z^{-\nu} - a_+ \sum_{k=1}^{\nu} \alpha_k^{(n)} z^{-k} = O(1) \\ &\text{uniformly in } z, \text{ on } \rho \le |z| \le \rho^{-1}, \text{ for all } \rho \text{ defined by (9.10).}\end{aligned} \tag{I.19}$$

The second term in (I.13) is equal to

$$\left[a_-^{-1} U^{(n)} z^n\right]_- = \left[a_-^{-1} z^{n+\nu}\left(U^{(n)} z^{-\nu} - a_+ \sum_{k=1}^{\nu} \alpha_k^{(n)} z^{-k}\right)\right]_- + \left[a_+ a_-^{-1} \sum_{k=1}^{\nu} \alpha_k^{(n)} z^{n+\nu-k}\right]_-. \tag{I.20}$$

Applying Lemma 2 on the first term in (I.20) gives

$$\left[a_-^{-1} U^{(n)} z^n\right]_- = \left[a_+ a_-^{-1} \sum_{k=1}^{\nu} \alpha_k^{(n)} z^{n+\nu-k}\right]_- + O(\rho^n), \tag{I.21}$$

where $O(\rho^n)$ holds on $\rho \le |z| \le \rho^{-1}$, uniformly in z, for all ρ satisfying (9.10). From now on it is always the case and we don't write every time that O holds uniformly

in z on $\rho \le |z| \le \rho^{-1}$, for all ρ satisfying (9.10). We can thus write (I.13) as

$$V^{(n)}(z) = -a_-(z)\left[a_-^{-1}Y^{(n)}\right]_-(z) - a_-(z)\sum_{k=1}^{\nu}\alpha_k^{(n)}\left[a_+a_-^{-1}z^{n+\nu-k}\right]_-(z) + O(\rho^n). \quad \text{(I.22)}$$

We use (9.33) to rewrite the first term on the RHS of (I.22) as

$$\left[a_-^{-1}Y^{(n)}\right]_- = e^{-\imath(n-1)\theta_0}\left[\frac{a_-^{-1}z^n}{z-e^{\imath\theta_0}}\right]_-^{(<)} - e^{\imath\theta_0}\left[\frac{a_-^{-1}}{z-e^{\imath\theta_0}}\right]_-^{(<)}. \quad \text{(I.23)}$$

The first term here is $O(\rho^n)$ by Lemma 2. Applying Lemma 1 to the second term gives

$$\left[a_-^{-1}Y^{(n)}\right]_-(z) = -e^{\imath\theta_0}\frac{a_-^{-1}(z)-a_-^{-1}(e^{\imath\theta_0})}{z-e^{\imath\theta_0}} + O(\rho^n) \quad \text{for } z \neq e^{\imath\theta_0}, \rho \le |z| \le \rho^{-1}. \quad \text{(I.24)}$$

The value at $z = e^{\imath\theta_0}$ is obtained by continuity and from now on we omit writing $z \neq e^{\imath\theta_0}, \rho \le |z| \le \rho^{-1}$ every time. It follows

$$V^{(n)}(z) = e^{\imath\theta_0}a_-(z)\frac{a_-^{-1}(z)-a_-^{-1}(e^{\imath\theta_0})}{z-e^{\imath\theta_0}} - a_-(z)\sum_{k=1}^{\nu}\alpha_k^{(n)}\left[a_-^{-1}a_+z^{n+\nu-k}\right]_-(z) + O(\rho^n)\,. \quad \text{(I.25)}$$

This expression can be used in (I.16) to find $U^{(n)}$. Before we do so, we use (9.33) again to get for the first term on the RHS of (I.16):

$$\left[a_+^{-1}Y^{(n)}z^{-(n+\nu)}\right]_+ = e^{-\imath(n-1)\theta_0}\left[\frac{a_+^{-1}z^{-\nu}}{z-e^{\imath\theta_0}}\right]_+^{(>)} - e^{\imath\theta_0}\left[\frac{a_+^{-1}z^{-(n+\nu)}}{z-e^{\imath\theta_0}}\right]_+^{(>)}. \quad \text{(I.26)}$$

The second term is $O(\rho^n)$ by Lemma 2. Applying Lemma 1 to the first term we get

$$\left[a_+^{-1}Y^{(n)}z^{-(n+\nu)}\right]_+(z) = e^{-\imath(n-1)\theta_0}\frac{[a_+^{-1}z^{-\nu}]_+(z)-[a_+^{-1}z^{-\nu}]_+(e^{\imath\theta_0})}{z-e^{\imath\theta_0}} + O(\rho^n)\,. \quad \text{(I.27)}$$

We can now substitute (I.25) in (I.16) and apply Lemma 2 to the second term on the RHS of (I.16) to get

$$\left[a_+^{-1}V^{(n)}z^{-(n+\nu)}\right]_+(z) = -\sum_{k=1}^{\nu}\alpha_k^{(n)}\left[a_-a_+^{-1}z^{-(n+\nu)}\left[a_-^{-1}a_+z^{n+\nu-k}\right]_-\right]_+(z) + O(\rho^n)\,. \quad \text{(I.28)}$$

Collecting everything it follows from (I.16)

$$\begin{aligned} U^{(n)}z^{-\nu} = &-e^{-\imath(n-1)\theta_0}a_+(z)\frac{[a_+^{-1}z^{-\nu}]_+(z)-[a_+^{-1}z^{-\nu}]_+(e^{\imath\theta_0})}{z-e^{\imath\theta_0}} + \\ &+ a_+(z)\sum_{k=1}^{\nu}\alpha_k^{(n)}\left(z^{-k} + \left[a_-a_+^{-1}z^{-(n+\nu)}\left[a_-^{-1}a_+z^{n+\nu-k}\right]_-\right]_+(z)\right) + O(\rho^n). \end{aligned} \quad \text{(I.29)}$$

The coefficients $\alpha_1^{(n)}, \alpha_2^{(n)}, \ldots, \alpha_\nu^{(n)}$ remain to be determined. However, if we assume that, for sufficiently small ρ, they satisfy

$$\alpha_k^{(n)}O(\rho^{2n}) = O(1), \quad \text{for } k = 1, 2, \ldots, \nu, \quad \text{(I.30)}$$

then, taking a ρ_1 such that $\rho_- < \rho_1 < \rho < 1 < \rho^{-1} < \rho_1^{-1} < \rho_+$, the last term in (I.29) is, by Lemma 2,

$$a_+(z)\sum_{k=1}^{\nu}\alpha_k^{(n)}\left[a_-a_+^{-1}z^{-(n+\nu)}\left[a_-^{-1}a_+z^{n+\nu-k}\right]_-\right]_+(z) = a_+(z)\sum_{k=1}^{\nu}\alpha_k^{(n)}O(\rho_1^{2n}) = O\big((\rho_1/\rho)^2\big),$$

on $\rho \le |z| \le \rho^{-1}$.

(I.31)

It follows

$$U^{(n)}z^{-\nu} = -e^{-\imath(n-1)\theta_0}a_+(z)\frac{[a_+^{-1}z^{-\nu}]_+(z) - [a_+^{-1}z^{-\nu}]_+(e^{\imath\theta_0})}{z-e^{\imath\theta_0}} + a_+(z)\sum_{k=1}^{\nu}\alpha_k^{(n)}z^{-k} + O(\sigma^n), \tag{I.32}$$

where $\sigma = \max\{(\rho_1/\rho)^2, \rho\}$. Then (I.32) is consistent with the starting assumption (I.19), while assumption (I.30) will be checked below for its consistency.

Finally, $X^{(n)}$ is computed using (I.12). The first term in (I.12) is found from (9.33) and (I.24), using

$$\left[a_-^{-1}Y^{(n)}\right]_+ = a_-^{-1}Y^{(n)} - \left[a_-^{-1}Y^{(n)}\right]_- . \tag{I.33}$$

We get

$$\left[a_-^{-1}Y^{(n)}\right]_+(z) = e^{-\imath(n-1)\theta_0}\frac{a_-^{-1}(z)z^n - a_-^{-1}(e^{\imath\theta_0})e^{\imath n\theta_0}}{z-e^{\imath\theta_0}} + O(\rho^n). \tag{I.34}$$

The second term in (I.12) is found from (I.21) and (I.32),

$$\begin{aligned}
\left[a_-^{-1}U^{(n)}z^n\right]_+ &= a_-^{-1}U^{(n)}z^n - \left[a_-^{-1}U^{(n)}z^n\right]_- \\
&= -e^{-\imath(n-1)\theta_0}a_-^{-1}(z)a_+(z)z^{n+\nu}\frac{a_+^{-1}(z)z^{-\nu} - a_+^{-1}(e^{\imath\theta_0})e^{-\imath\nu\theta_0}}{z-e^{\imath\theta_0}} \\
&\quad + e^{-\imath(n-1)\theta_0}a_-^{-1}(z)a_+(z)z^{n+\nu}\sum_{k=0}^{\nu-1}(a_+^{-1})_k\frac{z^{k-\nu} - e^{\imath(k-\nu)\theta_0}}{z-e^{\imath\theta_0}} \\
&\quad + \left[a_+a_-^{-1}\sum_{k=1}^{\nu}\alpha_k^{(n)}z^{n+\nu-k}\right]_+(z) + O(\sigma^n) ,
\end{aligned} \tag{I.35}$$

where we used

$$\left[a_+^{-1}z^{-\nu}\right]_+ = a_+^{-1}z^{-\nu} - \sum_{k=0}^{\nu-1}(a_+^{-1})_k z^{k-\nu} . \tag{I.36}$$

Now, summing (I.34) and (I.35) in (I.12) gives

$$\begin{aligned}
X^{(n)}(z)z^{\nu} =& e^{-\imath(n+\nu-1)\theta_0}a_+^{-1}(z)a_+^{-1}(e^{\imath\theta_0})\frac{a_+(z)a_-^{-1}(z)z^{n+\nu} - a_+(e^{\imath\theta_0})a_-^{-1}(e^{\imath\theta_0})e^{\imath(n+\nu)\theta_0}}{z-e^{\imath\theta_0}} \\
&+ e^{-\imath(n-1)\theta_0}a_-^{-1}(z)z^{n+\nu}\sum_{k=0}^{\nu-1}(a_+^{-1})_k\frac{z^{k-\nu} - e^{\imath(k-\nu)\theta_0}}{z-e^{\imath\theta_0}} \\
&+ a_+^{-1}(z)\sum_{k=1}^{\nu}\alpha_k^{(n)}\left[a_-^{-1}a_+z^{n+\nu-k}\right]_+(z) + O(\sigma^n) .
\end{aligned} \tag{I.37}$$

It remains to determine the coefficients $\alpha_1^{(n)}, \alpha_2^{(n)}, ..., \alpha_\nu^{(n)}$ from requirement (I.18) and to see whether (I.30) is satisfied. We compute the coefficients $(X^{(n)}z^{-\nu})_j$ by (9.31), integrating at $|w| = \rho$. All the terms in (I.37) containing the factor z^n result in

$O(\rho^n)$ corrections, while

$$\frac{1}{2\pi\imath}\oint_{|w|=\rho}\frac{a_+^{-1}(w)}{w-e^{\imath\theta_0}}\frac{dw}{w^{j+1}}=-e^{-\imath\theta_0}\sum_{k=0}^{j}\left(a_+^{-1}\right)_k e^{-\imath(j-k)\theta_0}. \tag{I.38}$$

It follows

$$\left(X^{(n)}z^\nu\right)_j=\sum_{k=1}^{\nu}\alpha_k^{(n)}\left(a_+^{-1}\left[cz^{n+\nu-k}\right]_+\right)_j+a_-^{-1}(e^{\imath\theta_0})\sum_{k=0}^{j}\left(a_+^{-1}\right)_k e^{-\imath(j-k)\theta_0}+O(\sigma^n), \tag{I.39}$$

where $c=a_+a_-^{-1}$.

Thus if the coefficients $\alpha_1^{(n)},\alpha_2^{(n)},...,\alpha_\nu^{(n)}$ satisfy

$$0=\sum_{k=1}^{\nu}\alpha_k^{(n)}\left(a_+^{-1}\left[cz^{n+\nu-k}\right]_+\right)_j+a_-^{-1}(e^{\imath\theta_0})\sum_{k=0}^{j}\left(a_+^{-1}\right)_k e^{-\imath(j-k)\theta_0},\quad \text{for } j=0,1,...,\nu-1, \tag{I.40}$$

then

$$\left(X^{(n)}z^\nu\right)_j=O(\sigma^n),\quad \text{for } j=0,1,...,\nu-1. \tag{I.41}$$

Using

$$\left(a_+^{-1}\left[cz^{n+\nu-k}\right]_+\right)_j=\sum_{m=0}^{j}\left(a_+^{-1}\right)_m c_{j-m-n-\nu+k} \tag{I.42}$$

it's easy to see that (I.40) is equivalent to

$$\sum_{k=1}^{\nu}\alpha_k^{(n)}c_{j-n-\nu+k}=-a_-^{-1}(e^{\imath\theta_0})e^{-\imath j\theta_0},\quad \text{for } j=0,1,...,\nu-1. \tag{I.43}$$

The set of equations (I.43) is solved by Cramer's rule. The solution is

$$\alpha_j^{(n)}=-a_-^{-1}(e^{\imath\theta_0})e^{-\imath(\nu-1)\theta_0}\frac{\tilde{\Delta}_{\nu,n}(j)}{\Delta_{\nu,n}} \tag{I.44}$$

where $\Delta_{\nu,n}$ and $\tilde{\Delta}_{\nu,n}(j)$ are defined by (9.12) and (9.14) respectively. We see that the condition (I.19) of Theorem 4 ensures that the assumption (I.30) is satisfied.

The solution of equations (I.12), (I.13) and (I.16) we have found is consistent with assumptions (I.19) and (I.30), that we have made to find it, up to $O(\sigma^n)$ terms. On the basis of this solution we construct the functions $X_1^{(n)}$, $U_1^{(n)}$ and $V_1^{(n)}$ discussed in sections 9.2.4 and 9.2.5.

I.3 Remarks on rigor

To prove theorems 3 and 4 we have used the intuitive property that a small perturbation to the functional equation (I.9) results only in a small perturbation to the solutions. Here we show it rigorously for the case of a zero winding number of the symbol, and thus make Theorem 3 rigorous.

The result we need is given by Lemma 3, that we are going to state and prove. The proof of the lemma uses a similar procedure to the one used in the proof of Szegő theorem in chapter X of [204], based on the Wiener-Hopf equations. Let us note that the complication with non-zero winding number is the presence of the third term in (I.16) and we omit this case.

Before introducing the lemma let us introduce two norms for functions analytic on an annulus around the unit circle. The first one is the supremum norm on the unit circle. Let g be analytic on the annulus $\rho_- < |z| < \rho_+$ that includes the unit circle. We define

$$\|g\| = \sup_{z\in\mathbb{C}:|z|=1} |g(z)|. \tag{I.45}$$

The second norm is defined as the sum of the absolute values of Laurent series coefficients of g, which is well defined since the Laurent series is absolutely convergent in the interior of its annulus. If $g(z) = \sum_{j=-\infty}^{\infty} g_j z^j$, we denote

$$\|g\|_1 = \sum_{j=-\infty}^{\infty} |g_j|. \tag{I.46}$$

We have clearly

$$\|g\| \le \|g\|_1 . \tag{I.47}$$

Let us discuss the properties of the norms related to the components (9.25). From their integral representation (9.30) we have

$$\|[g]_-\| \le \frac{\rho_1}{1-\rho_1} \sup_{z:|z|=\rho_1} \{|g(z)|\}, \qquad \|[g]_+\| \le \frac{\rho_2}{\rho_2-1} \sup_{z:|z|=\rho_2} |g(z)|, \tag{I.48}$$

for any choice $\rho_1 \in (\rho_-, 1), \rho_2 \in (1, \rho_+)$. On the other hand, the second norm clearly satisfies

$$\|[g]_-\|_1 \le \|g\|_1 , \qquad \|[g]_+\|_1 \le \|g\|_1 . \tag{I.49}$$

If g and h are two functions analytic on an annulus around the unit circle we have

$$\|gh\| \le \|g\|\,\|h\| , \qquad \|gh\|_1 \le \|g\|_1\,\|h\|_1 , \tag{I.50}$$

where the first inequality is trivial and the second is proven easily using the absolute convergence of the Laurent series inside the annulus. Finally, for a sequence of functions $(g^{(n)})_{n\in\mathbb{N}}$ analytic on an annulus around the unit circle and a sequence of positive numbers $(s_n)_{n\in\mathbb{N}}$ we have clearly that

$$\begin{aligned} &g^{(n)}(z) = O(s_n) \quad \text{uniformly in } z \text{ on the unit circle } |z| = 1 \\ &\text{if and only if} \quad \left\|g^{(n)}\right\| = O(s_n). \end{aligned} \tag{I.51}$$

Lemma 3. *Let a be non-zero analytic function on an annulus around the unit circle, defined by (9.7), and with a zero winding number. Let $Y_j^{(n)}$, for $j = 1, 2$ and $n \in \mathbb{N}$, be polynomials of degree not greater than $n-1$, i.e. analytic functions with*

$$\left[Y_j^{(n)}\right]_- = 0, \quad \left[Y_j^{(n)} z^{-n}\right]_+ = 0, \tag{I.52}$$

and let $X_j^{(n)}, U_j^{(n)}, V_j^{(n)}$, for $j = 1, 2$, be analytic solutions of the functional equation

$$aX_j^{(n)} = Y_j^{(n)} + U_j^{(n)} z^n + V_j^{(n)} \tag{I.53}$$

on the annulus, such that they satisfy the properties

$$\left[X_j^{(n)}\right]_- = 0, \quad \left[X_j^{(n)} z^{-n}\right]_+ = 0, \quad \left[U_j^{(n)}\right]_- = 0, \quad \left[V_j^{(n)}\right]_+ = 0 . \tag{I.54}$$

If

$$Y_1^{(n)}(z) - Y_2^{(n)}(z) = O(s_n) \quad \textit{uniformly in } z \textit{ on the unit circle } |z| = 1 \tag{I.55}$$

then

$$X_1^{(n)}(z) - X_2^{(n)}(z) = O(ns_n) \quad \textit{uniformly in } z \textit{ on the unit circle } |z| = 1. \tag{I.56}$$

Proof. Defining

$$Y^{(n)} = Y_1^{(n)} - Y_2^{(n)}, \quad X^{(n)} = X_1^{(n)} - X_2^{(n)}, \quad U^{(n)} = U_1^{(n)} - U_2^{(n)}, \quad V^{(n)} = V_1^{(n)} - V_2^{(n)}, \tag{I.57}$$

proving the lemma becomes equivalent to showing that if $\left\|Y^{(n)}\right\| = O(s_n)$ then the solution $X^{(n)}$ of the problem (I.9) (for $\nu = 0$) and (I.10) satisfies $\left\|X^{(n)}\right\| = O(ns_n)$.

The lines of the proof are the following. First we use the Wiener-Hopf equations (I.13) and (I.16) to show that $\left\|U^{(n)}\right\| = O(ns_n)$ and $\left\|V^{(n)}\right\| = O(ns_n)$. Then we recognize that directly from (I.9) and the properties of the norm it follows

$$\|X^n\| \leq \left\|a^{-1}\right\| \left(\left\|Y^{(n)}\right\| + \left\|U^{(n)}\right\| + \left\|V^{(n)}\right\| \right), \tag{I.58}$$

and conclude that since the right hand side of the inequality is $O(ns_n)$, so is the left side.

We now work out the details. Note first that the Laurent series coefficients $y_j^{(n)}$ of the function $Y^{(n)}(z) = \sum_{j=0}^{n-1} y_j^{(n)} z^j$ satisfy $|y_j^{(n)}| \leq \left\|Y^{(n)}\right\|$, which can be seen easily from the integral representation of the coefficients. It follows

$$\left\|Y^{(n)}\right\|_1 \leq n \left\|Y^{(n)}\right\|. \tag{I.59}$$

From the Wiener-Hopf equation (I.13) we get

$$\left\|V^{(n)}\right\| = \|a_-\| \left\|\left[a_-^{-1} Y^{(n)}\right]_-\right\| + \|a_-\| \left\|\left[a_-^{-1} U^{(n)} z^n\right]_-\right\|. \tag{I.60}$$

To bound the first term we notice

$$\left\|\left[a_-^{-1} Y^{(n)}\right]_-\right\| \leq \left\|\left[a_-^{-1} Y^{(n)}\right]_-\right\|_1 \leq \left\|a_-^{-1} Y^{(n)}\right\|_1 \leq \left\|a_-^{-1}\right\|_1 \left\|Y^{(n)}\right\|_1 \leq \left\|a_-^{-1}\right\|_1 n \left\|Y^{(n)}\right\|, \tag{I.61}$$

where all the inequalities except the last follow simply from the discussed properties of the norms, and the last one follows from (I.59). To bound the second term in (I.60) we use (I.48) with $\rho_1 = \rho$ for some ρ defined by (9.10). We have

$$\left\|\left[a_-^{-1} U^{(n)} z^n\right]_-\right\| \leq \frac{\rho^{n+1}}{1-\rho} \sup_{z:|z|=\rho} \{|a_-^{-1}(z) U^{(n)}(z)|\}. \tag{I.62}$$

Since the Laurent series coefficients of $U^{(n)}$ define a function analytic inside the whole circle $|z| < \rho^{-1}$ we can apply the maximum modulus principle to conclude

$$\sup_{z:|z|=\rho} \{|U^{(n)}(z)|\} \leq \sup_{z:|z|=1} \{|U^{(n)}(z)|\} = \left\|U^{(n)}\right\|. \tag{I.63}$$

It follows

$$\left\| \left[a_-^{-1} U^{(n)} z^n \right]_- \right\| \leq \frac{\rho^{n+1}}{1-\rho} \sup_{z:|z|=\rho} \{ |a_-^{-1}(z)| \} \left\| U^{(n)} \right\| . \tag{I.64}$$

We conclude that there are positive constants λ_1 and λ_2 (independent of n) such that

$$\left\| V^{(n)} \right\| \leq \lambda_1 n \left\| Y^{(n)} \right\| + \lambda_2 \rho^n \left\| U^{(n)} \right\| . \tag{I.65}$$

Using the same methods we conclude from the Wiener-Hopf equation (I.16) that there are positive constants λ_3 and λ_4 such that

$$\left\| U^{(n)} \right\| \leq \lambda_3 n \left\| Y^{(n)} \right\| + \lambda_4 \rho^n \left\| V^{(n)} \right\| . \tag{I.66}$$

We have obtained a system of two inequalities. Inserting the second into the first, and rearranging the terms, we get

$$(1 - \lambda_2 \lambda_4 \rho^{2n}) \left\| V^{(n)} \right\| \leq (\lambda_1 + \lambda_2 \lambda_3 \rho^n) n \left\| Y^{(n)} \right\| . \tag{I.67}$$

For sufficiently large n the factor on the right is positive and greater than, say, $1/2$, so we conclude

$$\left\| V^{(n)} \right\| = O(n s_n). \tag{I.68}$$

Using (I.66) again we get also

$$\left\| U^{(n)} \right\| = O(n s_n). \tag{I.69}$$

Finally, from (I.58) we get then $\left\| X^{(n)} \right\| = O(n s_n)$, which completes the proof. □

In applying Lemma 3 for functions $Y_2^{(n)}$ and $Y^{(n)}$ in section 9.2.4 we have $s_n = \rho^n$, for any ρ defined by (9.10). Note that since ρ can always be made smaller, the factor n in $O(n s_n)$ in (I.56) is irrelevant.

Bibliography

[1] V. Marić, S. M. Giampaolo, D. Kuić, and F. Franchini, "The frustration of being odd: how boundary conditions can destroy local order", New Journal of Physics **22**, 083024 (2020).

[2] V. Marić, S. M. Giampaolo, and F. Franchini, "Quantum phase transition induced by topological frustration", Communications Physics **3**, 220 (2020).

[3] V. Marić and F. Franchini, "Asymptotic behavior of toeplitz determinants with a delta function singularity", Journal of Physics A: Mathematical and Theoretical **54**, 025201 (2020).

[4] G. Torre, V. Marić, F. Franchini, and S. M. Giampaolo, "Effects of defects in the xy chain with frustrated boundary conditions", Phys. Rev. B **103**, 014429 (2021).

[5] V. Marić, F. Franchini, D. Kuić, and S. M. Giampaolo, "Resilience of the topological phases to frustration", Scientific Reports **11**, 6508 (2021).

[6] V. Marić, S. M. Giampaolo, and F. Franchini, *The fate of local order in topologically frustrated spin chains*, 2021, arXiv:2101.07276 [cond-mat.stat-mech].

[7] V. Marić, G. Torre, F. Franchini, and S. M. Giampaolo, *Topological frustration can modify the nature of a quantum phase transition*, 2021, arXiv:2101.08807 [cond-mat.stat-mech].

[8] G. Torre, V. Marić, D. Kuić, F. Franchini, and S. M. Giampaolo, *An odd thermodynamic limit for the loschmidt echo*, 2021, arXiv:2105.06483 [cond-mat.stat-mech].

[9] G. Mussardo, *Statistical field theory: an introduction to exactly solved models in statistical physics*, eng, 2nd ed., Oxford Graduate Texts (Oxford University Press, Oxford, 2020), p. 1024.

[10] S. Sachdev, *Quantum phase transitions*, 2nd ed. (Cambridge University Press, 2011).

[11] A. J. Beekman, L. Rademaker, and J. van Wezel, "An Introduction to Spontaneous Symmetry Breaking", SciPost Phys. Lect. Notes, 11 (2019).

[12] H. T. Diep and H. Giacomini, "Frustration — exactly solved frustrated models", in *Frustrated spin systems*, 2nd (World Scientific, Singapore, 2013), pp. 1–58.

[13] J. T. Chalker, "Geometrically frustrated antiferromagnets: statistical mechanics and dynamics", in *Introduction to frustrated magnetism: materials, experiments, theory*, edited by C. Lacroix, P. Mendels, and F. Mila (Springer Berlin Heidelberg, Berlin, Heidelberg, 2011), pp. 3–22.

[14] G. H. Wannier, "Antiferromagnetism. the triangular ising net", Phys. Rev. **79**, 357–364 (1950).

[15] R. Houtappel, "Order-disorder in hexagonal lattices", Physica **16**, 425–455 (1950).

[16] J. Stephenson, "Ising-model spin correlations on the triangular lattice. iii. isotropic antiferromagnetic lattice", Journal of Mathematical Physics **11**, 413–419 (1970).

[17] R. Moessner and J. T. Chalker, "Properties of a classical spin liquid: the heisenberg pyrochlore antiferromagnet", Phys. Rev. Lett. **80**, 2929–2932 (1998).

[18] R. Moessner and J. T. Chalker, "Low-temperature properties of classical geometrically frustrated antiferromagnets", Phys. Rev. B **58**, 12049–12062 (1998).

[19] S. T. Bramwell, M. J. P. Gingras, and P. C. W. Holdsworth, "Spin ice", in *Frustrated spin systems*, 2nd (World Scientific, Singapore, 2013), pp. 383–474.

[20] C. L. Henley, "Power-law spin correlations in pyrochlore antiferromagnets", Phys. Rev. B **71**, 014424 (2005).

[21] D. A. Huse, W. Krauth, R. Moessner, and S. L. Sondhi, "Coulomb and liquid dimer models in three dimensions", Phys. Rev. Lett. **91**, 167004 (2003).

[22] C. Castelnovo, R. Moessner, and S. L. Sondhi, "Magnetic monopoles in spin ice", Nature **451**, 42–45 (2008).

[23] D. J. P. Morris, D. A. Tennant, S. A. Grigera, B. Klemke, C. Castelnovo, R. Moessner, C. Czternasty, M. Meissner, K. C. Rule, J.-U. Hoffmann, K. Kiefer, S. Gerischer, D. Slobinsky, and R. S. Perry, "Dirac strings and magnetic monopoles in the spin ice dy2ti2o7", Science **326**, 411–414 (2009).

[24] J.-P. C. J. Villain R. Bidaux and R. Conte, "Order as an effect of disorder", Journal de Physique **41**, 1263–1272 (1980).

[25] R. Moessner, "Magnets with strong geometric frustration", Canadian Journal of Physics **79**, 1283–1294 (2001).

[26] J. T. Chalker, P. C. W. Holdsworth, and E. F. Shender, "Hidden order in a frustrated system: properties of the heisenberg kagomé antiferromagnet", Phys. Rev. Lett. **68**, 855–858 (1992).

[27] C. M. Dawson and M. A. Nielsen, "Frustration, interaction strength, and ground-state entanglement in complex quantum systems", Phys. Rev. A **69**, 052316 (2004).

[28] M. M. Wolf, F. Verstraete, and J. I. Cirac, "Entanglement and frustration in ordered systems", Int. Journal of Quantum Information **1**, 465 (2003).

[29] S. M. Giampaolo, G. Gualdi, A. Monras, and F. Illuminati, "Characterizing and quantifying frustration in quantum many-body systems", Phys. Rev. Lett. **107**, 260602 (2011).

[30] U. Marzolino, S. M. Giampaolo, and F. Illuminati, "Frustration, entanglement, and correlations in quantum many-body systems", Phys. Rev. A **88**, 020301 (2013).

[31] H. Tasaki, *Physics and mathematics of quantum many-body systems* (Springer, Cham, 2020).

[32] C. Lhuillier and G. Misguich, "Introduction to quantum spin liquids", in *Introduction to frustrated magnetism: materials, experiments, theory*, edited by C. Lacroix, P. Mendels, and F. Mila (Springer Berlin Heidelberg, Berlin, Heidelberg, 2011), pp. 23–41.

[33] G. Misguich and C. Lhuillier, "Two-dimensional quantum antiferromagnets", in *Frustrated spin systems*, 2nd (World Scientific, Singapore, 2013), pp. 235–319.

[34] B. Canals, "From the square lattice to the checkerboard lattice: spin-wave and large-n limit analysis", Phys. Rev. B **65**, 184408 (2002).

[35] J.-B. Fouet, M. Mambrini, P. Sindzingre, and C. Lhuillier, "Planar pyrochlore: a valence-bond crystal", Phys. Rev. B **67**, 054411 (2003).

[36] P. Lecheminant, "One-dimensional quantum spin liquids", in *Frustrated spin systems*, 2nd (World Scientific, Singapore, 2013), pp. 321–381.

[37] T. Giamarchi, *Quantum physics in one dimension* (Clarendon Press, Oxford, 2003).

[38] L. Faddeev and L. Takhtajan, "What is the spin of a spin wave?", Physics Letters A **85**, 375–377 (1981).

[39] I Affleck, D Gepner, H. J. Schulz, and T Ziman, "Critical behaviour of spin-s heisenberg antiferromagnetic chains: analytic and numerical results", Journal of Physics A: Mathematical and General **22**, 511–529 (1989).

[40] R. R. P. Singh, M. E. Fisher, and R. Shankar, "Spin-(1/2 antiferromagnetic xxz chain: new results and insights", Phys. Rev. B **39**, 2562–2567 (1989).

[41] T. Giamarchi and H. J. Schulz, "Correlation functions of one-dimensional quantum systems", Phys. Rev. B **39**, 4620–4629 (1989).

[42] H. Bethe, "Zur theorie der metalle", Zeitschrift für Physik **71**, 205–226 (1931).

[43] S. R. White and I. Affleck, "Dimerization and incommensurate spiral spin correlations in the zigzag spin chain: analogies to the kondo lattice", Phys. Rev. B **54**, 9862–9869 (1996).

[44] B. S. Shastry and B. Sutherland, "Excitation spectrum of a dimerized next-neighbor antiferromagnetic chain", Phys. Rev. Lett. **47**, 964–967 (1981).

[45] F. D. M. Haldane, "Spontaneous dimerization in the $S = \frac{1}{2}$ heisenberg antiferromagnetic chain with competing interactions", Phys. Rev. B **25**, 4925–4928 (1982).

[46] I Affleck, "Quantum spin chains and the haldane gap", Journal of Physics: Condensed Matter **1**, 3047–3072 (1989).

[47] C. K. Majumdar and D. K. Ghosh, "On next-nearest-neighbor interaction in linear chain. ii", Journal of Mathematical Physics **10**, 1399–1402 (1969).

[48] R. J. Cava, K. L. Holman, T. McQueen, E. J. Welsh, D. V. West, and A. J. Williams, "The geometries of triangular magnetic lattices", in *Introduction to frustrated magnetism: materials, experiments, theory*, edited by C. Lacroix, P. Mendels, and F. Mila (Springer Berlin Heidelberg, Berlin, Heidelberg, 2011), pp. 131–154.

[49] B. D. Gaulin and J. S. Gardner, "Experimental studies of pyrochlore antiferromagnets", in *Introduction to frustrated magnetism: materials, experiments, theory*, edited by C. Lacroix, P. Mendels, and F. Mila (Springer Berlin Heidelberg, Berlin, Heidelberg, 2011), pp. 177–206.

[50] P. Mendels and A. S. Wills, "Kagomé antiferromagnets: materials vs. spin liquid behaviors", in *Introduction to frustrated magnetism: materials, experiments, theory*, edited by C. Lacroix, P. Mendels, and F. Mila (Springer Berlin Heidelberg, Berlin, Heidelberg, 2011), pp. 207–238.

[51] H. Takagi and S. Niitaka, "Highly frustrated magnetism in spinels", in *Introduction to frustrated magnetism: materials, experiments, theory*, edited by C. Lacroix, P. Mendels, and F. Mila (Springer Berlin Heidelberg, Berlin, Heidelberg, 2011), pp. 155–175.

[52] B. D. Gaulin and J. S. Gardner, "Experimental studies of frustrated pyrochlore antiferromagnets", in *Frustrated spin systems*, 2nd (World Scientific, Singapore, 2013), pp. 475–507.

[53] P. Hohenberg and A. Krekhov, "An introduction to the ginzburg-landau theory of phase transitions and nonequilibrium patterns", Physics Reports **572**, 1–42 (2015).

[54] P. Coleman, *Introduction to many-body physics* (Cambridge University Press, 2015).

[55] G. Delfino, "Fields, particles and universality in two dimensions", Annals Phys. **360**, 477–519 (2015).

[56] F. Franchini, *An introduction to integrable techniques for one-dimensional quantum systems*, Vol. 940 (Springer International Publishing, Cham, 2017).

[57] L.-M. Duan, E. Demler, and M. D. Lukin, "Controlling spin exchange interactions of ultracold atoms in optical lattices", Phys. Rev. Lett. **91**, 090402 (2003).

[58] X.-W. Guan, M. T. Batchelor, and C. Lee, "Fermi gases in one dimension: from bethe ansatz to experiments", Rev. Mod. Phys. **85**, 1633–1691 (2013).

[59] J. Simon, W. S. Bakr, R. Ma, M. E. Tai, P. M. Preiss, and M. Greiner, "Quantum simulation of antiferromagnetic spin chains in an optical lattice", Nature **472**, 307–312 (2011).

[60] I. Bloch, "Quantum coherence and entanglement with ultracold atoms in optical lattices", Nature **453**, 1016–1022 (2008).

[61] I. M. Georgescu, S. Ashhab, and F. Nori, "Quantum simulation", Rev. Mod. Phys. **86**, 153–185 (2014).

[62] G. G. Cabrera and R. Jullien, "Universality of finite-size scaling: role of the boundary conditions", Phys. Rev. Lett. **57**, 393–396 (1986).

[63] G. G. Cabrera and R. Jullien, "Role of boundary conditions in the finite-size ising model", Phys. Rev. B **35**, 7062–7072 (1987).

[64] M. N. Barber and M. E. Cates, "Effect of boundary conditions on the finite-size transverse ising model", Phys. Rev. B **36**, 2024–2029 (1987).

[65] D. B. Abraham, L. F. Ko, and N. M. Švrakić, "Ising model with adjustable boundary conditions: exact results for finite lattice mass gaps", Phys. Rev. Lett. **61**, 2393–2396 (1988).

[66] C. R. Laumann, R. Moessner, A. Scardicchio, and S. L. Sondhi, "Quantum adiabatic algorithm and scaling of gaps at first-order quantum phase transitions", Phys. Rev. Lett. **109**, 030502 (2012).

[67] M. Campostrini, A. Pelissetto, and E. Vicari, "Quantum transitions driven by one-bond defects in quantum ising rings", Phys. Rev. E **91**, 042123 (2015).

[68] M. Campostrini, J. Nespolo, A. Pelissetto, and E. Vicari, "Finite-size scaling at first-order quantum transitions", Phys. Rev. Lett. **113**, 070402 (2014).

[69] M. Campostrini, A. Pelissetto, and E. Vicari, "Quantum ising chains with boundary fields", Journal of Statistical Mechanics: Theory and Experiment **2015**, P11015 (2015).

[70] J.-J. Dong and P. Li, "The a-cycle problem in xy model with ring frustration", Modern Physics Letters B **31**, 1750061 (2017).

[71] J.-J. Dong, P. Li, and Q.-H. Chen, "The a-cycle problem for transverse ising ring", Journal of Statistical Mechanics: Theory and Experiment **2016**, 113102 (2016).

[72] J.-J. Dong, Z.-Y. Zheng, and P. Li, "Rigorous proof for the nonlocal correlation function in the transverse ising model with ring frustration", Phys. Rev. E **97**, 012133 (2018).

[73] S. M. Giampaolo, F. B. Ramos, and F. Franchini, "The Frustration of being Odd: Universal Area Law violation in local systems", J. Phys. Comm. **3**, 081001 (2019).

[74] T. W. Burkhardt and I Guim, "Finite-size scaling of the quantum ising chain with periodic, free, and antiperiodic boundary conditions", Journal of Physics A: Mathematical and General **18**, L33–L38 (1985).

[75] M Karbach and K. H. Mutter, "The antiferromagnetic spin- 1/2 -XXZ model on rings with an odd number of sites", Journal of Physics A: Mathematical and General **28**, 4469–4479 (1995).

[76] P. Li and Y. He, "Ring frustration and factorizable correlation functions of critical spin rings", Phys. Rev. E **99**, 032135 (2019).

[77] A. Polkovnikov and V. Gritsev, "Breakdown of the adiabatic limit in low-dimensional gapless systems", Nature Physics **4**, 477–481 (2008).

[78] A. Polkovnikov, K. Sengupta, A. Silva, and M. Vengalattore, "Colloquium: nonequilibrium dynamics of closed interacting quantum systems", Rev. Mod. Phys. **83**, 863–883 (2011).

[79] P. Calabrese and J. Cardy, "Evolution of entanglement entropy in one-dimensional systems", Journal of Statistical Mechanics: Theory and Experiment **2005**, P04010 (2005).

[80] P. Calabrese and J. Cardy, "Quantum quenches in 1+1 dimensional conformal field theories", Journal of Statistical Mechanics: Theory and Experiment **2016**, 064003 (2016).

[81] A. Mitra, "Quantum quench dynamics", Annual Review of Condensed Matter Physics **9**, 245–259 (2018).

[82] N. D. Mermin and H. Wagner, "Absence of ferromagnetism or antiferromagnetism in one- or two-dimensional isotropic heisenberg models", Phys. Rev. Lett. **17**, 1133–1136 (1966).

[83] S. Coleman, "There are no goldstone bosons in two dimensions", Communications in Mathematical Physics **31**, 259–264 (1973).

[84] I. Affleck, "Field Theory Methods and Quantum Critical Phenomena", in Les Houches Summer School in Theoretical Physics: Fields, Strings, Critical Phenomena (June 1988).

[85] J. Cardy, *Scaling and renormalization in statistical physics*, Cambridge Lecture Notes in Physics (Cambridge University Press, 1996).

[86] P. Pfeuty, "The one-dimensional ising model with a transverse field", Annals of Physics **57**, 79 –90 (1970).

[87] M. B. Hastings, "Locality in quantum and markov dynamics on lattices and networks", Phys. Rev. Lett. **93**, 140402 (2004).

[88] M. B. Hastings and T. Koma, "Spectral gap and exponential decay of correlations", Communications in Mathematical Physics **265**, 781–804 (2006).

[89] N Iorgov, V Shadura, and Y. Tykhyy, "Spin operator matrix elements in the quantum ising chain: fermion approach", Journal of Statistical Mechanics: Theory and Experiment **2011**, P02028 (2011).

[90] E. Barouch and B. M. McCoy, "Statistical mechanics of the XY model. ii. spin-correlation functions", Phys. Rev. A **3**, 786–804 (1971).

[91] E. Lieb, T. Schultz, and D. Mattis, "Two soluble models of an antiferromagnetic chain", Annals of Physics **16**, 407 –466 (1961).

[92] V Korepin and P Zinn-Justin, "Thermodynamic limit of the six-vertex model with domain wall boundary conditions", Journal of Physics A: Mathematical and General **33**, 7053–7066 (2000).

[93] F. Colomo and A. G. Pronko, "The arctic curve of the domain-wall six-vertex model", Journal of Statistical Physics **138**, 662–700 (2010).

[94] F. Colomo and A. Sportiello, "Arctic curves of the six-vertex model on generic domains: the tangent method", Journal of Statistical Physics **164**, 1488–1523 (2016).

[95] F. Colomo, A. G. Pronko, and A. Sportiello, "Arctic curve of the free-fermion six-vertex model in an l-shaped domain", Journal of Statistical Physics **174**, 1–27 (2019).

[96] N. Allegra, J. Dubail, J.-M. Stéphan, and J. Viti, "Inhomogeneous field theory inside the arctic circle", Journal of Statistical Mechanics: Theory and Experiment **2016**, 053108 (2016).

[97] P. D. Francesco and E. Guitter, "Arctic curves for paths with arbitrary starting points: a tangent method approach", Journal of Physics A: Mathematical and Theoretical **51**, 355201 (2018).

[98] L. F. Cugliandolo, "Artificial spin-ice and vertex models", Journal of Statistical Physics **167**, 499–514 (2017).

[99] H. Cohn, N. Elkies, and J. Propp, "Local statistics for random domino tilings of the Aztec diamond", Duke Mathematical Journal **85**, 117 –166 (1996).

[100] N. Elkies, G. Kuperberg, M. Larsen, and J. Propp, "Alternating-sign matrices and domino tilings (part i)", Journal of Algebraic Combinatorics **1**, 111–132 (1992).

[101] N. Elkies, G. Kuperberg, M. Larsen, and J. Propp, "Alternating-sign matrices and domino tilings (part ii)", Journal of Algebraic Combinatorics **1**, 219–234 (1992).

[102] "Exact methods in low-dimensional statistical physics and quantum computing: lecture notes of the les houches summer school: volume 89", in, edited by J. Jacobsen, S. Ouvry, V. Pasquier, D. Serban, and L. Cugliandolo (Oxford University Press, Oxford, 2010) Chap. R. Kenyon: The dimer model.

[103] A. Borodin, V. Gorin, and E. M. Rains, "Q-distributions on boxed plane partitions", Selecta Mathematica **16**, 731–789 (2010).

[104] H. Cohn, M. Larsen, and J. Propp, "The shape of a typical boxed plane partition.", eng, The New York Journal of Mathematics [electronic only] **4**, 137–165 (1998).

[105] "Phase transitions and critical phenomena", in, Vol. 1, edited by C. Domb and M. S. Green (Academic Press, London, 1972) Chap. Rigorous Results and Theorems, R. B. Griffiths.

[106] B. Simon, *The statistical mechanics of lattice gases* (Princeton University Press, Princeton, 1993).

[107] L. D. Landau, "On the theory of phase transitions", Zh. Eksp. Teor. Fiz. **7**, 19–32 (1937).

[108] P. W. Anderson, *Basic notions of condensed matter physics* (The Benjamin/Cummings Publishing Company, Inc., 1984).

[109] B. Zeng, X. Chen, D.-L. Zhou, and X.-G. Wen, *Quantum information meets quantum matter* (Springer, New York, 2019).

[110] M. Greiner, O. Mandel, T. W. Hänsch, and I. Bloch, "Collapse and revival of the matter wave field of a bose–einstein condensate", Nature **419**, 51–54 (2002).

[111] T. Kinoshita, T. Wenger, and D. S. Weiss, "A quantum newton's cradle", Nature **440**, 900–903 (2006).

[112] S. Hofferberth, I. Lesanovsky, B. Fischer, T. Schumm, and J. Schmiedmayer, "Non-equilibrium coherence dynamics in one-dimensional bose gases", Nature **449**, 324–327 (2007).

[113] M. Rigol, V. Dunjko, and M. Olshanii, "Thermalization and its mechanism for generic isolated quantum systems", Nature **452**, 854–858 (2008).

[114] F. H. L. Essler and M. Fagotti, "Quench dynamics and relaxation in isolated integrable quantum spin chains", Journal of Statistical Mechanics: Theory and Experiment **2016**, 064002 (2016).

[115] J.-S. Caux and F. H. L. Essler, "Time evolution of local observables after quenching to an integrable model", Phys. Rev. Lett. **110**, 257203 (2013).

[116] J. Eisert, M. Friesdorf, and C. Gogolin, "Quantum many-body systems out of equilibrium", Nature Physics **11**, 124–130 (2015).

[117] L. D'Alessio, Y. Kafri, A. Polkovnikov, and M. Rigol, "From quantum chaos and eigenstate thermalization to statistical mechanics and thermodynamics", Advances in Physics **65**, 239–362 (2016).

[118] H. Tasaki, "From quantum dynamics to the canonical distribution: general picture and a rigorous example", Phys. Rev. Lett. **80**, 1373–1376 (1998).

[119] P. Reimann, "Foundation of statistical mechanics under experimentally realistic conditions", Phys. Rev. Lett. **101**, 190403 (2008).

[120] N. Linden, S. Popescu, A. J. Short, and A. Winter, "Quantum mechanical evolution towards thermal equilibrium", Phys. Rev. E **79**, 061103 (2009).

[121] K. Sengupta, S. Powell, and S. Sachdev, "Quench dynamics across quantum critical points", Phys. Rev. A **69**, 053616 (2004).

[122] R. A. Jalabert and H. M. Pastawski, "Environment-independent decoherence rate in classically chaotic systems", Phys. Rev. Lett. **86**, 2490–2493 (2001).

[123] T. Gorin, T. Prosen, T. H. Seligman, and M. Žnidarič, "Dynamics of loschmidt echoes and fidelity decay", Physics Reports **435**, 33–156 (2006).

[124] H. T. Quan, Z. Song, X. F. Liu, P. Zanardi, and C. P. Sun, "Decay of loschmidt echo enhanced by quantum criticality", Phys. Rev. Lett. **96**, 140604 (2006).

[125] A. Silva, "Statistics of the work done on a quantum critical system by quenching a control parameter", Phys. Rev. Lett. **101**, 120603 (2008).

[126] A. Chenu, J. Molina-Vilaplana, and A. del Campo, "Work Statistics, Loschmidt Echo and Information Scrambling in Chaotic Quantum Systems", Quantum **3**, 127 (2019).

[127] Z.-G. Yuan, P. Zhang, and S.-S. Li, "Loschmidt echo and berry phase of a quantum system coupled to an XY spin chain: proximity to a quantum phase transition", Phys. Rev. A **75**, 012102 (2007).

[128] D. Rossini, T. Calarco, V. Giovannetti, S. Montangero, and R. Fazio, "Decoherence by engineered quantum baths", Journal of Physics A: Mathematical and Theoretical **40**, 8033–8040 (2007).

[129] D. Rossini, T. Calarco, V. Giovannetti, S. Montangero, and R. Fazio, "Decoherence induced by interacting quantum spin baths", Phys. Rev. A **75**, 032333 (2007).

[130] M. Zhong and P. Tong, "Loschmidt echo of a two-level qubit coupled to nonuniform anisotropic XY chains in a transverse field", Phys. Rev. A **84**, 052105 (2011).

[131] S. Sharma, V. Mukherjee, and A. Dutta, "Study of loschmidt echo for a qubit coupled to an xy-spin chain environment", The European Physical Journal B **85**, 143 (2012).

[132] S. Montes and A. Hamma, "Phase diagram and quench dynamics of the cluster-XY spin chain", Phys. Rev. E **86**, 021101 (2012).

[133] J. Cardy, "Thermalization and revivals after a quantum quench in conformal field theory", Phys. Rev. Lett. **112**, 220401 (2014).

[134] J.-M. Stéphan and J. Dubail, "Local quantum quenches in critical one-dimensional systems: entanglement, the loschmidt echo, and light-cone effects", Journal of Statistical Mechanics: Theory and Experiment **2011**, P08019 (2011).

[135] A. Rajak and U. Divakaran, "Fidelity susceptibility and loschmidt echo for generic paths in a three-spin interacting transverse ising model", Journal of Statistical Mechanics: Theory and Experiment **2014**, P04023 (2014).

[136] R. Jafari and H. Johannesson, "Loschmidt echo revivals: critical and noncritical", Phys. Rev. Lett. **118**, 015701 (2017).

[137] Z. P. Karkuszewski, C. Jarzynski, and W. H. Zurek, "Quantum chaotic environments, the butterfly effect, and decoherence", Phys. Rev. Lett. **89**, 170405 (2002).

[138] M. Diez, N. Chancellor, S. Haas, L. C. Venuti, and P. Zanardi, "Local quenches in frustrated quantum spin chains: global versus subsystem equilibration", Phys. Rev. A **82**, 032113 (2010).

[139] E. J. Torres-Herrera and L. F. Santos, "Local quenches with global effects in interacting quantum systems", Phys. Rev. E **89**, 062110 (2014).

[140] A. Peres, "Stability of quantum motion in chaotic and regular systems", Phys. Rev. A **30**, 1610–1615 (1984).

[141] P. P. Mazza, J.-M. Stéphan, E. Canovi, V. Alba, M. Brockmann, and M. Haque, "Overlap distributions for quantum quenches in the anisotropic heisenberg chain", Journal of Statistical Mechanics: Theory and Experiment **2016**, 013104 (2016).

[142] B. Damski and M. M. Rams, "Exact results for fidelity susceptibility of the quantum ising model: the interplay between parity, system size, and magnetic field", Journal of Physics A: Mathematical and Theoretical **47**, 025303 (2013).

[143] G. H. Hardy, "Weierstrass's non-differentiable function", Transactions of the American Mathematical Society **17**, 301–325 (1916).

[144] M. V. Berry, Z. V. Lewis, and J. F. Nye, "On the weierstrass-mandelbrot fractal function", Proceedings of the Royal Society of London. A. Mathematical and Physical Sciences **370**, 459–484 (1980).

[145] B. B. Mandelbrot, *The fractal geometry of nature* (W. H. Freeman and Company, New York, 1982).

[146] C. Gao, H. Zhai, and Z.-Y. Shi, "Dynamical fractal in quantum gases with discrete scaling symmetry", Phys. Rev. Lett. **122**, 230402 (2019).

[147] B. Yan, L. Cincio, and W. H. Zurek, "Information scrambling and loschmidt echo", Phys. Rev. Lett. **124**, 160603 (2020).

[148] E. Ercolessi, S. Evangelisti, F. Franchini, and F. Ravanini, "Modular invariance in the gapped XYZ spin-$\frac{1}{2}$ chain", Phys. Rev. B **88**, 104418 (2013).

[149] P. Jordan and E. Wigner, "Über das paulische Äquivalenzverbot", Zeitschrift für Physik **47**, 631–651 (1928).

[150] B. M. McCoy, "Spin correlation functions of the $X-Y$ model", Phys. Rev. **173**, 531–541 (1968).

[151] L. Dell'Anna, O. Salberger, L. Barbiero, A. Trombettoni, and V. E. Korepin, "Violation of cluster decomposition and absence of light cones in local integer and half-integer spin chains", Phys. Rev. B **94**, 155140 (2016).

[152] "Phase transitions and critical phenomena, volume 10", in, edited by C. Domb and J. L. Lebowitz (Academic Press, London, 1986) Chap. H. W. Diehl.

[153] D. Bonn and D. Ross, "Wetting transitions", Reports on Progress in Physics **64**, 1085–1163 (2001).

[154] D. Bonn, J. Eggers, J. Indekeu, J. Meunier, and E. Rolley, "Wetting and spreading", Rev. Mod. Phys. **81**, 739–805 (2009).

[155] G. Delfino, "Interface localization near criticality", Journal of High Energy Physics **2016**, 32 (2016).

[156] G. Toulouse, "Theory of the frustration effect in spin glasses: i", Communications on Physics **2**, 115–119 (1977).

[157] J. Vannimenus and G. Toulouse, "Theory of the frustration effect. II. ising spins on a square lattice", Journal of Physics C: Solid State Physics **10**, L537–L542 (1977).

[158] S. M. Giampaolo, B. C. Hiesmayr, and F. Illuminati, "Global-to-local incompatibility, monogamy of entanglement, and ground-state dimerization: theory and observability of quantum frustration in systems with competing interactions", Phys. Rev. B **92**, 144406 (2015).

[159] C. Schuster and U. Eckern, "Quantum spin chains with various defects", Annalen der Physik **11**, 901–915 (2002).

[160] T. J. G. Apollaro, F. Plastina, L. Banchi, A. Cuccoli, R. Vaia, P. Verrucchi, and M. Paternostro, "Effective cutting of a quantum spin chain by bond impurities", Phys. Rev. A **88**, 052336 (2013).

[161] P. Smacchia, L. Amico, P. Facchi, R. Fazio, G. Florio, S. Pascazio, and V. Vedral, "Statistical mechanics of the cluster ising model", Phys. Rev. A **84**, 022304 (2011).

[162] S. M. Giampaolo and B. C. Hiesmayr, "Genuine multipartite entanglement in the cluster-ising model", New Journal of Physics **16**, 093033 (2014).

[163] G Zonzo and S. M. Giampaolo, "N-cluster models in a transverse magnetic field", Journal of Statistical Mechanics: Theory and Experiment **2018**, 063103 (2018).

[164] T. Koffel, M. Lewenstein, and L. Tagliacozzo, "Entanglement entropy for the long-range ising chain in a transverse field", Phys. Rev. Lett. **109**, 267203 (2012).

[165] Z.-X. Gong, M. Foss-Feig, S. Michalakis, and A. V. Gorshkov, "Persistence of locality in systems with power-law interactions", Phys. Rev. Lett. **113**, 030602 (2014).

[166] M. Foss-Feig, Z.-X. Gong, C. W. Clark, and A. V. Gorshkov, "Nearly linear light cones in long-range interacting quantum systems", Phys. Rev. Lett. **114**, 157201 (2015).

[167] D. Vodola, L. Lepori, E. Ercolessi, and G. Pupillo, "Long-range ising and kitaev models: phases, correlations and edge modes", New Journal of Physics **18**, 015001 (2015).

[168] J. K. Pachos and M. B. Plenio, "Three-spin interactions in optical lattices and criticality in cluster hamiltonians", Phys. Rev. Lett. **93**, 056402 (2004).

[169] S. Montes and A. Hamma, "Phase diagram and quench dynamics of the cluster-XY spin chain", Phys. Rev. E **86**, 021101 (2012).

[170] S. M. Giampaolo and B. C. Hiesmayr, "Topological and nematic ordered phases in many-body cluster-ising models", Phys. Rev. A **92**, 012306 (2015).

[171] G. Mussardo, A. Trombettoni, and Z. Zhang, "Prime suspects in a quantum ladder", Phys. Rev. Lett. **125**, 240603 (2020).

[172] G Mussardo, G Giudici, and J Viti, "The coprime quantum chain", Journal of Statistical Mechanics: Theory and Experiment **2017**, 033104 (2017).

[173] D. García-Martín, E. Ribas, S. Carrazza, J. Latorre, and G. Sierra, "The Prime state and its quantum relatives", Quantum **4**, 371 (2020).

[174] B. Sutherland, *Beautiful models* (WORLD SCIENTIFIC, 2004).

[175] J. Zinn-Justin, *Quantum field theory and critical phenomena* (Oxford University Press, Oxford, 2002).

[176] M. den Nijs and K. Rommelse, "Preroughening transitions in crystal surfaces and valence-bond phases in quantum spin chains", Phys. Rev. B **40**, 4709–4734 (1989).

[177] X. G. Wen, F. Wilczek, and A. Zee, "Chiral spin states and superconductivity", Phys. Rev. B **39**, 11413–11423 (1989).

[178] X. G. Wen, "Topological orders in rigid states", International Journal of Modern Physics B **04**, 239–271 (1990).

[179] R. Moessner and J. E. Moore, *Topological phases of matter* (Cambridge University Press, 2021).

[180] F. Pollmann, E. Berg, A. M. Turner, and M. Oshikawa, "Symmetry protection of topological phases in one-dimensional quantum spin systems", Phys. Rev. B **85**, 075125 (2012).

[181] X. Chen, Z.-C. Gu, and X.-G. Wen, "Classification of gapped symmetric phases in one-dimensional spin systems", Phys. Rev. B **83**, 035107 (2011).

[182] R. Verresen, R. Moessner, and F. Pollmann, "One-dimensional symmetry protected topological phases and their transitions", Phys. Rev. B **96**, 165124 (2017).

[183] T. Senthil, "Symmetry-protected topological phases of quantum matter", Annual Review of Condensed Matter Physics **6**, 299–324 (2015).

[184] I. Affleck, T. Kennedy, E. H. Lieb, and H. Tasaki, "Rigorous results on valence-bond ground states in antiferromagnets", Phys. Rev. Lett. **59**, 799–802 (1987).

[185] I. Affleck, T. Kennedy, E. H. Lieb, and H. Tasaki, "Valence bond ground states in isotropic quantum antiferromagnets", Comm. Math. Phys. **115**, 477–528 (1988).

[186] A. Y. Kitaev, "Unpaired majorana fermions in quantum wires", Physics-Uspekhi **44**, 131–136 (2001).

[187] W. Son, L. Amico, R. Fazio, A. Hamma, S. Pascazio, and V. Vedral, "Quantum phase transition between cluster and antiferromagnetic states", EPL (Europhysics Letters) **95**, 50001 (2011).

[188] M. B. Hastings and X.-G. Wen, "Quasiadiabatic continuation of quantum states: the stability of topological ground-state degeneracy and emergent gauge invariance", Phys. Rev. B **72**, 045141 (2005).

[189] G. C. Wick, "The evaluation of the collision matrix", Phys. Rev. **80**, 268–272 (1950).

[190] M. Gaudin, "Une démonstration simplifiée du théorème de wick en mécanique statistique", Nuclear Physics **15**, 89–91 (1960).

[191] X.-G. Wen, *Quantum field theory of many-body systems*, eng, Oxford Graduate Texts (Oxford University Press, Oxford, 2007).

[192] L. G. Molinari, *Notes on wick's theorem in many-body theory*, 2017, arXiv:1710.09248 [math-ph].

[193] A. Böttcher and B. Silbermann, *Introduction to large truncated toeplitz matrices* (Springer-Verlag New York, 1999).

[194] M. Rao and H. Stetkaer, *Complex analysis: an invitation* (World Scientific Publishing Co., Singapore, 1991).

[195] G. Szegö, "On certain hermitian forms associated with the fourier series of a positive function", Festschrift Marcel Riesz, 228–238 (1952).

[196] P. Deift, A. Its, and I. Krasovsky, "Toeplitz matrices and toeplitz determinants under the impetus of the ising model: some history and some recent results", Communications on Pure and Applied Mathematics **66**, 1360–1438 (2013).

[197] B. Simon, *Orthogonal polynomials on the unit circle* (Colloquium Publications, 2004).

[198] A. Böttcher and B. Silbermann, *Analysis of toeplitz operators* (Springer-Verlag Berlin Heidelberg, 2006).

[199] R. E. Hartwig and M. E. Fisher, "Asymptotic behavior of toeplitz matrices and determinants", Archive for Rational Mechanics and Analysis **32**, 190–225 (1969).

[200] M. E. Fisher and R. E. Hartwig, "Toeplitz determinants: some applications, theorems, and conjectures", in *Advances in chemical physics* (John Wiley and Sons, Ltd, 1969), pp. 333–353.

[201] A. Böttcher and B. Silbermann, "Notes on the asymptotic behavior of block toeplitz matrices and determinants", Mathematische Nachrichten **98**, 183–210 (1980).

[202] A. Böttcher and H. Widom, "Szegö via jacobi", Linear Algebra and its Applications **419**, 656 –667 (2006).

[203] I. Krasovsky, "Aspects of toeplitz determinants", in Random walks, boundaries and spectra, edited by D. Lenz, F. Sobieczky, and W. Woess (2011), pp. 305–324.

[204] B. McCoy and T. T. Wu, *The two-dimensional ising model* (Harvard University Press, 1973).

[205] T. T. Wu, "Theory of toeplitz determinants and the spin correlations of the two-dimensional ising model. i", Phys. Rev. **149**, 380–401 (1966).